Immune regulation of *Chlamydia psittaci* persistence in Sheep

Thesis submitted to the University of Edinburgh (Faculty of Medicine) for the Degree of Doctor of Philosophy

by

Jeremy Keith Brown

1999

Declaration

I declare that all the work presented in this thesis has been composed and performed by myself. Contributions to the work of this thesis by colleagues are fully acknowledged in the text.

This work has not been, and is not currently being submitted for candidature for any other degree.

Table of Contents

Acknowledgements *IX*

List of Abbreviations *X*

Abstract *XV*

1.0 General Introduction 1
1.1. Introduction 2
1.2. Genus Chlamydia 3
1.2.1. Developmental cycle of *Chlamydia* 3
1.3.2.Taxonomy 4
1.3. Ovine Enzootic Abortion 7
1.3.1. Transmission of OEA 8
1.3.2. Pathology of OEA in non-pregnant sheep 9
1.3.3. Pathology of OEA in pregnant sheep 11
1.3.4. Zoonotic infection 11
1.3.5. Diagnosis of OEA 12
1.3.6. Vaccination strategies 13
1.4. Murine models of in vivo chlamydial infection 17
1.5. The innate immune response to C. psittaci 18
1.5.1. Recruitment and activation of immune cells 18
1.5.2. Interaction between *C. psittaci* and neutrophils 20
1.5.3. Interaction between *C. psittaci* and mononuclear cells 22
1.5.4. Interaction between *C. psittaci* and dendritic cells 25
1.5.5. Interaction between *C. psittaci* and NK cells 27
1.6. Acquired immunity to C. psittaci 28
1.6.1. Immunity to *C. psittaci* in naive sheep infected outwith pregnancy 28
1.6.2. The secondary ovine immune response to *C. psittaci* 29
1.6.3 Humoral immunity to chlamydiae 29
1.6.4 CD4 +ve $\alpha\beta$ T-cells and immunity to chlamydiae 32
1.6.5 CD8 +ve $\alpha\beta$ T-cells and immunity to chlamydiae 35
1.6.6 $\gamma\delta$ T-cells and immunity to chlamydiae 36
1.6.7 Cytokines and immunity to chlamydiae 36
1.6.8. IFN-γ mediated persistence of chlamydiae *in vitro* 37
1.7. Aims of the study 39

2.0 Materials and Methods 40
2.1. Cell culture and C. psittaci 41
2.1.1. General culture conditions 41
2.1.2. Fetal bovine sera 41
2.1.3. Cryopreservation 41
2.1.4. ST.6 cells 42

2.1.5. RAW 264.7 cell line 42
2.1.6. Collection of bronchoalveolar lavage cells 43
2.1.7. Collection of ovine peripheral blood mononuclear cells 43
2.1.8. *C. psittaci* S26/3 44
2.2. Phenotypic analysis of primary ovine cells 45
2.2.1. Flow cytometry 45
2.2.2. Non-specific esterase staining of adherent BAL cells 45
2.2.3. Phagocytic characterisation of adherent BAL cells 46
2.3. Recombinant ruminant cytokines 47
2.3.1. Recombinant ovine IFN-γ 47
2.3.2. Recombinant bovine IFN-α 47
2.3.3. Ovine anti-viral interferon bioassay 48
2.4. Histology and imaging 49
2.4.1. Cytospins 49
2.4.2. Modified Ziehl Neelsen's (MZN) Stain 49
2.4.3. Giemsa Stain 49
2.4.4. *C. psittaci* specific immunoperoxidase (IPX) staining 50
2.4.5. Image Acquisition and Storage 50
2.4.6. Image Processing 51
2.5. Measurement of C. psittaci multiplication 53
2.5.1. Chlamydial LPS-ELISA 53
2.5.2. Titration of chlamydial infectivity 54
2.6. Recombinant MOMP 55
2.6.1. Production of recombinant MOMP in *Escherichia coli* 55
2.6.2. Direct dot-immunobinding assay for TMOMP 56
2.6.3. Polyacrylamide gel chromatography 57
2.6.4. Purification of Recombinant TMOMP 58
2.6.5. SDS-PAGE 59
2.6.6. 1D gel densitometery 60
2.7. Lymphocyte stimulation assay 61

3.0 Initial feasibility studies and development of an automated image analysis solution for measuring chlamydial growth *in vitro* 62
3.1. Introduction 63
3.2. Materials and Methods 64
3.2.1 Preparation of cells and chlamydiae for imaging 64
3.2.2 Image acquisition 65
3.2.3 Manual image analysis of *C. psittaci* inclusion bodies 65
3.2.4 Automated enumeration and measurement of inclusions 66
3.2.5 Semi-automated measurement of *C. psittaci* inclusion bodies 66
3.2.6 Statistical Analysis 66
3.3 Results 67
3.3.1 Chlamydial growth and image acquisition 67
3.3.2 Preliminary image analysis 70
3.3.3 Development of an automated image

analysis system for the enumeration and measurement of Chlamydial inclusion bodies 89
3.3.3.1 Universal colour segmentation 89
3.3.3.2 Guard frame design 90
3.3.3.3 Calculation of the 2-D rolling ball 94
3.3.3.4 Automation of the 2-D rolling ball background subtraction 95
3.3.3.5 Calculation of the scaling factor of the images 96
3.3.3.6 Automation of enumeration and measurement of Inclusion Bodies 97
3.3.4 Computer aided manual enumeration and measurement of inclusion bodies 98
3.3.5 Statistical comparison of the results generated by automated image analysis and manual image analysis 102
3.4 Discussion 107

4.0 Improved colour segmentation of chlamydial inclusion bodies 113
4.1. Introduction 114
4.2 Materials and Methods 115
4.2.1. Image acquisition 115
4.2.2 Automated enumeration and measurement of inclusions 115
4.2.3 Statistical Analysis 115
4.3 Results 116
4.3.1 "Point and click" colour segmentation in Inclusion Counter v2.0 117
4.3.2 Batch processing using the Colour Range Record 121
4.3.3. Length and width measurement by best fit ellipse 122
4.3.4. Implementation of the HSV colour model in Object-Image 1.62n6 122
4.3.5. Implementation of the HSV model in Inclusion Counter v2.0 126
4.3.6. Analysis of the results generated by Inclusion Counter v2.0 126
4.4 Discussion 132

5.0 Mechanisms of ROvIFN-γ mediated inhibition of *C. psittaci* growth in ovine cells 134
5.1. Introduction 135
5.2. Materials and Methods 137
5.2.1. Pretreatment and infection of ovine ST.6 cells 137
5.2.2. Measurement of *C. psittaci* multiplication in ST.6 cells 137
5.2.3. Sheep 138
5.2.4. Phenotypic characterisation of ovine BAL cells 138
5.2.5. Stimulation of murine RAW 264.7 cells 139

5.2.6. Stimulation of ovine BAL cells 139
5.2.7. Measurement of nitric oxide production using the Griess reaction 139
5.2.6. ROvIFN-γ mediated restriction of *C. psittaci* in ovine BAL cells 140
5.3. Results 141
5.3.1. Comparative analysis of the anti-chlamydial effects of RBovIFN-α and ROvIFN-γ. 141
5.3.2. Comparative analysis of the anti-chlamydial effects of PolyI: PolyC and ROvIFN-γ. 142
5.3.3. Mechanisms of ROvIFN-γ mediated inhibition of *C. psittaci* in ST.6 cells. 144
5.3.4. Phenotypic analysis of ovine BAL cells 152
5.3.5. Nitric oxide production in murine RAW 264.7 cell controls 156
5.3.6. Direct comparison of nitric oxide production in ovine BAL cells and murine RAW 264.7 cells 157
5.3.7. ROvIFN-γ mediated restriction of chlamydial growth in ovine alveolar macrophages 161
5.4. Discussion 165

6.0 Persistent *C. psittaci* Infection of Ovine Cells 171
6.1 Introduction 172
6.2 Materials and Methods 173
6.2.1 Infection of ST-6 cells and treatment with ROvIFN-γ 173
6.2.2 Maintenance of persistently infected ST.6 cells 173
6.2.3 Measurement of *C. psittaci* multiplication 174
6.2.4 Statistics 174
6.3 Results 176
6.3.1 Restriction of *C. psittaci* growth in ovine ST.6 cells maintained in ROvIFN-γ for 21 days 176
6.3.2 Persistence *C. psittaci* infection of ovine ST.6 cells maintained in ROvIFN-γ for up to 28 days after infection 178
6.3.2.1 Analysis of *C. psittaci* growth on day 14 180
6.3.2.2 Analysis of *C. psittaci* growth on day 21 180
6.3.2.3 Analysis of *C. psittaci* growth on day 28 182
6.4 Discussion 184

7.0 Long-Term Persistent *C. psittaci* Infection of Ovine Cells 187
7.1 Introduction 188
7.2 Materials and Methods 189
7.2.1 Infection of ST-6 cells and treatment with ROvIFN-γ 189
7.2.2 Maintenance of persistently infected ST.6 cells 189
7.2.3 Measurement of *C. psittaci* multiplication 189
7.2.4 Statistics 190
7.3 Results 191
7.3.1 Infected control ST.6 Cell Cultures 191
7.3.2 Cultures maintained in medium containing ROvIFN-γ for 7 Days 192
7.3.3 Cultures maintained in medium containing ROvIFN-γ for 14 Days 193
7.3.4 Cultures maintained in medium containing ROvIFN-γ for 21 Days 195
7.3.5 Cultures maintained in medium containing ROvIFN-γ for 28 Days 197
7.3.6 Cultures maintained in medium containing ROvIFN-γ for 35 Days 199
7.3.7 Cultures maintained in medium containing ROvIFN-γ for 49 Days 200
7.3.8 Cultures maintained in medium containing ROvIFN-γ for 63 Days 201
7.4 Discussion 217

8.0 A Role for the Tryptophan Pathway in Interferon-γ Mediated Persistence of *Chlamydia psittaci* 222
8.1 Introduction 223
8.2 Materials and Methods 224
8.2.1 Infection of ST-6 cells and treatment with ROvIFN-γ 224
8.2.2 Maintenance of persistently infected ST.6 cells 224
8.2.3 Measurement of *C. psittaci* multiplication 225
8.2.4 Addition of exogenous L-tryptophan to persistently infected cultures 225
8.3 Results 226

8.3.1 Infected controls 226
8.3.2 Induction of *C. psittaci* persistence by ROvIFN-γ 226
8.3.3 Addition of exogenous L-tryptophan to ST.6 cultures at the time of infection 229
8.3.4 Addition of exogenous L-tryptophan to persistently infected ST.6 cells 235
8.4 Discussion 238

9.0 Stimulation of *C. psittaci* specific PBM proliferation by recombinant MOMP 240
9.1. Introduction 241
9.2. Materials and Methods 242
9.2.1. Sheep 242
9.2.2. Recombinant MOMP 242
9.2.3. *C. psittaci* specific lymphocyte stimulation assay 244
9.3 Results 245
9.3.1. Screening of Post-OEA ewes and controls for FMOMP specific PBM proliferation 243
9.3.2. Screening of selected post-OEA ewes and controls for TMOMP specific PBM proliferation 245
9.3.4. TMOMP-specific ovine T-cell lines 248
9.4. Discussion 249

10.0 General Discussion 251

References 267

Appendix 293
Appendix 1: Reagents 294
Appendix 2: Surface marker expression of ovine BAL cells 298
Appendix 3: Peer reviewed publications arising from the work detailed in this thesis 299

Acknowledgements

I would like to thank the following people for their help and encouragement during the course of my studies.

Dr. Gary Entrican (Moredun Research Institute) and Dr. Sarah Howie (Department of Pathology, The University of Edinburgh) for their advice and supervision.

Many thanks must go to all the members of the Moredun Research Institute, particularly Jackie, Ann, Sandy, Jo, Annie, Dr. Elisabeth Innes, David Dean, Dr. David Haig, Steven Maley and anyone else I've omitted. Dr. Alex Schock for her help and advice with microscopy and immunohistochemistry, to name but two things. Gareth Jones, Dr. Alan Herring, Dr. David Longbottom, Dr. Susan Wyllie and Susanna Dunbar for help and advice with the MOMP side of things. Dr. Hugh Reid for helping to find the funding required for these endeavours and the Moredun Foundation for putting up the cash.

Andrew Sanderson (ICAPB, The University of Edinburgh) for help with FACS analysis. Scott Cunningham and Stuart McKenzie (Imaging Unit, Department of pathology, The University of Edinburgh) for their help with image acquisition.

To every member of the international NIH Image community, with special thanks to the following people. Wayne Rasband, for getting the whole thing started and for his continual support for NIH Image and his new Java Image software (NIH: USA). Dr. Christopher Coulon (GAIA group: USA) for his enthusiasm, help and encouragement during the initial stages of my excursions into image analysis, not to mention showing me around the Napa Valley. Norbert Vischer (Universiteit van Amsterdam, The Netherlands), who not only single-handedly wrote the best image analysis software package in the world and made it freely available in the public domain, but also included the ability to automate image processing using the HSV colour model at my rather presumptuous request. Greg Joss (School of Biological Sciences, Macquarie University, Australia) for beta testing Inclusion Counter v2.0, unfaltering support and enthusiastic discussions.

SmithKline Beecham for their kind donation of the Power Macintosh 7100/80 AV which was used for image acquisition and processing during the course of these studies.

Last, but not least, my love and thanks go to Alex and my parents for putting up with me over the last many months. Many thanks to all my friends outside of work, even Palmer, who are alas to numerous to mention on this page.

List of Abbreviations

(αβ T-cell)	Alpha beta T-cell
(β-2m -/-)	Beta 2-microglobulin gene knockout
(BAL)	Bronchoalveolar Lavage
(BMDM)	Bone marrow derived macrophages
(BSA)	Bovine serum albumin
(BVDV)	Bovine virus diarrhoea virus
(CCD)	Charge coupled device
(CD)	Cluster of differentiation
(CD4 -/-)	CD4 gene knockout
(CFT)	Complement fixation test
(CHO)	Chinese Hamster Ovary
(CMI)	Cell mediated immune
(ConA)	Concanavalin A
(CPE)	Cytopathic effect
(CPM)	Counts per minute
(CR1)	Complement receptor 1
(CR3)	Complement receptor 3
(DAB)	3, 3'-Diaminobenzidine Tetrahydrochloride
(DC)	Dendritic cells
(DMSO)	Dimethyl-sulfoxide
(DTH)	Delayed type hypersensitivity
(EB)	Elementary body
(ELISA)	Enzyme linked immunosorbent assays
(FACS)	Fluorescence activated cell sorter
(FBS)	Fetal bovine serum
(FITC)	Fluorescein isothiocyanate
(FMOMP)	Fusion protein derived recombinant major outer membrane protein
(GB)	Gigabyte
(γδ -/-)	Gamma delta T-cell gene knockout

(γδ T-cell)	Gamma delta T-cell
(GM-CSF)	Granulocyte-macrophage colony-stimulating factor
(GMEM)	Glasgow's Modified Eagle's Medium without glutamine
(GRO)	Growth-related oncogene family of chemokines
(H_2O_2)	Hydrogen peroxide
(HBSS)	Hanks Balance Salt Solution
(HCl)	Hydrochloric acid
(HSV)	Hue, Saturation and Value
(IDO)	Indoleamine 2,3-dioxygenase
(IFAT)	indirect immuno-fluorescence test
(IFN-α)	Interferon-alpha
(IFN-β)	Interferon-beta
(IFN-γ -/-)	IFN-γ gene knockout mice
(IFN-γ)	Interferon-gamma
(IFN-γR -/-)	IFN-γ receptor gene knockout mice
(IFU)	Inclusion forming units
(IFU/ml)	Inclusion-forming units/ml
(IgA)	Immunoglobulin A
(IgG)	Immunoglobulin G
(Igμ -/-)	Immunoglobulin μ heavy chain gene knockout mice
(IL-10)	Interleukin-10
(IL-12)	Interleukin-12
(IL-1α)	Interleukin-1 alpha
(IL-1β)	Interleukin-1 beta
(IL-6)	Interleukin-6
(IL-8)	Interleukin-8
(IL4-/-)	Interleukin-4 gene knockout
(IMDM)	Iscove's modified Dulbecco's medium
(iNOS)	Inducible nitric oxide synthase

(IPTG)	Isopropyl-β-thiogalactopyranoside
(IPX)	Immunoperoxidase
(IU/ml)	International units/ml
(KDa)	Kilodalton
(KO)	Gene knockout
(L-NMMA)	N-guanidino-monomethyl L-arginine
(LC)	Langerhans cells
(LCR)	Ligase chain reaction
(LPS)	Lipopolysaccharide
(LST assay)	Lymphocyte stimulation assay
(Mab)	Monoclonal antibody
(MALT)	Mucosal-associated lymphoid tissue
(MB)	Megabyte
(MHC I)	Major histocompatibility complex class one
(MHC II -/-)	MHC II gene knockout
(MHC II)	Major histocompatibility complex class two
(MOMP)	Major outer membrane protein
(MoPn)	Mouse pneumonitis strain of *C. trachomatis*
(MRI)	Moredun Research Institute
(MSX)	Methionine sulphoxamine
(MZN)	Modified Ziehl Neelsen's stain
(NK)	Natural killer
($NO^{\bullet}$)	Nitric oxide
(NTSC)	National Television System Committee
(nu/nu)	Athymic nude mouse
(OD)	Optical density
(OEA)	Ovine Enzootic Abortion
(OMP1)	Major outer membrane protein gene
(OMP90)	A family of four chlamydial genes which describe a group of membrane proteins of approximately 90 kilodaltons in size.
(OPD)	o-phenylenediamine dihydrochloride

(PAF)	Platelet-activating factor
(PAL)	Phase Alternation Line colour system
(PBM)	Peripheral blood mononuclear cells
(PBS)	Phosphate buffered saline
(PBST)	PBS containing 0.05% Tween 20
(PBST-BSA)	PBS containing 0.05% Tween 20 and 3% bovine serum albumin
(PCR)	Polymerase chain reaction
(PhF-DMEM)	Phenol red-free Dulbecco's Modified Eagle's Medium
(PICT)	Macintosh picture image format
(PolyI:PolyC)	Polyinosinic Acid-Polycytidylic Acid
(RAM)	Random access memory
(RB)	Reticulate body
(RBovIFN-α)	Recombinant bovine interferon-alpha
(rDNA)	16S ribosomal deoxyribonucleic acid
(RGB)	Red, green and blue
(RHuIFN-α)	Recombinant human interferon-alpha
(RHuIFN-β)	Recombinant human interferon-beta
(RHuIFN-γ)	Recombinant human interferon-gamma
(ROI)	Region of interest
(ROvIFN-γ)	Recombinant ovine interferon-gamma
(RT)	Room temperature
(RT-PCR)	Reverse transcriptase-PCR
(SCID)	Severe combined immunodeficiency
(SDS)	Sodium dodecyl sulfate-polyacrylamide
(SDS-PAGE)	Sodium dodecyl sulfate-polyacrylamide gel electrophoresis
(SFV)	Semliki Forest Virus
(SI)	stimulation index
(SPF)	Specific pathogen free
(TCR)	T-cell receptor

(Th1-like)	T-helper-1-like
(TIFF)	Tag Image File Format
(TMB)	Tetramethylbenzidine
(TMOMP)	Truncated recombinant major outer membrane protein
(TNF-α)	Tumour necrosis factor-alpha
(Tris)	Tris- (Hydroxymethyl) aminomethane
(UV)	Ultraviolet radiation

Abstract

Chlamydia psittaci is the causative agent of ovine enzootic abortion (OEA), the single most common cause of diagnosed infectious ovine abortion in the United Kingdom. The immune effector mechanisms responsible for microbistatic and microbicidal control of *C. psittaci* in ovine cells were investigated with a long term view to improving the diagnosis and prophylactic control of OEA.

Characterisation of the immunological and pharmacological control of *Chlamydia spp* is dependent of the accurate measurement of chlamydial growth *in vitro*. Traditionally this has required manual enumeration of the replicating masses of *Chlamydiae* or inclusion bodies that form within infected cells, which is both time consuming and subjective. A novel technique for counting and measuring chlamydial inclusions was developed using image analysis. A software solution, Inclusion Counter, was developed using the public domain image analysis packages NIH Image and Object Image. Results generated by Inclusion Counter were not only accurate with respect to counting chlamydial inclusions but also provided additional information about chlamydial growth that were previously unavailable or impractical to measure.

Diagnosis and control of OEA is complicated by the ability of *C. psittaci* to establish a chronic low level or persistent infection in ewes infected out-with pregnancy. Persistent *C. psittaci* infection was reproduced *in vitro* by maintaining infected ovine fibroblastic ST.6 cells in the presence of recombinant ovine interferon gamma (ROvIFN-γ) at physiologically relevant concentrations for up to 63 days after infection. ROvIFN-γ restricted *C. psittaci* growth in a dose dependent manner; concentrations of 25-100 units of biological activity per millilitre (U/ml) induced and maintained persistence whereas concentrations of 250 U/ml or more eradicated *C. psittaci* from infected cultures. Attempts to identify and characterise the source of IFN-γ in immune sheep using T-cell lines raised against recombinant *C. psittaci* proteins were unsuccessful.

The mechanisms of ROvIFN-γ mediated restriction of *C. psittaci* were investigated. Pretreatment of ST.6 cells with recombinant interferon alpha or double stranded RNA at concentrations matched with ROvIFN-γ for anti-viral activity did not restrict *C. psittaci* growth in ST.6 cells, indicating that the mechanism through which ROvIFN-γ restricts *C. psittaci* in ovine cells is independent from its anti-viral activities. Nitric oxide was not detected in the supernates of infected ST.6 cells pretreated with ROvIFN-γ and addition of L-NMMA, a potent inhibitor of inducible nitric oxide synthase, did not alter the anti-*C. psittaci* effects of ROvIFN-γ in this cell line. Furthermore, nitric oxide production could not be demonstrated in primary ovine alveolar macrophages treated with combinations of ROvIFN-γ, LPS, heat

inactivated *C. psittaci* and/or live *C. psittaci*. Addition of exogenous L-tryptophan partially reversed the anti-chlamydial effects of ROvIFN-γ in ST.6 cells that had been infected with *C. psittaci* over a 7 day period and also resulted in the recovery of infectious *Chlamydiae* from persistently infected ST.6 cells maintained in 50 U/ml of ROvIFN-γ. These findings support a role for up-regulation of tryptophan catabolism in ROvIFN-γ mediated restriction of both *C. psittaci* growth and persistence in ovine cells.

Chapter 1.0
General Introduction

1.1. Introduction

Chlamydia psittaci is a major cause of infectious ovine abortion. However, what makes this pathogen interesting is its ability to survive for prolonged periods in ewes infected outwith pregnancy without causing pathology or inducing protective immunity. Thus, the interaction between the ovine immune system and *C. psittaci* appears to strike a fine balance between restriction of pathology in the non-pregnant ewe and maintenance of a chronic low level or persistent infection. When persistently infected ewes become pregnant this balance is altered allowing *C. psittaci* to invade the placenta and cause fetopathology.

Figure 1.1: *C. psittaci* inclusion bodies (arrow) in ovine ST.6 cells

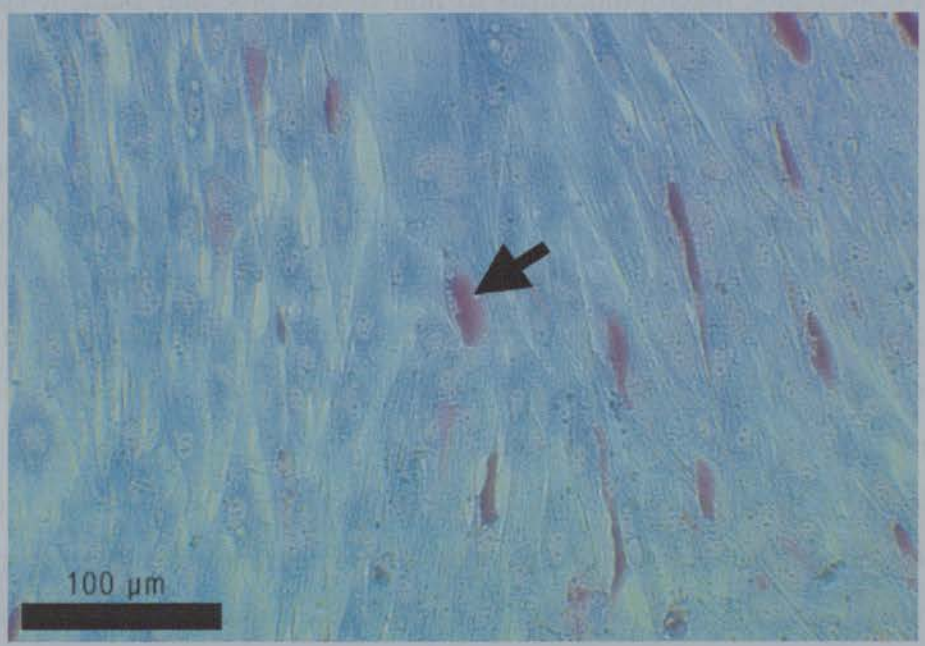

Typical appearance of the inclusion bodies of the S26/3 ovine abortion strain of *C. psittaci* after 48 hours growth in ovine ST.6 cells. Inclusion bodies are stained with Ziehl Neelsen's carbo fuchsin, cellular background is counter-stained with Methyl Blue.

1.2. Genus *Chlamydia*

1.2.1. Developmental cycle of *Chlamydia*

Members of the genus *Chlamydia* are obligate intracellular gram-negative bacteria. Chlamydiae are restricted in metabolic capacity and are thus dependent on a eukaryotic host cell for the provision of a wide variety of metabolic intermediates [Moulder, 1991]. The developmental cycle of *Chlamydia* is unique and involves two morphologically and functionally distinct stages (Figure 1.2), an infectious metabolically inactive extracellular form, the elementary body (EB), and a non-infectious but metabolically active intracellular reticulate body (RB).

EB are non motile and rely on Brownian motion to instigate contact with potential host cells [Moulder, 1991]. Numerous mechanisms of attachment and uptake of chlamydial EB have been proposed, including receptor-mediated endocytosis in clathrin-coated pits, macropinocytosis in non coated pits, and parasite-specified phagocytosis [Wyrick, 1998]. Following uptake, EB evade phagolysosomal fusion and over the following 6-10 hours reorganise into RB which multiply by binary fission within a membrane-bound vesicle that, at least in the case of *C. trachomatis*, appears to share several characteristics with the recycling endosomes of the host cell [Van Ooij *et al*, 1997]. RB start the process of differentiation back into infectious EB at approximately 16-20 hrs after invasion. RB multiplication and differentiation continues for a further 24-48 hours, by which point inclusion bodies (vesicles of replicating chlamydiae) can be resolved in the host cell by light microscopy (Figure 1.1) [McClarty, 1994]. Infectious EB may be released into the extracellular milieu by lysis of the host cell, fusion of the inclusion membrane with the cytoplasmic membrane of the host cell or possibly through the breakdown of the inclusion membrane and release of EB into the cytoplasm [Wyrick, 1998].

Figure 1.2: Developmental cycle of *Chlamydia*

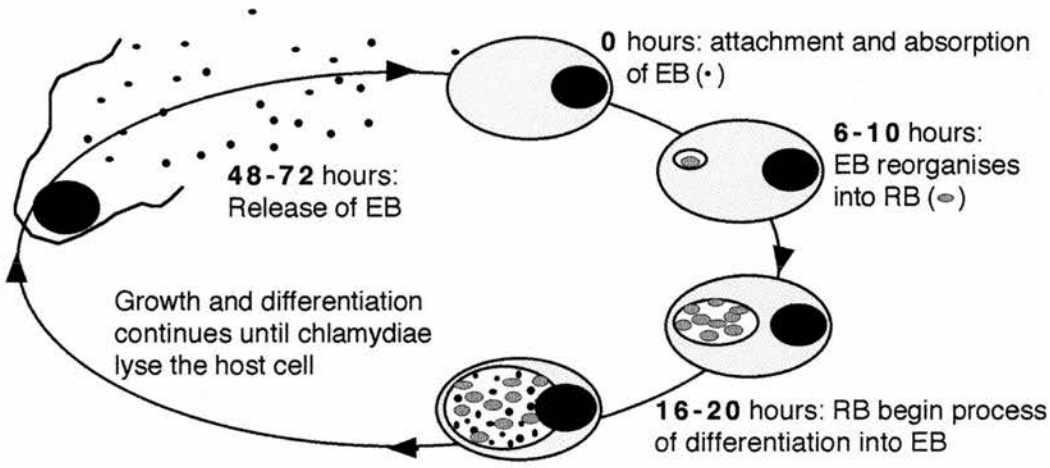

The developmental cycle of *Chlamydia* begins with the attachment and absorption of one or more chlamydial elementary bodies (EB) by a suitable host cell. EB subsequently reorganise into reticulate bodies (RB) which multiply by binary fission. RB differentiate into EB which are released into the extracellular milieu to complete the cycle.

1.3.2. Taxonomy

There are currently four recognised species within the genus *Chlamydia*: *C. trachomatis*, *C. psittaci*, *C. pneumoniae*, and *C. pecorum*. Historically, the genus was originally divided into *C. psittaci* and *C. trachomatis* on the basis of inclusion body morphology, glycogen content and sulphadiazine resistance [Page, 1968]. The TWAR strain of *C. psittaci* was reclassified as *C. pneumoniae* in 1989 by Grayston *et al* (1989), on the basis of DNA-DNA homology, EB ultrastructure and serology. The fourth species, *C. pecorum*, was proposed in 1992 by Fukushi and Hirai (1992) based on DNA-DNA homology analysis. The current taxonomic classification, host specificity, range of diseases and morphological characteristics of the genus *Chlamydia* are summarised in Table 1.1 (adapted from Fukushi and Hirai (1992), Grayston *et al* (1989), Kaltenboeck *et al* (1993), Page (1968), Pudjiatmoko *et al* (1997), Takahashi *et al*, (1997) and Vanrompay *et al* (1995)).

Table 1.1: Genus *Chlamydia*: taxonomy, host specificity, pathology and morphology

Order	***Chlamydiales***								
Family	***Chlamydiaceae***								
Genus	***Chlamydia***								
Species	***trachomatis***				***psittaci***			***pneumoniae***	***pecorum***
Biotype / Hosts	Trachoma / humans	LGV / humans	Swine	Mouse pneumonitis (MoPn)/Rodents	Avian and Abortion strains / ruminants, birds, koalas + others	guinea pig inclusion conjunctivitis (GPIC)	Feline	Humans (horses)	Ruminants, pigs and koalas
Diseases	Trachoma (Serovars A-C). Urogenital diseases, conjunctivitis and infant pneumonia (Serovars D-K).	Lymphogranuloma venereum (LGV).	Conjunctivitis, intestinal, urogenital, and respiratory diseases.	Pneumonia, proliferative ileitis.	Psittacosis, abortion, pneumonia, conjunctivitis, hepatitis, polyarthritis, enteritis, .	Inclusion conjunctivitis.	Pneumonia, conjunctivitis.	Pneumonia, conjunctivitis. Association with atherosclerosis.	Abortion, enteritis, polyarthritis, encephalomyelitis, pneumonia, urogenital infection.
Zoonotic diseases	NA	NA	None as yet have been identified.	None as yet have been identified.	Psittacosis associated with avian strains and abortion associated with ovine abortion strains.	None as yet have been identified.	None as yet have been identified.	NA	None as yet have been identified.
Elementary body morphology	Round				Round			Pear shape	Round
Inclusion morphology	Oval, vacuolar				Variable, dense			Oval, dense	Oval, dense
Glycogen in inclusion	Yes				No			No	No
Resistance to sulphadiazine	No				Yes			Yes	Yes

Of the four species of *Chlamydia* currently recognised, *C. psittaci* remains the most heterogeneous in terms of host specificity, disease (Table 1.1) and intra-species DNA-DNA homology (Table 1.2), although there are also significant differences between the human, murine and swine biotypes of *C. trachomatis* [Kaltenboeck *et al*, 1993; Pudjiatmoko *et al*, 1997]. Further reclassification of those strains of *Chlamydia* currently classified as *C. psittaci* and *C. trachomatis* is supported by phylogenetic analysis of the major outer membrane protein gene (omp1) [Kaltenboeck *et al*, 1993] and the 16S ribosomal deoxyribonucleic acid (rDNA) [Pudjiatmoko *et al*, 1997]. Pudjiatmoko *et al* (1997) identified eight genetic groups of *Chlamydia* that might form the basis for reclassification of the genus: (1) avian and ovine abortion strains of *C. psittaci*; (2) the guinea pig inclusion conjunctivitis strain of *C. psittaci* (GPIC); (3) feline strains of *C. psittaci*; (4) *C. pecorum*; (5) *C. pneumoniae*; (6) human trachoma,urogenital and LGV strains of *C. trachomatis*; (7) swine strains of *C. trachomatis*; and (8) the mouse pneumonitis strain of *C. trachomatis* (MoPn).

Table 1.2: DNA-DNA homology within the genus *Chlamydia*

	Percentage homology with:			
Species	*C. trachomatis*	*C. psittaci*	*C. pneumoniae*	*C. pecorum*
C. trachomatis	20-92 ‡	1-33	1-7	1-10
C. psittaci		14-95	1-8	1-19
C. pneumoniae			94-96	10
C. pecorum				88-100

This table was adapted from Fukushi and Hirai (1992) and is based on a DNA-DNA liquid hybridisation assay adapted for chlamydiae [Cox *et al*, 1988]. ‡ LGV and trachoma strains of *C. trachomatis* show up to 92% homology with each other, a value of 20% homology was obtained between the mouse pneumonitis strain of *C. trachomatis* and the LGV/trachoma strains.

1.3. Ovine Enzootic Abortion

Ovine Enzootic Abortion (OEA) occurs in most sheep-rearing countries [Buxton, 1994] and is a major problem in the sheep industry. OEA is the single most common cause of diagnosed infectious ovine abortion in the United Kingdom (Figure 1.3) [Veterinary Laboratories Agency, 1997]. Estimates place the economic burden of this disease at £10 million - £20 million per annum for the British sheep industry alone [Aitken *et al*, 1990].

Figure 1.3: Relative incidence of diagnosed ovine abortion in the United Kingdom during the period January 1996 - January 1997

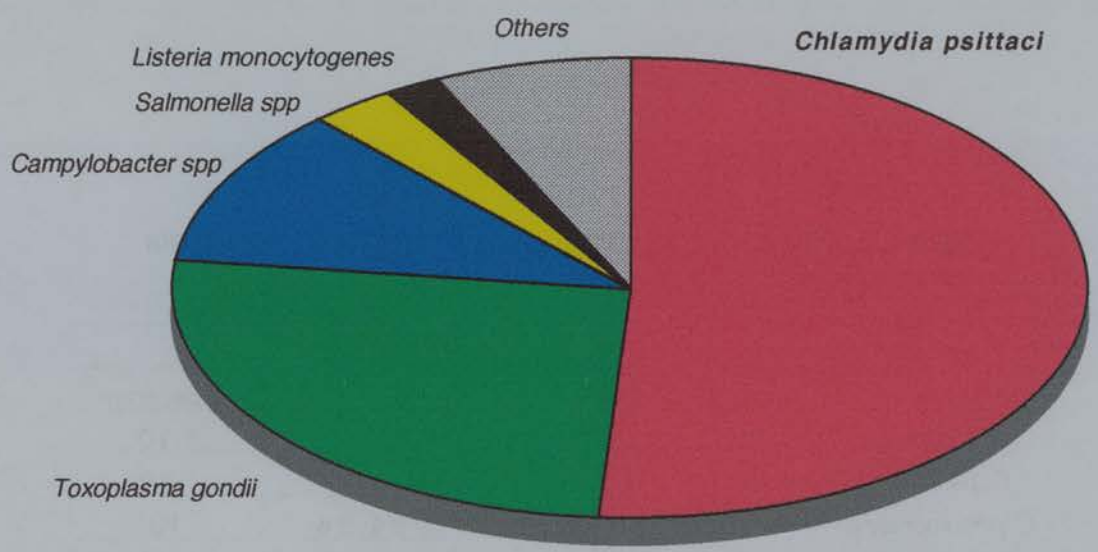

[Veterinary Laboratories Agency, 1997]

1.3.1. Transmission of OEA

OEA was first described by Greig (1936) who named it enzootic abortion of ewes and suggested, but did not present evidence, that it was due to a dietary deficiency. Stamp *et al* (1950) later demonstrated that crude suspensions of material prepared from aborted and premature lambs from suspected cases of enzootic abortion could induce abortion when inoculated into naive ewes during pregnancy. In addition, suspensions which had been passed through a 0.4 μm filter did not induce abortion, supporting the involvement of an infectious agent rather than a soluble factor. Whilst attempts to culture extracellular bacteria from infected ewes and aborted lambs were unsuccessful, micro-organisms were observed within cells in the chorionic villi of infected placentas and in large numbers in smears made from infected placentas. The intracellular location, morphology and staining characteristics of the organism led Stamp *et al* (1950) to speculate that it was related to *Rickettsia* or to the psittacosis-lymphogranuloma group of infectious agents, later classified as genus *Chlamydia*.

The discovery that OEA was caused by an infectious agent made understanding the natural mode of transmission of OEA a priority. Transmission of OEA by sheep ticks was discounted by Stamp *et al* (1950) because the epidemiology of the disease was not consistent with tick distribution. In contrast, *Ornithodoros coriaceus* ticks have been shown to transmit strains of *C. psittaci* which cause abortion in cattle [Kimsey *et al*, 1983; McKercher *et al*, 1980]. However, there is still no evidence in the literature to suggest that ticks can transmit OEA strains of *C. psittaci*. The close phylogenetic relationship of avian and OEA strains of *C. psittaci* is interesting [Kaltenboeck *et al*, 1993; Pudjiatmoko *et al*, 1997] since it suggests that birds may represent a possible reservoir for OEA. However, whilst it is possible that OEA strains of *C. psittaci* are originally derived from avian strains it seems unlikely that the most closely related avian strains, those isolated from parakeets [Takahashi *et al*, 1997], could represent a reservoir of OEA given the distribution of the disease.

The anatomical site of entry for *C. psittaci* in the ewe is likely to be a mucosal surface. Experimental oral inoculation of pregnant ewes with OEA strains of *C.*

psittaci has been shown to result in pathology similar to that seen in naturally occurring OEA [Dawson *et al*, 1986; McEwen *et al*, 1951a; Wilsmore *et al*, 1984] and tonsillar tissue has been identified as the most likely route of infection for *C. psittaci* when delivered in this manner [Jones and Anderson, 1988]. Whilst it remains unclear as to how *C. psittaci* disseminates to the reproductive tract in the ewe, macrophages have been shown to play a role in the dissemination of *C. pneumoniae* in mice [Moazed *et al*, 1998] and may play a similar role in OEA.

Early attempts to demonstrate sexual transmission of OEA did not induce fetopathology [Appleyard *et al*, 1985; Wilsmore *et al*, 1984]. However, in a more recent study, intravaginal inoculation of non-pregnant ewes with *C. psittaci* was shown to result in abortion during the next pregnancy [Papp and Shewen, 1996a], suggesting that venereal transmission is possible. In this case, infection could be established directly in the urogenital tract. However, ingestion or inhalation of contaminated material around the time of lambing remains the most likely mode of transmission for OEA strains of *C. psittaci*, especially under intensive lambing conditions [Aitken *et al*, 1990].

1.3.2. Pathology of OEA in non-pregnant sheep

There is little evidence to suggest that OEA strains of *C. psittaci* cause pathology in ewes prior to pregnancy, although experimental infection of non-pregnant ewes is associated with a brief febrile response at the time of infection [Amin and Wilsmore, 1995; Huang *et al*, 1990]. Chronic infection of the vagina, uterus, and oviducts [Papp and Shewen, 1996b], in conjunction with shedding of infectious chlamydiae during estrus [Papp *et al*, 1994], has been described in ewes after pregnancy failure due to experimental infection with an OEA strain of *C. psittaci*. These findings have led to speculation that *C. psittaci* may cause chronic pathology in the reproductive tract of post-OEA ewes, similar to that observed in women infected with *C. trachomatis* [Papp and Shewen, 1997]. However, there is little evidence that post-OEA ewes are in any way compromised in their ability to conceive or carry lambs to full-term [Rodolakis *et al*, 1998].

Despite the apparent absence of pathology in the non-pregnant ewe, the ability of *C. psittaci* to infect ewes outwith pregnancy is critical for its survival and dissemination. Latent or persistent subclinical infection of non-pregnant ewes with the agent responsible for OEA was first reported in 1951 [McEwen *et al*, 1951b]. In that study, significant numbers of ewes born in infected flocks and moved to clean pasture two months prior to conception showed clinical symptoms of OEA in their first pregnancy (7% aborted and a further 27% shed infectious material at the time of lambing). Wilsmore *et al* (1984) later confirmed that ewes infected during the perinatal period often go on to experience clinical disease during their first pregnancy after infection.

Because *C. psittaci* has been difficult to isolate from naive ewes infected outwith pregnancy, the phenotype and location of the host cell of persistent *C. psittaci* infection has not been identified *in vivo*. *C. psittaci* antigen and DNA have been detected in the draining lymph nodes of non-pregnant ewes for up to 18 days after subcutaneous challenge with live *C. psittaci* [Buxton *et al*, 1996; Huang *et al*, 1990]. However, live chlamydiae were not recovered in either of these studies and the presence of DNA and chlamydial antigens in draining lymphoid tissue shortly after infection is not clearly demonstrative of a persistent infection. Similar studies detected the presence of *C. psittaci* antigens in epithelial cells and lymphocytes in a variety of tissues following nasopharyngeal or subcutaneous inoculation of naive non-pregnant ewes with an OEA strain of *C. psittaci*, but as in the case described above, the presence of live chlamydiae was not demonstrated [Amin and Wilsmore, 1995]. Cells containing *C. psittaci* have been detected in vaginal and cervical samples from chronically infected post-OEA ewes [Papp *et al*, 1998]. However, it remains to be confirmed if the same is true for ewes persistently infected with *C. psittaci* prior to abortion.

The ability of *C. psittaci* to enter a latent or persistent state in ewes infected prior to pregnancy not only allows the pathogen to survive from one breeding season to the next, but also severely complicates the diagnosis and management of OEA. This is particularly problematic for farmers who wish to replace stock with ewes or lambs purchased at market and it is not uncommon for flocks which were previously free

from OEA to experience extremely high rates of abortion following the introduction of infected replacement animals [Aitken *et al*, 1990].

1.3.3. Pathology of OEA in pregnant sheep

The timing of the events leading to fetopathology in OEA are remarkably consistent. Regardless of when ewes are infected during pregnancy, *C. psittaci* is not found in the placenta or fetus until day 60 of gestation [Buxton *et al*, 1990]. This coincides with the normal physiological invasion of the maternal caruncular stroma by chorionic villi of the placenta and haemorrhage of maternal blood vessels. The haematomas that result from this process may represent one less barrier for *C. psittaci* to cross in order to infect the placenta. Despite the presence of *C. psittaci* in the placenta from day 60 of gestation onward, pathological changes do not occur until the later stages of pregnancy (around day 90 of gestation), resulting in fetopathology and abortion at or just before the time of normal parturition (between days 120-140 of gestation) [Buxton *et al*, 1990]. This pattern of pathology results in the delivery of infectious material into the local environment at a time when there are naive animals present that are susceptible to infection.

1.3.4. Zoonotic infection

In addition to its economic burden, OEA is also of potential zoonotic importance. Infection in non-pregnant individuals is generally asymptomatic or results in mild upper respiratory tract symptoms which may not always be diagnosed as *C. psittaci*. However, a more severe influenza-like disease was reported in a group of laboratory workers who were accidentally infected with the S26/3 strain of *C. psittaci* while producing a vaccine for OEA [Baker and Cooper, 1983]. In contrast to non-pregnant individuals, infection in pregnant women can be life threatening and commonly involves abortion with severe systemic complications including, renal dysfunction, hepatic dysfunction and disseminated intravascular coagulation [Aitken, 1991; Hadley *et al*, 1992; Hyde and Benirschke, 1997; Jorgensen, 1997].

Fortunately, zoonotic infection of pregnant women is rare [Sanghi *et al*, 1997] and there is no evidence to support human to human transmission of the OEA strain of *C. psittaci* [Hadley *et al*, 1992].

1.3.5. Diagnosis of OEA

Diagnosis of OEA is largely limited to retrospective identification of OEA as a cause of abortion, rather than identifying persistently infected ewes which are at risk of abortion. This is largely due to the absence of clinical disease, the poor immune response induced by *C. psittaci* in ewes infected prior to pregnancy and difficulties associated with detection of *C. psittaci* in the non-pregnant ewe. As a result, diagnosis can only be used to determine whether OEA is present within a given flock and to identify those ewes which are already immune to OEA but may still shed infectious chlamydiae [Papp *et al*, 1994].

There are numerous options available for the diagnosis of OEA. Traditionally, vital dyes such as modified Ziehl Nielsen's carbo fuchsin or Giemsa [Stamp *et al*, 1950] have been used to identify chlamydial EB and inclusion bodies in smears or tissue sections prepared from aborted material. However, vital dyes are nonspecific and interpretation of the results requires an experienced pathologist. Genus- or species–specific monoclonal antibodies, in conjunction with immuno-fluorescence or immunohistochemistry, significantly increase the certainty with which OEA can be diagnosed [Amin and Wilsmore, 1994]. Advances in molecular biology have led to routine use of the polymerase chain reaction (PCR) and ligase chain reaction (LCR) to diagnose *C. trachomatis* infections in humans [Taylor-Robinson, 1997] and these technologies may equally well be applied to the diagnosis of OEA [Hewinson *et al*, 1991; Rodolakis *et al*, 1998].

Serological diagnosis is complicated by the existence of non-pathogenic enteric forms of *C. pecorum* which do not cause abortion but share antigenic markers with OEA strains of *C. psittaci*. Attempts to develop more specific enzyme linked immunosorbent assays (ELISA) [Anderson *et al*, 1995; Donn *et al*, 1997; Griffiths *et*

al, 1996; Jones *et al*, 1997; Sting and Hafez, 1992] or indirect immuno-fluorescence test (IFAT) [Markey *et al*, 1993] to distinguish between antibody raised against *C. psittaci* and non-pathogenic *C. pecorum* strains have met with varying degrees of success. More recently, a competitive ELISA based on monoclonal antibodies raised against peptide sequences of the major outer membrane protein (MOMP) that are specific to abortion strains of *C. psittaci*, was shown to be extremely sensitive and specific and may provide a viable alternative to traditional laborious pathological examination of aborted material [Salti-Montesanto *et al*, 1997]. The recent discovery and characterisation of a family of 90 kilodalton (KDa) proteins from the outer membrane of *C. psittaci* should also further improve diagnosis of OEA. These proteins are recognised by the sera of post-OEA ewes and show little or no genetic homology with *C. pecorum* strains [Longbottom *et al*, 1996; Longbottom *et al*, 1998a; Longbottom *et al*, 1998b].

Despite advances in the diagnosis of OEA as the cause of abortion and the identification of post-OEA ewes on the basis of serology, an effective approach to the diagnosis of persistent infection in ewes remains elusive.

1.3.6. Vaccination strategies

Attempts to develop a vaccine for OEA were undertaken shortly after the discovery that the disease was transmitted by an infectious agent [Stamp *et al*, 1950]. Initial experiments demonstrated that formalin-inactivated vaccines, prepared from aborted placental material or from *C. psittaci* grown in chicken egg yolk sacs, protected ewes from subcutaneous challenge with live *C. psittaci* during pregnancy and significantly reduced the overall rate of abortion in field studies [McEwen *et al*, 1951b]. These findings led to the development of a commercially available vaccine composed of liquid paraffin and Falba-adjuvanted formalin-inactivated *C. psittaci* (Strain A.22) [McEwen *et al*, 1955]. However, the inactivated vaccine did not prevent shedding of chlamydiae at parturition [Rodolakis and Souriau, 1979] and further field studies during the late 1970's indicated that the vaccine was either not as effective as was initially thought or that widespread use of the vaccine had

resulted in the selection of resistant strains of *C. psittaci* [Linklater and Dyson, 1979]. A second OEA strain of *C. psittaci* (S26/3) was added in 1981 [Aitken *et al*, 1981] but did not improve the efficacy of the vaccine, which was eventually withdrawn in 1992. An experimental vaccine based on semi-purified formalin-inactivated EB, derived from S26/3 and A.22 strains of *C. psittaci* grown to high titres in tissue culture, has been shown to provide some degree of protection against heterogeneous OEA strains of *C. psittaci* when delivered in conjunction with a variety of adjuvants [Jones *et al*, 1995].

Live attenuated vaccines have a number of advantages over inactivated vaccines. Live vaccines require a smaller initial dose to induce protection than inactivated vaccines, thereby reducing production costs. In addition, it has become increasingly apparent that the local tissue microenvironment and context in which antigen is presented to T-cells can greatly influence the type of immune response elicited [Del Prete, 1998]. Antigens derived from an inactivated vaccine, which is essentially extracellular, are unlikely to be processed and presented in the same way that they would in a natural chlamydial infection. This is supported by the finding that heat inactivated chlamydiae induce different levels of pro-inflammatory cytokines compared with live chlamydiae in human monocytic cells [Bianchi *et al*, 1997], ovine alveolar macrophages [Entrican *et al*, 1999] and human umbilical vein endothelial cells [Molestina *et al*, 1998]. Furthermore, live vaccines may disseminate and induce immune responses at more appropriate anatomical sites than inactivated vaccines which typically result in a localised inflammatory response at the site of inoculation [Buxton, 1994].

Rodolakis (1983) developed a live attenuated vaccine against OEA by using N-methyl-N'nitro-N-nitrosoguanidine enhanced mutagenesis to generate temperature sensitive mutants from a virulent OEA strain of *C. psittaci* (AB7). One of the resultant mutants, designated 1B, has been shown to induce protective immunity in mice [Rodolakis, 1983] , ewes [Souriau *et al*, 1988; Rodolakis and Souriau, 1983] and goats [Rodolakis and Souriau, 1986] without causing disease in pregnant animals. The 1B vaccine strain has also been shown to protect ewes against challenge with heterogeneous OEA strains of *C. psittaci* and to prevent shedding of

infectious chlamydiae at parturition [Chalmers *et al*, 1997; Rodolakis and Bernard, 1984]. Following confirmation of the genetic stability of the 1B vaccine strain [Rodolakis and Souriau, 1989] and compliance with other safety criteria, it is now fully licensed and commercially available within the UK, France and Spain (Enzovax, Intervet, Chlamydia Vetoquinol) [Rodolakis *et al*, 1998].

A major drawback to vaccines based on inactivated or live attenuated *C. psittaci* is that their use largely precludes serological diagnosis of OEA and severely complicates epidemiological surveillance of the disease. As a result of this, and the absence of long-term field data on the efficacy of the 1B vaccine strain of *C. psittaci*, there is still a great deal of interest in the development of a recombinant protein or peptide vaccine for OEA.

Initial attempts to generate a vaccine based on the *C. psittaci* MOMP were stimulated by the observation that an experimental vaccine prepared from the outer membrane of *C. psittaci*, consisting predominantly (90%) of MOMP, protected ewes against challenge with the S26/3 OEA strain of *C. psittaci* during pregnancy [Tan *et al*, 1990]. Two monoclonal antibodies, which react with purified MOMP in its native trimeric form [De Sa *et al*, 1995; Herring *et al*, 1994; McCafferty *et al*, 1995], have been shown to reduce fetal and placental infection in mice [Buzoni-Gatel *et al*, 1990]. However, vaccine trials with recombinant MOMP have been unsatisfactory and the lack of protective immunity induced by recombinant MOMP has been suggested to be due, at least in part, to its failure to adopt the natural trimeric conformation of native MOMP [Herring *et al*, 1994, 1998].

Cevenini *et al* (1991) identified an 89 KDa protein in outer membrane complexes derived from the A.22 OEA strain of *C. psittaci* which was recognised by sera from post-OEA ewes. A family of four genes has since been identified, cloned and characterised as encoding a group of proteins of approximately 90 KDa present in the outer membrane of the S26/3 OEA strain of *C. psittaci* [Longbottom *et al*, 1996; Longbottom, 1998a; Longbottom, 1998b]. This group of outer membrane proteins (OMP90) appear, on the basis of immunoblotting of chlamydial outer membrane complexes with sera from post-OEA ewes, to be immunogenic and in addition to

their potential value in diagnosis, described previously, may also be suitable vaccine candidates.

1.4. Murine models of in vivo chlamydial infection

Although OEA can be studied directly *in vivo* in the ewe, *in vivo* studies in inbred strains of mice offer a number of advantages over sheep. Experiments using mice are generally cheaper, more rapid, permit adoptive transfer of cells between MHC-matched animals and the use of congenitally immune deficient, transgenic and gene knockout (KO) mouse strains allow detailed dissection of the immune response.

A mouse model of OEA does exist and is likely to be very useful in extending the understanding of the immune response to *C. psittaci* in the ewe [Rodolakis *et al*, 1981]. However, at the time of writing, there have been few attempts to use this model to dissect the immune response to OEA strains of *C. psittaci*. Consequently, much of what is know about the *in vivo* immune response the *C. psittaci* in the ewe must be extrapolated from experiments using strains of chlamydiae which induce distinct pathology in the mouse from that seen in sheep infected with OEA strains of *C. psittaci*. Whilst, these studies should not be taken out of context, they do provide a useful insights into the interaction of the immune system with chlamydiae.

1.5. The innate immune response to *C. psittaci*

1.5.1. Recruitment and activation of immune cells

C. psittaci infection in the ewe appears to be established at a mucosal surface, either in the epithelium of the vaginal [Papp and Shewen, 1996a] or nasopharyngeal / gastrointestinal tract, possibly via lymphocytes and epithelial cells within mucosal-associated lymphoid tissue (MALT) [Jones and Anderson, 1988]. Initial interaction between *C. psittaci* and the immune system is therefore likely to involve the recruitment and activation of immune cells from the underlying mucosa and local vasculature by pro-inflammatory cytokines released from infected epithelial cells and lymphocytes. The range of chemokines and pro-inflammatory cytokines produced *in vitro* by cells infected with chlamydiae is consistent with the recruitment and activation of a variety of immune cells involved in inflammatory responses (Table 1.3) [Bianchi *et al*, 1997; Entrican *et al*, 1999; Entrican, unpublished results; Heinemann *et al*, 1996; Ingalls *et al*, 1995; Kaukoranta-Tolvanen *et al*, 1996; Manor *et al*, 1993; Molestina *et al*, 1998; Paguirigan *et al*, 1994; Rasmussen *et al*, 1997; Van Westreenen *et al*, 1998]. There is also evidence of both systemic production of granulocyte-macrophage colony-stimulating factor (GM-CSF) [Magee *et al*, 1991] and local production of Interleukin-1α/β (IL-1α/β) and Interleukin-6 (IL-6) by mice infected with MoPn [Magee *et al*, 1992].

The components of chlamydiae that mediate pro-inflammatory cytokine release appear to be heat-labile and/or dependent on chlamydial replication in the host cell [Bianchi *et al*, 1997; Entrican *et al*, 1999; Molestina *et al*, 1998; Ojcius *et al*, 1998a]. Ingalls *et al* (1995) were able to induce tumour necrosis factor-alpha (TNF-α) production in *ex vivo* preparations of unfractionated human blood cells with both live *C. trachomatis* EB and purified *C. trachomatis* LPS, albeit at much lower levels than live *Salmonella minnesota* R595, *S. minnesota* R595 LPS or *Neisseria gonorrhoea* LPS. Addition of LPS antagonists to cultures inhibited TNF–α release for unfractionated human blood cells incubated with *C. trachomatis* EB.

Table 1.3: Chemokine and pro-inflammatory cytokine production by cells infected with chlamydiae

Reference	Chlamydia species	Cell type	Chemokines/Cytokines
(Bianchi *et al*, 1997)	*trachomatis*	human monocytic cell line	IL-8
(Entrican *et al*, 1999)	*psittaci*	ovine alveolar macrophages	IL-1β, GM-CSF and IL-8
(Entrican, unpublished results)	*psittaci*	ovine fibroblastic cell line	IL-8
(Heinemann *et al*, 1996)	*pneumoniae*	human monocytic cell line	IL-1β, IL-6 and TNF-α
(Kaukoranta-Tolvanen *et al*, 1996)	*pneumoniae*	human peripheral blood mononuclear cells	TNF-α, IL-1β, IL-6 and IFN-α
(Ingalls *et al*, 1995)	*trachomatis* / LPS	human whole blood *(& CD14 transfected CHO cells)*	TNF-α *(NK-κB translocation)*
(Manor *et al*, 1993)	*trachomatis*	human macrophages	TNFα
(Molestina *et al*, 1998)	*pneumoniae*	human umbilical vein endothelial cells	IL-8, MCP-1 and sICAM-1
(Paguirigan *et al*, 1994)	*psittaci*	human macrophages	IL-1 and type-1 IFNs
(Rasmussen *et al*, 1997)	*trachomatis and psittaci*	cervical and colonic epithelial cells	IL-8, GRO-α, GM-CSF and IL-6
(Van Westreenen *et al*, 1998)	*trachomatis*	human mesothelial cells	IL-1β and IL-8

Abbreviations: Chinese hamster ovary cells (CHO cells); Granulocyte-macrophage colony-stimulating factor (GM-CSF); growth-related oncogene alpha (GRO-α); type-1 interferons (type-1 IFNs); interferon-alpha (IFN-α); Interleukin-1 alpha/beta (IL-1α/β); Interleukin-6 (IL-6); Interleukin-8 (IL-8); Monocyte chemoattractant protein 1 (MCP-1); Nuclear factor kappa B (NK-κB); soluble intercellular adhesion molecule-1 (sICAM-1); and tumour necrosis factor-alpha (TNF–α).

The lack of reagents currently available has limited the range of pro-inflammatory cytokines that can be quantified in the supernatants of ovine cells infected with OEA strains of *C. psittaci* to IL-1, interleukin-8 (IL-8) and GM-CSF [Entrican *et al*, 1999]. However, given the central role played by IL-1 in the inflammatory response [Dinarello, 1998], it seems plausible that OEA strains of *C. psittaci* could induce the full spectrum of pro-inflammatory mediators that are released by human and murine cells infected with other strains of chlamydiae (Table 1.3). In addition, IL-8 has been shown to up–regulate the production of other pro-inflammatory cytokines, including IL-1β, IL-6 and TNF–α in human mononuclear cells [Yu *et al*, 1994]. Precisely how *C. psittaci* manages to survive the ovine inflammatory response and establish a persistent infection in the non-pregnant ewe or disseminate to the placenta and cause fetopathology in the pregnant ewe remains unclear.

1.5.2. Interaction between *C. psittaci* and neutrophils

Recruitment and activation of neutrophils occurs rapidly following the induction of inflammatory responses [Smith, 1994]. The presence of neutrophils has long been recognised as a cytological indicator of the presence of chlamydiae [Yoneda *et al*, 1975] and their role in controlling chlamydial infections has been highlighted by *in vivo* depletion studies [Barteneva *et al*, 1996]. Mice rendered neutrophil deficient by monoclonal antibodies have been shown to suffer exacerbated and prolonged infection compared to control mice following intravaginal infection with MoPn. Furthermore, circumstantial evidence suggests that defects in neutrophil function may play a role in host susceptibility to *C. trachomatis* in humans [Monno *et al*, 1991].

Neutrophil adherence to vascular endothelium and transendothelial migration to the site of inflammation is mediated primarily through the action of IL-8 [Zhang *et al*, 1995] and related neutrophil chemoattractants, including the growth-related oncogene (GRO) family of chemokines [Wu *et al*, 1994]. There is considerable interplay between the pro-inflammatory cytokines, and the release of IL-8 and related chemoattractants may be regulated by macrophage derived IL-1 and TNF-α

[Wu *et al*, 1995; Zhang *et al*, 1995]. However, an ovine fibroblastic cell line (ST.6) has been shown to produce IL-8 in the absence of exogenous stimuli following infection with the S26/3 strain of *C. psittaci* [Entrican, unpublished results], suggesting that infection of epithelial cells alone may be sufficient to recruit neutrophils to the site of *C. psittaci* infection in sheep. Neutrophils may also be recruited to the site of chlamydial infections by chemotactic products of the alternative complement pathway [Megran *et al*, 1985].

Neutrophils appear to be able to kill chlamydiae in the absence of exogenous stimuli. Elementary bodies of trachoma and LGV strains of *C. trachomatis* do not appear to be able to evade phagosome-granule fusion in human neutrophils and have been shown to be rapidly degraded following uptake by these cells in the absence of exogenous cytokines or opsonins [Register *et al*, 1986; Yong *et al*, 1982, 1986; Zvillich and Sarov, 1985]. However, Register *et al* (1986) showed that human neutrophils are less efficient at killing *C. psittaci* EB than *C. trachomatis* EB. Similarly, *C. psittaci* EB are more resistant to damage by the contents of human neutrophil granules than *C. trachomatis* EB [Register *et al*, 1987].

In addition to their direct anti-microbial effects, neutrophils can cause host tissue damage and are associated with immunopathology in a number of disease processes [Smith, 1994]. Persistent neutrophil activation is associated with the chronic and/or acute inflammation and pathology typical of chlamydial infections [Cvenkel and Globocnik, 1997; Darville *et al*, 1995; Pizzichini *et al*, 1997; Rasmussen *et al*, 1997; Yang *et al*, 1994]. Although persistent infection in the non-pregnant ewe is not associated with immunopathology or inflammation, accumulation of neutrophils at the maternal-fetal interface has recently been described in the murine model of OEA [Buendia *et al*, 1998].

Traditionally, neutrophils were thought to be largely incapable of protein synthesis and their role in the immune response was considered to be restricted to phagocytosis and the release of proteolytic and cytotoxic compounds. However, studies in the late 1980s and early 1990s demonstrated that neutrophils can express a variety of cytokines and surface receptors including: IFN-alpha (IFN-α); IL-1; IL-6;

IL-8; interleukin-10 (IL-10); interleukin-12 (IL-12); TNF-α; platelet-activating factor (PAF); major histocompatibility complex class I molecules (MHC I); complement receptor 1 (CR1); and complement receptor 3 (CR3) [Cicco *et al*, 1990; Dubravec *et al*, 1990; Jack and Fearon, 1988; Lord *et al*, 1991; Moore *et al*, 1992; Neuman *et al*, 1990; Romani *et al*, 1997]. Activation of neutrophils at the site of infection is therefore likely to create a positive feedback loop leading to further recruitment and activation of immune cells.

1.5.3. Interaction between *C. psittaci* and mononuclear cells

The interaction between chlamydiae and mononuclear cells is complex. Large numbers of *Chlamydial* EB have been shown to induce an immediate cytotoxic response in murine [Wyrick and Brownridge, 1978; Wyrick *et al*, 1978] and ovine macrophages [Entrican *et al*, 1999]. This ability appears to be mediated by a structural component of the EB outer membrane [Wyrick and Davis, 1984]. Heat inactivation, but not UV inactivation, of EB prevents cytotoxicity [Su and Caldwell, 1995], suggesting that the mediator is heat-labile. At lower EB to macrophage ratios, *C. psittaci* and *C. trachomatis* appear to be able to infect and multiply within macrophages of human [Manor and Sarov, 1986], murine [Wyrick and Brownridge, 1978; Wyrick *et al*, 1978; Zhong and De La Maza, 1988] and ovine [Entrican *et al*, 1999] origin. In contrast, *C. pneumoniae* growth appears to be restricted in human macrophages *in vitro* [Gaydos *et al*, 1996].

Peripheral blood monocytes are more resistant to chlamydial infection than mature macrophages. However, during tissue culture, peripheral blood monocytes become increasingly macrophage-like in phenotype and more susceptible to infection with chlamydiae [Yong *et al*, 1987]. Differences in the literature with regard to the resistance of monocytes to identical strains of chlamydiae probably arise as a result of variations in the time for which peripheral blood monocytes were cultured prior to infection. It is therefore necessary to interpret the literature concerning *in vitro* infection of peripheral blood mononuclear cells with some caution.

Where direct comparisons have been made between macrophages and peripheral blood derived monocytes, it appears that the ability of different strains of *C. psittaci* and *C. trachomatis* to grow in monocytes correlates with their ability to cause systemic infections *in vivo*. Human monocytes have been shown to inhibit the growth of *C. trachomatis* serovar K but are less effective at restricting LGV strains of *C. trachomatis* [Yong *et al*, 1987], which causes more invasive pathology *in vivo* [Pitche *et al*, 1998]. However, it has since been reported that *C. trachomatis* serovar K can persist in human monocytes in a viable but non productive form [Koehler *et al*, 1996, 1997]. Similarly, human monocytes are more susceptible to infection with the 6BC avian strain of *C. psittaci* (which causes systemic disease [Pudjiatmoko *et al*, 1997; Vanrompay *et al*, 1995]) than they are to LGV strains of *C. trachomatis* [Manor and Sarov, 1986]. Less is known about the interaction between monocytes and *C. pneumoniae*. However, a recent clinical study found that *C. pneumoniae* DNA was common in peripheral blood mononuclear cells of patients with coronary heart disease and in middle-aged blood donors, suggesting that *C. pneumoniae* may infect human monocytes *in vivo* [Boman *et al*, 1998].

In contrast to the ability of un-stimulated macrophages to support chlamydial growth, activated macrophages are capable of restricting the growth and development of chlamydiae. Peritoneal macrophages recovered from mice in remission following a potentially lethal intraperitoneal challenge with the 6BC strain of *C. psittaci* were shown to inhibit chlamydial growth when challenged *in vitro* [Huebner and Byrne, 1988]. The principal factor responsible for macrophage activation has since been extensively characterised as T-cell or Natural killer (NK) cell derived interferon-gamma (IFN-γ) [Chen *et al*, 1996; Rothermel *et al*, 1983; Yong *et al*, 1987; Zhong and De La Maza, 1988].

The interaction between chlamydiae and monocytes/macrophages is likely to act as a double-edged sword, simultaneously exacerbating pathology whilst contributing to the protective immune response. Infected mononuclear phagocytes may play a role in the dissemination of chlamydiae from the initial site of infection [Moazed *et al*, 1998]. They may also contribute to chronic inflammation and tissue damage through the release of pro-inflammatory cytokines [Delannoy *et al*, 1993], which are at the

same time critical for the recruitment and activation of immune effector cells and lymphocytes.

Ovine macrophages infected with the S26/3 OEA strain of *C. psittaci* produce IL-8 *in vitro* [Entrican *et al*, 1999] and are likely to play a role in the recruitment and activation of neutrophils to kill chlamydiae *in vivo* [Zhang *et al*, 1995]. Similarly, production of IL-1 by infected ovine [Entrican *et al*, 1999] and human [Ingalls *et al*, 1995; Kaukoranta-Tolvanen *et al*, 1996; Paguirigan *et al*, 1994] macrophages suggests that chlamydial infection of macrophages may be important in the activation of lymphocytes and NK cells *in vivo*. In addition, IL-1 has multi functional effects on a wide variety of cell types and can induce the production of other pro-inflammatory cytokines by macrophages, including TNF-α [Dinarello, 1998] which can act synergistically with IL-12 to activate NK cells [Bancroft, 1993]. IL–12 is produced by human and murine mononuclear cells in response to challenge with a variety of pathogens [Bancroft, 1993] and up-regulation of IL-12 expression has been demonstrated by reverse transcriptase-PCR (RT-PCR) in conjunctival samples from patients with ocular inflammation, but not scarring, associated with trachoma caused by *C. trachomatis* [Bobo *et al*, 1996]. In addition to their pro-inflammatory role, some cytokines released by macrophages infected with chlamydiae have been reported to have direct anti-chlamydial effects.

Macrophages have the potential to process and present chlamydial antigens to CD4 +ve T-cells in the context of MHC II. Murine bone marrow derived macrophages (BMDM) have been demonstrated to process and present antigens from heat inactivated chlamydiae to CD4 +ve T-cell, but are not as effective as mixed spleen cells [Su and Caldwell, 1995]. MHC II expression is induced in the chlamydial inclusion vacuole in a human monocytic cell line, THP1, following activation with IFN-γ [Ojcius *et al*, 1997]. However, mononuclear phagocytes are not thought to be the major APC involved in antigen presentation to CD4 +ve T-cells during the primary immune response [Knight and Stagg, 1993] and the presence of dendritic cells (DC) is required for presentation of chlamydial antigen to naive human T-cells [Stagg *et al*, 1993a].

1.5.4. Interaction between *C. psittaci* and dendritic cells

Dendritic cells are professional APCs and are thought to play a central role in antigen presentation during primary immune responses. After acquiring antigen, DC migrate to local lymphoid tissue via the afferent lymphatic system. Interdigitating cells, located in the paracortex of lymph nodes, are thought to include DC which have migrated into the lymph node following antigen acquisition in the periphery [Knight and Stagg, 1993]. This may explain the appearance of chlamydial antigen in "macrophage-like" cells associated with the cortex and medullary chords of draining lymph nodes from ewes following primary subcutaneous challenge with *C. psittaci* [Buxton *et al*, 1996].

Internalisation of chlamydiae by DC was originally observed using avidin conjugated with fluorescein isothiocyanate (FITC) to probe permeabilised peripheral blood derived DC previously incubated with biotinylated *C. trachomatis* EB. Fluorescence activated cell sorter (FACS) analysis revealed significant amounts of internalised biotinylated EB [Stagg *et al*, 1993b], refuting the previously held concept that DC were incapable of internalising complex antigens. More recently, DC have been shown to internalise live *C. trachomatis* and *C. psittaci* through nonspecific macropinocytosis. Macropinosomes containing EB fuse with DC lysosomes expressing MHC class II and the chlamydiae are subsequently killed and degraded, allowing efficient antigen presentation to CD4 +ve T-cells [Ojcius *et al*, 1998b]. Differences in the duration and severity of *C. trachomatis* (serovar-F) genital infections observed between BALB/c and C3H mouse strains, appear to correlate with the ability of these mice to recruit a population of large, CD45 +ve, MHC II +ve mononuclear cells into uterine tissue shortly after intravaginal challenge. FACS analysis also revealed increased expression of CD40 and CD86, costimulatory surface ligands involved in T-cell activation, indicative of an APC phenotype. Furthermore, increased expression of CD11a, CD11b and CD11c was evident and CD11c is preferentially, but not exclusively, expressed by DC. However, further characterisation of these cells was confounded by their weak expression of both F4/80, a mature macrophage surface marker, and DEC205, a DC antigen [Stagg *et al*, 1998].

DC may also contribute to the development of immunity through the production of cytokines. Fixed *Staphylococcus aureus* and *Escherichia coli* LPS have been shown to induce high levels of IL-12 p40 mRNA transcripts and secretion of active IL-12 in murine and human DC [Heufler *et al*, 1996]. Human DC, generated *in vitro* by culturing plastic-adherent PBMC in presence of IL-4 and GM-CSF, produce high levels of TNF-α, IL-6, IL-8, IL-12, in response to *E coli* LPS [Verhasselt *et al*, 1997]. More recent studies, using single cell resolution intracellular cytokine staining in epidermal Langerhans cells (LC) and *ex vivo*-derived CD14-, CD1a+, CD83+, CD40+ DC, also support a role for DC in the production of pro-inflammatory cytokines following stimulation with LPS [Lore *et al*, 1998]. These finding suggest that DC might also contribute, although perhaps to a lesser extent than macrophages, to the production of pro-inflammatory cytokines and chemokines following stimulation by chlamydial LPS.

In addition to producing cytokines and chemokines in responses to LPS, DC have also been shown to produce IL-12 in response to antigen-specific interaction with T-cells in the absence of exogenous stimuli [Heufler *et al*, 1996; Macatonia *et al*, 1995]. This characteristic of DC, which appears to be mediated through CD40-CD40L ligation [Cella *et al*, 1996], has also been shown to profoundly influence the cytokine profile of T-cells. Thus, DC appear to be able to drive naive CD4+ T-cells towards a T-helper-1-like (Th1-like) cytokine profile [Macatonia *et al*, 1995]. Furthermore, DC have been shown to induce Th1-like cytokine production by resting T-cells in allogeneic mixed lymphocyte reactions without the need for any exogenous cytokines or stimuli such as microorganisms [Heufler *et al*, 1996]. It would therefore appear that DC and DC-derived IL-12 play an important role in skewing the immune system towards a Th1-like response. These findings, when considered together with what is known about the ability of DC to kill chlamydiae and present their antigens to CD4 +ve T-cells [Ojcius *et al*, 1998b], suggest a significant role for DC in the induction of the primary immune response to chlamydiae.

1.5.5. Interaction between *C. psittaci* and NK cells

There is considerable evidence to support a critical role for NK cells during the primary immune response to a variety of intracellular bacteria [Bancroft, 1993]. Their principal role in this context appears to be the production of IFN-γ at a time when the host does not have a significant number of pathogen-specific T-cells [Kaufmann, 1993]. Increased NK activity has been observed in the spleen and lung of both naive athymic nude (nu/nu) mice and heterozygous (nu/+) mice during the initial stages of pulmonary infection with MoPn. However, anti-asialo GM-1 antibody-mediated depletion of NK cells or stimulation of NK activity by immunomodulators did not affect the outcome of MoPn infection in nu/nu mice [Williams *et al*, 1987a]. In a later study, *in vivo* depletion of IFN-γ was associated with increased pathology in naive nu/nu mice infected with MoPn and depletion of NK cells using anti-asialo GM1 antibody significantly reduced IFN-γ production in the lung suggesting a putative role for NK-derived IFN-γ in this model [Williams *et al*, 1993]. More recently, IFN-γ and NK cells have been shown to appear concomitantly in the genital tract of female BALB/c mice shortly after intravaginal infection with MoPn. Furthermore, mice treated with anti-asialo GM1 antibodies suffer prolonged MoPn infections compared to mice treated with control antibody, lending further support for a role for NK cells in the primary immune response to chlamydiae [Tseng and Rank, 1998].

1.6. Acquired immunity to *C. psittaci*

It has long been recognised that ewes which abort or suffer fetopathology as a result of placental infection with *C. psittaci* rarely experience repeated episodes of clinical OEA [Stamp *et al*, 1950]. This suggests that events associated with infection of the placenta or generalised chlamydaemia during pregnancy can induce immunological memory. However, ewes do not develop sterile immunity *C. psittaci* and shed chlamydiae during estrus for several years after developing protective immunity to clinical OEA [Papp *et al*, 1994]. The immune response to OEA during secondary challenge is therefore likely to be focused on prevention of fetopathology rather than eradication of chlamydiae.

1.6.1. Immunity to *C. psittaci* in naive sheep infected outwith pregnancy

The question as to how *C. psittaci* persists in apparently immunocompetent sheep without causing disease or inducing protective immunity to OEA remains largely unresolved. Since *C. psittaci* does not appear to cause significant pathology in naive ewes infected outwith pregnancy, it must be assumed that the immune response is able to restrict the pathogen in a manner that does not confer protection to fetopathology or abortion. Experimental infection of non-pregnant ewes is associated with transient low level seroconversion as determined by complement fixation test (CFT) [Dawson *et al*, 1986; Wilsmore *et al*, 1984] and more recently by ELISA [Amin and Wilsmore, 1995]. However, serum antibody titres are not indicative of protective immunity, since animals which seroconvert following primary infection often abort during their next pregnancy [Dawson *et al*, 1986]. In contrast, the ability of individual ewes to mount a strong cell mediated immune (CMI) response, measured using a delayed type hypersensitivity (DTH) skin test to semi-purified *C. psittaci* whole EB antigen, has been reported to correlate with reduced fetopathology during the first pregnancy after infection [Dawson *et al*, 1986]. Although this is perhaps not unexpected for an intracellular pathogen, it does not explain why the ewe fails to eradicate *C. psittaci* at the time of primary infection or how persistent *C. psittaci* can be reactivated during pregnancy.

1.6.2. The secondary ovine immune response to *C. psittaci*

The development of acquired immunity to OEA that follows abortion or fetopathology has been shown to be associated with a prolonged increase in both humoral and CMI responses. On the basis that CMI responses correlate better with reduced susceptibility to abortion than seroconversion does, it has been suggested that the high antibody titres observed in ewes that develop clinical disease are a result of increased chlamydaemia during pregnancy. High antibody titres may be a result of failure to mount an effective anti-chlamydial CMI response rather than an absolute indicator of the development of acquired immunity [Dawson *et al*, 1986]. However, the possibility that antibody contributes to the immune response during secondary challenge with *C. psittaci* in subsequent pregnancies can not be excluded.

1.6.3 Humoral immunity to chlamydiae

The current consensus of opinion on protective immunity to chlamydiae favours a Th1-like immune response but does not preclude a role for antibody [Rasmussen, 1998]. Passive transfer of immune sera has been shown to prolong survival in both athymic nu/nu mice (BALB/c background) and their normal heterozygous nu/- siblings following lethal challenge with MoPn. Delivery of immunoglobulin A (IgA) or immunoglobulin G (IgG) monoclonal antibodies into the serum and vaginal secretions of naive mice has been reported to reduce upper genital tract pathology in mice infected with MoPn [Cotter *et al*, 1995]. More recently, the ability of neutralising anti-MOMP IgA monoclonal antibodies to protect mice infected with MoPn against infertility has been confirmed in passive transfer experiments [Pal *et al*, 1997]. Similarly, and of more relevance to OEA, passive transfer of two different monoclonal antibodies (which recognise the MOMP of B577 OEA strain of *C. psittaci* [De Sa *et al*, 1995; McCafferty *et al*, 1995]) completely ablates fetopathology in female Swiss mice challenged during pregnancy with the AB7 OEA strain of *C. psittaci* [Buzoni-Gatel *et al*, 1990].

In addition to the ability of antibody to neutralise chlamydiae, certain IgG isotypes

have been shown to enhance the *in vitro* infectivity of *C. trachomatis* in cells bearing the low affinity receptor for antibody, Fc gamma RIII (CD16) [Su *et al*, 1991]. Furthermore, passive immunisation of mice with IgG2b monoclonal antibodies raised against EB surface antigens has been demonstrated to enhance the infectivity of a serovar E strain of *C. trachomatis* in mice, suggesting that chlamydiae may be able to take advantage of antibody to infect cells bearing CD16 [Peterson *et al*, 1997].

Despite the ability of passively transferred antibody to confer protection against challenge with chlamydiae, experiments with B-cell deficient mice have suggested that antibody is not a prerequisite for protection. Rendering BALB/c mice B-cell deficient, by treatment from birth with goat or rabbit anti-mouse μ chain polyclonal antibodies, was shown to have no effect on their susceptibility to primary intranasal or intravaginal infection with MoPn [Ramsey *et al*, 1988; Williams *et al*, 1987b]. Furthermore, BALB/c mice rendered B-cell deficient in this way were also shown to be as resistant to secondary intravaginal challenge as normal BALB/c controls [Ramsey *et al*, 1988].

Recent studies using immunoglobulin μ heavy chain KO mice (Igμ -/-), which do not develop functionally mature B-cells [Kitamura *et al*, 1991], have added further weight to the argument that antibody and B-cells are not a critical component of the immune response to chlamydiae [Johansson *et al*, 1997a; Su *et al*, 1997; Williams *et al*, 1997]. Female Igμ -/- C57BL/6 mice do not differ significantly from female C57BL/6 controls in their ability to resolve primary genital tract infections with human serovar D or MoPn strains of *C. trachomatis* [Johansson *et al*, 1997a; Su *et al*, 1997]. Furthermore, Igμ -/- C57BL/6 mice and control C57BL/6 mice mounted equally effective memory responses during secondary challenge with the serovar D strain of *C. trachomatis* [Johansson *et al*, 1997a].

Whilst the induction of immunological memory and the ability to mount a more effective immune response during secondary challenge does not appear to be compromised in Igμ -/- mice, they have been shown to be marginally more susceptible to reinfection of the genital tract [Su *et al*, 1997] and lung [Williams *et al*, 1997] with MoPn when compared to normal control mice. However, Williams *et al*

(1997) reported anomalies in Th1-like cytokine production by Igμ -/- mice during secondary infection with MoPn which may have contributed to the differences in susceptibility of these mice to reinfection. IFN-γ production was slightly suppressed and TNF-α production was greatly enhanced in Igμ -/- mice during secondary infection compared to control mice. The anti-chlamydial effects of TNF-α may compensate for the absence of antibody, masking its role in the secondary immune response. Alternatively a reduction in IFN-γ production by Igμ -/- mice may contribute to the slight increase in their susceptibility to *C. trachomatis*. The later of these two possibilities seems less plausible given that in the same study IFN-γ deficient mice (IFN-γ -/-) actually appeared to be less susceptible to reinfection than control mice and like Igμ -/- mice, produced almost twice as much TNF-α compared to the controls [Williams *et al*, 1997].

Regardless of whether relative changes in IFN-γ and TNF-α expression in B-cell deficient mice compensate for the absence of a functional humoral response, there does not appear to be an absolute requirement for B-cells or antibody in the resolution of primary *C. trachomatis* infection or acquired immunity to *C. trachomatis* in the mouse. At the same time the increased susceptibility of Igμ -/- mice, albeit marginal, to secondary infection with *C. trachomatis* suggests that chlamydiae-specific B-cells may contribute to the secondary immune response, either directly through the production of neutralising antibody [Buzoni-Gatel *et al*, 1990; Cotter *et al*, 1995; Pal *et al*, 1997; Williams *et al*, 1982] or by acting as *C. trachomatis*-specific APCs. However, until similar experiments are repeated in the context of the murine model of OEA [Rodolakis *et al*, 1981] it can only be speculated upon as to whether the same is true for pregnant mice, or sheep, infected with OEA strains of *C. psittaci*.

1.6.4 CD4 +ve αβ T-cells and immunity to chlamydiae

Studies involving the experimental infection of B-cell deficient mice with Serovar D and MoPn strains of *C. trachomatis* have been unanimous in concluding that CMI plays a more dominant role than antibody in the protective immune response to chlamydiae [Johansson *et al*, 1997a; Ramsey *et al*, 1988; Su *et al*, 1997; Williams *et al*, 1987b; Williams *et al*, 1997].

In contrast to B-cell deficient mice, athymic nu/nu mice are much more susceptible to infection with MoPn than functionally intact heterozygous nu/+ controls [Williams *et al*, 1981]. However, in addition to being largely devoid of functionally mature αβ T-cells, nu/nu mice fail to mount a humoral response to chlamydiae [Coalson *et al*, 1987]. Reconstitution of nu/nu BALB/c mice with thymuses explanted from neonatal +/+ BALB/c mice restores their ability to produce functionally mature αβ T-cells and affords significantly more protection against intranasal challenge with MoPn than passive transfer of immune sera. Reconstituted nu/nu mice also produce antibody in response to MoPn, suggesting that both CMI and humoral immunity to chlamydiae are αβ T-cell dependent [Williams *et al*, 1982].

Severe combined immunodeficiency (SCID) mice, which do not produce functional B-cells, αβ T-cells or γδ T-cells [Yancopoulos and Alt, 1988], are more susceptible to pneumonia caused by MoPn than nu/nu mice [Magee *et al*, 1993], possibly as a result of the presence of subpopulations of γδ T-cells in nu/nu mice [Williams *et al*, 1987a, 1996]. SCID mice have been shown to be partially protected from challenge with MoPn by passive transfer of a MoPn-specific Th1-like CD4 +ve αβ T-cell clone lending further support to the role for CMI in immunity to chlamydiae [Magee *et al*, 1993].

More recent studies have concentrated on the use of KO mice and antibody targeted depletion to dissect the primary and secondary immune responses to chlamydiae. Antibody mediated depletion of CD4 +ve or CD8 +ve T-cells has been shown to significantly increase chlamydial burden in C57BL/6 mice infected intranasally with MoPn during the primary immune response. However, mortality was significantly

higher in mice after CD4 targeted depletion, when compared to CD8 depleted mice which did not differ significantly from control mice. Depletion of CD 4 +ve T-cells (but not CD8 +ve T-cells) was also associated with a significant reduction in both serum IgG and the ability of spleen cells to produce IFN-γ in response to UV-inactivated MoPn EB [Magee *et al*, 1995].

CD4 KO (CD4 -/-) C57BL/6 mice experience increased chlamydial burdens and prolonged infection with MoPn compared to control C57BL/6 mice or beta 2-microglobulin KO (β-2m -/-) C57BL/6 mice. Although antibody mediated depletion of CD8 +ve T-cells did not result in significantly increased mortality, a significant increase in mortality has been reported in β-2m -/- mice relative to normal control mice [Magee *et al*, 1995]. In a parallel experiment, Morrison *et al* (1995) showed that whilst CD4 -/- C57BL/6 mice suffered significantly prolonged infection compared to controls and β-2m -/- mice, they were able to resolve primary genital tract infection with MoPn. In the same study, both β-2m -/- and CD4 -/- mice mounted an effective memory response to secondary challenge. In contrast to the findings of Magee *et al* (1995), there was no evidence that IgG production was significantly affected in CD4 -/- mice during genital tract infection with MoPn, although IgA production was delayed in CD4 -/- mice compared to β-2m -/- and control mice. However, MHC II KO (MHC II -/-) C57BL/6 mice produce significantly reduced amounts of antibody, fail to resolve primary infection and do not develop immunological memory following intravaginal challenge with MoPn [Morrison *et al*, 1995]. The discrepancy between the outcome of infection in CD4 -/- and MHC II -/- mice is surprising since both models are thought to be completely CD4 +ve αβ T-cell deficient [Grusby *et al*, 1991; Killeen *et al*, 1993; Rahemtulla *et al*, 1991].

Like MHC II -/- C57BL/6 mice, MHC II -/- BALB/c mice have been shown to be very susceptible to secondary infection in the lung with MoPn when compared to normal BALB/c controls, β-2m -/-, Igμ-/- or interleukin-4 KO (IL4-/-) BALB/c mice [Williams *et al*, 1997]. On the basis of these findings, CD4 +ve T-cells appear to play the pivotal role in both the primary and secondary immune response to *C. trachomatis* in the mouse.

The ability of different inbred strains of mice to resist primary infection with MoPn has been shown to correlate with quantitative differences in cytokine expression. C57BL/6 mice are more resistant than BALB/c mice to both intravaginal and intranasal challenge with MoPn [Stagg *et al*, 1998; Yang *et al*, 1996]. Whilst both mouse strains have an apparently functionally intact immune system, BALB/c mice were shown to express higher levels of IL-10, more IgG1 antibody, weaker DTH responses and less IFN-γ than C57BL/6 mice [Yang *et al*, 1996].

The protective immune response to primary infection with MoPn is profoundly compromised in IL-12 depleted and IFN-γ KO (IFN-γ -/-) C57BL/6 mice [Perry *et al*, 1997]. IL-12 depleted mice were shown to have decreased numbers of infiltrating CD4 +ve T-cells in infected tissues and took almost twice as long to clear chlamydiae from the reproductive tract when compared to mice treated with a control antibody. Neutralisation of IL-12 also caused qualitative and quantitative changes in immunoglobulin isotype expression, including expression of IgG1 which is associated with a Th2-like response. Furthermore, spleen cells from IL-12 depleted mice produced significantly less IFN-γ in response to heat-inactivated chlamydiae, indicating that the Th1-like immune response was suppressed in these mice. IFN-γ -/- mice initially appeared to control genital tract infection with MoPn but went on to develop systemic infections often resulting in mortality. These mice also showed abnormalities in cytokine and immunoglobulin isotype expression, including failure to produce IgG2a and significantly depressed IL-6 production during the initial stages of infection. However, IL-10 production was shown to be depressed in IFN-γ -/- mice when compared to control mice, suggesting that suppression of IFN-γ production does not necessarily skew the immune response toward Th2-like cytokine production. In contrast to IL-12 depleted and IFN-γ -/- mice, IL-4 depleted mice were indistinguishable from control mice with respect to time taken to resolve infection, cytokine production and immunoglobulin isotype production [Perry *et al*, 1997]. These findings lend substantial support to earlier studies which demonstrate that antibody mediated depletion of IFN-γ can induce exacerbated and prolonged disease in naive mice challenged with *C. trachomatis* [Rank *et al*, 1992; Williams *et al*, 1988] or with the S26/3 OEA strain of *C. psittaci* [McCafferty *et al*, 1994].

Whilst IFN-γ has been shown to play a significant role in the primary immune response to MoPn [Perry *et al*, 1997; Yang *et al*, 1996], its role appears to be less important during the secondary immune response to chlamydiae. Although, there appears to be an absolute requirement for CD4 +ve T-cells for the generation of immunological memory to chlamydiae, IFN-γ -/- mice have been shown to be equally resistant to reinfection as normal mice of the same genetic background [Cotter *et al*, 1997; Williams *et al*, 1997]. IFN-γ -/- mice were reported to produce significantly elevated levels of TNF-α during the secondary response to MoPn and it has been suggested that additional CMI mechanisms may operate during the secondary response to MoPn [Williams *et al*, 1997]. In contrast, experimental infection of IFN-γ receptor deficient mice (IFN-γR -/-) does not result in the development of immunological memory and these mice develop significantly increased pathology compared to control mice following secondary intravaginal challenge with MoPn [Johansson *et al*, 1997b].

1.6.5 CD8 +ve αβ T-cells and immunity to chlamydiae

Whilst studies using β-2m -/- mice suggest that CD8 +ve αβ T-cells are not an essential component of the primary or secondary immune response to MoPn [Magee *et al*, 1995; Morrison *et al*, 1995; Williams *et al*, 1997] there is considerable evidence that CD8 +ve T-cells contribute to the resolution of chlamydial infections. Adoptive transfer of chlamydiae-specific CD8+ T-cell clones has been shown to increase the frequency with which nu/nu mice eliminate MoPn, although the ability of individual clones to contribute to protection was shown to be dependent on their capacity to produce IFN-γ and TNF-α [Igietseme *et al*, 1994]. Similarly, adoptive transfer of a CD8 +ve cytotoxic T-cell line, derived from a mouse infected with a LGV strain of *C. trachomatis*, was also shown to partially protect normal female BALB/c mice from infection with an LGV strain of *C. trachomatis* through an IFN-γ dependent mechanism [Starnbach *et al*, 1994]. Furthermore, epidemiological studies have also implicated *C. trachomatis*-specific CD8 +ve T-cells in the resolution of trachoma in humans [Holland *et al*, 1997; Reacher *et al*, 1991].

1.6.6 γδ T-cells and immunity to chlamydiae

Little is known about the contribution of γδ T-cells to the protective immune response to chlamydiae and even less about their role in the ovine immune response to OEA. The presence of γδ T-cells in nu/nu mice has been cited as a potential source of IFN-γ and may be the reason why nu/nu mice are more resistant to chlamydial infections than SCID mice [Williams *et al*, 1987a]. However, experimental infection of γδ T-cell deficient (γδ -/-) mice with MoPn has shown that whilst γδ T-cells may play a positive role in protection during the initial stages of infection, their role in the later stages of infection is less clear and they may even contribute to pathology [Williams *et al*, 1996].

1.6.7 Cytokines and immunity to chlamydiae

The anti-chlamydial properties of cytokines have been extensively scrutinised *in vitro*. Early studies showed that a cocktail of cytokines, derived in this case from concanavalin A (ConA) stimulated spleen cells of immune mice, could activate murine macrophages to restrict the growth of the 6BC avian strain of *C. psittaci* [Byrne and Faubion, 1982]. IFN-γ was subsequently identified as the component responsible for restricting the growth of *C. psittaci* in human macrophages [Rothermel *et al*, 1983] and murine fibroblasts [Byrne and Krueger, 1983]. IFN-γ has since been reported to restrict the growth of *C. psittaci*, *C. trachomatis* and more recently *C. pneumoniae* in a variety of different cells of human, murine and ovine origin [Chen *et al*, 1996; De La Maza *et al*, 1987a, 1987b; Graham *et al*, 1995; Kane and Byrne, 1998; Mehta *et al*, 1998; Rapoza *et al*, 1991; Yong *et al*, 1987; Zhong and De La Maza, 1988].

IFN-γ is not the only cytokine that can restrict the growth of chlamydiae directly. TNF-α has been shown to inhibit the growth of a LGV strain of *C. trachomatis* in human HEp-2 cells (derived from a carcinoma of the larynx) through a mechanism that was dependent on endogenous Interferon-beta (IFN-β) production by HEp-2 cells [Shemer-Avni *et al*, 1988; 1989]. IFN-β has also been shown to restrict the

growth of *C. trachomatis* in the absence of TNF-α [Shemer-Avni *et al*, 1989]. TNF-α may act synergistically with IFN-γ to restrict *C. pneumoniae* growth in human HEp-2 cells [Summersgill *et al*, 1995] and IL-1 has been demonstrated to act synergistically with IFN-γ in restricting the growth of *C. psittaci* in human monocyte derived macrophages [Carlin and Weller, 1995].

1.6.8. IFN-γ mediated persistence of chlamydiae *in vitro*

Chlamydial diseases are commonly characterised by long-term persistent infections. Persistent subclinical *C. psittaci* infection is well documented in the context of OEA in the non-pregnant ewe [Rodolakis *et al*, 1998]. Similarly, chlamydial persistence is thought to be involved in both long-term asymptomatic infections and chronic inflammatory pathology, characteristic of genital and ocular *C. trachomatis* infections in humans [Ward, 1995]. Furthermore, there is mounting evidence of an association between persistent *C. pneumoniae* infection and cardiovascular disease [Gibbs *et al*, 1998]. Consequently, there has been considerable interest in the mechanisms through which chlamydial persistence is mediated.

Penicillin was the first anti-microbial agent shown to induce chlamydial persistence *in vitro* [Matsumoto and Manire, 1970]. The presence of penicillin in cultures of murine L-cells infected with *C. psittaci* resulted in the formation of aberrant RB which did not undergo binary fission or develop into infectious EB. However, penicillin did not eradicate RB from infected cultures and *C. psittaci* resumed its normal cytolytic growth cycle when persistently infected cells were transferred into penicillin-free culture conditions. Similar results have also been reported in murine McCoy cells infected with *C. psittaci* or *C. trachomatis* under amino acid-free or -depleted culture conditions [Coles *et al*, 1993].

At the same time that Coles *et al* (1993) were investigating the role of amino acid deprivation in chlamydial persistence, it became clear that IFN-γ could induce a persistent *C. trachomatis* infection in human cells that shared several characteristics with penicillin mediated persistence. The effect of IFN-γ on *C. trachomatis* growth in

the human epithelial HeLa 229 cell line was shown to be dose dependent and at relatively low concentrations resulted in the formation of morphologically aberrant chlamydiae that did not mature into infectious EB [Beatty *et al*, 1993]. *C. trachomatis* development and production of infectious EB was restored when IFN-γ was removed from the culture conditions [Beatty *et al*, 1993]. Further characterisation of this model revealed that *C. trachomatis* could be maintained in a non-productive persistent state for over 30 days when infected cells were maintained in the presence of IFN-γ and that persistence was mediated by host cell tryptophan catabolism [Beatty *et al*, 1994a, 1995]. IFN-γ has since been reported to mediate chlamydial persistence in human in polarised human epithelial cells infected with *C. trachomatis* [Kane and Byrne, 1998] and human HEp-2 cells infected with *C. pneumoniae* [Mehta *et al*, 1998].

1.7. Aims of the study

The ability of *C. psittaci* to cause a persistent infection in the non-pregnant ewe without inducing protective immunity to OEA severely confounds both diagnosis and vaccine strategies. The mechanisms through which persistent *C. psittaci* infection is mediated in sheep have not been previously defined. The main purpose of this work was to investigate whether the ovine immune response can contribute to the induction and maintenance of *C. psittaci* persistence. To which end the following studies were pursued:

- An image analysis software solution was developed with a view to automating the otherwise laborious and error prone task of measuring chlamydial growth *in vitro*.

- The mechanisms responsible for ovine IFN-γ mediated restriction of *C. psittaci* growth in ovine cells were investigated.

- The ability of ovine IFN-γ to induce and mediate persistent *C. psittaci* infection of an ovine cell line was investigated.

- The mechanisms responsible for IFN-γ mediated *C. psittaci* persistence were investigated.

- Attempts were made to generated and characterise *ex vivo* T-cell lines, raised against the predominant *C. psittaci* surface antigen MOMP, with a view to clarifying the phenotype of IFN-γ producing T-cells from immune sheep.

Chapter 2.0

Materials and Methods

2.1. Cell culture and *C. psittaci*

2.1.1. General culture conditions

All aspects of cell culture, handling of *C. psittaci* and Semliki Forest Virus (SFV) were performed under biosafety level two conditions. All cell lines and primary cultures were propagated and maintained in antibiotic free media (unless stated otherwise) in a 37°C humidified 5% CO_2 environment. Cell viability was determined by nigrosine exclusion (BDH Chemicals, Poole, UK).

Unless stated otherwise, reagents were obtained from Moredun Research Institute (MRI) scientific services.

2.1.2. Fetal bovine sera

Fetal bovine serum (FBS: Boehringer Mannheim, Lewes, UK) was screened at MRI and shown to be free of *C. psittaci*-specific antibodies [Jones *et al*, 1997]. In addition, each batch of FBS was tested to ensure that it did not influence *C. psittaci* infectivity or inclusion formation. FBS was also screened for bovine virus diarrhoea virus (BVDV) specific antibodies and infectious BVDV. BVDV can establish persistent infections in ruminant cell lines and has the potential to alter cell function [Nettleton and Entrican, 1995]. The ruminant cell lines used throughout these experiments were routinely screened for BVDV by IFAT. In addition, cell lines were tested every 6 months for the presence of mycoplasmas using a commercially available ELISA (Boehringer Mannheim).

2.1.3. Cryopreservation

Cells were cryopreserved at a density of $5x10^6$ - $1x10^7$ viable cells/ml in freezing medium: 50% of the appropriate culture medium, 40% FBS and 10% dimethyl-sulfoxide (DMSO; Sigma-Aldrich Poole, UK). Cell suspensions were aliquoted into

1 ml Nunc Cryotubes (GIBCO BRL, Paisley, UK), cooled to -70°C at a rate of approximately 1°C/minute, using a Nalgene Cryo freezing vessel containing isopropanol (GIBCO BRL), then transferred to long-term storage in liquid nitrogen.

2.1.4. ST.6 cells

The ovine fibroblastic cell line, ST.6, was originally derived from a metastatic tumour explanted from the posterior mediastinal lymph node of an adult ewe identified as having a naturally occurring adenocarcinoma of the small intestine [Norval *et al*, 1981].

ST.6 cells were maintained in Iscove's modified Dulbecco's medium (IMDM; GIBCO BRL) supplemented with 5% FBS (IMDM+5% FBS). ST.6 cultures were routinely maintained in IMDM + 5% FBS in 225 cm^2 vented tissue culture flasks (Corning Costar, High Wycombe, UK). Cultures were passaged 1 in 3 every 3-4 days or when the cell monolayers became confluent. Cell monolayers were washed twice with sterile pH 7.4 phosphate buffered saline (PBS; Appendix 1.1), detached with 2 ml of trypsin/versene (Appendix 1.2) and resuspended to 9 ml in IMDM+5% FBS. Fresh 225 cm^2 flasks were seeded with 3 ml of cell suspension and made up to 25 ml with IMDM+5% FBS.

2.1.5. RAW 264.7 cell line

The murine macrophage cell line RAW 264.7 [Raschke *et al*, 1978] was obtained from the European Collection of Animal Cell Cultures.

Raw 264.7 cells were maintained in IMDM+5% FBS in 75 cm^2 vented tissue culture flasks (Corning Costar). Cultures were passaged 1 in 10 every 3-4 days or when the cell monolayers became confluent. The monolayer was mechanically disrupted using a sterile plastic cell scraper (Corning Costar), the cell suspension was centrifuged at 400 g for 5 minutes and the pellet was resuspended in 10 ml of IMDM+5% FBS. Fresh flasks were seeded with 1 ml of cell suspension and made up to 10 ml with

IMDM+5% FBS.

2.1.6. Collection of bronchoalveolar lavage cells

Bronchoalveolar Lavage (BAL) cells were collected using a modified version of the protocol described by Burrells (1985). Conventionally reared adult ewes and specific pathogen free (SPF) ewe lambs were euthanized by intravenous injection with sodium pentobarbital (Euthetal; Rhone Mereux, Harlow, UK). The lungs were excised with the trachea clamped shut to avoid contaminating the interior of the lung with blood. Approximately one litre of PBS was poured into the trachea, after which lungs were briefly massaged and the resultant suspension of BAL cells was decanted into a sterile container through sterile gauze. At this stage, any BAL suspensions contaminated with blood were discarded. Cells were washed three times by centrifugation at 500 g for 30 minutes in cold (4°C) Hanks Balance Salt Solution (HBSS; GIBCO BRL), supplemented with 2% FBS, 100 μg/ml gentamicin sulphate (Sigma-Aldrich), 200 international units/ml (IU/ml) of penicillin (Britannia Pharmaceuticals, Redhill, UK), 100 μg/ml of streptomycin (GIBCO BRL), 4 μg/ml Amphotericin B (Sigma-Aldrich), 10 IU/ml Heparin (Sigma-Aldrich). The cells were washed a final time in cold (4°C) antibiotic-free IMDM + 10% FBS and cryopreserved in 1 ml aliquots of freezing medium at a density of $1X10^7$ viable cells/ml.

2.1.7. Collection of ovine peripheral blood mononuclear cells

Adult ewes which had previously aborted as a result of experimental infection with the S26/3 EAE strain of *C. psittaci* during pregnancy [Jones *et al*, 1995] were isolated and kept at the MRI animal facilities. Adult ewes which were seronegative by CFT for *C. psittaci* S26/3 and had no previous record of EAE were also isolated and kept at MRI animal facilities for use as controls.

Whole peripheral blood, drawn from the jugular vein, was collected in 20 ml vacutainers coated with preservative-free heparin (Becton Dickinson, Oxnard,

USA). The blood was transferred into sterile 25 ml universal tube (Bibby Sterilin, Stone, UK) and centrifuged at 800 g for 20 minutes at 10°C with the centrifuge brake mechanism disabled. The resultant buffycoats, containing the peripheral blood mononuclear cells (PBM), were removed and diluted in cold (4°C) PBM wash medium (HBSS supplemented with 2% FBS, 100 μg/ml gentamicin sulphate and 10 IU/ml Heparin). The buffycoat suspension was layered onto Lymphoprep: specific gravity 1.077 g/l (Nycomed, Oslo, Norway) and centrifuged at 800 g for 30 minutes at 10°C with the centrifuge brake mechanism disabled. The interface was collected, washed three times with PBM wash medium and counted using a haematocytometer before resuspending the cells at $2X10^6$ viable cells/ml in IMDM supplemented with 10% FBS, 25 μg/ml gentamicin sulphate (PBM Culture medium).

2.1.8. *C. psittaci* S26/3

Tissue culture-derived stocks of the S26/3 ovine abortion strain of *C. psittaci* [McClenaghan *et al*, 1984] were obtained by incubating confluent ST.6 cultures in 225 cm^2 vented tissue culture flasks for 6 hours with 8 ml of IMDM+5% FBS containing $2x10^7$ inclusion forming units (IFU) of *C. psittaci* grown in chicken egg yolk sacs [Stamp *et al*, 1950]. Chlamydiae were harvested after 5 days by disrupting the ST.6 cells with 3 mm diameter sterile glass beads. The resultant suspension was centrifuged at 500 g for 10 minutes to remove debris. Supernatants were collected and centrifuged at 10000 g for 10 minutes to pellet chlamydiae which were then resuspended in chlamydial transport medium (Appendix 1.3) and stored at -70°C [Graham *et al*, 1995].

2.2. Phenotypic analysis of primary ovine cells

2.2.1. Flow cytometry

Surface marker expression on ovine BAL cells was characterised using flow cytometry. Single cell suspensions containing approximately $2x10^6$ cells/ml were prepared in cold (4°C) fluorescent activated cells sorter medium (FACS medium; HBSS supplemented with 0.01% sodium azide (Sigma-Aldrich) and 2% FBS). 50 µl aliquots of the resultant cell suspensions were added to Nunc V-bottomed 96-well microtitre plates (GIBCO BRL) and centrifuged for 10 minutes at at 500 g (4 °C). The supernatant was discarded and the cell pellets were resuspended by gentle agitation using a benchtop vortex (Fisher Scientific, Loughburgh, UK). Non-specific antibody binding was blocked by incubating the cells at 4 °C for 20 minutes in FACS medium supplemented with 2% normal rabbit serum, after which the cells were centrifuged and washed twice with FACS medium as described before. The cells were then incubated for 30 minutes at 4 °C with primary antibodies diluted appropriately in FACS medium. After three washes in FACS medium, cells were incubated at 4 °C for 30 minutes in 50 µl of rabbit anti-mouse immunoglobulin conjugated with fluorescein isothiocyanate (rabbit anti-mouse-FITC; DAKO A/S, Denmark) diluted 1/50 in FACS medium. Cells were then washed three more times with FACS medium, fixed in FACS medium supplemented with 1% paraformaldehyde (Sigma-Aldrich) and stored in the dark at at 4 °C. Analysis was performed a using flow cytometer (Facscan; Becton Dickinson, California, USA) with linear amplification for forward/side scatter and logarithmic amplification for FITC green fluorescence. Events were gated to exclude erythrocytes and dead cells on the basis of forward and side scatter.

2.2.2. Non-specific esterase staining of adherent BAL cells

Ovine BAL cells were adjusted to $2x10^6$ cells/ml in IMDM supplemented with 10 % FBS and 25 µg/ml gentamicin sulphate. 300 µl aliquots of the resultant cell

suspension were seeded into 8-well Permanox chamber-slides (Fisher Scientific) and incubated for 6 hours under standard cell culture conditions. Non-adherent cells were discarded and the adherent cells were washed once in IMDM+10% FBS. Non-specific esterase activity was determined using a commercially available kit following the procedure described by the manufacturer (α-napthyl acetate esterase assay; Sigma-Aldrich). The percentage of α-napthyl acetate esterase positive cells was determined using image analysis.

2.2.3. Phagocytic characterisation of adherent BAL cells

Ovine BAL cells were adjusted to $1x10^6$ cells/ml in IMDM supplemented with 10 % FBS and 25 μg/ml gentamicin sulphate. 300 μl aliquots of the resultant cell suspension were seeded into 8-well Permanox chamber-slides and incubated for 6 hours under standard cell culture conditions. Non-adherent cells were discarded and the culture medium was replaced with 300 μl of IMDM+10% FBS containing $1x10^7$ latex beads/ml (3 μm diameter; Sigma-Aldrich). After a further 12 hours chamber-slides were fixed in absolute methanol (Fisher Scientific) and stained with 0.5% Methyl blue (Sigma-Aldrich) in deionised water for 2 minutes and the percentage of cells containing latex beads was determined using image analysis.

2.3. Recombinant ruminant cytokines

2.3.1. Recombinant ovine IFN-γ

Ovine IFN-γ cDNA was originally cloned using the polymerase chain reaction [McInnes *et al*, 1990]. Chinese Hamster Ovary (CHO) cells which had been stably transfected with OvIFN-γ cDNA inserted into the pEE14 mammalian expression plasmid vector (Celltech, Slough, UK) were maintained in antibiotic-free Glasgow's Modified Eagle's Medium without glutamine (GMEM; GIBCO BRL) supplemented with 7.5% dialysed FBS and 100 μM methionine sulphoxamine (MSX; Sigma-Aldrich). The pEE14 expression vector contains a glutamine synthase gene as a selection marker which allows transfected clones to grow in glutamine free medium in the presence of low levels of MSX.

Recombinant OvIFN-γ (ROvIFN-γ) was produced by, washing the transfected CHO cell monolayers with PBS to remove MSX and FBS, then incubating cultures in serum-free GMEM in the absence of MSX for 4 days. Culture supernatants were harvested, centrifuged for 10 minutes at 500 g to remove cell debris and passed through a sterile low protein binding 0.22 μm filter unit (Millipore, Bedford, USA). Supernatants were aliquoted into 1 ml volumes and stored in sterile 1.5 ml microcentrifuge tubes (Corning Costar) at –70°C before being assayed for biological activity.

2.3.2. Recombinant bovine IFN-α

Recombinant bovine interferon-alpha (RBovIFN-α) was kindly donated by CIBA-GEIGY (CIBA-GEIGY, Switzerland).

2.3.3. Ovine anti-viral interferon bioassay

The biological activity of rOvIFN-γ and RBovIFN-α were measured using an ovine interferon bioassay [Entrican *et al*, 1989, 1992]. ST.6 cells were suspended in IMDM + 5% FBS at a density of $5X10^4$ cells/ml, seeded in volumes of 100 μl into 96-well flat-bottomed microtitre plates (Corning Costar) and allowed to grow for two days. Log_2 serial dilutions of samples to be tested were prepared in IMDM + 2% FBS. Plates were incubated for 12 hours with triplicate 100 μl aliquots of each dilution. Culture supernatants were discarded from the plates and replaced with 200 μl of IMDM + 2% FBS containing 100 $TCID_{50}$ of SFV (a kind gift from Dr Alan Morris, Warwick, UK). After a further 48 hour incubation the plates were examined for cytopathic effect (CPE) induced by SFV. One unit of interferon biological activity was defined as the maximum dilution of sample capable of inhibiting the CPE of SFV by 50%. The activity of the original samples were extrapolated from the dilution corresponding to 1 U/ml.

2.4. Histology and imaging

2.4.1. Cytospins

100 μl aliquots of cell suspensions, adjusted to a density of between $1X10^5$ and $2X10^5$ cells/ml, were centrifuged onto glass slides at 90 g for 5 minutes using a Cytospin 3 cytocentrifuge (Shandon Scientific, Runcorn, UK) after which the slides were allowed to air dry before fixation and staining.

2.4.2. Modified Ziehl Neelsen's (MZN) Stain

ST.6 cultures were fixed in absolute methanol for 15 minutes, air dried and incubated at 60°C with 2% Ziehl Neelsen's carbo fuchsin (Pro-Lab Diagnostics, Neston, UK) for 1 hour, washed thoroughly in tap water, and destained in 1% acetic acid for 4 seconds. Cells were then counter-stained with 0.5% Methyl blue in 1% acetic acid (Fisher Scientific) in deionised water, washed thoroughly in tap water and allowed to air dry.

2.4.3. Giemsa Stain

ST.6 cultures and cytocentrifuge preparations were fixed in absolute methanol for 15 minutes, air dried and incubated in a solution of 10% Giemsa's improved R66 stain (BDH Chemicals) in deionised water for 45 minutes at room temperature (RT). Cultures that had been maintained in 96-well flat-bottomed microtitre plates were washed in tap water and air dried. Slides were washed in tap water, dehydrated in graded ethanol, cleared in xylene and mounted with coverslips using Shandon's synthetic mountant (Shandon Scientific).

2.4.4. *C. psittaci* specific immunoperoxidase (IPX) staining

Ovine bronchoalveolar macrophages which had previously been maintained in 8-well Permanox chamber slides were fixed for 15 minutes in absolute methanol and allowed to air dry. Non-specific antibody binding was blocked by incubating wells at 37 °C for 60 minutes with 200 µl of normal rabbit serum diluted 1/50 in PBST-BSA (PBS containing 0.05% Tween 20 (Sigma-Aldrich, UK) and 3% bovine serum albumin (BSA; Sigma-Aldrich)). The wells were then washed three times in PBST-BSA and incubated at 37 °C for 60 minutes with 200 µl of anti-*C. psittaci* MOMP monoclonal antibody (Mab) 4/11 (MRI) diluted appropriately in PBST-BSA. The optimal working concentration of Mab 4/11 ascites (typically 1/50) was determined by titration on ST.6 cells infected with *C. psittaci* prior to use. Wells were washed a further three times in PBST-BSA and incubated at RT for 10 minutes in PBST-BSA containing 3% hydrogen peroxide (H_2O_2; Sigma-Aldrich) to block endogenous peroxidase activity. After three more washes with PBST-BSA, wells were incubated at 37 °C for 60 minutes in the presence of 200 µl of goat anti-mouse Mab conjugated to horse radish peroxidase (goat anti-mouse-HRP; DAKO A/S) diluted 1/500 in PBST-BSA. Wells were washed a final three times with PBST-BSA and then incubated for 30 minutes at 37 °C with 180 µl of 3, 3'-Diaminobenzidine Tetrahydrochloride (DAB) substrate prepared using SIGMA FAST tablets as instructed by the manufacturer (Sigma-Aldrich). At this stage, the chamber slide well housings and gaskets were discarded and the slides were washed thoroughly in tap water. Slides were then counterstained for 2 minutes in Meyer's hematoxylin (Sigma-Aldrich), washed in tap water, dehydrated in graded ethanol and cleared in xylene. Permanox slides were not mounted with coverslips.

2.4.5. Image Acquisition and Storage

Images were acquired with a JVC KY-F30 3 charge coupled device (CCD) camera module attached to a Olympus BH2-RFCA conventional compound microscope (Olympus Optical CO, London, UK). Live 24-bit red, green and blue (RGB) European television standard (PAL) video was digitised using a Video Desk HR-24

NuBus card mounted in a Power Macintosh 7100/66 fitted with 16 megabytes (MB) of random access memory (RAM), running System 7.5.3 (Apple Computer, California, USA) and ColourVision 1.5 (Improvision, University of Warwick Science Park, UK). Colour images were captured in ColourVision at a resolution of 700 x 572 pixels and stored as 24-bit colour Tag Image File Format (TIFF) files on one gigabyte (1GB) Jaz Disks (Iomega Corporation, Utah, USA).

Images were also acquired with a JVC TK-1280E single CCD colour camera module attached to a Olympus BX-50 conventional compound microscope (Olympus Optical CO). Live 24-bit super-VHS colour PAL video was digitised using the standard AV digitiser mounted in a Power Macintosh 7100/80 AV (Apple Computer) fitted with 80 MB RAM, running Mac OS 8.1 (Apple Computer) and NIH Image 1.61 [Rasband and Bright, 1995]. NIH Image is a public domain software package developed at the U.S. National Institute of Health and is available from the internet by anonymous FTP from zippy.nimh.nih.gov/pub/NIH Image/ or on floppy disk from the national Technical Information Service, Springfield, Virginia, part number PB95-500195GEI. Colour images were captured in NIH Image 1.61 using Plug-in Digitiser v1.2.4 (Cyrus Daboo, Cambridge, UK) at a resolution of 752 x 576 pixels and stored as 24-bit colour TIFF files on 1GB Jaz Disks.

2.4.6. Image Processing

Images were processed on a Power Macintosh Performa 6320 fitted with 48 MB RAM running Mac OS 8.1 (Apple Computer) or a Power Macintosh 7100/80 AV fitted with 80 MB RAM, running Mac OS 8.1. Standard image analysis procedures such as cell counting and scoring were performed using Object Image 1.62n6 [Vischer *et al*, 1994]. Object Image is a public domain software package, based on NIH Image, developed by Norbert Vischer (Universiteit van Amsterdam, Amsterdam, The Netherlands) and is available from the internet by anonymous FTP from ftp://simon.bio.uva.nl/object-Image.html.

Software for the automated measurement of chlamydial inclusion bodies, Inclusion

Counter v1.0 , was developed using NIH Image 1.61 [Rasband and Bright, 1995] (ftp://codon.nih.gov/pub/nih-image/user-macros/inclusion_counter.hqx). Updated versions, Inclusion Counter v2.0 (ftp://codon.nih.gov/pub/nih-image/user-macros/inclusion_counterv2.sit.hqx), were developed in Object Image 1.62n6 [Vischer *et al*, 1994].

2.5. Measurement of *C. psittaci* multiplication

2.5.1. Chlamydial LPS-ELISA

The concentration of lipopolysaccharide (LPS) in experimental culture supernatants was determined using an ELISA. The anti-LPS Mab 13/4 was produced as ascites and titrated to determine the optimal concentration for use in the ELISA. Flat-bottomed F-type 96-well ELISA plates (Dynatech, UK) were coated over night at 4°C with 100 µl of Mab 13/4 diluted in pH 9.6 carbonate coating buffer (Appendix 1.4). Plates were emptied, washed three times with PBST (PBS containing 0.05% Tween 20) and blotted dry. Plates were blocked with 200 µl/well of donor horse serum (Northumbria Biologicals, Cramlington, UK) diluted 1/5 in pH 9.6 carbonate coating buffer for one hour at 37°C. Plates were washed three times with PBST, after which 100 µl aliquots of samples were added to each well in triplicate. Duplicate $\log_2$ serial dilutions of *S. minnesota* RE-595 LPS (Sigma-Aldrich) were used as standards. Plates were incubated at 37°C for one hour and then washed three times in PBST and blotted dry as before. 100 µl of affinity purified 13/4 Mab conjugated to horse radish peroxidase (13/4-HRP) diluted in PBST to approximately 50 µg/ml, was added to each well after which the plates were incubated for one hour at 37°C. Plates were washed and blotted dry as before after which substrate was added. Two different substrates were used:

1; Plates were incubated for 10 minutes at RT in the presence of 100 µl/well of Sigma Fast o-phenylenediamine dihydrochloride substrate (OPD; Sigma-Aldrich). The reaction was stopped using 50 µl/well of 2.5 M sulphuric acid (Fisher Scientific). Optical density (OD) was measured with a Titretec Multiscan ELISA Reader (Flow, High Wycombe, UK) using an absorbance filter of 492 nm.

2; Plates were incubated at RT in the presence of 100 µl/well of Tetramethylbenzidine (TMB; Kirkegaard & Perry Laboratories, Maryland, USA) and the reaction was stopped using 0.1 M Hydrochloric acid (Fisher Scientific). OD was measured with a Titretec Multiscan ELISA Reader using an absorbance filter of

450 nm.

2.5.2. Titration of chlamydial infectivity

The infectivity of *C. psittaci* stocks and experimental culture supernatants was determined by titration on confluent monolayers of ST.6 cells in 96-well flat-bottomed microtitre plates. Culture supernatants were discarded from plates and 100 μl of serial dilutions ($\log_2$ or $\log_{10}$) in IMDM+2% FBS, were added in triplicate. The plates were incubated for two days, after which the cell monolayers were fixed and stained using the Giemsa or Modified Ziehl Neelsen's methods. The total number of inclusion bodies in each well was counted by eye with the aid of an 16 mm eye-piece graticule (Graticules, Tonebridge, UK) over a range of dilutions and the number of inclusion-forming units/ml (IFU/ml) was determined by extrapolation for each sample.

2.6. Recombinant MOMP

2.6.1. Production of recombinant MOMP in *Escherichia coli*

The MOMP gene of the S26/3 strain of *C. psittaci* was originally cloned and sequenced by Herring *et al* (1989). The coding region for the C-terminal 351 amino acids of S26/3 MOMP was transfected into *E. coli* using the pET-22b vector (Novangen: Calbiochem-Novabiochem UK Ltd, Nottingham, UK). On induction with Isopropyl-β-thiogalactopyranoside (IPTG; Bioline, London, UK), the construct produces large quantities of a truncated protein lacking the first 16 amino acids of S26/3 MOMP (TMOMP) which accumulate as inclusion bodies inside transfected *E. coli* [Herring *et al*, 1998].

Stably transfected *E. coli* were stored at -70°C in L-broth (Appendix 1.5) supplemented with 30% glycerol (Fisher Scientific) in 1 ml Nunc Cryo Tubes. A sample of *E. coli* was removed from storage and streaked onto solid L-agar gel (Appendix 1.6) to form single colony isolates using a nichrome wire inoculating loop (Fisher Scientific). After incubation overnight at 37°C, a single colony was removed using a nichrome wire inoculating loop and suspended in 20 ml of L-broth supplemented with 100 μg/ml of ampicillin (Sigma-Aldrich) in a glass conical flask. The flask was then incubated in an Aerotron shaking incubator (Fisher Scientific) at 37°C. After 6 hours, the flask was removed and stored at 4°C over night. The flask was removed from storage and mixed by gentle agitation. 16 ml of the *E. coli* suspension were withdraw and centrifuged at 5000 g for 15 minutes. The pellet was resuspend in 2 ml of L-Broth and 0.8 ml of cell suspension was added to each of two 400 ml of prewarmed L-Broth supplemented with 100μg/ml of ampicillin in 2 litre conical flasks in the Aerotron at 37°C. Samples were periodically removed and the OD of the *E. coli* suspension was measured using a spectrophotometer (Fisher Scientific). When the *E. coli* suspension reached an OD of 0.6, IPTG was added to each flask to give a final concentration of 1 mM. The cultures were grown for a further 3 hrs, after which they were centrifuged at 5000 g for 15 minutes, resuspended in 100 ml of PBS, centrifuged for a further 15 minutes at 5000 g and

stored as a pellet over night at 4°C. The pellet was resuspended and incubated for 30 minutes at RT in 100 ml of pH 8.0 Tris (Hydroxymethyl) aminomethane/HCL buffer (Tris-HCL; Sigma-Aldrich) supplemented with 0.5 mM EDTA (Sigma-Aldrich), 1 M sucrose (Sigma-Aldrich) and 120 μg/ml of chicken egg white lysozyme (Calbiochem, Nottingham, UK). The suspension was then centrifuged at 25 000 g for 10 minutes. The pellet was resuspended in 50 ml of pH 8.0 Tris buffer containing with 0.5 mM EDTA and 1 M sucrose and centrifuged at 25 000 g for a further 10 minutes. The cells were resuspended in 50 ml Tris supplemented with 0.5 mM EDTA and sonicated with an W385 ultrasonic processor (Jencons Scientific, Leighton Buzzard, UK) 6 times for 15 seconds on ice with one minute standing in between. The product was centrifuged at 6000 g for 15 minutes and resuspended in 40 ml of sterile PBS three times, after which the pellet was resuspended in 8 ml of sterile PBS.

The presence of TMOMP in the sample was confirmed by using a direct dot-immunobinding technique. The concentration and purity of TMOMP in the product was determined by sodium dodecyl sulfate-polyacrylamide gel electrophoresis (SDS-PAGE) and 1D gel densitometery. The product was adjusted to 10 mg/ml of TMOMP in PBS and stored at –20°C in 200 μl aliquots.

2.6.2. Direct dot-immunobinding assay for TMOMP

TMOMP samples were spotted directly onto a nitrocellulose membrane in duplicate and allowed to air dry. Non-specific antibody binding was blocked by incubating the nitrocellulose membrane at 37 °C for 60 minutes with normal rabbit serum diluted 1/50 in PBST-BSA. The nitrocellulose membrane was then washed three times in PBST-BSA. One of the duplicate spots was incubated at 37 °C for 30 minutes with the Mab 4/11. The nitrocellulose membrane was washed three more times in PBST-BSA, after which both duplicates were incubated for 30 minutes at 37 °C in the presence of goat anti-mouse-HRP diluted 1/1000 in PBST-BSA. The nitrocellulose membrane was washed three more times with PBST-BSA and then incubated for 10 minutes at 37 °C with DAB substrate. Specific binding of Mab

4/11 to TMOMP in the sample was confirmed by macroscopic examination.

2.6.3. Polyacrylamide gel chromatography

TMOMP was purified for use in cell culture using a conventional adjustable bed column (Isco, Nebraska, USA) filled with Bio-Gel P-60 polyacrylamide gel: 45-90 μm hydrated particle size; with an exclusion limit of 3 - 60 KDa (Bio-Gel P-60, Bio-Rad Laboratories Laboratories, Hemel Hempstead, UK). 18 g of anhydrous Bio-Gel P-60 was weighed out into a 2.5 l Conical Buchner flask. 360 ml of degassed deionised water was added to the flask gradually with continuous mixing to ensure that a uniform suspension of was formed. The gel was allowed to hydrate and settle out of suspension overnight. Approximately half the supernatant was decanted off and the side arm of the flask attached to a vacuum pump. The flask was sealed and the contents degassed under 100 mBars of pressure for 20 minutes at RT. A further 360 ml of degassed deionised water was added and mixed with the gel. The flask was allowed to stand at RT for 2 hours or until >95% of the gel particles had settled out of suspension, at which point, approximately 80% of the supernatant was was decanted off and discarded. This process was repeated three times to remove all the fine particles. A 250 ml reservoir was attached to top of the column. In order to void any air bubbles from the lower outlet tubbing, the column was filled with degassed deionised water and the lower column outlet opened until the water fell to approximately 20% of the column height. Hydrated gel was then added until it filled the column and over half the reservoir. Degassed distilled water was layered on top of the gel, the lower outlet was opened and the column was left overnight to pack. A P-3 peristaltic pump (Fisher Scientific) was attached to the lower outlet of the column and run in reverse for a few seconds to void any air bubbles, after which the lower outlet was closed. The upper reservoir was removed and a flow adapter (Isco) was inserted into the top of the column down to the level of the flow bed. A one litre reservoir of column buffer (degassed 40 mM Phosphate buffer (Appendix 1.7) containing 0.1% sodium dodecyl sulfate-polyacrylamide (SDS; Sigma-Aldrich)) was prepared and attached to to lower outlet of the column. 360 ml of column buffer was passed through the column over 96 hours at a operating flow rate of 3.8

ml/hour. After this period, the reservoir was replenished with column buffer.

2.6.4. Purification of Recombinant TMOMP

Two mg of TMOMP suspended in 200 μl of PBS were diluted with 800μl of 40 mM Phosphate Buffer containing 2% SDS and 5% 2-mercaptoethanol (ICN Biomedicals, Basingstoke, Hampshire, UK) in a 1.5 ml micro centrifuge tube. A small perforation was made in the cap of the micro centrifuge tube before it was closed and incubated in a water bath at 100°C for 5 minutes to dissolve the TMOMP. The resultant solution was allowed to cool to RT before it was loaded onto the Bio-Gel P-60 column. The peristaltic pump attached to the column was stopped and the lower column outlet removed from the column buffer reservoir. The pump was reversed for a few seconds to void air bubbles and the lower outlet tubing was carefully placed into the micro centrifuge tube containing the TMOMP solution. The pump was allowed to draw up the TMOMP solution until the first air bubble appeared in the tubing. At this point the pump was stopped and the end of the lower outlet tubing which had been in contact with the TMOMP solution was gently washed with column buffer to avoid contamination of the buffer reservoir. The outlet was then placed into a second microfuge tube containing column buffer, reversed briefly to void air bubbles and allowed to draw up approximately 0.5 ml of column buffer. The pump was then stopped and inserted into the buffer reservoir, again briefly reversing the pump to void any air bubbles. The pump was switched to forward and the lower outlet tubing securely fixed in the buffer reservoir. The upper outlet of the column was attached to a fraction collector (Isco) set to collect one fraction ever hour in 5 ml sample tubes (Corning Costar). The flow rate of the pump was set to 3.4 ml/hour and the column was run for 36 hours.

The protein content of the fractions was estimated using a Beckman DU 650 Spectrophotometer (Beckman Instruments, California, USA) at an absorbance of 260 nm. The two fractions with the highest absorbance values were mixed and concentrated by centrifugation at 5000 g for 20 minutes in Centricon-30 concentrators: <30 KDa exclusion limit (Amicon, Stonehouse, UK). This was done

repeatedly with 2 ml aliquots until the TMOMP had been concentrated to a volume of approximately 500 μl. The concentration of TMOMP was estimated by SDS-PAGE and 1D gel densitometery.

2.6.5. SDS-PAGE

SDS-PAGE was used to confirm the molecular weight and amount of TMOMP present in samples prepared using the *E. coli* system outlined above. SDS-PAGE was performed using the Mini-PROTEAN® II electrophoresis system (Bio-Rad Laboratories Laboratories). Gels were hand cast as follows. Approximately 4 ml of 12% acrylamide resolving gel (Appendix 1.8) was added to each cast and 75 % ethanol (Fisher Scientific) was then layered on top of the resolving gel to void any air bubbles. Once the resolving gel had set, the ethanol was decanted off and allowed to evaporate. The cast was then topped up with 4% acrylamide stacking gel (Appendix 1.9), and a Teflon comb (Bio-Rad Laboratories) was used to make the loading wells and the gel allowed to polymerise.

After polymerisation, gels were transferred into a Mini-PROTEAN® II electrophoresis tank and electrode buffer (Appendix 1.10) was added to the inner and outer cells. TMOMP samples and standards (2.5 μg, 7.5, μg and 15 μg) were heated to 100°C for five minutes diluted 1:1 in sample buffer (Appendix 1.11) before loading onto gels along with medium range molecular weight markers (Sigma-Aldrich) diluted 1:1 in sample buffer. Gels were electrophoresed at 200 mV and 70 mA for 45 minutes or until the bromophenol blue in the sample buffer passed the end of the gel matrix. The gels were carefully removed and stained with Coomassie Blue (Sigma-Aldrich) for five minutes, after which they were destained over night in acid-alcohol (Appendix 1.12) and imaged using a flatbed gel-scanner (Bio-Rad Laboratories).

2.6.6. 1D gel densitometery

The protein concentration in SDS-PAGE bands was estimated by densitometery using the software package Molecular Analyst/PC (Bio-Rad Laboratories). Briefly, the OD of the TMOMP standards were used to generate a standard curve from which the amount of TMOMP present in the samples was extrapolated. TMOMP samples were then diluted to 2 mg/ml in column buffer, filter sterilised and stored in 200μl aliquots at -70°C. The molecular weight of the product was compared against the molecular weight standards.

2.7. Lymphocyte stimulation assay

Antigens and mitogens were added to the central 60 wells of Nunc 96-well round bottomed microtitre plates (GIBCO BRL) diluted in 100 μl volumes of PBM culture medium. In the case of TMOMP, which was insoluble at the low concentrations of SDS required for cell culture, volumes of 0.5 - 2 μl of 1 mg/ml TMOMP in 40 mM Phosphate buffer + 0.1% SDS were added directly to the bottom of empty wells before being made up to 100 μl with PBM culture medium. 100 μl/well of ovine PBM at a density of $2X10^6$ viable cells/ml in PBM culture medium were then added to plates and cultured for 3 days. 50 μl of PBM culture medium containing 100 nmol of ^{3}H–thymidine with a specific activity of 185Gbq/mmol (Amersham Pharmacia Biotech UK, Little Chalfont, UK) were added to each well and the culture incubated for a further 16 hours. Cultures were then harvested onto glass fibre filters (Packard Instruments B. V. Chemical Operations, Groningen, The Netherlands) using a Micromate 196 Harvester (Packard Instruments, Pangbourne, UK). Wells were then washed with deionised water and harvested a further three times. The filters were allowed to dry before the cell associated radioactivity (Counts per minute: CPM) was measured using a MATRIX Direct β Counter 96 (Packard Instruments).

Chapter 3.0

Initial feasibility studies and development of an automated image analysis solution for measuring chlamydial growth *in vitro*

3.1. Introduction

Much of the work published on anti-chlamydial pharmaceuticals and immune mechanisms has been heavily dependent on the accurate measurement of chlamydial growth *in vitro*. Traditionally, enumeration of chlamydial inclusion bodies by eye has been the most common method of measuring chlamydial growth *in vitro* and it is still widely used today [Kane and Byrne, 1998; Mehta *et al*, 1998; Pudjiatmoko *et al*, 1998; Roblin and Hammerschlag, 1998; Ramsey *et al*, 1998; Su and Caldwell, 1998]. However, there are several drawbacks to measuring chlamydial growth in this way. Considerable amounts of time must be set aside for counting inclusions, and without the implementation of double blind counting systems, results are open to subjective error. In addition, measurement of secondary parameters of chlamydial growth such as host cell lysis and inclusion size are so time consuming that they are usually ignored or only speculated upon.

Procedures for staining inclusions vary widely, but cultures are typically fixed at 48-72 hours after infection to ensure that any inclusion bodies present can be resolved by light microscopy. Chlamydiae can be differentiated from cellular background using a number of vital dyes. These include: Giemsa [Johnson, 1975]; Ziehl Neelsen's Carbo fuchsin [Stamp *et al*, 1950]; methylene blue [Johnson *et al*, 1978]; and toluidine blue [Mohammed and Hillary, 1984]. Alternatively, infected cells can be probed with anti-chlamydial monoclonal or polyclonal antibodies which in turn can be labelled by antibodies conjugated to fluorochromes or enzymes allowing inclusions to be differentiated from cellular background on the basis of deposition of insoluble coloured product or fluorescence.

Whilst the technology to automate the measurement and enumeration of chlamydial inclusion bodies has existed for some time, it has not as yet been implemented. The requirement for an rapid, easy to use and accurate replacement for counting and measurement of chlamydial inclusion bodies by eye, precipitated the development of a suite of NIH Image based macros, Inclusion Counter v1.0. This chapter describes the development and evaluation of Inclusion Counter v1.0.

3.2. Materials and Methods

3.2.1 Preparation of cells and chlamydiae for imaging

100 μl aliquots of ST.6 cells were seeded into a 96-well flat-bottomed microtitre plate at a concentration of $5x10^4$ cells/ml in IMDM+5% FBS and propagated under standard conditions (Chapter 2.1.1.). *C. psittaci* (ovine abortion strain S26/3) was removed from storage at -70°C (Chapter 2.1.8.) and diluted in IMDM+2% FBS to give a final concentration of $2x10^5$ IFU/ml. The resultant suspension of chlamydiae was diluted a further 8 times at a ratio of 1:1 in IMDM+2% FBS to give a total of 9 Log_2 serial dilutions of S26/3 *C. psittaci* (Table 3.1).

Table 3.1: Concentrations of chlamydiae used to infect ST.6 cultures

Dilution	IFU/ml	IFU/well
1	200000	20000
2	100000	10000
3	50000	5000
4	25000	2500
5	12500	1250
6	6250	625
7	3125	312.5
8	1562.5	156.25
9	781.25	78.125

After 48 hours the supernatants of the ST.6 cultures were discarded. 100 μl aliquots of IMDM+2% FBS were added to the outermost wells of the plate and to all the wells in column 11. Six replicates of 100 μl of each dilution of S26/3 *C. psittaci* were added to the remaining wells. Cultures were incubated under standard conditions (Chapter 2.1.1.) for 6 hours, after which the supernatants were discarded and replaced with 200 μl of IMDM+2% FBS. The cultures were then incubated for a further 66 hours, after which they were fixed and stained with MZN by the procedure described previously, using methyl blue as a counter stain (Chapter 2.4.2.).

3.2.2 Image acquisition

200 24-bit RGB colour images were acquired at a magnification of x125 following the procedure described in Chapter 2.4.5. During acquisition the images were automatically saved with a sequentially numbered suffix in the following format: image.0001; image.0002 .... image.0200.

3.2.3 Manual image analysis of *C. psittaci* inclusion bodies

Five images were selected for preliminary image analysis to determine which of the morphological features of chlamydial inclusion bodies could be used as the basis of an automated system for their enumeration and measurement. Each 24-bit colour TIFF image was opened in NIH Image 1.61 [Rasband and Bright, 1995] as a stack of three greyscale images (RGB stack), each image in the stack representing one of the Red (Figure 3.1B), Green (Figure 3.1C) and Blue colour (Figure 3.1D) channels. An indexed colour image was then automatically created from the RGB stack using NIH Image's custom 256 colour palette. The entire image was outlined using the *rectangular selection tool* to create a region of interest (ROI) that excluded any spurious data produced by the frame grabber along edges of the image. Using NIH Image's *histogram function*, pixel greylevel values were plotted against frequency for each colour channel of all five images.

In the Indexed colour image, inclusion bodies were manually outlined using the *freehand selection tool*. After outlining each inclusion body, the outline was transposed to the RGB stack using the *Restore Selection* command. The area, mean greylevel value, Standard deviation from the mean greylevel value and roundness of each inclusion was then measured for each channel in the RGB stack. The results of these measurements were used as the basis for the design of Inclusion Counter v1.0.

3.2.4 Automated enumeration and measurement of inclusions

Inclusion Counter v1.0, a suite of macros written for NIH Image 1.61, was designed and developed for counting and measuring chlamydial inclusion bodies in cell culture. The result generated by Inclusion Counter v1.0 were compared for accuracy against results generated by manually measuring inclusions in 200 images.

3.2.5 Semi-automated measurement of *C. psittaci* inclusion bodies

A semi-automated system was designed and used to assign definitive and verifiable values for the number of inclusions, mean inclusion area and total area occupied by inclusions to each of the 200 digital images.

3.2.6 Statistical Analysis

Results obtained using manual and automated methods were compared by simple linear regression.

3.3 Results

3.3.1 Chlamydial growth and image acquisition

S26/3 *C. psittaci* EBs were titrated onto ST.6 cultures previously grown to confluence in a 96-well flat-bottomed microtitre plate. The concentration range of EBs used to infect the ST.6 cultures resulted in a logarithmic (Log_2) distribution of inclusion bodies across the plate, allowing acquisition of images containing a broad range of inclusion numbers. After the cultures had been stained and air dried, the 96-well flat-bottomed microtitre plate was inverted and imaged at a magnification of x125 using a conventional compound microscope. In general the specificity of the MZN stain was acceptable, although there were some notable exceptions. Some of the smaller inclusions stained poorly (Figure 3.1A; inclusion bodies #9 and #10) and in some cases cellular debris stained positively with MZN (Figure 3.1A: arrow). Images were digitised at a resolution of 700x572 pixels and 24-bit colour depth using a 3-CCD Camera module and a frame grabber mounted in a Power Macintosh desktop computer. The resultant images were of a high enough quality to be used for image analysis (Figure 3.1A), despite the fact that they were acquired through plastic with a conventional objective lens designed for imaging through glass coverslips.

Cells which had been infected with the highest concentration of EBs were heavily lysed by 72 hours and were not used for imaging. Four non-overlapping images were acquired from each well of the remaining infected cultures giving a total of 192 images of cells infected with various numbers of chlamydiae. A further 8 images were acquired from wells containing uninfected cultures to provide negative controls.

Figure 3.1A: 24-bit RGB colour image of ST.6 cells and inclusion bodies

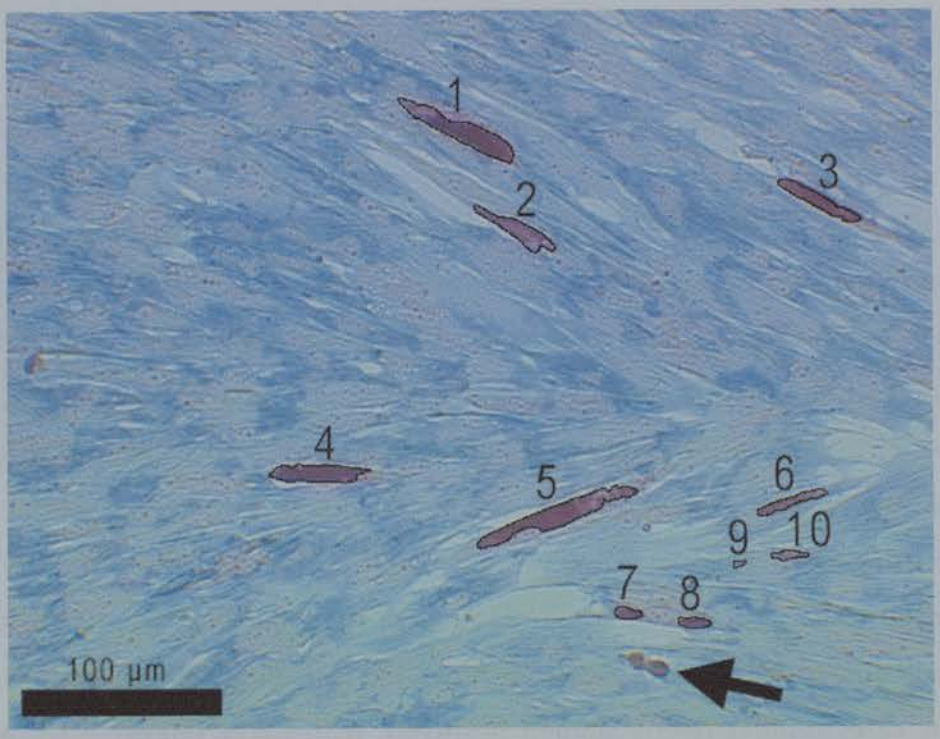

Inclusion Bodies are outlined and numbered, artefacts are highighted (arrow).

Figure 3.1B: The red channel component of Figure 3.1A

Figure 3.1C: The green channel component of Figure 3.1A

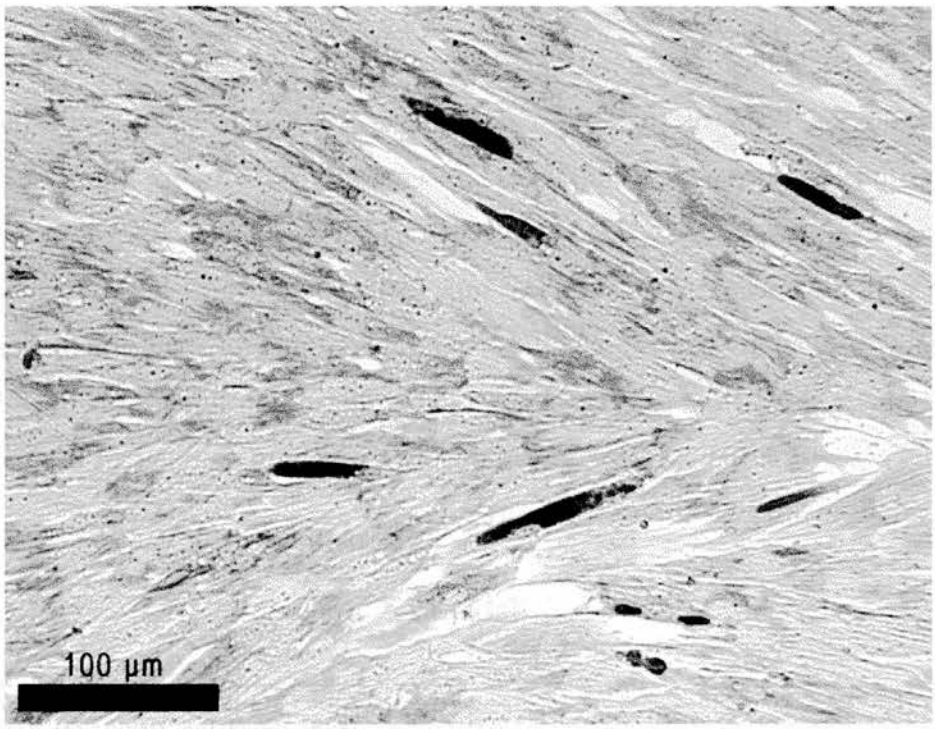

Figure 3.1D: The blue channel component of Figure 3.1A

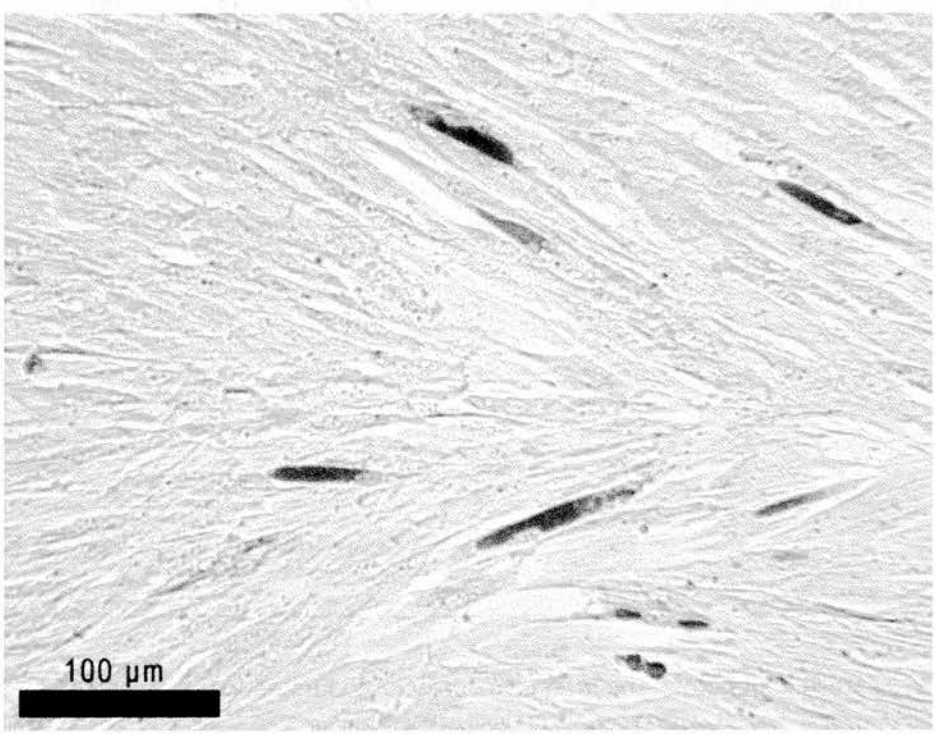

3.3.2 Preliminary image analysis

Images of ST.6 cells infected with 26/3 *C. psittaci* were selected for preliminary analysis on the basis of the following criteria: the intensity and specificity of staining in selected images should be representative of the entire batch of images; variations in inclusion body size should also be representative; each image should contain enough infected cells to allow morphology studies to be performed on a significant number of inclusion bodies; but the number of inclusion bodies in a selected image should not be high enough to significantly influence the overall pixel frequency/greylevel value histogram in any of the colour channels of the image. A typical example image is shown in Figure 3.1.

Table 3.2

Inclusion Body #	AREA /pixels	Roundness	MEAN Greylevel Value: Red	Standard deviation from the mean Greylevel Value: Red	MEAN Greylevel Value: Green	Standard deviation from the mean Greylevel Value: Green	MEAN Greylevel Value: Blue	Standard deviation from the mean Greylevel Value: Blue
1	1103	0.2375	135	25	185	28	132	32
2	563	0.2251	110	22	150	25	94	19
3	535	0.2913	124	14	191	15	141	14
4	601	0.2908	152	12	193	10	146	14
5	1221	0.1679	122	22	173	28	130	26
6	253	0.2252	108	17	153	23	114	16
7	117	0.5871	125	17	176	19	130	18
8	121	0.5141	133	15	181	16	130	25
9	13	0.7786	99	7	123	9	81	9
10	88	0.2851	95	10	127	13	87	11
Mean Value	462	0.3603	120	16	165	19	118	18
Std. Dev. from mean	427	0.1983	18	6	26	7	23	7
Minimum Threshold	N.A.	N.A.	85	5	114	5	72	4
Maximum Threshold	N.A.	N.A.	156	27	216	33	165	33
Minimum Value	13	0.1679	95	7	123	9	81	9
Maximum Value	1221	0.7786	152	25	193	28	146	32

Table 3.2: Results generated by manually outlining and measuring the individual inclusion bodies in Figure 3.1. Inclusion body number correlates directly to the number assigned to inclusion bodies in figure 3.1A.

Area was calculated using the standard procedure employed by NIH Image. The number of pixels within a selection, the outline of each inclusion body, were counted and the results were then converted into real units using a predetermined scaling factor for the image. In this case assigning real units to the area measurement was not of interest and the area of inclusion bodies was expressed in pixels, using a scaling factor of 1. The perimeter of each inclusion body was also measured using the standard procedure applied by NIH image (data not shown). A number of approaches to perimeter measurement exist in the literature [Russ, 1998]. NIH image uses the following approach, perimeter pixels of an object or those pixels which make up the outline selection of the object are recorded. Corner and non-corner pixels are defined and the perimeter is then calculated using the following equation:

$$\text{Perimeter} = \sqrt{2}\sum \text{Pixels}_{\text{Corner}} + \sum \text{Pixels}_{\text{Non-Corner}}$$

Roundness was then calculated from the area and perimeter values using the following equation:

$$\text{Roundness} = \frac{4 \times \pi \times \text{Area}}{\text{Perimeter}^{2}}$$

This is one of the most commonly used equations for defining the roundness or circularity of an object, usually referred to as Formfactor [Russ, 1998], and produces a value between 0 and 1, where a perfect circle has a value of 1. In this case, roundness was calculated in NIH image using a custom designed macro. Alternatively, it can be calculated in a separate spreadsheet application.

The mean greylevel values of the pixels and the standard deviation from the mean greylevel value within each inclusion body image were calculated for all three colour channels for each inclusion body. Area values for inclusion bodies varied significantly, standard deviation from the mean area was almost as large as the mean area value itself, and the smallest inclusions had area values close to the resolution of the CCD camera at this level of magnification. Roundness values for inclusion bodies varied widely. The standard deviation from the mean greylevel

values within each inclusion body were generally quite low, approximately 10% of the mean greylevel value of each inclusion body.

The mean and standard deviation from the mean of the mean greylevel values of each inclusion body was then calculated for the image as a whole. These values were used to calculate a threshold for the image in each colour channel as follows:

Minimum Threshold = Mean Greylevel Value - 2(Standard Deviations)

and

Maximum Threshold = Mean Greylevel Value + 2(Standard Deviations)

Defining a threshold for the greylevel values of the pixels within an image instructs the computer to ignore any pixels which fall outside the range of the threshold. The results of applying the calculated threshold ranges to the images in Figure 3.1 are shown as insets in Figure 3.2.

Histograms of pixel frequency plotted against the pixel greylevel values were generated for each colour channel using NIH Images built in *histogram function* (Figure 3.2). The overall profile of the histograms did not differ significantly from the histograms produced for images of uninfected cells (Figures 3.3A and 3.4) and there was no evidence of a second population of pixels with higher greylevel values as seen in images of heavily infected cells (Figure 3.3B and 3.5). The calculated values for the threshold ranges in the green and blue channels produced relatively good segmentation of inclusion bodies from cellular background compared to the red channel. This was expected since the threshold range in the red channel intruded into the main peak of the histogram in that channel. However, some components of the cellular background were segmented with inclusion bodies in both the green and blue channels. This was particularly obvious when similar threshold ranges calculated from all five of the images selected for preliminary analysis (Table 3.3) were applied to images of uninfected cells (Figure 3.4B and Figure 3.4C).

Table 3.3: Results generated by manually outlining and measuring *C. psittaci* inclusion bodies from 5 different images

Inclusion Body #	AREA /pixels	Roundness	MEAN Greylevel Value: Red	Standard deviation from the mean Greylevel Value: Red	MEAN Greylevel Value: Green	Standard deviation from the mean Greylevel Value: Green	MEAN Greylevel Value: Blue	Standard deviation from the mean Greylevel Value: Blue
1	3	0.5890	140	18	187	21	57	14
2	12	0.8507	139	9	197	11	98	14
3	13	0.7786	99	7	123	9	80	8
4	26	0.3620	107	12	119	17	65	14
5	26	0.6325	110	13	141	12	97	8
6	37	0.7457	109	9	128	8	66	16
7	40	0.6239	128	17	159	11	99	14
8	40	0.7089	157	10	194	9	129	10
9	41	0.5493	115	13	158	14	99	8
10	44	0.9680	136	14	190	18	99	25
11	77	0.3669	101	13	129	17	80	12
12	80	0.4437	93	9	119	14	68	10
13	87	0.3434	69	7	112	14	68	12
14	88	0.2851	95	10	127	13	83	10
15	101	0.3615	150	14	186	11	113	12
16	115	0.8652	104	15	166	24	97	20
17	117	0.5871	125	17	176	19	130	16
18	121	0.5141	133	15	181	16	130	24
19	128	0.5939	97	12	155	15	81	16
20	142	0.8208	111	15	170	16	99	14
21	211	0.4211	118	16	177	17	98	24
22	237	0.4010	113	23	163	31	129	14
23	244	0.4508	117	13	189	21	132	16
24	253	0.2252	108	17	153	23	114	16
25	295	0.3350	140	16	185	16	131	14
26	299	0.1958	131	17	159	21	100	16
27	309	0.6018	117	15	186	13	97	16
28	396	0.3355	123	10	164	12	98	10
29	428	0.3244	116	12	176	20	114	16
30	439	0.4680	106	11	145	23	112	16
31	471	0.6196	161	13	198	14	128	17
32	486	0.3346	97	13	126	17	82	10
33	527	0.4131	135	19	175	24	115	16
34	528	0.5201	123	17	179	25	115	21
35	535	0.2913	124	14	191	15	133	12
36	563	0.2251	110	22	150	25	82	17
37	565	0.3969	146	19	188	19	135	14
38	601	0.2908	152	12	193	10	130	12
39	603	0.2996	134	16	195	18	134	16
40	721	0.2652	126	15	167	21	98	17
41	743	0.5061	119	14	189	10	130	14
42	773	0.2587	102	15	141	18	83	12
43	783	0.4398	123	11	180	16	116	12
44	811	0.2538	81	13	128	24	64	21
45	842	0.5355	147	12	196	13	131	16
46	958	0.2689	124	15	164	26	113	20
47	1037	0.3563	87	12	157	25	98	21
48	1103	0.2375	135	25	185	28	132	29
49	1167	0.4024	159	16	197	14	133	17
50	1221	0.1679	122	22	173	28	130	25
51	1297	0.3747	153	14	192	17	134	16
Mean Value	408	0.4550	121	14	166	18	105	16
Std. Dev. from mean	367	0.1924	21	4	25	6	23	5
Minimum Threshold	N.A.	N.A.	79	7	116	6	59	7
Maximum Threshold	N.A.	N.A.	162	22	217	29	152	25
Minimum Value	3	0.1679	69	7	112	8	57	8
Maximum Value	1297	0.9680	161	25	198	31	135	29

Figure 3.2

A: Pixel frequency plotted against pixel greylevel value for the Red channel of the image in Figure 3.1A. The cursor bar represents the threshold range calculated from the measurements in Table 3.2. The result of applying this threshold to the image in Figure 3.1B are displayed as a binary image inset in the top right of the figure.

B: Pixel frequency plotted against pixel greylevel value for the green channel of the image in Figure 3.1A. The cursor bar represents the threshold range calculated from the measurements in Table 3.2. The result of applying this threshold to the image in Figure 3.1C are displayed as a binary image inset in the top right of the figure.

C: Pixel frequency plotted against pixel greylevel value for the green channel of the image in Figure 3.1A. The cursor bar represents the threshold range calculated from the measurements in Table 3.2. The result of applying this threshold to the image in Figure 3.1D are displayed as a binary image inset in the top right of the figure.

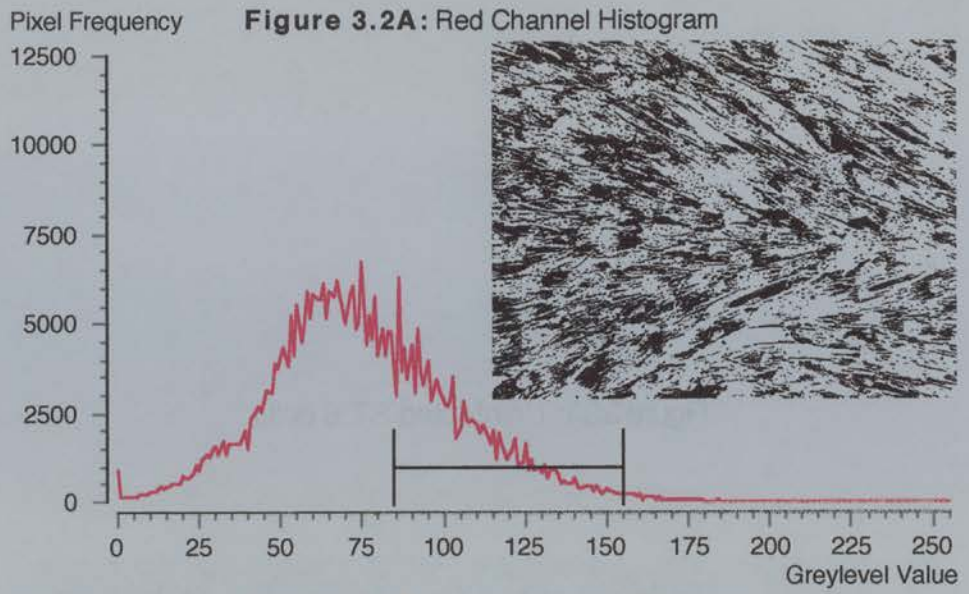

Figure 3.2A: Red Channel Histogram

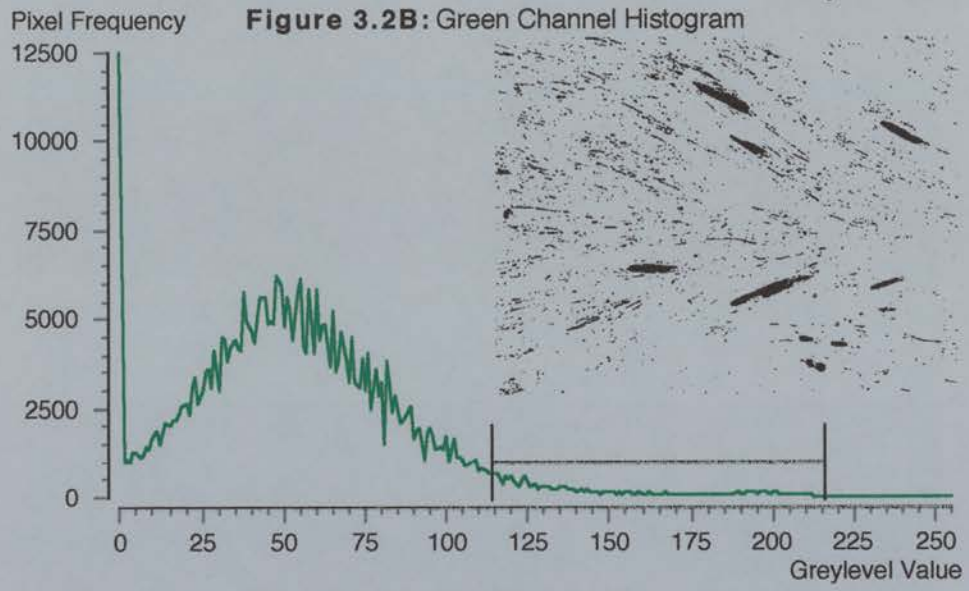

Figure 3.2B: Green Channel Histogram

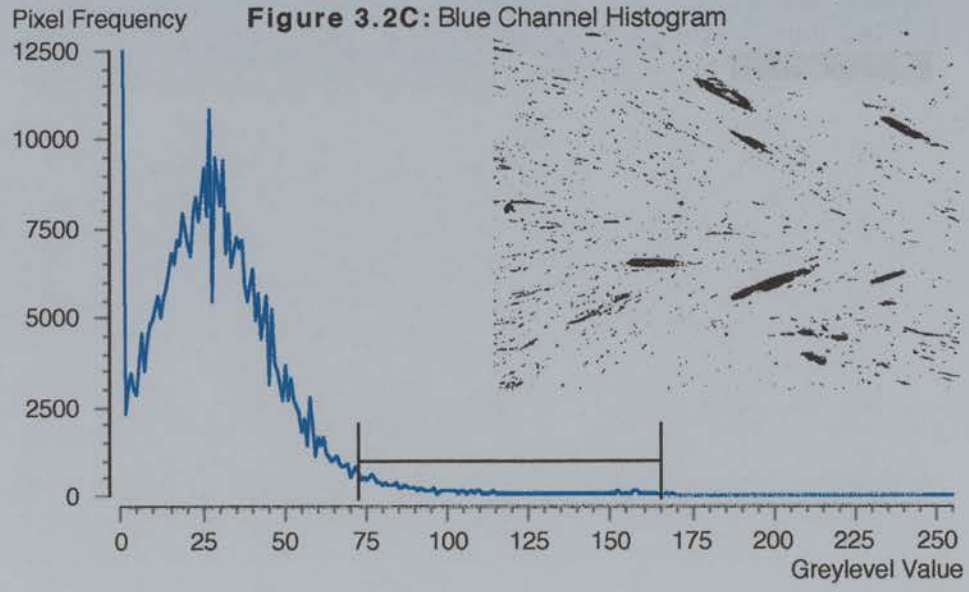

Figure 3.2C: Blue Channel Histogram

Figure 3.3A: Uninfected ST.6 cells

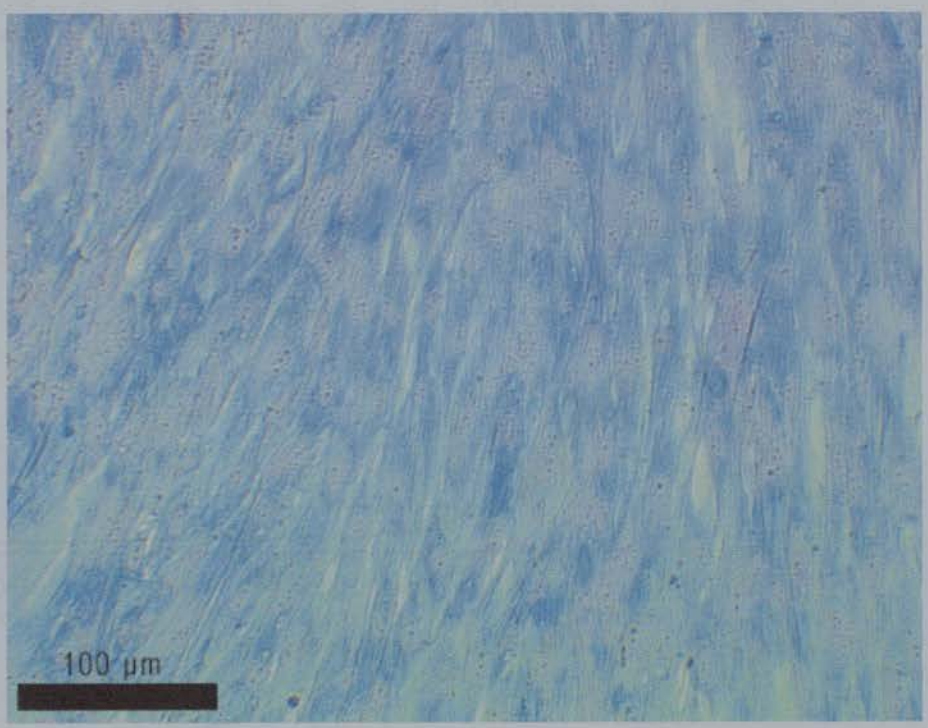

Figure 3.3B: Heavily infected ST.6 cells

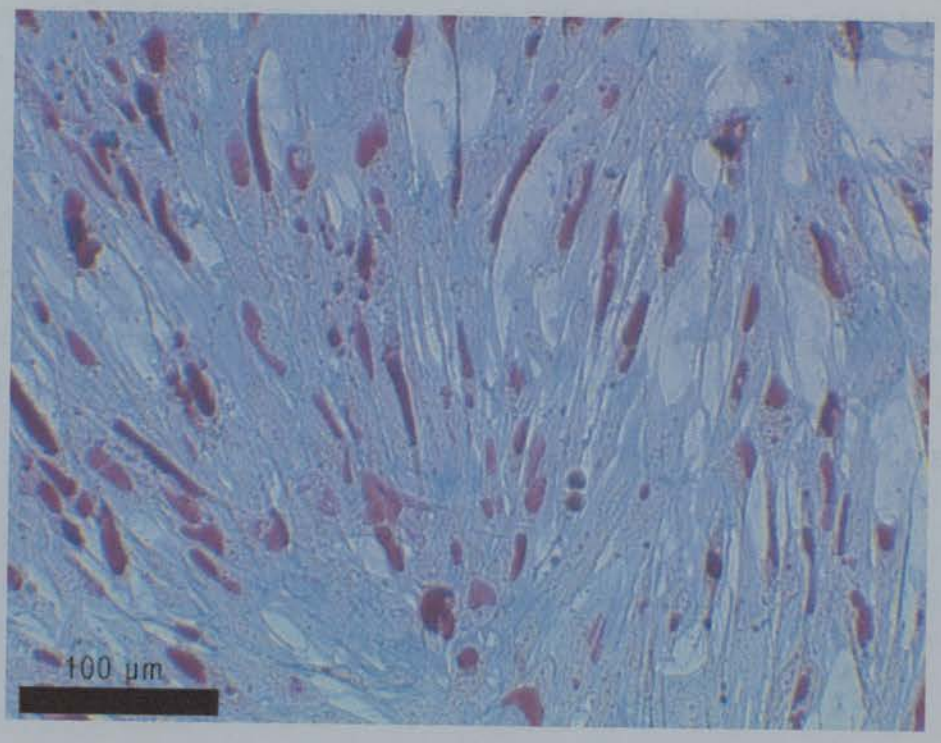

Figure 3.4

A: Pixel frequency plotted against pixel greylevel value for the Red channel of the image of uninfected cells in Figure 3.3A. The cursor bar represents the threshold range calculated from the measurements in Table 3.3. The result of applying this threshold to the red channel component of the image in Figure 3.3A are displayed as a binary image inset in the top right of the figure.

B: Pixel frequency plotted against pixel greylevel value for the green channel of the image of uninfected cells in Figure 3.3A. The cursor bar represents the threshold range calculated from the measurements in Table 3.3. The result of applying this threshold to the green channel component of the image in Figure 3.3A are displayed as a binary image inset in the top right of the figure.

C: Pixel frequency plotted against pixel greylevel value for the blue channel of the image of uninfected cells in Figure 3.3A. The cursor bar represents the threshold range calculated from the measurements in Table 3.3. The result of applying this threshold to the blue channel component of the image in Figure 3.3A are displayed as a binary image inset in the top right of the figure.

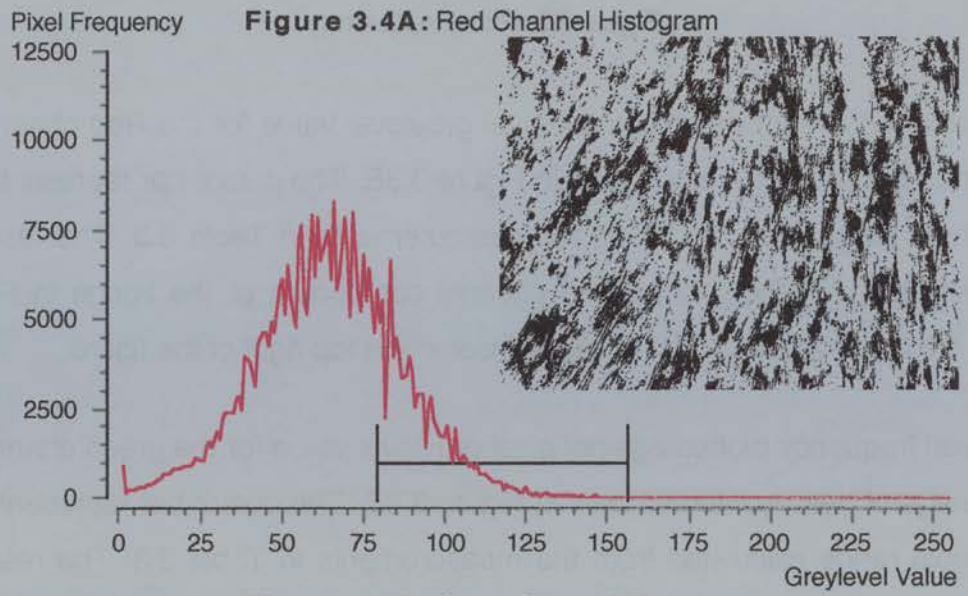

Figure 3.4A: Red Channel Histogram

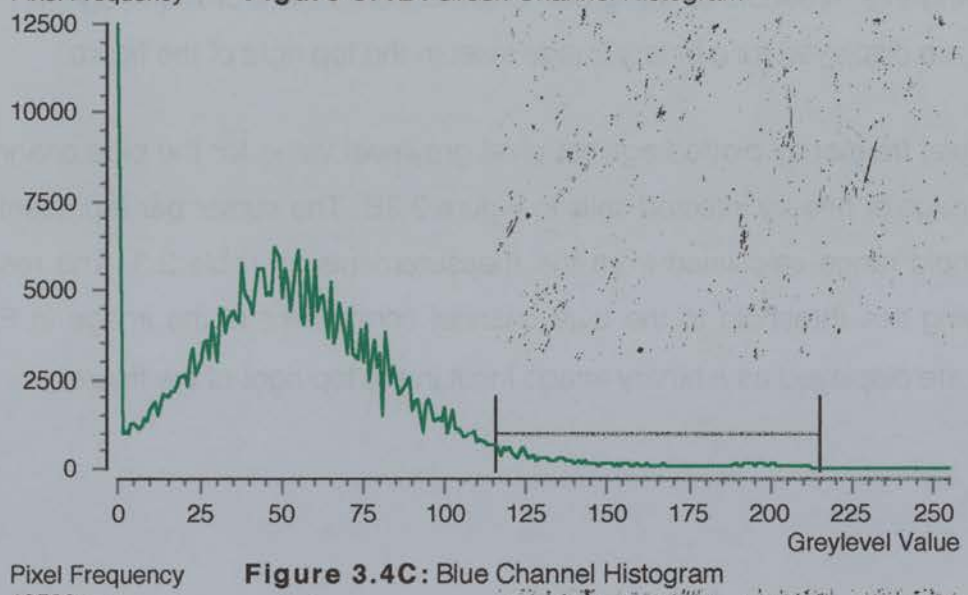

Figure 3.4B: Green Channel Histogram

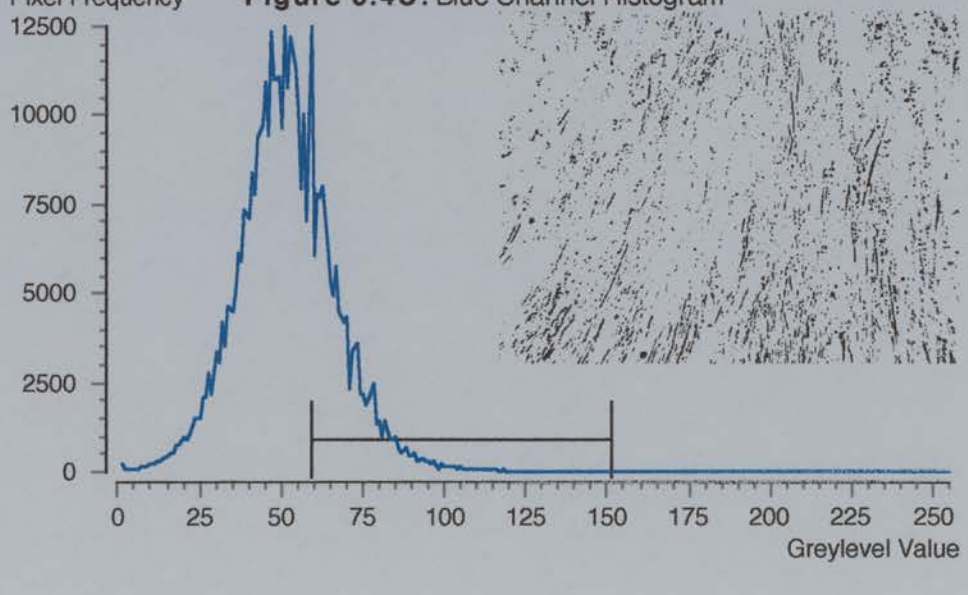

Figure 3.4C: Blue Channel Histogram

Figure 3.5: Pixel frequency

A: Pixel frequency plotted against pixel greylevel value for the Red channel of the image of heavily infected cells in Figure 3.3B. The cursor bar represents the threshold range calculated from the measurements in Table 3.3. The result of applying this threshold to the red channel component of the image in Figure 3.3B are displayed as a binary image inset in the top right of the figure.

B: Pixel frequency plotted against pixel greylevel value for the green channel of the image of heavily infected cells in Figure 3.3B. The cursor bar represents the threshold range calculated from the measurements in Table 3.3. The result of applying this threshold to the green channel component of the image in Figure 3.3B are displayed as a binary image inset in the top right of the figure.

C: Pixel frequency plotted against pixel greylevel value for the blue channel of the image of heavily infected cells in Figure 3.3B. The cursor bar represents the threshold range calculated from the measurements in Table 3.3. The result of applying this threshold to the blue channel component of the image in Figure 3.3B are displayed as a binary image inset in the top right of the figure.

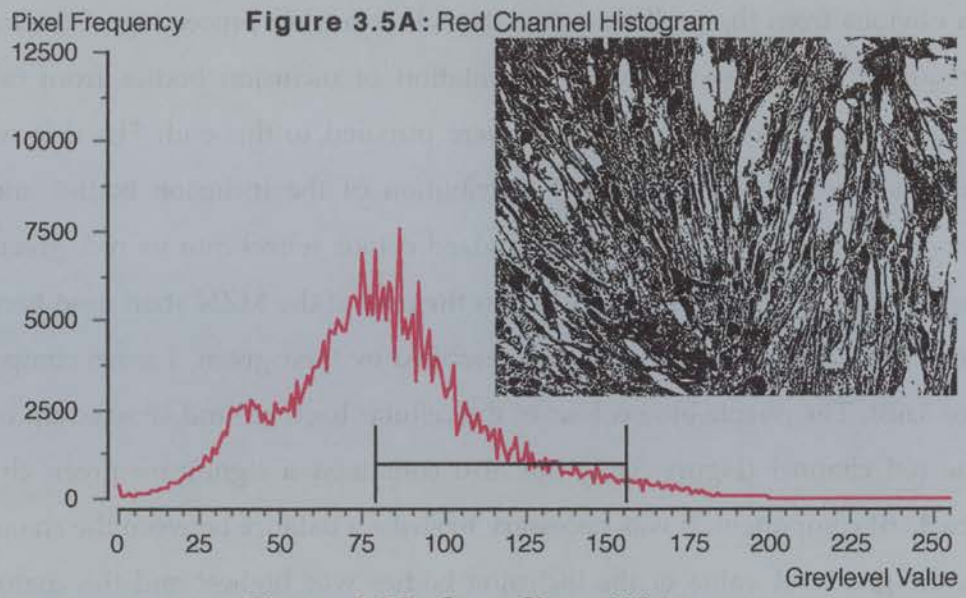

Figure 3.5A: Red Channel Histogram

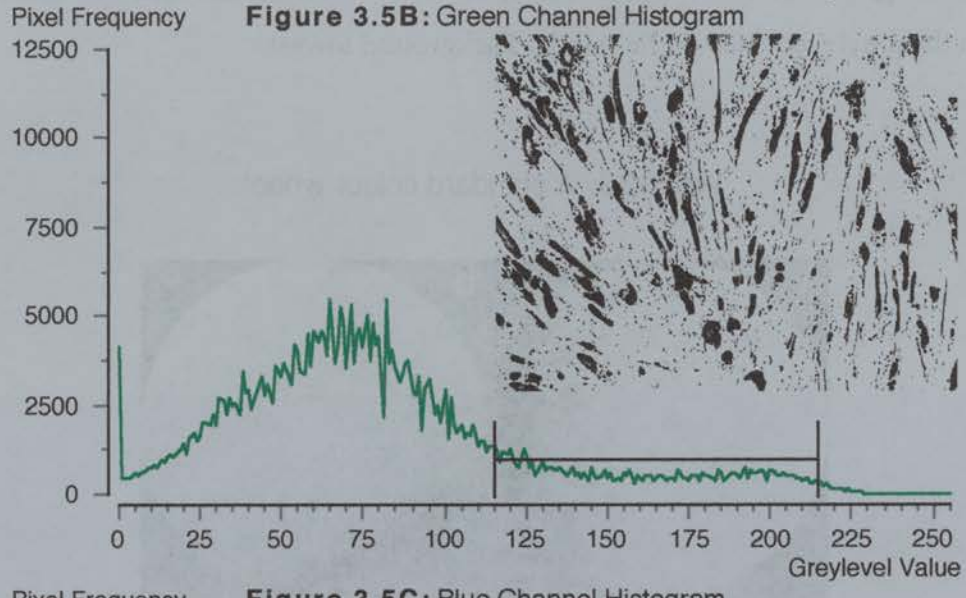

Figure 3.5B: Green Channel Histogram

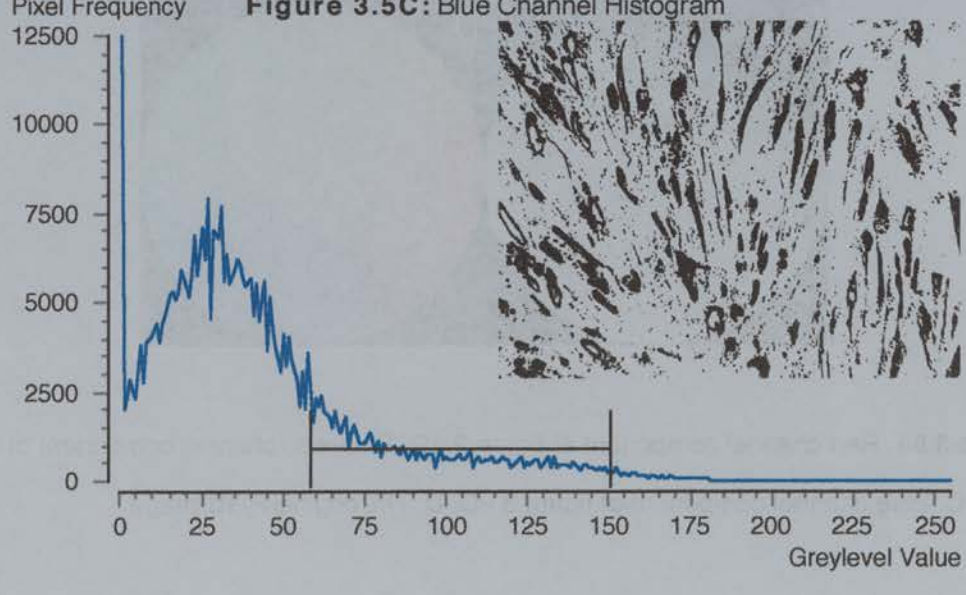

Figure 3.5C: Blue Channel Histogram

It was obvious from the preliminary analysis that further processing of the images was required to achieve optimal segmentation of inclusion bodies from cellular background. A number of approaches were pursued to this end. The first was to further examine the colour channel distribution of the inclusion bodies and the cellular background. Dissection of a standard colour wheel into its red, green and blue components is shown in figure 3.6. In the case of the MZN stain used here, the colour of the inclusion bodies was best described by their green channel component (Figure 3.6B). The purple-blue colour of the cellular back ground showed up best in the the red channel (Figure 3.6A) but also contained a significant green channel (Figure 3.6B) component. It was necessary to strike a balance between the channel in which the greylevel value of the inclusion bodies was highest and the channel in which the greylevel value of the cellular background lowest.

Figure 3.6: A standard colour wheel

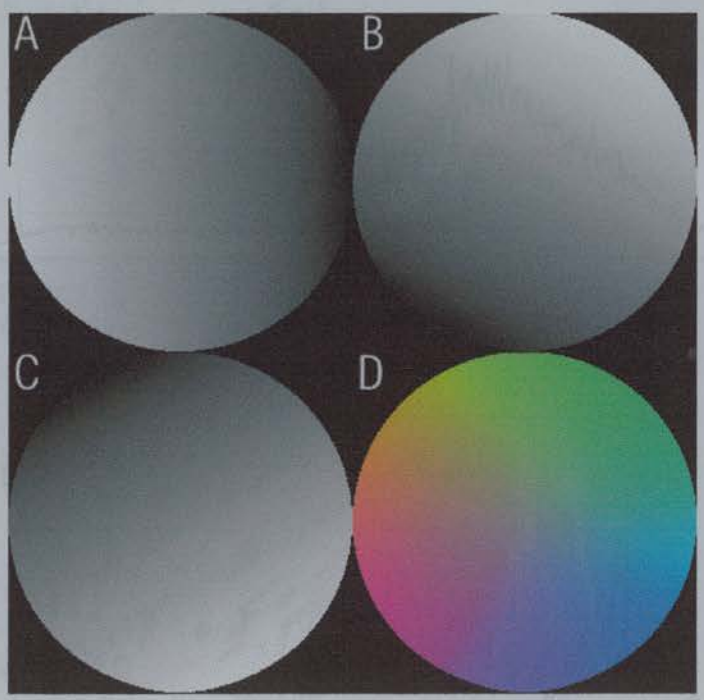

Figure 3.6A: Red channel component of figure 3.6D. B: Green channel component of figure 3.6D. C: Blue channel component of figure 3.6D. D: The original RGB image

The highest contrast between inclusion bodies and the cellular back ground (Figure 3.7) was achieved by averaging the green (Figure 3.1B) and blue channels (Figure 3.1C).

Figure 3.7: The result of averaging the green and blue channels of the image in Figure 3.1A

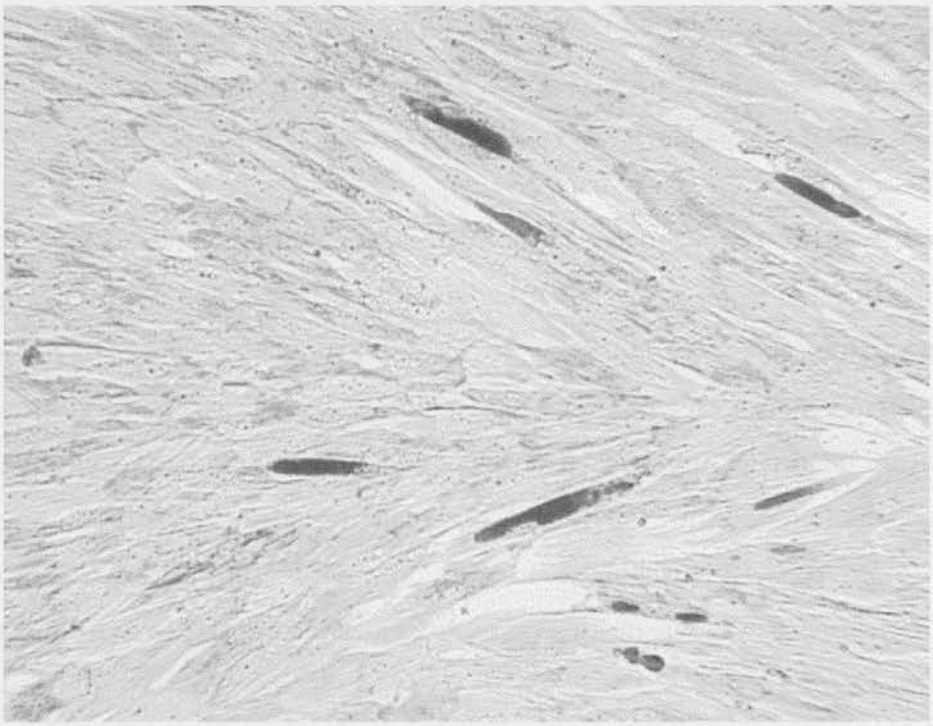

A number of different background subtraction techniques were examined with respect to improving the segmentation of inclusion bodies from the cellular background. The standard approach to correcting images for a variation in light levels resulting from defects in the optical quality of the microscope or CCD camera used for acquisition of the images is simply to subtract an image of the background, in this case an empty well from a 96–well flat-bottomed microtitre plate, from the images which require correction [Russ, 1998]. The problems associated with segmenting inclusion bodies from cellular background, encountered here, arose from irregularities in the optical quality of individual wells and from differences in the growth and arrangement of the ST.6 cell monolayers. Whilst the above approach is very useful for removing constant background irregularities, due for example to a misaligned condenser, it was not used here since the variations in cellular

background differed from image to image.

Rank levelling, another approach to background subtraction, is more useful when dealing with local variations in background and is strictly dependent on the content of the image to which it is applied. The procedure for rank levelling is fairly straightforward. Briefly, a copy was made of the original image (Figure 3.7), the copy was then subjected to 7 iterations of NIH image's built-in 3x3 neighbourhood minimum rank filter (see Russ (1998) for a full description of rank and kernel based filters) and the result (Figure 3.8A) was subtracted from the original image to produce the final background corrected image (Figure 3.8B).

The problem with this approach is that the number of applications of the minimum rank filter applied to an image must be balanced between removing the objects of interest and preserving variations in background greylevel values. In this case, a relatively large number of iterations was required to remove the largest inclusion bodies from the image in figure 3.8A. As a result, much of the background variation remained unaltered (figure 3.8B) and segmentation of inclusion bodies was not greatly improved by this technique. In addition, rank levelling altered the greylevel values of the pixels in the inclusion bodies as well as the cellular background.

Figure 3.8A: The result of applying 7 iterations of a 3x3 minimum rank filter to the image in Figure 3.7

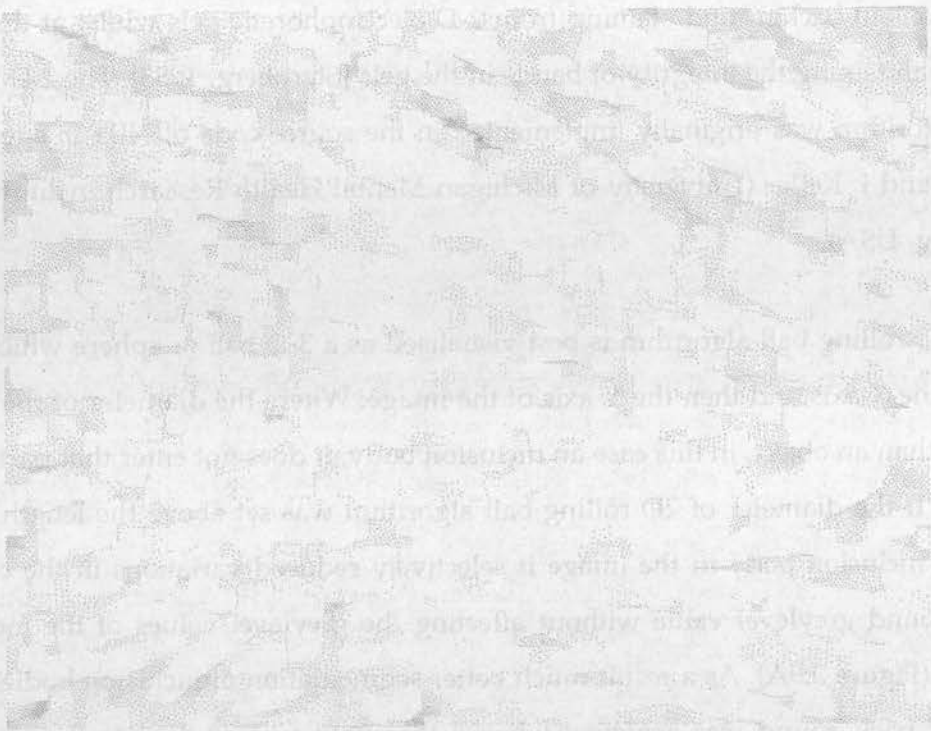

Figure 3.8B: The result of subtracting the image in Figure 3.8A from the image in Figure 3.7

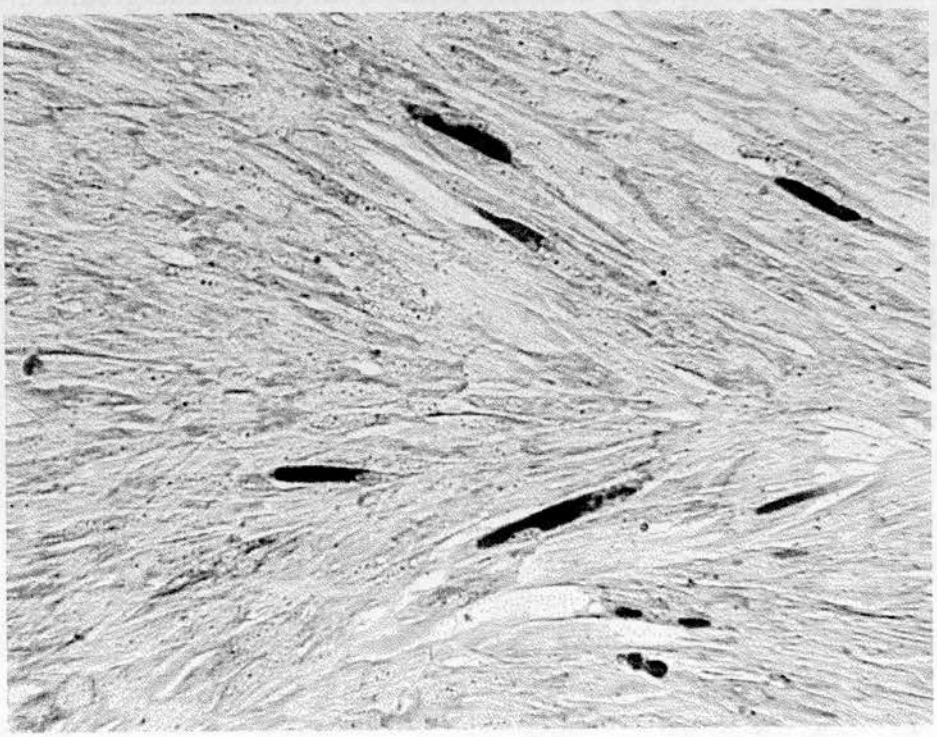

Another form of background subtraction that was investigated was a 2-D rolling ball algorithm. The 2D rolling ball algorithm was originally designed for removing variations in background staining from 2-D electrophoretic gels whilst at the same time maintaining the integrity of bands in the gels [Sternberg, 1983]. The 2-D rolling ball algorithm was originally implemented in the source code of NIH Image by M. Castle and J. Keller (University of Michigan Mental Health Research Institute, East Lansing, USA).

The 2-D rolling ball algorithm is best visualised as a 3-D ball or sphere which rolls along the X-axis and then the Y-axis of the image. Where the diameter of the ball is larger than an object, in this case an inclusion body, it does not enter that part of the image. If the diameter of 2D rolling ball algorithm was set above the length of the largest inclusion body in the image it selectively reduced variations in the cellular background greylevel value without affecting the greylevel values of the inclusion bodies (Figure 3.9A). As a result much better segmentation of inclusion bodies from cellular background was achieved when a threshold was applied to the resultant image (Figure 3.9B). Most importantly it normalised the pixel frequency / greylevel value histograms of the images to which it was applied (Figure 3.10) making and made it much easier to segment inclusion bodies from cellular background in a large number of images by applying the same threshold range to all of the images.

Despite the improvements made in the segmentation of inclusion bodies from cellular background errors in segmentation still occurred. Inclusion bodies #9 and #10 (Figure 3.1A) were not segmented and the cellular debris (Figure 3.1A; arrow) was segmented with the inclusion bodies.

Figure 3.9A: Result of applying a 100 pixel diameter 2-D rolling ball algorithm to figure 3.7

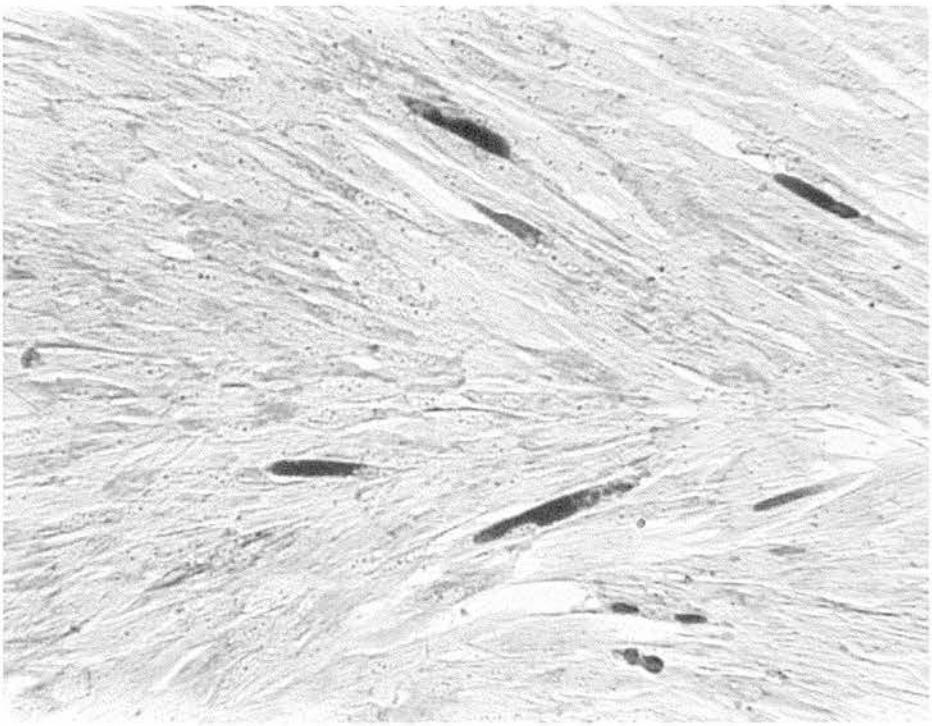

Figure 3.9B: A binary image of Figure 3.9A produced by applying the threshold values calculated for the green channel in Table 3.3

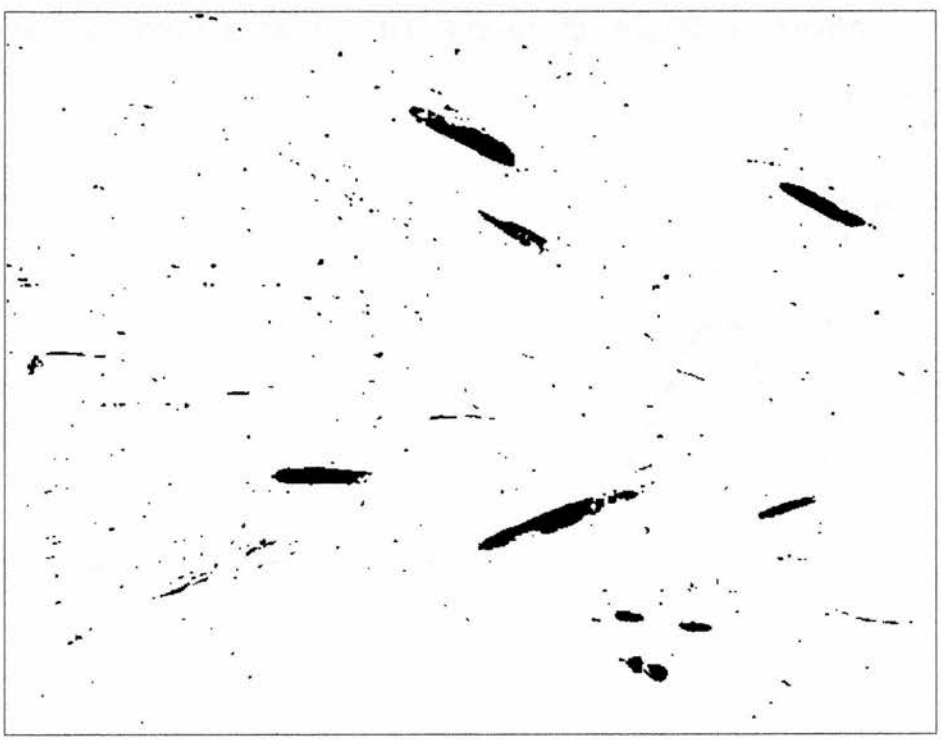

Figure 3.10A: Pixel frequency / greylevel value histograms of the average of the green and blue channels of images from Figures 3.1A(—), 3.3A(—) and 3.3B(—).

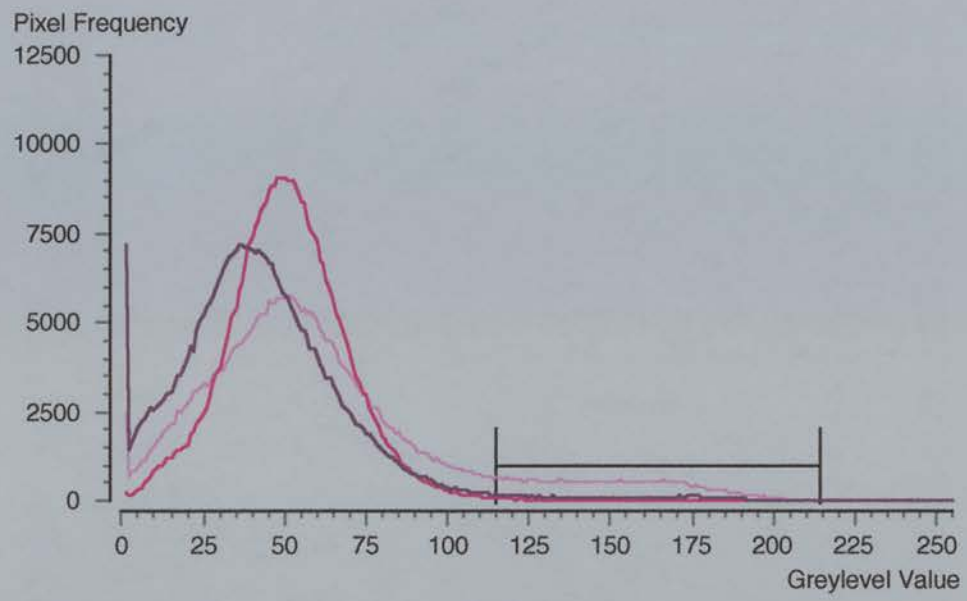

Figure 3.10B: Pixel frequency / greylevel value histograms of the average of the green and blue channels of images from Figures 3.1A(—), 3.3A(—) and 3.3B(—) following a 100 pixel diameter 2-D rolling ball background subtraction.

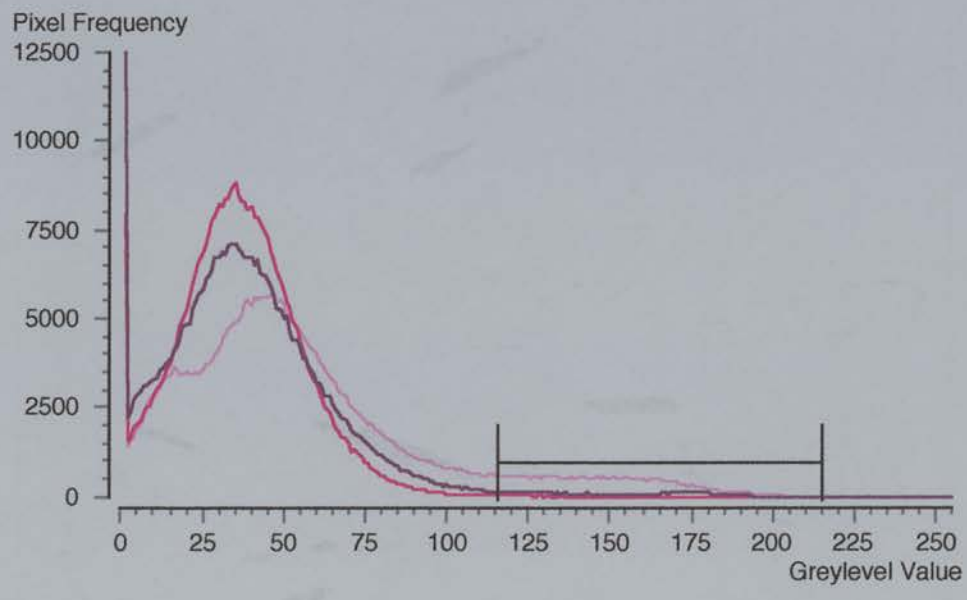

3.3.3 Development of an automated image analysis system for the enumeration and measurement of Chlamydial inclusion bodies

The results of the preliminary image analysis of *C. psittaci* inclusions stained with MZN in ST.6 cells were used as the basis for the design of Inclusion Counter v1.0, an automated image analysis solution for counting and measuring chlamydial inclusion bodies in cell culture based on NIH Image.

3.3.3.1 Universal colour segmentation

The first problem addressed during the design of Inclusion Counter v1.0 was the need for a universal method of colour segmentation that performed equally well with different staining protocols. Inclusion Counter v1.0 was designed not only to allow the operator to choose between a variety of different colour segmentation options but also to prompt the operator into selecting the correct version. A menu option called *Choose a Colour Channel* was developed which produced a range of greyscale images, 3-D surface plots and line profiles of selected inclusion bodies and cellular background in all of the colour channel combinations available. This allowed the operator to see how well inclusion bodies would be differentiated from cellular background using the options available in Inclusion Counter v1.0. The range of colour segmentation options available in Inclusion Counter v1.0 are listed in Table 3.4 in conjunction with suitability for segmenting different hues of stain in both bright field and dark field applications.

Table 3.4: Colour segmentation options available in Inclusion Counter v1.0

Menu Command	Hue of Stain						Black & White	Bright Field/Dark Field
	Magenta	Blue	Cyan	Green	Yellow	Red		
Grey Scale	Variable	Variable	Variable	Variable	Variable	Variable	++	Yes/Yes
24-bit to grey scale	Variable	Variable	Variable	Variable	Variable	Variable	++	Yes/Yes
Red Channel	+	++	+++	++	+	-	+	Yes/Yes
Green Channel	+++	++	+	-	+	++	+++	Yes/Yes
Blue Channel	+	-	+	++	+++	++	++	Yes/Yes
Red and Green Channels	++	+++	++	-	-	-	+	Yes/Yes
Red and Blue Channels	-	-	++	+++	++	-	+	Yes/Yes
Green and Blue Channels	++	-	-	-	++	+++	+	Yes/Yes

3.3.3.2 Guard frame design

The resolution at which digital images can be acquired varies widely. Images acquired using analogue CCD cameras, like the one used here, vary depending on both the video signal (usually PAL or NTSC standard) and the resolution of the frame grabber mounted in the computer. In addition, the wide range of digital cameras that are now available for this kind of application do not adhere to any form of standard with respect to resolution. Another problem that commonly arises during image acquisition is the appearance of spurious information along one or more of the edges of images digitised by a frame grabber (Figure 3.11A). Such

spurious information varies in its location between different cameras and frame grabber boards. It was therefore necessary to design a customisable counting or guard frame that could be adjusted to suit any resolution of image and to exclude areas of the images containing spurious information.

Whilst NIH Image provided a variety of ROI tools which could be used to restrict the area of the images that was measured, it does not implement a true guard frame. Correct implementation of a guard frame is an absolute requirement for accurate counting and measurement of objects within a specified ROI. Figure 3.11A shows a thresholded image and the ROI that was used as a guard frame for processing the image. When NIH Image was instructed to count and measure the thresholded objects within the ROI, it did so regardless of whether they touched the edges of the ROI or not. As a result the number of objects in the ROI was overestimated, since objects were counted when touching all four edges of the image, and the area and morphological measurements were miscalculated because some of the objects touching the edges of the ROI were either truncated by the edge of the image or touched other objects outside the ROI. A customisable guard frame was designed to correct this error. The thresholded image (Figure 3.11A) was converted into a binary image (Figure 3.11B). Objects touching the top and left edges of the guard frame were deleted (Figure 3.11C). NIH Image was then used to return the corrected number of objects within the ROI. The guard frame was then applied to the image for a second time and objects that touched any edge of the guard frame were deleted (Figure 3.11D).

Figure 3.11A: Thresholded image with visible region of interest (dashed line) and spurious information generated by the frame grabber (arrows).

Figure 3.11B: Binary image of thresholded objects in figure 3.11A with visible region of interest (dashed line).

Figure 3.11C: Binary image with visible region of interest (dashed line), objects touching top and left edges were not included in the count (Red)

Figure 3.11D: Binary image with visible region of interest (dashed line), objects touching edges were not measured (RED)

NIH Image was then instructed to perform an analyse particles routine and returned the corrected values for the mean area, standard deviation from the mean area and total area occupied by the objects in the ROI. Table 3.5 illustrates the level of error that occurred when the guard frame was not used.

Table 3.5: Errors incurred by incorrect implementation of the guard frame

	Standard ROI	Guard frame	% Error
Inclusion bodies / ROI	114	105	7.90
Mean Area (Pixels)	395.91	327.01	17.40
Standard deviation (Pixels)	750.55	259.56	65.41
Total area (Pixels)	45134	32047	28.99

The guard frame was implemented in the macro language of NIH Image, allowing the operator to set and record an appropriate guard frame by choosing *Set ROI* from the *Special* menu. Inclusion Counter v1.0 would only analyse images if a guard frame had been set prior to image processing and returned an error message if there was no guard frame available. In addition, the area of the guard frame itself was also measured providing a precise value for the area of the cell monolayer sampled by each image. This approach also allowed a backup copy of the ROI file which specified the guard frame to be saved for later use.

3.3.3.3 Calculation of the 2-D rolling ball

Correct estimation of the diameter of the background subtraction algorithm was critical. If the Diameter was set too low the greyscale values of the inclusion bodies were adversely effected. If the diameter was set too high the background correction was ineffective and computation time was increased. A routine for calculating the diameter of the 2-D rolling ball was adapted from a macro written by Mark Vivino

[Vivino, 1992]. Inclusion Counter v1.0 prompted the operator to measure the length of the largest inclusion body present in the images and returned an estimate of the diameter of the 2-D rolling ball required. In addition it generated a circular ROI which could be moved around each image to ensure that the diameter was correct (Figure 3.12).

Figure 3.12: The interface provided for calculating of the 2-D rolling ball diameter

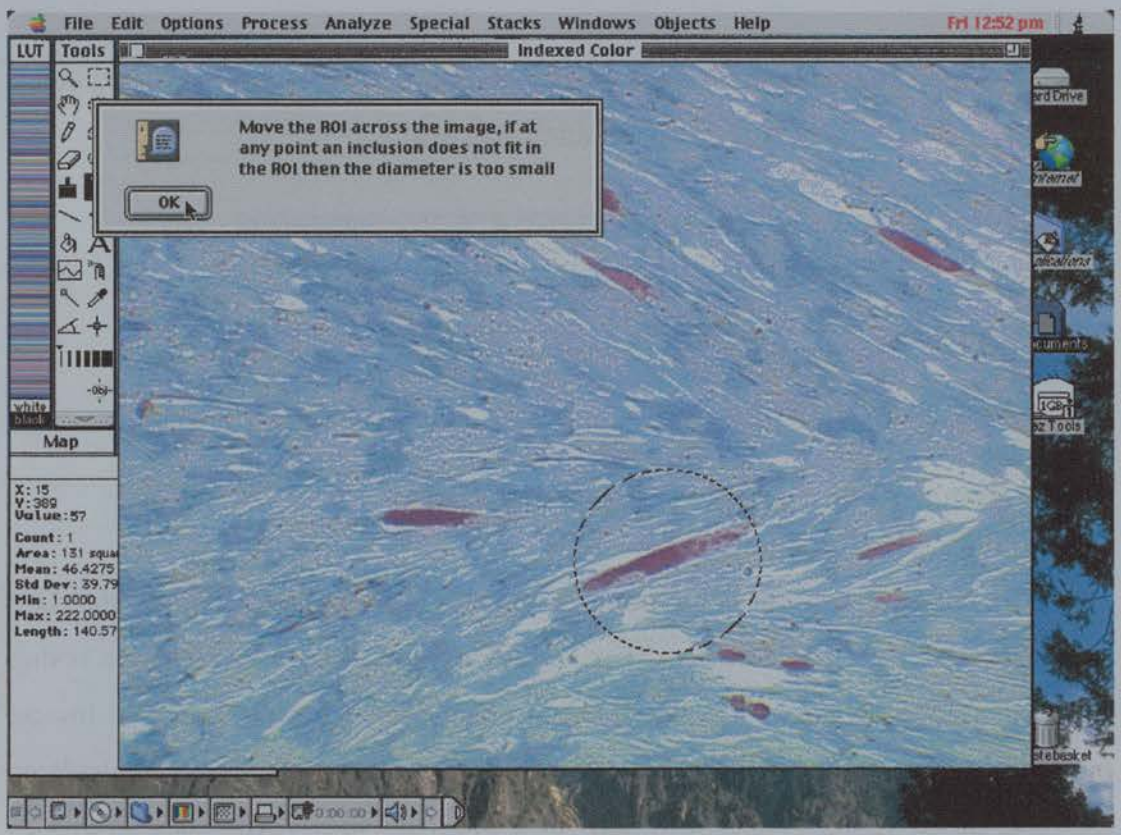

3.3.3.4 Automation of the 2-D rolling ball background subtraction

The operator selected the appropriate menu command from the special menu (Figure 3.13) defining the combination of colour channels to be analysed and entered a value for the diameter of the 2-D rolling ball background subtraction algorithm when prompted. Inclusion Counter v1.0 then automatically preprocessed the images. Automation was achieved through the implementation of a Boolean argument that made use of the numerical suffix of the images.

```
.....
For n:= 1 to 1000 do begin;
Open('Image.',q:4);
.....
```

The Boolean argument above instructed Inclusion Counter v1.0 to sequentially open and process all of the images with names conforming to the format *Image.000n*, where the maximum number of images that can be processed is 999. The results were saved as greyscale images with names in the format of *Subtracted.000n*.

Figure 3.13: The menu commands available for the automated 2-D rolling ball background subtraction algorithm

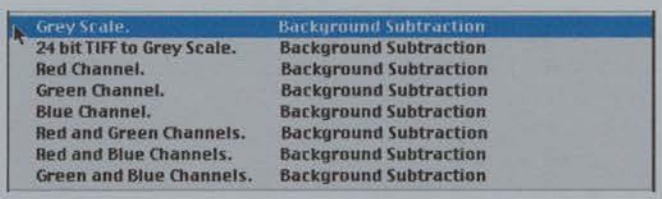

3.3.3.5 Calculation of the scaling factor of the images

Values obtained using Inclusion Counter v1.0 for mean inclusion area, standard deviation from the mean inclusion area and total area occupied by inclusion bodies within the ROI were converted into real units using a scaling factor. Once the images had been preprocessed with the 2-D rolling ball algorithm, the operator calculated the scale of the images using an image of a graticule slide (Graticules LTD, UK) acquired at the same magnification as the images. This process was facilitated by two macro implemented menu commands, *Set Scale Part 1* and *Set Scale Part 2*. The operator was then prompted to record the scaling factor of the images for future reference.

3.3.3.6 Automation of enumeration and measurement of Inclusion Bodies

Two separate methods of counting and measuring inclusion bodies were implemented. The first employed fixed value for the upper and lower greyscale value thresholds. These values were calculated by the operator as described in section 3.3.2. The second approach allowed the operator to rapidly set the thresholds for each image individually. This was achieved by developing two separate macro files, *Batch Count Inclusions v1.0* and *Manual Density Slice v1.0*. Both included identical components for selecting colour channels, setting and applying the guard frame, 2-D rolling ball background subtraction and scaling the images. They differed only in that the way the images were thresholded.

In *Batch Count Inclusions v1.0,* the images were analysed automatically by selecting the menu command, *Background Subtracted Images Automated Inclusion Enumeration*. The operator was prompted to enter the values for the scale of the images, the upper and lower threshold values and the values for the minimum and maximum area of the inclusion bodies. The operator opened the first image in the series of background subtracted grey scale images with names with the format *Subtracted.000n,* the guard frame was applied and its area was measured. Inclusion Counter v1.0 then used the threshold values previously specified by the operator to convert the greyscale image into a binary image. Inclusion bodies were counted and measured using the guard frame as described previously and the results were saved in a text file. Inclusion Counter v1.0 repeated this process for all of the image in the series *Subtracted.0001 - Subtracted.000n* using the Boolean argument below.

```
.....
For n:= 1 to 1000 do begin;
Open('Subtracted.',q:4);
.....
```

In *Manual Density Slice v1.0,* a threshold was assigned to each image by the operator. Inclusion Counter v1.0 prompted the operator to open the first image in the series *Subtracted.0001 - Subtracted.000n*. The upper threshold was set at a greylevel value of 254 and the operator adjusted the lower threshold limit manually as directed. Inclusion Counter v1.0 converted the thresholded image into a binary

image and saved it with the name in the format *Binary.0001*. Inclusion Counter v1.0 then automatically opened the next image in the series and allowed the operator to repeat the thresholding process. This was repeated for all of the images in the series for up to a maximum of 999 images. After all of the greyscale images had been converted into binary images the operator selected *Binary Images. Automated Inclusion Enumeration* from the *Special* menu. Inclusion Counter v1.0 prompted the operator to enter the scale of the images and the minimum and maximum values for the areas of the inclusion bodies, it then applied the guard frame and counted and measured the inclusion bodies in each of the images in the series, saving the results in a text file.

Text files generated by Inclusion Counter v1.0 can be opened in any spreadsheet software package allowing further data analysis.

3.3.4 Computer aided manual enumeration and measurement of inclusion bodies

A new layer was added to each image in Adobe Photoshop 4.0. Working in the new layer, the outline of each inclusion was traced and filled with black (Figure 3.14B). The background layer of cells and inclusions was then discarded, and the remaining layer flattened and saved in a separate folder as a binary image in Macintosh Picture (PICT) format (Figure 3.14C).

A macro was designed in NIH Image 1.61 to automatically count and measure the binary images of inclusion bodies generated manually in Photoshop (Photoshop Helper v1.0. The operator selected *Process Photoshop Images* from the *Special* menu in NIH Image 1.61. Inclusion Counter v1.0 prompted the operator to enter the scale of the images and to opened the first image in the series. A guard frame was then applied to the images as described previously, the number of inclusion bodies, the mean area of the inclusion bodies, standard deviation from the mean area of the inclusion bodies and total area occupied by inclusion bodies. The binary images of inclusions were replaced by numbered outlines and a text file was produced

containing the measurements. The image of outlined and numbered inclusion bodies was then pasted into a further layer of the original image in Photoshop 4.0 and the resultant image saved in Photoshop format. The final images produced by this technique consisted of the original cell monolayers with outlines and numbers superimposed over each inclusion in a separate layer (Figure 3.14D). This allowed a second user to verify the count and kept the original image intact enabling automated image analysis to be performed on the same image.

Figure 3.14A: 24-bit colour image of ST.6 cells and inclusion bodies

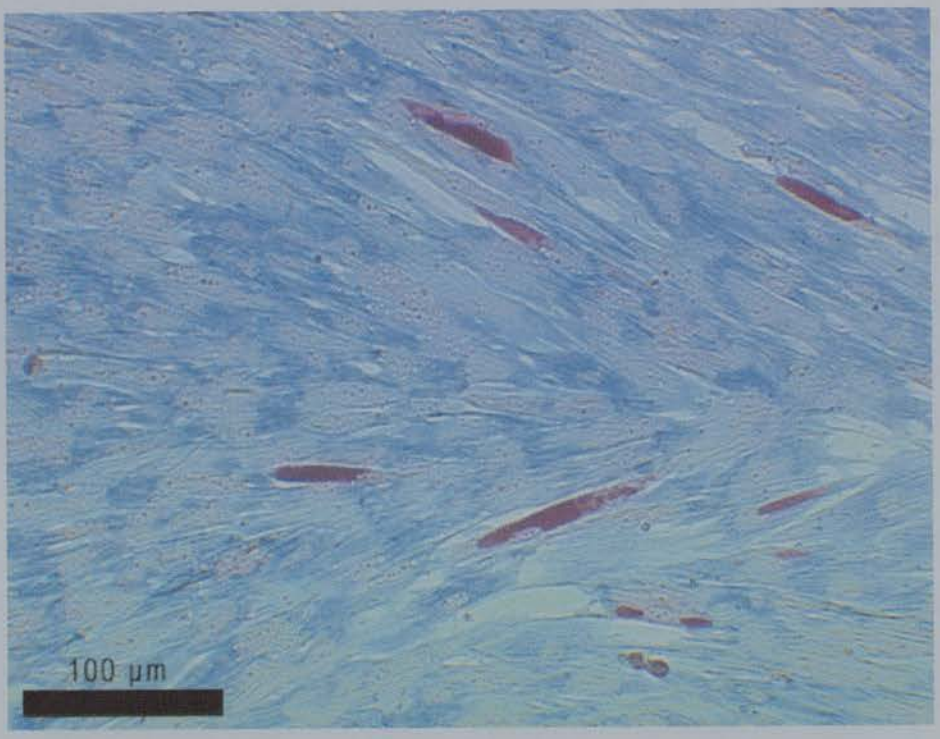

Figure 3.14B: The image from figure 3.14A with inclusion bodies traced and filled with black in a second layer in Photoshop 4.0

Figure 3.14C: The binary image of inclusion bodies produced by the layer containing the original image in Photoshop 4.0

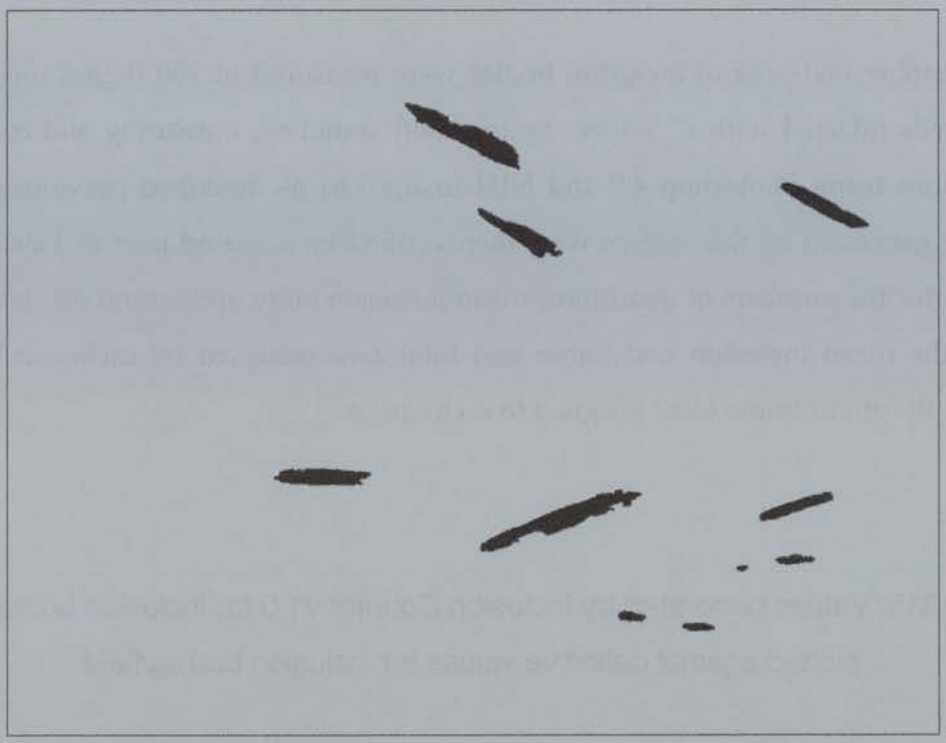

Figure 3.14D: The final composite image with inclusion bodies outlined and numbered by Inclusion Counter v1.0

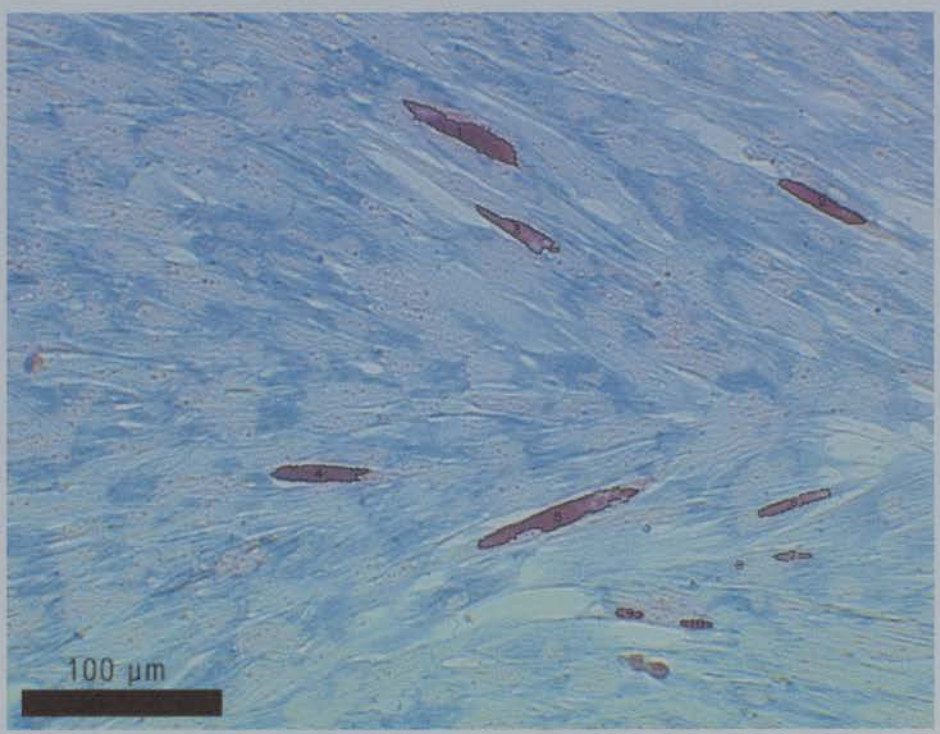

3.3.5 Statistical comparison of the results generated by automated image analysis and manual image analysis.

The number and area of inclusion bodies were measured in 200 digital images of ST.6 cells infected with *C. psittaci* by manually outlining, measuring and counting inclusions using Photoshop 4.0 and NIH Image 1.61 as described previously. The results generated by this system were then verified by a second user and definitive values for the numbers of inclusions, mean inclusion body area, standard deviation from the mean inclusion body area and total area occupied by inclusion bodies within the guard frame were assigned to each image.

Figure 3.15: Values generated by Inclusion Counter v1.0 for inclusion bodies/field plotted against definitive values for inclusion bodies/field

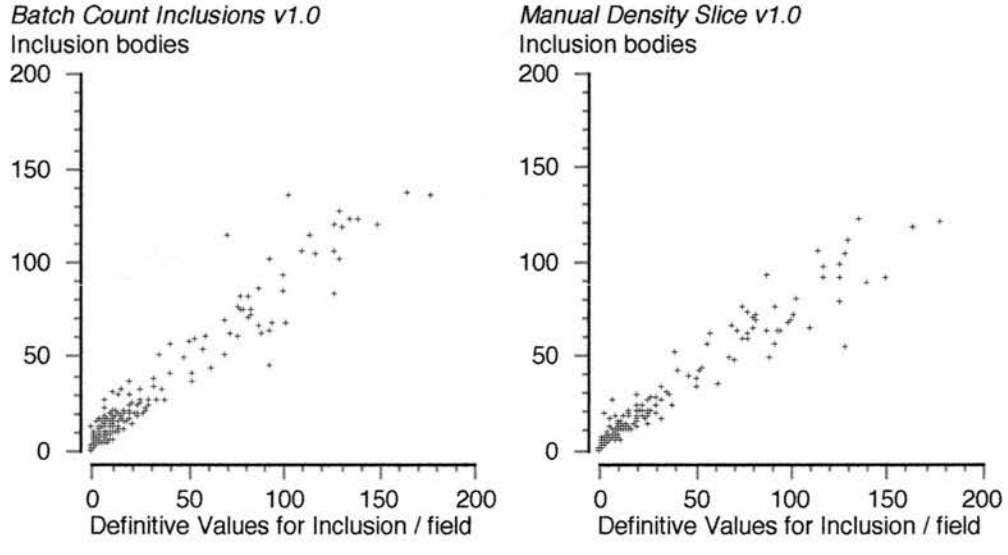

Batch Count Inclusions v1.0 and *Manual Density Slice v1.0* were evaluated for their accuracy in counting and measuring inclusion bodies. The relationship between the number of inclusions in each field obtained by manual counting and the values

generated by Inclusion Counter v1.0 are displayed in (Figure 3.15). Analysis of the results generated by both components of Inclusion Counter v1.0 by simple linear regression showed a significant positive correlation with the definitive values assigned to the images, *Batch Count Inclusions v1.0* (Correlation Coefficient = 0.9654; Slope = 0.8288; Intercept = 5.1173; P< 0.0001) and *Manual Density Slice v1.0* (Correlation Coefficient = 0.9699; Slope = 0.7134; Intercept = 3.1742; P< 0.0001).

A significant positive correlation was found between mean inclusion area values generated by Inclusion Counter v1.0 and the definitive values assigned to the images (Figure 3.16). There was a significant positive correlation between manual measurement and *Batch Count Inclusions v1.0* (Correlation Coefficient = 0.5691; Slope = 0.2783; Intercept = 171.7268; P< 0.0001) and between *Manual Density Slice v1.0* and manual measurement (Correlation Coefficient = 0.6609; Slope = 0.3665; Intercept = 147.4130; P< 0.0001).

Figure 3.16: Values generated by Inclusion Counter v1.0 for mean inclusion body area plotted against definitive values for mean inclusion body area

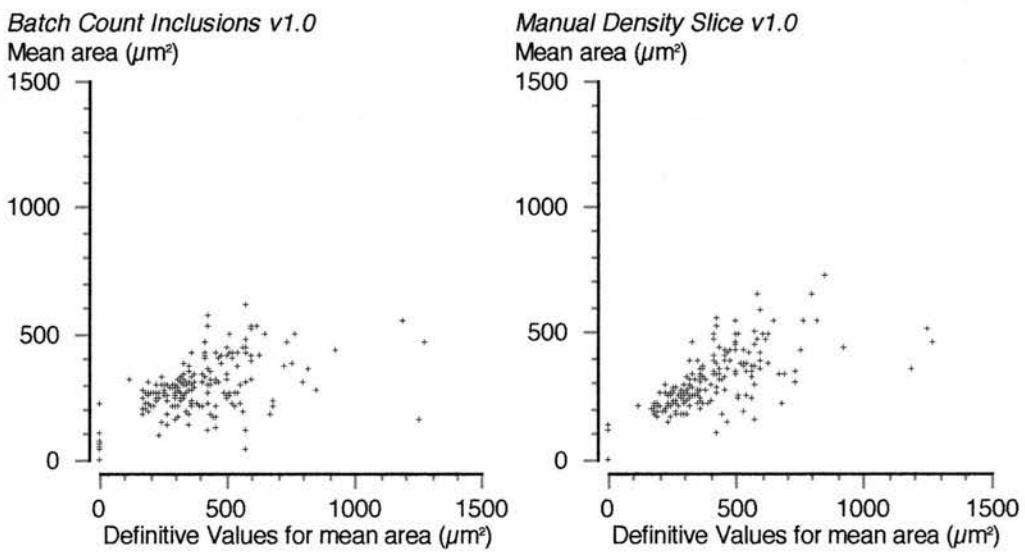

A significant positive correlation was found between the standard deviation from the mean inclusion area returned by Inclusion Counter v1.0 and the definitive values assigned to the images (Figure 3.17). There was a significant positive correlation between *Batch Count Inclusions v1.0* and manual measurement (Correlation Coefficient = 0.7028; Slope = 0.4646; Intercept = 147.4719; P< 0.0001) and between *Manual Density Slice v1.0* and manual measurement (Correlation Coefficient = 0.7367; Slope = 0.5392; Intercept = 86.5118; P< 0.0001).

Figure 3.17: Values generated by Inclusion Counter v1.0 for standard deviation from the mean inclusion body area plotted against definitive values for standard deviation from the mean inclusion body area

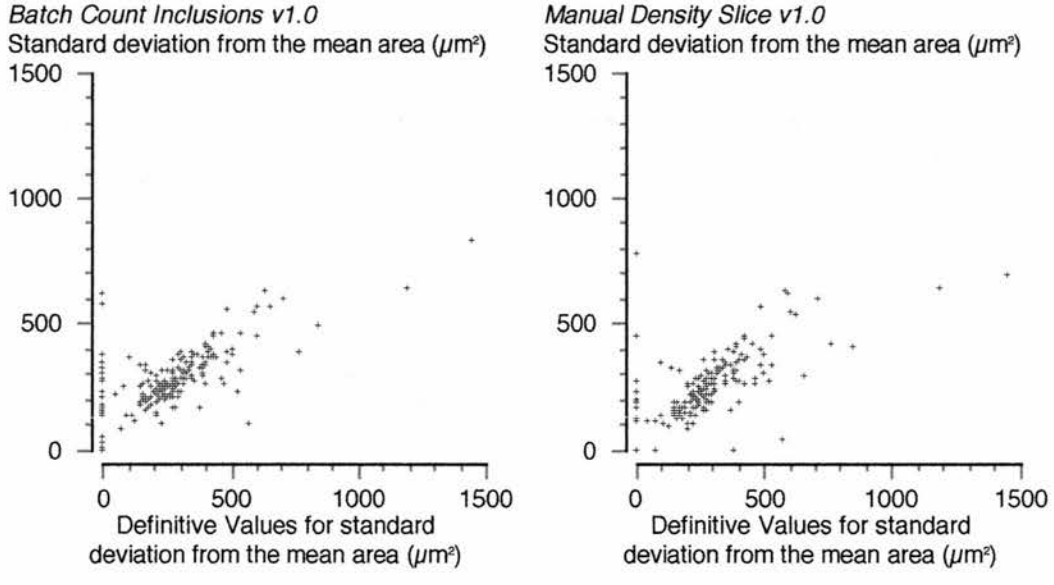

The relationship between values generated for the total area occupied by inclusion bodies within each field of view was also investigated. The Results are shown in Figure 3.18. Values for the total area occupied by inclusions obtained using Inclusion Counter v1.0 showed significant positive correlation with the definitive values assigned to the images, *Batch Count Inclusions v1.0* with manual measurement

(Correlation Coefficient = 0.9689; Slope = 1.0176; Intercept = -257.9802; P< 0.0001) and *Manual Density Slice v1.0* with manual measurement (Correlation Coefficient = 0.9639; Slope = 0.7308; Intercept = 270.1981; P< 0.0001).

Figure 3.18: Values generated by Inclusion Counter v1.0 for total inclusion body area plotted against definitive values for total inclusion body area

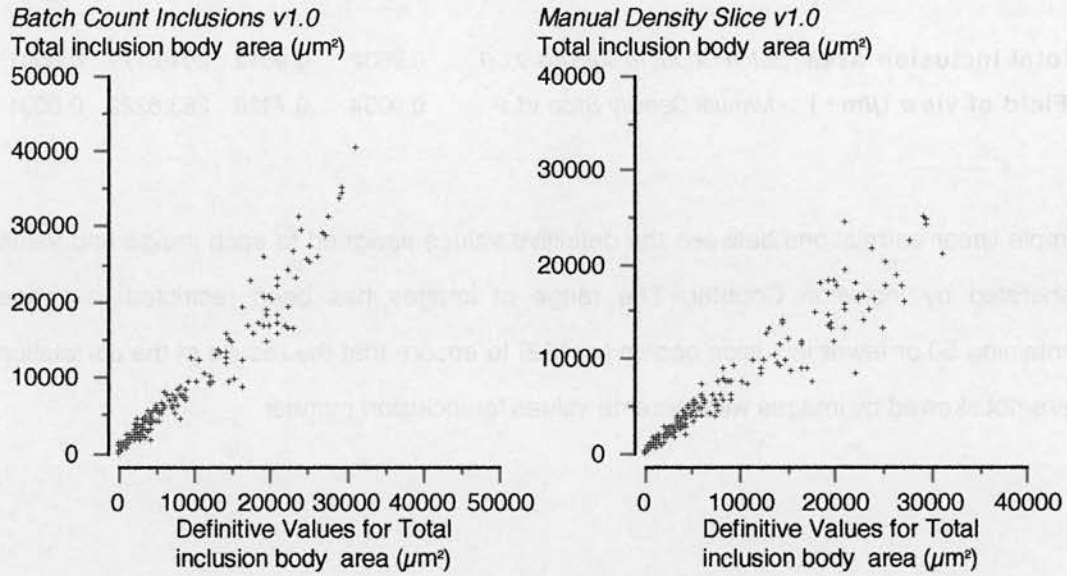

The range of inclusion numbers was not uniformly dispersed throughout the images, and the majority of fields of view contained less than 50 inclusions. Further statistical analysis was therefore performed to ensure that the statistics were not being skewed by the higher values obtained for some images. Table 3.6 shows the results of simple linear regression correlations between definitive values and Inclusion Counter v1.0 generated values over this range of images. All results generated by Inclusion Counter v1.0 over this range showed significant positive correlation coefficients with the definitive values assigned to images (P< 0.0001).

Table 3.6

Correlation investigated	*Macro*	correlation coefficient	Slope	Intercept	P<
Inclusions / field of view	*Batch Count Inclusions v1.0*	0.8651	0.8991	4.2655	0.0001
	Manual Density Slice v1.0	0.8992	0.7857	2.1587	0.0001
Mean Inclusion area (μm^2)	*Batch Count Inclusions v1.0*	0.5771	0.2956	157.5905	0.0001
	Manual Density Slice v1.0	0.4409	0.2489	200.8251	0.0001
Standard deviation from the mean area	*Batch Count Inclusions v1.0*	0.7066	0.4634	148.7181	0.0001
	Manual Density Slice v1.0	0.5500	0.3986	127.4296	0.0001
Total Inclusion Area /Field of view (μm^2)	*Batch Count Inclusions v1.0*	0.9632	0.9012	294.6179	0.0001
	Manual Density Slice v1.0	0.9054	0.7426	283.6222	0.0001

Simple linear correlations between the definitive values assigned to each image and values generated by Inclusion Counter. The range of images has been restricted to images containing 50 or fewer inclusion bodies (n=152) to ensure that the results of the correlations were not skewed by images with extreme values for inclusion number.

3.4 Discussion

In contrast to the *in vitro* setting where counting inclusion bodies by eye remains the method of choice for measuring chlamydial growth, clinical diagnosis of chlamydial infections has largely moved on from isolation and culture of live chlamydiae to the development and use of more automated techniques [Taylor-Robinson, 1997]. These include: antigen-specific ELISAs [Pugh *et al*, 1985; Souriau and Rodolakis, 1986; Mohanty *et al*, 1996]; anti-chlamydial antibody-specific ELISAs [Evans and Taylor-Robinson, 1982; Salti-Montesanto *et al*, 1997]; PCR [Corkish and Bevan, 1991; Palmer *et al*, 1991; Rasmussen *et al*, 1992]; and LCR [Dille *et al*, 1993]. Whilst these approaches have proved useful to varying degrees in the setting of clinical diagnosis [Taylor-Robinson, 1997], remarkable few of these techniques have been applied to the problem of measuring chlamydial growth *in vitro*. This is largely because these techniques were originally designed for qualitative rather than quantitative analysis or as in the case of anti-chlamydial antibody ELISAs cannot be applied to the situation *in vitro*. Despite this, a number of semi-automated techniques have been applied to the quantification of chlamydial growth *in vitro*. These include: a chlamydial-LPS specific ELISA that was used to measure the effects of ROvIFN-γ on *C. psittaci* growth in ovine ST.6 cells [Graham *et al*, 1995]; an RT-PCR based assay for evaluation of the in vitro antibiotic susceptibility of *C. pneumoniae* [Khan *et al*, 1996]; and most recently the use of flow cytometry to evaluate the antibiotic susceptibility of *C. trachomatis in vitro*[Dessus-Babus *et al*, 1998]. However, whilst the ELISA [Graham *et al*, 1995] and RT-PCR [Khan *et al*, 1996] assays are less time consuming than counting inclusion bodies by eye, they only provide an indirect measure of chlamydial growth and neither of these techniques have been widely adopted outside their original laboratories. In contrast, the flow cytometry based solution developed by Dessus-Babus *et al* (1998) provides a direct measure of the percentage of infected cells. It is too early to say if this technique will gain wide acceptance and counting inclusion bodies by eye remains the method of choice for measuring chlamydial growth *in vitro*.

The aim of the experiments detailed here was to assess the feasibility of using image

analysis for the measurement of chlamydial growth *in vitro* and if possible generate an automated system that would overcome the disadvantages of counting inclusions by eye without reducing sensitivity and add functionality that was previously unavailable. The image analysis software package, NIH Image, was chosen for this purpose on the grounds of its power, flexibility and public domain status. In addition, because it has attracted such a large number of users, the level of peer-based technical support for NIH Image remains largely unequalled.

Initial studies based on manual measurement of inclusion bodies (Tables 3.2 and 3.3) and pixel frequency/greylevel value histogram analysis of images (Figures 3.2, 3.4 and 3.5) indicated that segmentation of inclusion bodies was possible on the basis of differences between the greylevel values of inclusion bodies and the cellular background. When dealing with colour images, as was the case here, segmentation could be enhanced by selecting the combination of the red, green and blue colour channels in which there was maximum contrast between the greylevel values of inclusion bodies and the cellular background. In the case of inclusion bodies stained with MZN and cellular background counter stained with methyl blue this was achieved by averaging the greylevel values of the green and blue colour channels of the images. A threshold greylevel value was then applied to the images instructing the computer to exclude any pixels falling out with the range of greylevel values specified. In this way, the majority of the cellular background was excluded from the measurements. However, greylevel value alone was not sufficient to allow satisfactory segmentation of inclusion bodies since some components of the cellular background were included in the thresholded image. The second parameter by which objects in the thresholded image were defined as inclusion bodies was size. Objects were counted as inclusion bodies if the value returned for their area fell within the specified range. Superficially, the perimeter of the *C. psittaci* inclusion bodies appeared to be relatively smooth, suggesting that formfactor or roundness might have been used to further define objects as chlamydial inclusion bodies. However, roundness values obtained for inclusion bodies (Table 3.3) varied too widely to be used for this purpose and this approach was not pursued further.

In the experiments detailed here, the images were captured under variable lighting

conditions from plastic 96-well flat-bottomed microtitre plates, which are relatively poor in terms of optical quality compared to glass. Attempts to facilitate greylevel based segmentation of inclusion bodies by adjusting the background greylevel values were varied in their success. Standard procedures for background correction were inappropriate or adversely effected the greylevel values of the inclusion bodies. However, the implementation of the 2-D rolling ball background subtraction algorithm [Sternberg, 1983] greatly improved segmentation of chlamydial inclusion bodies. In addition the 2-D rolling ball algorithm normalised the light levels through out the entire batch of images (Figure 3.10) allowing a single threshold range to be applied to all of images in a given series. Images acquired using more sophisticated image capture systems which are capable of automated focusing and light level adjustment do not necessarily require preprocessing with the 2-D rolling ball background subtraction algorithm. Since computation of the 2-D rolling ball algorithm is relatively time consuming this process was made optional so that images captured with microscopes equipped with these features could be processed more rapidly.

The final version of Inclusion Counter v1.0 consisted of four main components: *Batch count Inclusions v1.0; Manual Density Slice v1.0; No Background Subtraction v1.0;* and *Photoshop Helper v1.0*. These allowed automated enumeration and measurement of chlamydial inclusion bodies to be performed on images independently of the type of the staining and microscopy used. In addition, *Photoshop Helper v1.0* and a separate Photoshop 4.0 actions file, *Help with Inclusion Counter,* provided a system for manual measurement of chlamydial inclusion bodies that could be used to verify the results obtained with the automated components of Inclusion Counter v1.0.

In order to assess the accuracy of Inclusion Counter v1.0, it was first necessary to assign a definitive value for inclusion body areas and number to each image. A number of approaches were considered. The system detailed in chapter 3.3.4 was chosen primarily because it was open to secondary verification and allowed measurement of inclusion bodies by eye to be performed on the same image that was processed automatically by Inclusion Counter v1.0, removing the requirement for

assumptions to be made about sample size and the spatial distribution of inclusion bodies. This approach, whilst extremely time consuming, was by far the most accurate available and allowed definitive values for inclusion body size and number to be assigned to each image.

In general, the results generated by Inclusion Counter v1.0 showed close correlation with values obtained using the method for manual measurement of inclusions described in section 3.3.4. In particular, the values for the number of inclusions and total area occupied by inclusions per field of view returned by Inclusion Counter v1.0 correlated closely with the definitive values assigned to each image (Figures 3.15 and 3.18). The correlation between the values generated by Inclusion Counter v1.0 for mean inclusion body area and those obtained by manually outlining inclusion bodies (Figure 3.16) was significant but were not as good as correlations obtained for inclusion body number (Figures 3.15). It is notable that in contrast to this, results obtained for the total area occupied by inclusion bodies were more accurate (Figure 3.18). This discrepancy was largely due to the lack of variability of mean inclusion body area between the images used in this study. Values obtained for the standard deviation from the mean area within images describe the population heterogeneity for inclusion body area (figure 3.17). The correlation between standard deviation from the mean area values generated by Inclusion Counter v1.0 and manual measurements was reasonably good. This measurement parameter may be useful when examining the effects of anti-chlamydial pharmaceuticals of immune effector mechanisms.

Whilst the results generated by *Batch count Inclusions v1.0* and *Manual Density Slice v1.0* were generally similar, the results generated by *Batch count Inclusions v1.0* were more accurate when analysis was restricted to images of cell monolayers containing 50 or fewer inclusion bodies (Table 3.6). This was most notable for the values returned for the total area occupied by inclusion bodies where the correlation coefficient, slope and intercept values were more precise for *Batch count Inclusions v1.0*.

There were a number of drawbacks to allowing the operator to set the threshold for

each image individually. Firstly, because the threshold was set by the operator in a greyscale image rather than a colour image accurate discrimination between artifacts/artefacts and inclusion bodies was difficult. A typical example of common artefacts of MZN staining is shown in figure 3.1A. In the colour image it was possible to discriminate between the artefacts and the inclusion bodies on the basis of their position in the focal plane and slight differences in saturation. However, it was much harder to discriminate between these artefacts and the inclusion bodies in the greyscale image which was used to set the threshold for the image (Figure 3.7). Secondly, allowing the operator to set the threshold of each image independently opened up Inclusion Counter v1.0 to subjective decision making by the operator, one of the key features that it was designed to avoid. This is particularly problematic in the case of uninfected controls where an operator will nearly always ensure that none of the cellular background is counted. This effectively nullifies the value of including uninfected controls and means that they cannot be used as measure of the level of error inherent in the system. It also means that the level of error is variable, as is apparent from the more scattered distribution of values for images with large numbers of inclusion bodies (Figures 3.16 and 3.18). By forcing the operator to calculate the threshold using the technique detailed in section 3.2.3, *Batch count Inclusions v1.0* avoids these problems entirely. In addition, whilst setting the threshold individually only take a few seconds for each of the images, this process become extremely time consuming when large numbers of images require processing.

The most useful feature of Inclusion Counter v1.0 was its ability to provide not only accurate values for the number of inclusion bodies in a given field of view but also the total area occupied by the inclusion bodies. The same approach can be easily implemented to calculate the area of the cell monolayer which was lysed due to chlamydial growth. This allows the progression of the infectious process to be measure after the first cycle of chlamydial growth and host cell lysis, providing useful information about the effects of anti-chlamydial agents beyond the initial phase of infection. Inclusion Counter v1.0 can be used in this way to allow rapid and accurate quantification of a wide variety of histological features both inside

and outside chlamydial biology, including cytokine expression, pathological changes and infectious processes that would otherwise be difficult to quantify.

Inclusion Counter v1.0 is largely automated and requires a fraction of the user's time compared with traditional methods of assessing chlamydial growth. It typically takes 20 minutes of the operators time to set up *Batch Count inclusions v1.0* or a few seconds for each image image if *Manual Density Slice v1.0* is used, after which Inclusion Counter v1.0 will process up to 999 images automatically. These features, combined with the public domain status of NIH Image and Inclusion Counter v1.0 provide a strong argument for the replacement of traditional counting methods.

Chapter 4.0

Improved colour segmentation of chlamydial inclusion bodies

4.1. Introduction

Inclusion Counter v1.0 provides an accurate, automated method of counting chlamydial inclusion bodies *in vitro*. Values returned by Inclusion Counter v1.0 for the total area occupied by inclusion bodies per field are also highly accurate (Chapter 3.0). However, the method used by Inclusion Counter v1.0 to segment chlamydial inclusion bodies from cellular background commonly results in the segmentation of cellular debris and other artefacts which reduce specificity. Furthermore, Inclusion Counter v1.0 will only return accurate results if the operator systematically goes through the process of selecting the appropriate combination of RGB colour channels, calculating the grey value thresholds and determining the minimum and maximum area of the inclusion bodies. In order to address these issues, a novel 24-bit colour segmentation system was developed and implemented for Inclusion Counter v2.0 using the public domain image analysis package Object-Image [Vischer *et al*, 1994]. This chapter describes the development and evaluation of Inclusion Counter v2.0.

4.2 Materials and Methods

4.2.1. Image acquisition

All aspects of this work were carried out using the same images that were used during the development of Inclusion Counter v1.0 (Chapter 3.0).

4.2.2 Automated enumeration and measurement of inclusions

Inclusion Counter v2.0 was designed and developed in Object-Image 1.62n6 (Norbert Vischer: November 1998) using Inclusion Counter v1.0 (Chapter 3.0) as a structural framework. The accuracy of the data generated by Inclusion Counter v2.0 was compared against the results generated by manual measurement of inclusion bodies in 200 digital images of ovine ST.6 cells infected with the S26/3 OEA strain of *C. psittaci* as described previously (Chapter 3.3.4).

4.2.3 Statistical Analysis

Results obtained using manual and automated methods were compared by simple linear regression.

4.3 Results

Inclusion Counter v2.0 used the same guard frame, 2-D rolling ball background subtraction [Sternberg, 1983], image scaling and automated batch processing routines as Inclusion Counter v1.0. However, it differed significantly from Inclusion Counter v1.0 in the way that it segmented chlamydial inclusion bodies from cellular background and to a lesser degree in the range of measurement parameters it returned.

Figure 4.1: "Point and click" colour segmentation

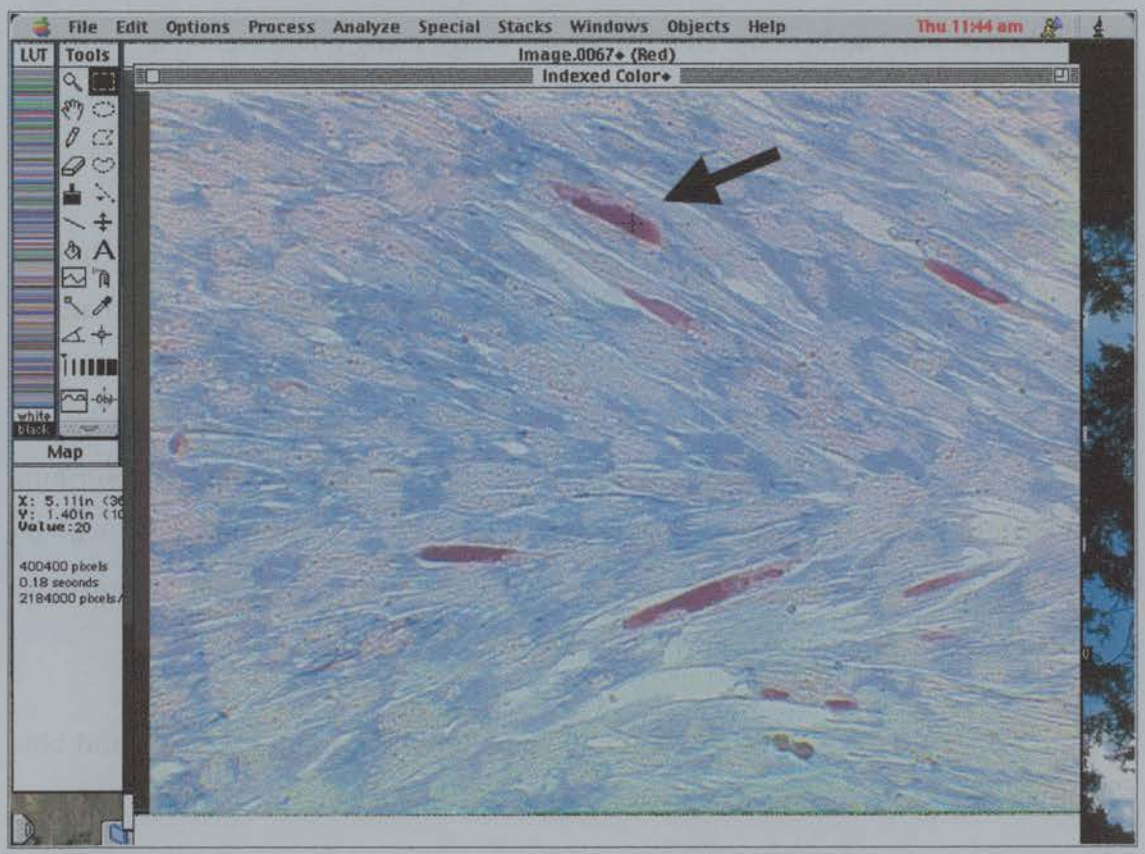

The cursor (highlighted by the arrow) is placed over an inclusion body in an indexed colour image generated from the original RGB image. When the mouse button is depressed, Inclusion Counter v2.0 samples the grey level values at that location in each of the colour channels of the original RGB image. Inclusion counter v2.0 then sets the grey level threshold for each of the red, green and blue channels.

4.3.1 "Point and click" colour segmentation in Inclusion Counter v2.0

Inclusion Counter v2.0 removed the requirement for the operator to manually calculate and set a grey level threshold. This was achieved by directly sampling the grey level values of each colour channel component of the inclusion bodies. Inclusion Counter v2.0 (Part 1) prompted the operator to open an image of ST.6 cells containing inclusion bodies and click on an inclusion (Figure 4.1). Using the x,y coordinate of the cursor as a reference, Inclusion Counter v2.0 measured the grey level values at that location in each of the component channels of the original image and used the resultant values to threshold each channel individually (Figures 4.2A, 4.2B and 4.2C). Inclusion Counter v2.0 then compared the resultant binary images from each channel and produced a composite image using a Boolean AND function. The resultant binary image generated by the Boolean AND function only contained pixels which occurred at the same place in all three binary images (Figure 4.2D).

Inclusion Counter v2.0 also kept a copy of the binary images of each channel allowing the operator the option of selectively discarding one or more channels during future analysis. In addition, both the size of the area sampled and the degree of sensitivity with which the thresholds were set could be easily adjusted by the operator. In the case of the image in Figure 4.2, the red channel did not contribute significantly to the segmentation process. Furthermore, the sensitivity level was set to a very low level (± 10 grey level values) resulting in excessive background segmentation in the Boolean AND image (Figure 4.2D).

Figure 4.3 shows the results of "point and click" thresholding in the green and blue channels only, with the sensitivity set to ±1 grey level values.

Figure 4.2A: "Point and click" threshold image of the red channel

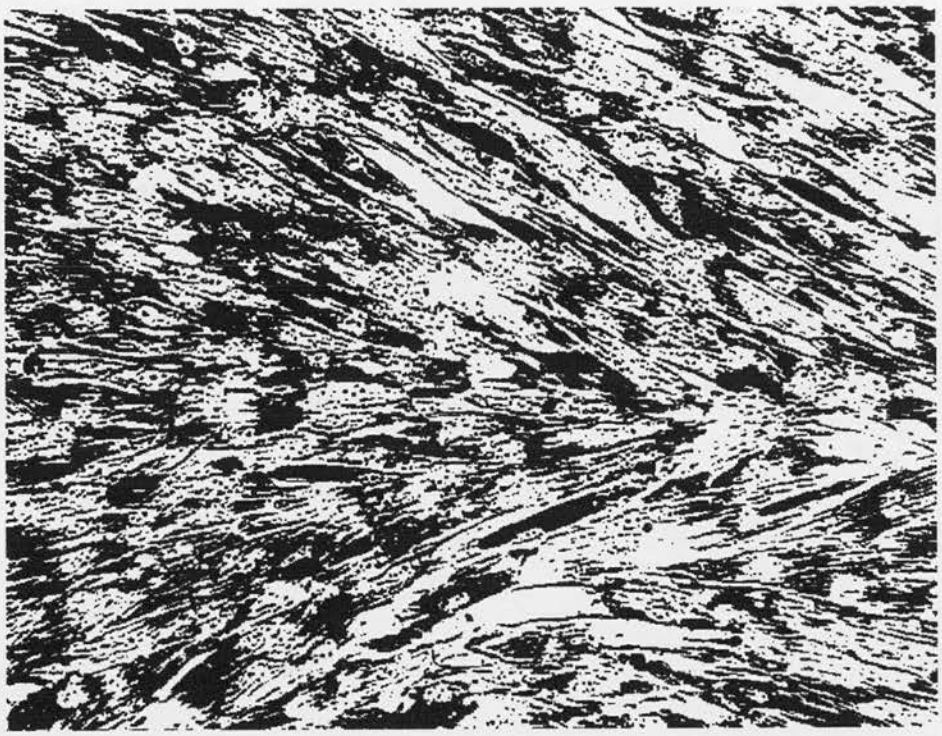

Figure 4.2B: "Point and click" threshold image of the green channel

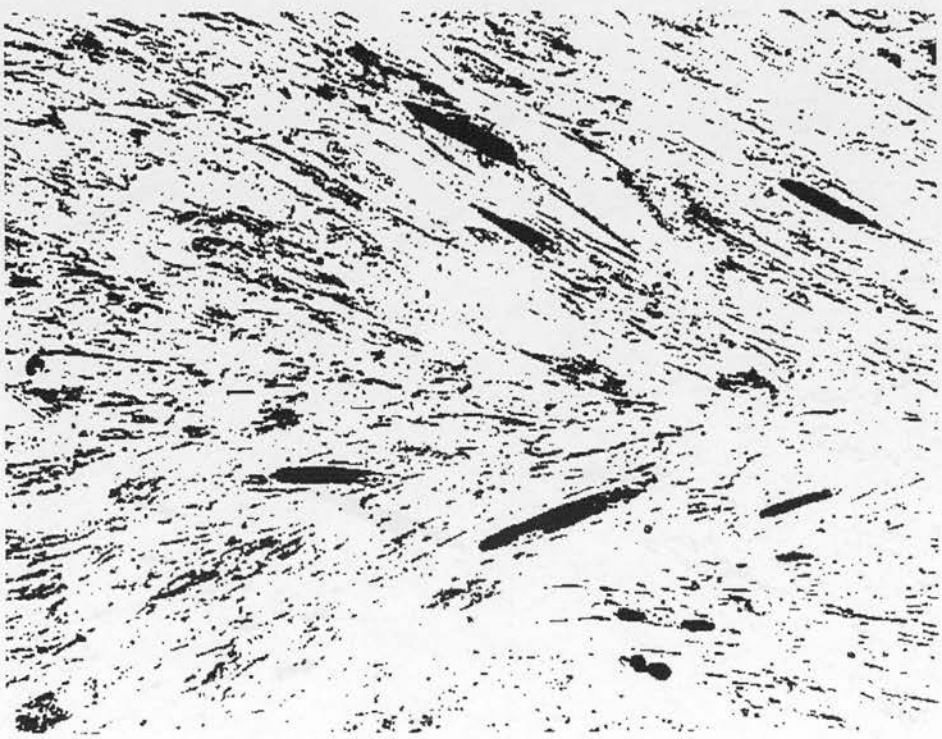

Figure 4.2C: "Point and click" threshold image of the blue channel

Figure 4.2D: Boolean AND image of figures 4.2A, 4.2B and 4.2C

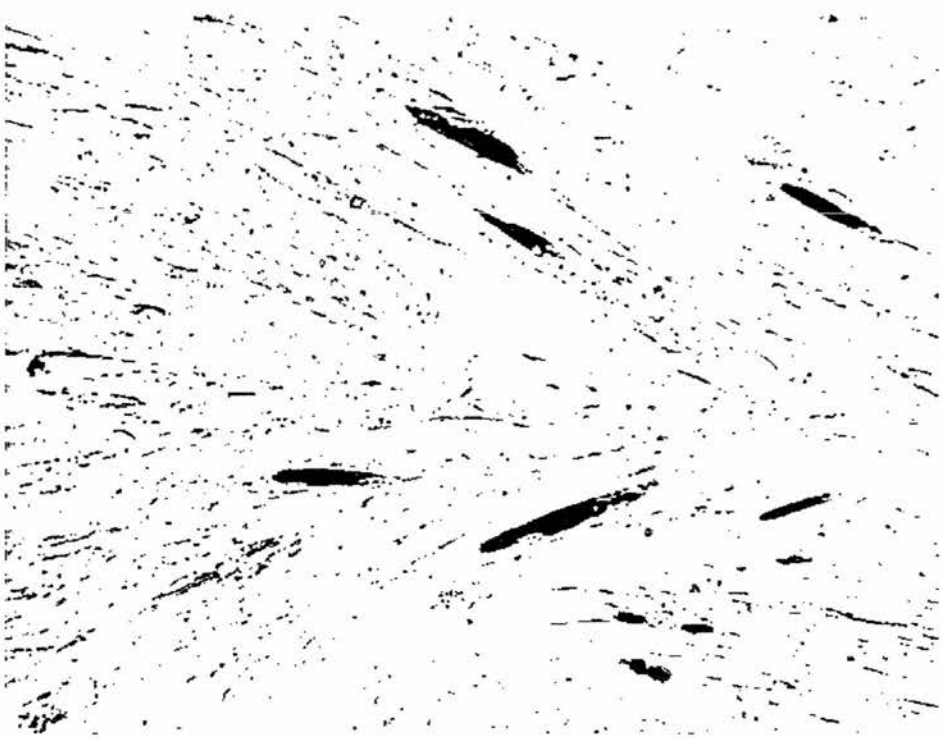

Figure 4.3: Boolean AND image derived from thresholding in the green and blue channels of the RGB image

(Area sampled:= 9x9 pixels and sensitivity:=1)

This process was repeated until satisfactory segmentation was achieved, at which point the operator saved the threshold values by selecting *New Colour Range Record* from the *Special* menu. This created a 'Colour Range Record', a 100x100 resolution image with a background grey level value of zero (white) and recorded the upper and lower grey value thresholds for each colour channel as pixels with x,y locations: red (lower=1,1/upper=1,2); green (lower=1,3/upper=1,4); and blue (lower=1,5/upper=1,6). This process was then repeated for at least two more images (picked at random from the batch of images requiring processing) with the minor modification that the operator added new threshold values to the existing 'Colour Range Record' file by choosing *Add To Open Colour Range Record* from the *Special* menu. *Add To Open Colour Range Record* added a further image to the 'Colour Range Record' stack in which it recorded the new upper and lower thresholds for each colour channel as described above. Once satisfied with the 'Colour Range Record' the operator could rename, close and save the *Colour Range Record* file as

required.

4.3.2 Batch processing using the Colour Range Record

Inclusion Counter v2.0 automatically processed up to 999 images at a time using a similar technique to Inclusion Counter v1.0 (Chapter 3.0). The operator selected the appropriate colour channels for analysis from the *Special* menu, set the scale, set the minimum and maximum size for inclusion bodies, opened the first image in the batch requiring processing and selected the correct 'Colour Range Record' file. Inclusion Counter v2.0 used the 'Colour Range Record' file to calculate a mean value (± 1 standard deviation) for the threshold settings in each colour channel and applied this to all of the images requiring processing. The results for inclusion number, total area occupied by inclusion bodies, percentage area occupied by inclusion bodies and the values for the mean/standard deviations from the mean inclusion body area, length and width of each image were exported to a separate text file. Further data analysis could then be performed in any spreadsheet package as required (Table 4.2).

Table 4.1: An example of the spreadsheet output of Inclusion Counter v2.0

ROI Area	*288408*		*µm²*					
Inclusions Per ROI	*Mean Area*	*STDEV (Area)*	*Total Area*	*% Area*	*Mean Length*	*STDEV (Length)*	*Mean Width*	*STDEV (Width)*
0	0	0	0	0	0	0	0	0
0	0	0	0	0	0	0	0	0
0	0	0	0	0	0	0	0	0
17	242	199	3866	1.34	27.15	11.92	9.94	5.54
13	166	133	1995	0.69	23.48	14.52	8.40	2.59
9	311	396	2803	0.97	27.71	20.01	11.08	6.63
19	194	212	3689	1.28	30.42	19.98	7.05	2.99
8	387	399	3096	1.07	35.71	22.15	11.34	5.44

4.3.3. Length and width measurement by best fit ellipse

Mean length and width of chlamydial inclusions within the guard frame of each image were calculated using Object-Image's built-in best fit ellipse algorithm and measuring the major and minor axes of the resultant ellipse (Figure 4.4). Object-Image uses a similar method for calculation of the best fit ellipse to that described by Russ (1998).

Figure 4.4: Best fit ellipse for a binary image of a *C. psittaci* inclusion body

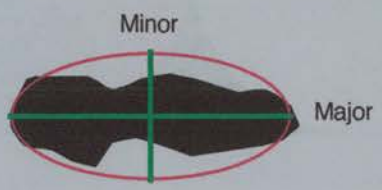

4.3.4. Implementation of the HSV colour model in Object-Image 1.62n6

A macro command for the conversion of RGB Images into Hue, Saturation and Value (HSV) images was implemented in Object-Image 1.62n6. This made it possible, for the first time, to include a HSV colour segmentation system in Inclusion Counter v2.0. Figure 4.5 shows the result of converting of a RGB 24-bit colour image of a standard colour wheel into its hue, saturation and value component channels.

Figure 4.5: The hue (A), saturation (B) and value (C) components of a standard colour wheel (D).

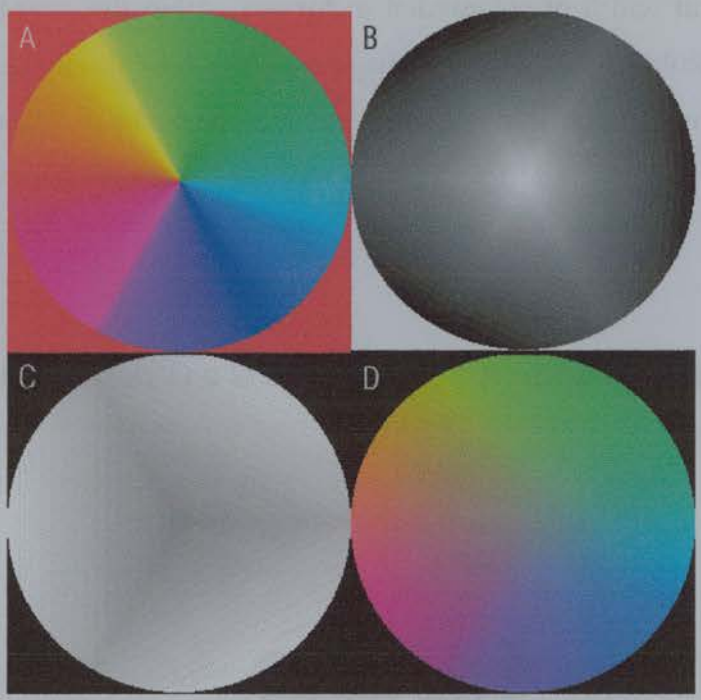

$$\text{Hue} = \frac{\left[\pi/2 - \arctan\left\{(2\cdot \text{R} - \text{G} - \text{B})/\sqrt{3}\cdot(G-B)\right\} + \pi; G < B\right]}{2\pi}$$

$$\text{Saturation} = \frac{[\text{Maximum(RGB)} - \text{Minimum(RGB)}]}{\text{Minimum(RGB)}}$$

$$\text{Value} = \text{Minimum (RGB)}$$

Figure 4.6A: A 24-bit RGB colour image of inclusion bodies in ST.6 cells, with artefacts (arrow), as displayed by a standard cathode ray tube monitor.

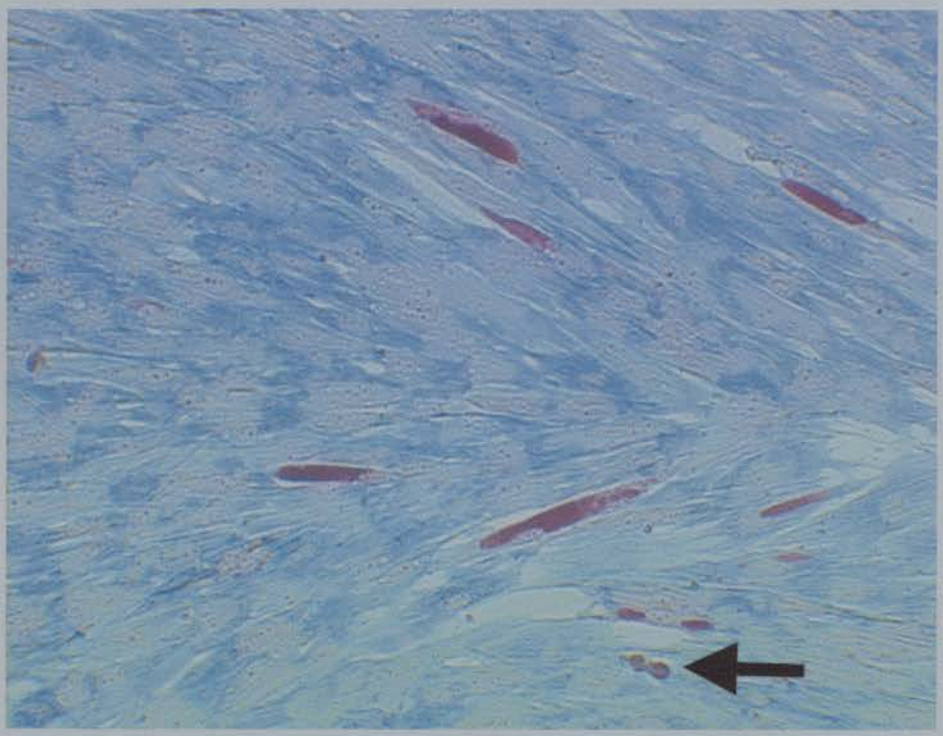

Figure 4.6B: The hue component of Figure 4.3A

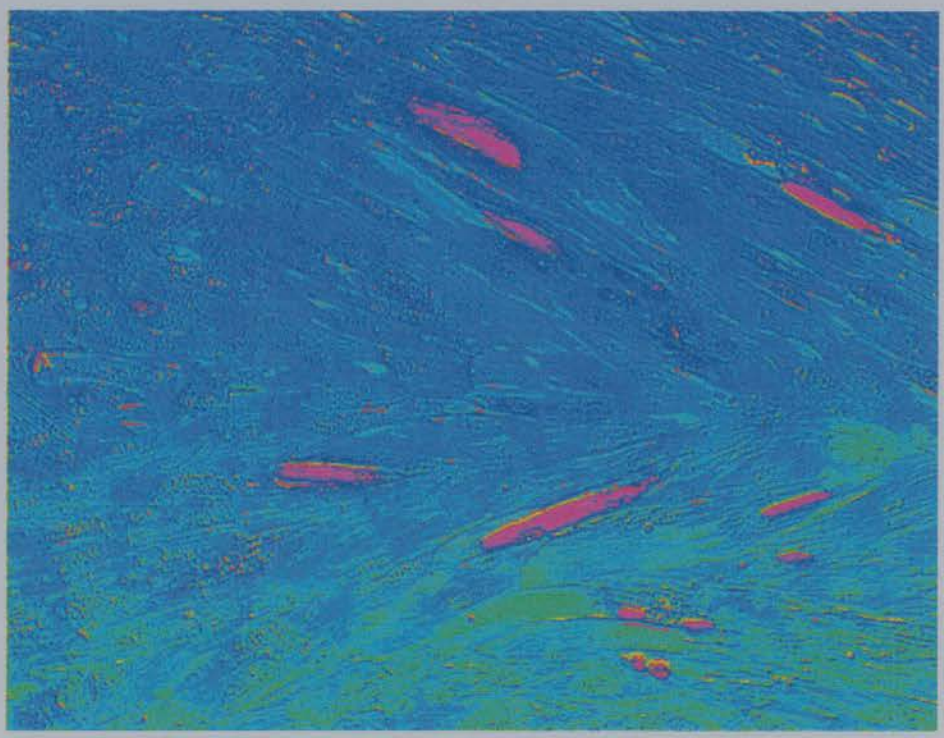

Figure 4.6C: The saturation component of Figure 4.3A

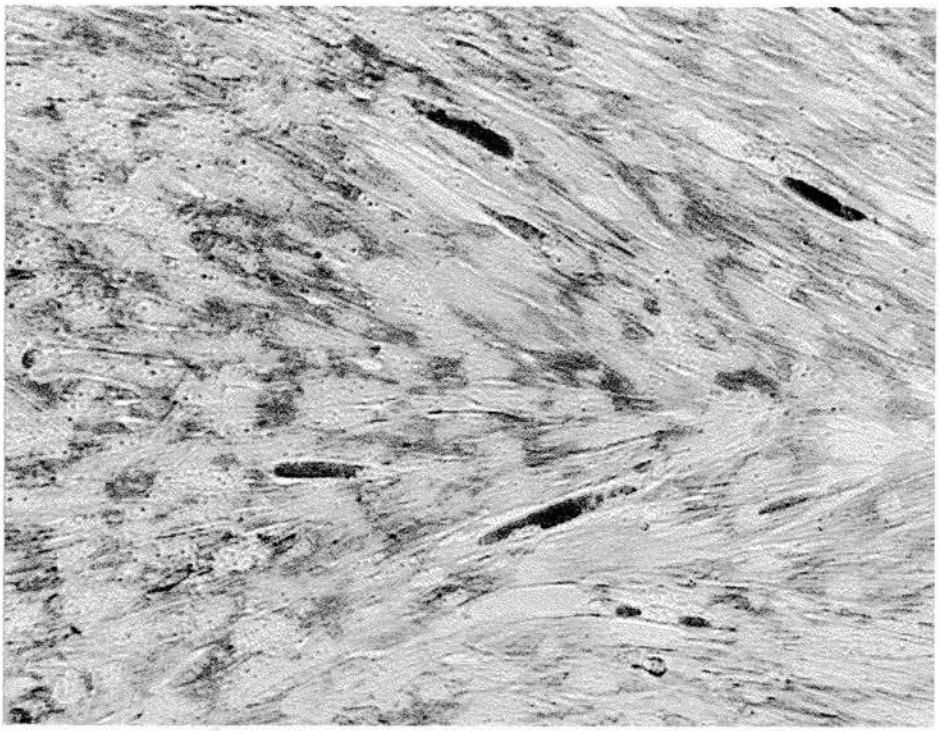

Figure 4.6D: The value component of Figure 4.3A

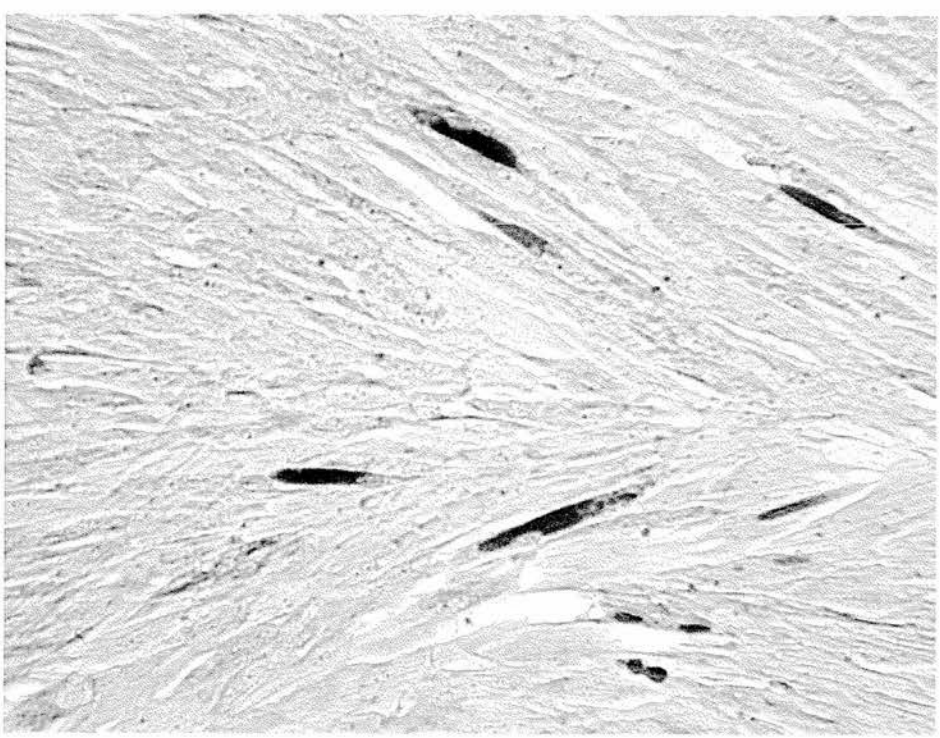

Figure 4.6 shows the results of converting a 24-bit RGB colour image of chlamydial inclusion bodies and ST.6 cells into its component HSV channels in Object-Image 1.62n6. Inclusion bodies appeared at greatest contrast to the cellular background in the hue channel (Figure 4.6B) and there was a total absence of cellular artefacts (Figure 4.6A: arrow) in the saturation channel (Figure 4.6C). These findings prompted the implementation of the HSV colour model in Inclusion Counter v2.0.

4.3.5. Implementation of the HSV model in Inclusion Counter v2.0

HSV based "point and click" colour segmentation (Inclusion Counter v2.0 **HSV**) was implemented using the same procedure as described for RGB based "point and click" colour segmentation (Inclusion Counter v2.0 **RGB)**.

4.3.6. Analysis of the results generated by Inclusion Counter v2.0

The semi-automated measurement system described in Chapter 3.0 was used to assign definitive and verifiable values for inclusion number, mean inclusion area, mean inclusion length, mean inclusion width, total area occupied by inclusion bodies, percentage area occupied by inclusion bodies and the standard deviations from the mean area, length and width to 200 digital images of ST.6 cells infected with chlamydiae. Inclusion Counter v2.0 **RGB** and Inclusion Counter v2.0 **HSV** were then evaluated for accuracy in counting and measuring inclusion bodies.

Figure 4.7: Comparison of the number of inclusion bodies in each image returned by Inclusion Counter v2.0 and the definitive values.

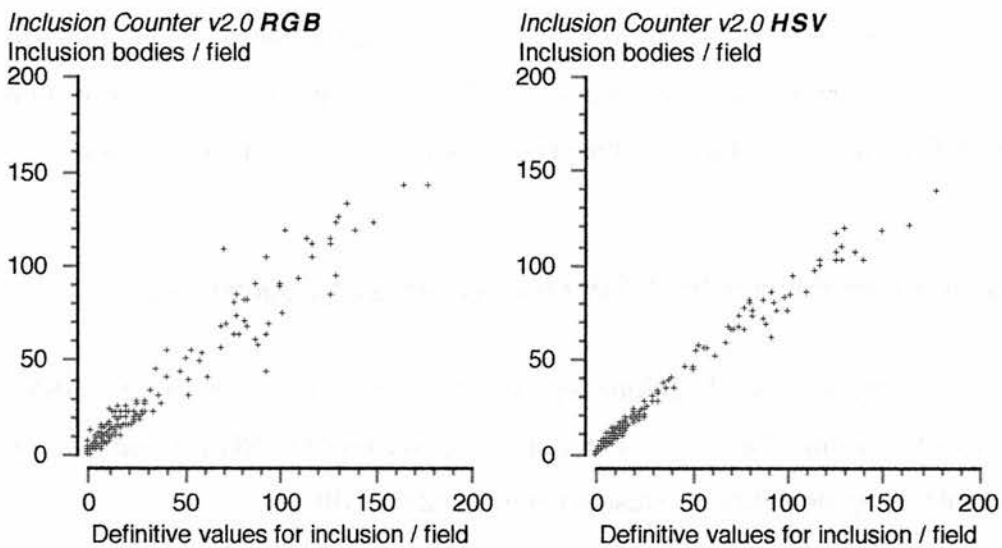

Simple linear regression analysis of the number of inclusion bodies per image returned by Inclusion Counter v2.0 showed a significant positive correlation with the definitive values assigned to the images (Figure 4.7). Inclusion Counter v2.0 **RGB** (correlation coefficient = 0.9733; slope = 0.8451; intercept = 3.1888; $P < 0.0001$) and Inclusion Counter v2.0 **HSV** (correlation coefficient = 0.9921; slope = 0.8249; intercept = 2.1498; $P < 0.0001$).

Figure 4.8: Comparison of the values generated by Inclusion Counter v2.0 for the total area occupied by inclusions in each image and the definitive values.

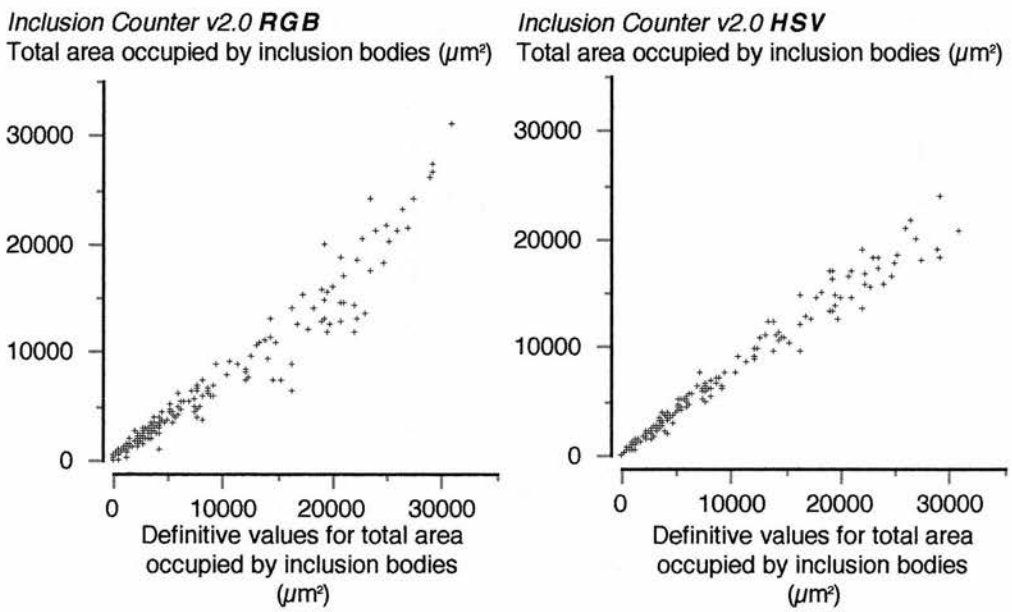

Simple linear regression analysis of the values for the total area occupied by inclusion bodies obtained using Inclusion Counter v2.0 showed a significant positive correlation with the definitive values assigned to the images (Figure 4.8). Inclusion Counter v2.0 **RGB** (correlation coefficient = 0.9714; slope = 0.7939; intercept = -139.6086; $P < 0.0001$) and Inclusion Counter v2.0 **HSV** (correlation coefficient = 0.9887; slope = 0.7319; intercept = 282.1805; $P < 0.0001$).

Correlation between the percentage area occupied by inclusions obtained using Inclusion Counter v2.0 and the definitive values assigned to the images was statistically identical to those obtained for the total area occupied by inclusion bodies.

Figure 4.9: Comparison of the values returned by Inclusion Counter v2.0 for mean inclusion body area in each image and the definitive values.

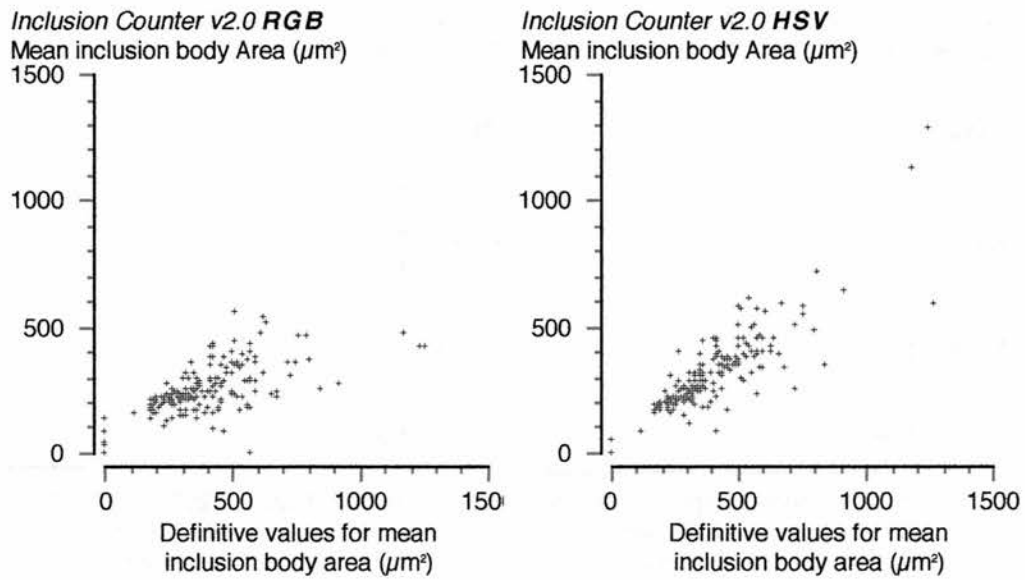

Simple linear regression analysis of the results generated by Inclusion Counter v2.0 for mean inclusion body area showed a significant positive correlation with the definitive values assigned to the images (Figure 4.9). Inclusion Counter v2.0 **RGB** (Correlation Coefficient = 0.6951; Slope = 0.3200; Intercept = 120.0956; $P < 0.0001$) and between Inclusion Counter v2.0 **HSV** and manual measurement (Correlation Coefficient = 0.8959; Slope = 0.6939; Intercept = 31.7685; $P < 0.0001$).

There was also a significant positive correlation between the values returned by Inclusion Counter v2.0 for the standard deviation from the mean inclusion area in each image and the definitive values assigned to the images. Inclusion Counter v2.0 **RGB** and manual measurement (Correlation Coefficient = 0.646; Slope = 0.411; Intercept = 121.6544; $P < 0.0001$) and between Inclusion Counter v2.0 **HSV** and manual measurement (Correlation Coefficient = 0.9049; Slope = 0.7756; Intercept = 32.1972; $P < 0.0001$).

Figure 4.10: Comparison of the values returned by Inclusion Counter v2.0 for mean inclusion body length in each image and the definitive values.

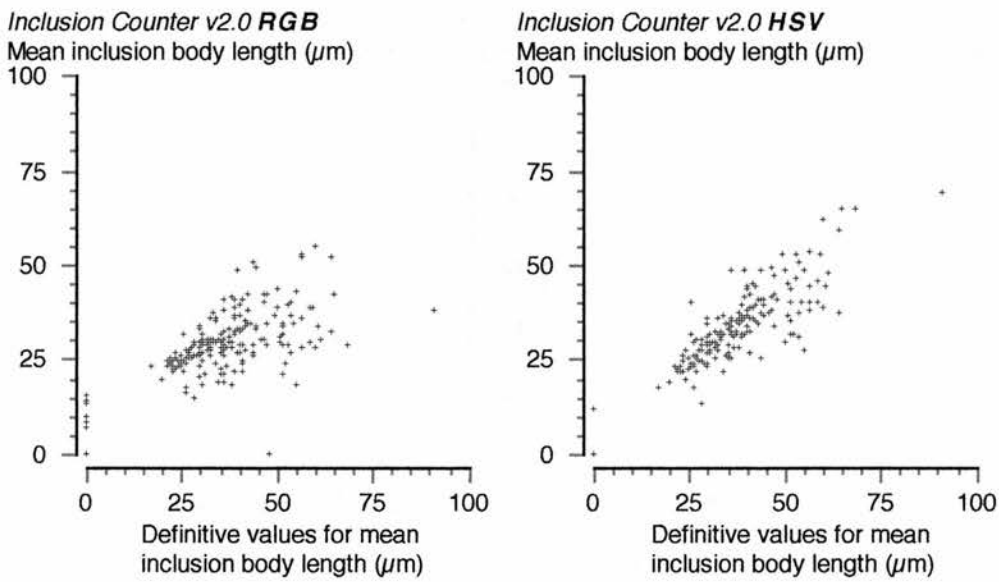

Simple linear regression analysis of the values for mean inclusion body length in each image returned by Inclusion Counter v2.0 showed a significant positive correlation with the definitive values assigned to the images (Figure 4.10). Inclusion Counter v2.0 **RGB** (Correlation Coefficient = 0.7016; Slope = 0.4608; Intercept = 11.9695; $P < 0.0001$) and Inclusion Counter v2.0 **HSV** (Correlation Coefficient = 0.8976; Slope = 0.7557; Intercept = 4.6024; $P < 0.0001$).

There was also a significant positive correlation between the values returned by Inclusion Counter v2.0 for the standard deviation from the mean inclusion body length in each image and the definitive values assigned to the images. Inclusion Counter v2.0 **RGB** and manual measurement (Correlation Coefficient = 0.5783; Slope = 0.4307; Intercept = 9.8662; $P < 0.0001$) and between Inclusion Counter v2.0 **HSV** and manual measurement (Correlation Coefficient = 0.8673; Slope = 0.8091; Intercept = 2.2846; $P < 0.0001$).

Figure 4.11: Comparison of the values returned by Inclusion Counter v2.0 for mean inclusion body width in each image and the definitive values.

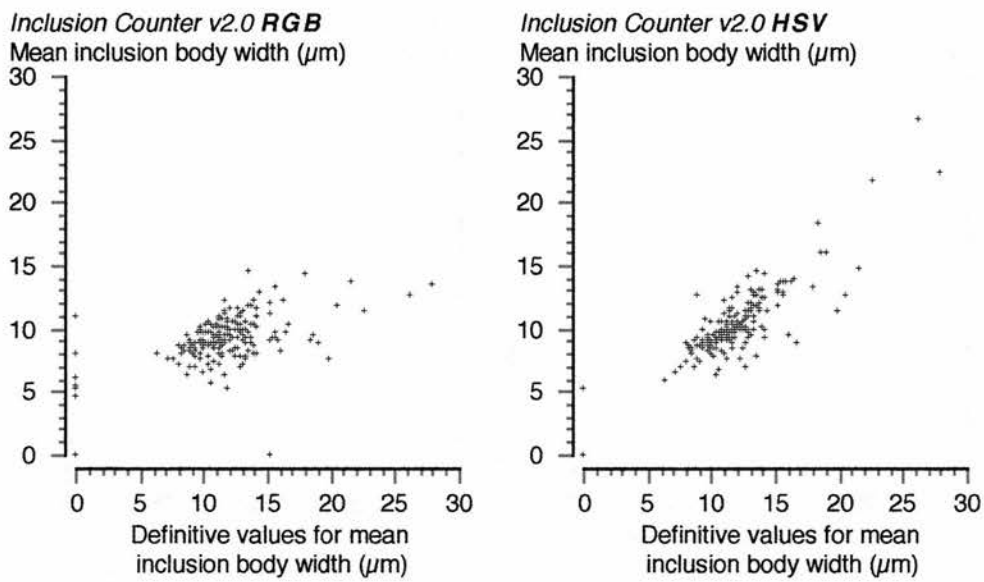

Simple linear regression analysis of the values returned by Inclusion Counter v2.0 for the mean inclusion body width in each image showed a significant positive correlation with the definitive values assigned to the images (Figure 4.11). Inclusion Counter v2.0 **RGB** (Correlation Coefficient = 0.6568; Slope = 0.3763; Intercept = 4.683; $P < 0.0001$) and Inclusion Counter v2.0 **HSV** (Correlation Coefficient = 0.9121; Slope = 0.775; Intercept = 1.0074; $P < 0.0001$).

There was also a significant positive correlation between the values returned by Inclusion Counter v2.0 for the standard deviation from the mean inclusion body width in each image and the definitive values assigned to the images. Inclusion Counter v2.0 **RGB** and manual measurement (Correlation Coefficient = 0.4971; Slope = 0.3770; Intercept = 2.7080; $P < 0.0001$) and between Inclusion Counter v2.0 **HSV** and manual measurement (Correlation Coefficient = 0.8667; Slope = 0.8481; Intercept = 0.5291; $P < 0.0001$).

4.4 Discussion

Interface design for colour segmentation is an extremely complex task in itself [Russ, 1998]. Inclusion Counter v1.0 (Chapter 3.0) avoided this problem by allowing the operator to perform analysis on 8-bit greyscale images derived from a combination of the red, green and blue channels of the original RGB colour image. In doing so, it essentially discarded much of the information present in the images. In contrast, Inclusion Counter v2.0 made full use of all of the information present within each image before summarising it as binary image prior to analysis. This approach resulted in much more stringent segmentation of inclusion bodies from the cellular background. Furthermore, the way in which this was achieved by "point and click" sampling of the grey level values of the inclusion bodies actually simplified the process for the operator.

The values returned by Inclusion Counter v2.0 **RGB** for inclusion body number, mean inclusion body area and total inclusion body area were marginally more accurate that those previously generated by Inclusion Counter v1.0 (*Batch count Inclusions v1.0*; Chapter 3.0). However, accuracy gains with Inclusion Counter v2.0 **HSV** were highly marked compared to both Inclusion Counter v1.0 and Inclusion Counter v2.0 **RGB**. Values returned by Inclusion Counter v2.0 **HSV** for inclusion body number and total area/% area occupied by inclusion bodies were exceptionally accurate (Figures 4.7 and 4.8). Furthermore, Inclusion Counter v2.0 **HSV** returned notably more accurate values for area (Figures 4.9 and 4.10), length (Figures 4.11 and 4.12) and width (Figures 4.13 and 4.14) compared to previous versions of Inclusion Counter.

Whilst Inclusion Counter v1.0 provided a solid argument for the use of image analysis in the measurement of chlamydial growth *in vitro*, the accuracy of Inclusion Counter v2.0 **HSV** exceeded initial expectations for this technology. Inclusion Counter v2.0 **HSV** provided highly accurate, robust and repeatable results using several different 'Colour Range Record' files. Its ability to return accurate values for area and length parameters should allow much more detailed analysis of chlamydial growth *in vitro* than any of the ELISA [Graham *et al*, 1995], RT-PCR [Khan et al,

1996] or FACS [Dessus-Babus *et al*, 1998] based technologies currently available. In addition, examination of tissue sections containing *Neospora caninum* parasites stained with IPX suggests that Inclusion Counter v2.0 **HSV** can be used for *in vitro* studies (data not shown).

Results generated by Inclusion Counter v1.0 are clearly dependent on the quality and specificity of the stain used and on the quality of the image capture system. MZN is a non-specific acid fast stain. Whilst it generally provides good differential staining of chlamydial inclusion bodies, it was not always uniform, and some inclusions stained only faintly. Specific staining protocols such as immunohistochemistry or *in situ*-hybridisation will significantly improve the accuracy of Inclusion Counter. Furthermore, the microscope used in these studies was not optimised for use with plastic 96-well plates and problems associated with maintaining a stable video signal required changes to be made to the illumination and condenser settings throughout image acquisition. This is not recommended when batch processing images using thresholding and is likely to have compromised the accuracy of the results generated by Inclusion Counter in these studies. The use of an inverted microscope with plastic optimised objectives would solve this problem and improve the accuracy of Inclusion Counter even further. There is no reason why results obtained using Inclusion Counter v2.0 **HSV** under optimal conditions should not approach 100% accuracy.

Chapter 5.0

Mechanisms of ROvIFN-γ mediated inhibition of *C. psittaci* growth in ovine cells.

5.1. Introduction

The ability of IFN-γ to restrict chlamydial growth in a wide variety of target cells has highlighted the importance of this cytokine in the immune response to chlamydiae. Consequently, a considerable amount of interest has focused on characterising the anti-chlamydial effects of IFN-γ. Whilst *in vivo* studies have established a significant role for IFN-γ in limiting chlamydial growth during the primary immune response, *in vitro* studies have been focused on the effects of IFN-γ on the intracellular growth of chlamydiae.

Initially, results from studies using murine and human mononuclear phagocytes were unanimous in agreement that the anti-chlamydial mechanism of IFN-γ was oxygen-independent [Rothermel *et al*, 1986; Byrne and Krueger, 1983]. However, it has since become clear that there are significant differences between the mechanisms through which IFN-γ restricts chlamydial growth in human and murine cells.

In 1986, Bryne *et al* (1986) showed that IFN-γ inhibited the growth of *C. psittaci* in a human uroepithelial cell line (T24) by upregulating tryptophan catabolism, which has been shown to be mediated by the enzyme indoleamine 2,3-dioxygenase (IDO) [Gupta *et al*, 1994], thereby restricting the availability of tryptophan to the pathogen. Furthermore, the anti-chlamydial effects of IFN-γ were almost completely reversed by the addition of excess exogenous tryptophan to the culture conditions [Byrne *et al*, 1986]. Upregulation of tryptophan catabolism has since been confirmed as the primary mechanism through which IFN-γ activates human cells to restrict the growth of *C. psittaci*, *C. trachomatis* and *C. pneumoniae* [Beatty *et al*, 1994; Mehta *et al*, 1998; Murray *et al*, 1989; Summersgill *et al*, 1995; Thomas *et al*, 1993].

Addition of exogenous tryptophan has also been reported to result in the restoration of near normal levels of chlamydial growth in human HEp-2 cells treated with TNF-α, suggesting the anti-chlamydial effects of TNF-α are also mediated through increased tryptophan catabolism in human cells. Similarly, IFN-α, IFN-β and IL-1 have also been shown upregulate tryptophan catabolism in human cells [Hu *et al*, 1995; Murray *et al*, 1989; Paguirigan *et al*, 1994].

In contrast to the situation in human cells, the mechanism by which IFN-γ restricts chlamydial growth in murine cells is not associated with upregulated tryptophan catabolism [De La Maza *et al*, 1985]. IFN-γ has been reported to lyse murine L cells infected with *C. psittaci* or *C. trachomatis* [Byrne *et al*, 1989]. IFN-γ pretreated murine McCoy cells have been shown to produce nitric oxide (NO•) following infection with *C. trachomatis*. More importantly, addition of exogenous N-guanidino-monomethyl L-arginine (L-NMMA), which inhibits the enzyme inducible nitric oxide synthase (iNOS), prevented NO• production in these cells and reversed anti-chlamydial effects of IFN-γ in a dose dependent manner, suggesting that NO• free radicals may have an anti-chlamydial function [Mayer *et al*, 1993]. More recently, IFN-γ mediated inhibition of *C. trachomatis* has been shown to correlate with NO• production in the murine RAW 264.7 macrophage cell line and can be reversed by exogenous L-NMMA [Chen *et al*, 1996]. Treatment of mice with L-NMMA has been shown to increase chlamydial replication *in vivo* and to reduce the ability of a chlamydiae-specific T-cell clone to protect mice against MoPn [Igietseme, 1996].

An *in vivo* study in sheep demonstrated local production of IFN-γ by an immune ewe following secondary challenge with live S26/3 *C. psittaci*. *In vitro* work, based on those observations, have shown that ROvIFN-γ restricts the growth of S26/3 *C. psittaci* in ovine ST.6 cells and, moreover, that this effect can be partially reversed by the addition of exogenous L-tryptophan [Graham *et al*, 1995].

The experiments detailed in this chapter were designed to clarify whether there are additional mechanisms involved in ROvIFN-γ mediated restriction of *C. psittaci* growth in ovine ST.6 cells and also to investigate its effects in *ex vivo* derived ovine BAL cells.

5.2. Materials and Methods

5.2.1. Pretreatment and infection of ovine ST.6 cells

ST.6 cells were suspended in IMDM+5% FBS at a density of $5X10^4$ cells/ml, seeded in volumes of 100 µl into 96-well flat-bottomed microtitre plates and allowed to grow to confluence. Cultures were then incubated for 24 hours in IMDM+2% FBS supplemented with ROvIFN-γ, RBovIFN-α or Polyinosinic Acid-Polycytidylic Acid (PolyI:PolyC; ICN Biomedicals, Thame, UK) at concentrations matched for anti-viral activity (Chapter 2.3.3.). Control cultures were incubated in the presence of IMDM+2% FBS alone. Cultures were then incubated with 100 µl of IMDM+5% FBS containing $1x10^5$ S26/3 *C. psittaci* IFU/ml for 6 hours, after which they were washed once in IMDM+5% FBS and incubated for a further 5 days in IMDM+2% FBS. Uninfected control were maintained in IMDM+2% FBS alone. The supernatants were harvested and stored at -20°C.

In a separate experiment, ST.6 cultures were pre-treated for 24 hours with various concentrations of ROvIFN-γ and infected with $1x10^4$ S26/3 *C. psittaci* IFU/ml (as described above). Cultures were subsequently maintained in either 200 µl of IMDM+2% FBS alone, IMDM+2% FBS supplemented with 500 µg/ml of L-tryptophan, IMDM+2% FBS supplemented with 0.5 µM of L-NMMA, or IMDM+2% FBS supplemented with 500 µg/ml of L-tryptophan and 0.5 µM of L-NMMA. Cultures were incubated for 7 days, after which the supernatants were harvested and stored at -20°C.

5.2.2. Measurement of *C. psittaci* multiplication in ST.6 cells

Culture supernatants were thawed and assayed for *C. psittaci* LPS using an LPS-ELISA (Chapter 2.5.1.).

5.2.3. Sheep

BAL cells were obtained from four SPF ewe lambs (approximately one year old) and 10 conventionally reared adult ewes by the procedure described previously (Chapter 2.1.6.).

5.2.4. Phenotypic characterisation of ovine BAL cells

BAL cells surface marker expression was characterised by flow cytometry using the monoclonal antibodies detailed in Table 5.1 (following the protocol described in Chapter 2.2.1.). Adherent cells were stained for non-specific esterase activity (Chapter 2.2.2.) and imaged under oil immersion at a magnification of x1000 using a JVC TK-1280E CCD colour camera module attached to a Olympus BX-50 conventional compound microscope (Chapter 2.4.5.). The ability of adherent BAL cells to phagocytose 3μm latex beads was also determined (Chapter 2.2.3.) and imaged at a magnification of x400 as described above. The percentages of non-specific esterase positive cells and cells containing latex beads were measured using a modified version of *CellCounting.obj* distributed with Object-Image1.62n6 (Norbert Vischer: November 1998).

Table 5.1: Antibodies used for phenotypic FACS analysis of ovine BAL cells

Antibody	Specific Target	Reference
VPM 49	Border Disease Virus	[Dutia *et al*, 1990]
Pooled VPM 22 and 49	Border Disease Virus	[Dutia *et al*, 1990]
SBU LCA (1.28)	CD45	[Maddox *et al*, 1985]
36F	CD2	[Mackay *et al*, 1988]
86D	TCR ($\gamma\delta$)	[Hunig, 1985]
CC21	CD21	[Naessens and Howard 1991]
VPM 30	B cell marker (uncharacterised)	[Hopkins *et al*, 1993]
VPM 65	CD14	[Gupta *et al*, 1996]
VPM 67	CD14	[Gupta *et al*, 1996]
VPM 8	Immunoglobulin light Chain	[Bird *et al*, 1995]

5.2.5. Stimulation of murine RAW 264.7 cells

Murine RAW 264.7 cells were adjusted to $2x10^4$ cells/ml in phenol red-free Dulbecco's Modified Eagle's Medium (GIBCO BRL) supplemented with 10% FBS (PhF-DMEM+10% FBS). 100 μl aliquots of the resultant suspension were seeded into the central 32 wells of 96-well flat-bottomed microtitre plates and incubated under standard conditions for 48 hours. RAW 264.7 cultures were then incubated with various combinations of RMuIFN-γ (Genzyme LTD, Suffolk, UK), bacterial LPS, live or heat inactivated S26/3 *C. psittaci* in 100 μl of PhF-DMEM+10% FBS. Culture supernatants were harvested after a further 8 - 96 hours and stored at –20°C. Cell viability was assessed by nigrosine exclusion. In later experiments, culture supernatants were supplemented with 100 μM of carboxy-PTIO in an attempt to enhance the sensitivity of the Griess reaction.

5.2.6. Stimulation of ovine BAL cells

BAL cells stored in liquid nitrogen were thawed, washed once and adjusted to $2x10^6$ cells/ml in IMDM+10% FBS supplemented with 25 μg/ml of gentamicin. 100 μl aliquots of the resultant cell suspensions were seeded into the central 32 wells of 96-well flat-bottomed microtitre plates and allowed to adhere for 6 hours. Adherent cells were washed once with 200 μl of PhF-DMEM+10% FBS and incubated for 12 hours in 100 μl of PhF-DMEM+10% FBS. BAL cells were then incubated (in parallel with murine RAW 264.7 cultures) with various combinations of ROvIFN-γ, bacterial LPS, live or heat inactivated S26/3 *C. psittaci* in 100 μl of PhF-DMEM+10% FBS and assayed for $NO^{\bullet}$ production as described above.

5.2.7. Measurement of nitric oxide production using the Griess reaction

Sodium nitrite standards (0.78-100 μM) were prepared in PhF-DMEM+10% FBS and stored on ice. Culture supernatants were removed from storage (at -20°C) and allowed to thaw for 30 minutes at RT. 50 μl aliquots of the culture supernatants, sodium nitrite standards and PhF-DMEM+10% FBS alone were then added to F-

type 96-well ELISA plates. 100 μl of Griess reagent (Appendix 1.13) was added to each well, the plates were incubated for 10 minutes at RT and the absorbance of the coloured azo product was measured at 540 nm using a Titretec Multiscan ELISA reader. The concentration of nitrite present in the samples was extrapolated from the standard curve provided by the sodium nitrite standards.

5.2.6. ROvIFN-γ mediated restriction of *C. psittaci* in ovine BAL cells

BAL cells were removed from liquid nitrogen, washed once and adjusted to $2x10^6$ cells/ml in IMDM+10% FBS supplemented with 25 μg/ml of gentamicin. 300 μl aliquots of the resultant cell suspension were incubated for 6 hours in 8-well Permanox chamber-slides. Non-adherent cells were discarded, after which adherent cells were washed once with 300 μl of PhF-DMEM+10% FBS and incubated for 12 hours in 200 μl of PhF-DMEM+10% FBS. 100 μl aliquots of ROvIFN-γ were added to BAL cultures to yield final concentrations of 2.5, 25 and 250 U/ml. 100 μl of PhF-DMEM+10% FBS alone was added to control cultures. After 24 hours, the culture supernatants were replaced with 300 μl of PhF-DMEM+10% FBS containing $2x10^4$ S26/3 *C. psittaci* IFU/ml. Uninfected control cultures were incubated with 300 μl of PhF-DMEM+10% FBS alone. BAL cells were incubated for a further 60 hours, after which they were fixed and stained with IPX (Chapter 2.4.4.). Chlamydial replication was analysed by semi-quantitative image analysis (Chapter 2.4.6.) of standard white light microscopy images acquired at a magnification of x1000 under oil immersion using a JVC TK-1280E CCD colour camera module attached to a Olympus BX-50 conventional compound microscope (Chapter 2.4.5.). Supernatants were assayed for nitrite as described previously.

5.3. Results

5.3.1. Comparative analysis of the anti-chlamydial effects of RBovIFN-α and ROvIFN-γ.

C. psittaci growth was measured indirectly by LPS-ELISA in ST.6 cultures pretreated with ROvIFN-γ and RBovIFN-α at concentration which were matched for anti-viral activity (Chapter 2.3.3.). ROvIFN-γ restricted *C. psittaci* growth in a dose dependent manner. In contrast, there was no evidence of reduced chlamydial growth in cultures pretreated with RBovIFN-α (Figure 5.1). Pretreatment of cultures with 0.25 or 2.5 U/ml of ROvIFN-γ significantly reduced chlamydial LPS production compared to both the infected controls (Table 5.2) and cultures pretreated with matched concentrations of RBovIFN-α (Figure 5.1). Very low LPS levels were detected in the supernatants of cultures which had been pretreated with 25 and 250 U/ml of ROvIFN-γ (Figure 5.1).

Table 5.2: Statistical analysis of the anti-chlamydial effects of ROvIFN-γ and RBovIFN-α at concentrations matched for anti-viral activity.

Anti-viral activity (U/ml)	*RBovIFN-α P value=*	*ROvIFN-γ P value =*
250	0.4824	0.0002
25	0.2842	0.0002
2.5	0.8416	0.0007
0.25	0.5835	0.0273

Results of unmatched two-tailed Student's 't' test analysis where the null hypothesis is: Differences between chlamydial LPS levels in the infected controls and in cultures pretreated with ROvIFN-γ or RBovIFN-α occurred by chance.

Figure 5.1: The chlamydial growth in ST.6 cells following pretreatment with ROvIFN-γ or RBovIFN-α.

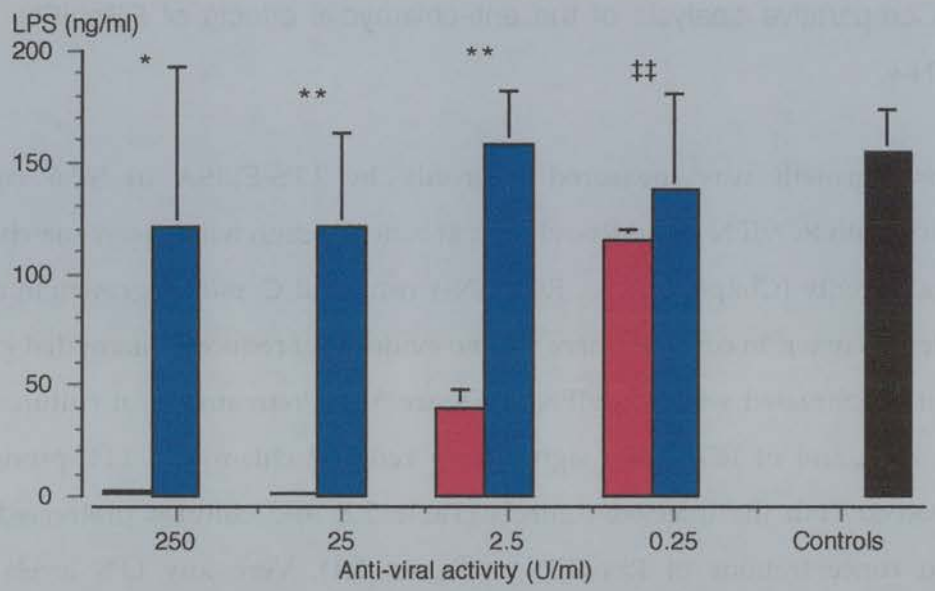

Triplicate cultures were pretreated with matched concentrations of ROvIFN-γ (■) or RBovIFN-α (■) for 24 hours prior to infection with $1x10^5$ IFU/ml of the OEA S26/3 strain of *C. psittaci*. Error bars represent ±1 standard deviation from the mean. Statistical significance was determined by unmatched two-tailed Student's 't' test analysis, where the null hypothesis was: Differences between chlamydial LPS production in cultures pretreated with ROvIFN-γ and RBovIFN-α occurred by chance. The null hypothesis was rejected at P value<0.05 (*) and P value<0.01 (**). The null hypothesis was accepted at P value>0.1 (‡‡). Infected controls (■) and uninfected controls (□ not visible).

5.3.2. Comparative analysis of the anti-chlamydial effects of PolyI: PolyC and ROvIFN-γ.

C. psittaci growth was measured indirectly by LPS-ELISA in ST.6 cultures pretreated with ROvIFN-γ and PolyI: PolyC at concentrations matched for anti-viral activity. ROvIFN-γ reduced in a *C. psittaci* growth in a dose dependent manner similar to that described above. 150 U/ml of PolyI: PolyC appeared to inhibit *C. psittaci* growth on the basis of results generated by the LPS-ELISA. However, microscopic analysis of the ST.6 cultures prior to infection indicated that PolyI:

PolyC was cytotoxic at this concentration (250 μg/ml). Similar results were also observed in the ovine interferon bioassay (data not shown). There was no evidence of reduced chlamydial growth in cultures pretreated with the lower concentrations of PolyI: PolyC (Figure 5.2). In contrast, as little as 1.5 U/ml of ROvIFN-γ significantly reduced chlamydial LPS production compared to the infected controls (Figure 5.2 and Table 5.3).

Figure 5.2: The chlamydial growth in ST.6 cells following pretreatment with ROvIFN-γ or Poly I: Poly C.

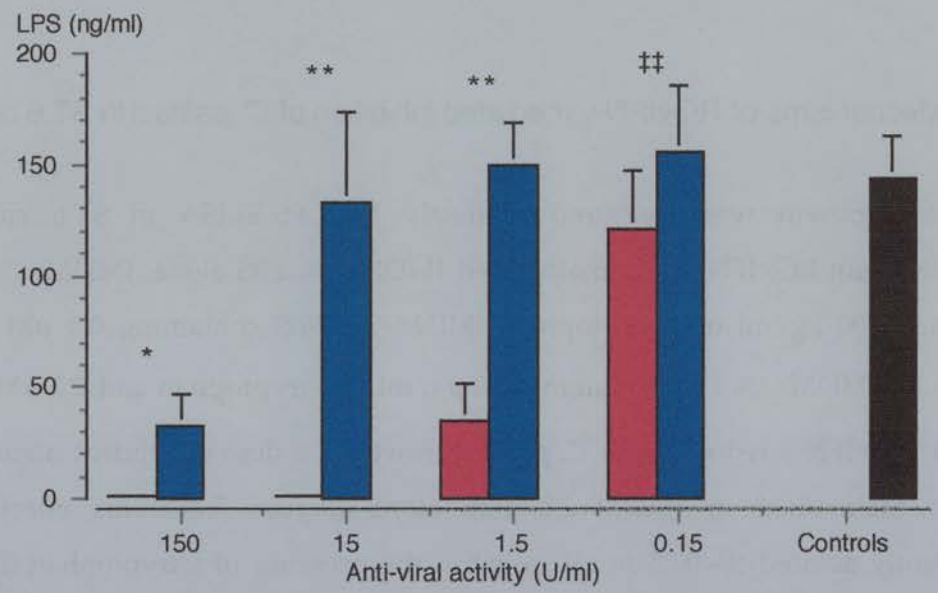

Triplicate cultures were pretreated with matched concentrations of ROvIFN-γ (■) or PolyI: PolyC (■) for 24 hours prior to infection with 1x10^5 IFU/ml of the OEA S26/3 strain of *C. psittaci*. Error bars represent ±1 standard deviation from the mean. Statistical significance was determined by unmatched two-tailed Student's 't' test analysis, where the null hypothesis was: Differences between chlamydial LPS production in cultures pretreated with ROvIFN-γ and RBovIFN-α occurred by chance. The null hypothesis was rejected at P value<0.05 (*) and P value<0.01 (**). The null hypothesis was accepted at P value>0.1 (‡‡). Infected controls (■) and uninfected controls (□ not visible).

Table 5.3: Statistical analysis of the anti-chlamydial effects of ROvIFN-γ and Poly I: Poly C at concentrations matched for anti-viral activity.

Anti-viral activity (U/ml)	*Poly I: Poly C P value=*	*ROvIFN-γ P value =*
150	0.0014	0.0002
15	0.7057	0.0002
1.5	0.7468	0.0018
0.15	0.6024	0.2909

Results of unmatched two-tailed Student's 't' test analysis where the null hypothesis is: Differences between chlamydial growth, measured indirectly by LPS-ELISA, in infected controls and cultures pretreated with ROvIFN-γ or Poly I: Poly C occurred by chance.

5.3.3. Mechanisms of ROvIFN-γ mediated inhibition of *C. psittaci* in ST.6 cells.

C. psittaci growth was measured indirectly by LPS-ELISA in ST.6 cultures pretreated with ROvIFN-γ and maintained IMDM+2% FBS alone, IMDM+2% FBS containing 500 μg/ml of L-tryptophan, IMDM+2% FBS containing 0.5 μM of L-NMMA, or IMDM+2% FBS containing 500 μg/ml of L-tryptophan and 0.5 μM of L-NMMA. ROvIFN-γ reduced in a *C. psittaci* growth in a dose dependent manner in cultures maintained in IMDM+2% FBS alone (Figure 5.3). This effect was significantly ablated ($P<0.05$ in all cases) in the presence of L-tryptophan (Figure 5.3). In contrast, the addition of 0.5 μM of exogenous L-NMMA was not associated with a significant reduction in the anti-chlamydial effects of ROvIFN-γ (Figure 5.4).

Figure 5.3: The effects of L-tryptophan on *C. psittaci* growth in ST.6 cells pretreated with ROvIFN-γ.

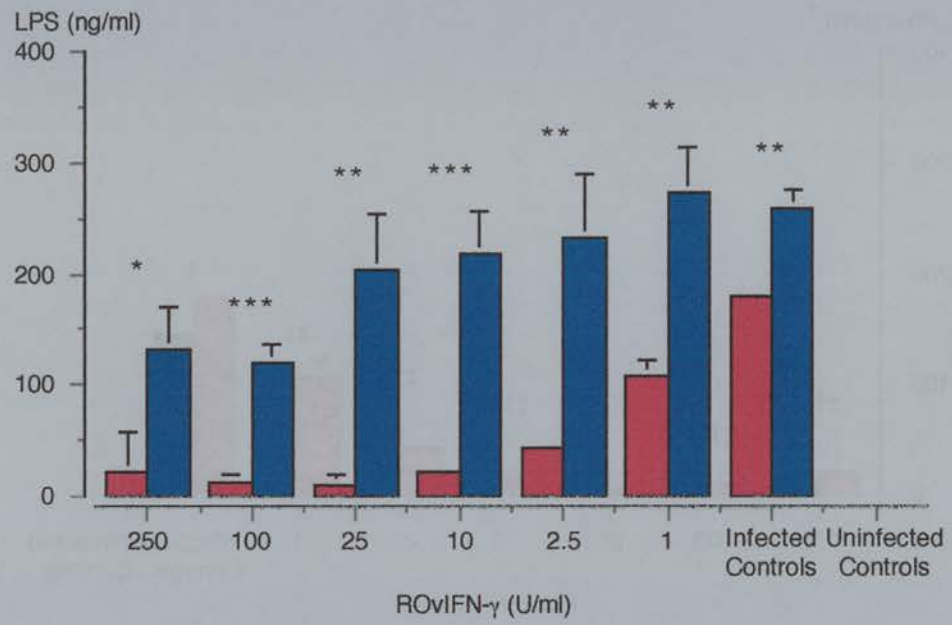

Triplicate cultures were maintained in IMDM+2% FBS alone (■) or IMDM+2% FBS supplemented with 500 μg/ml of L-tryptophan (■). Error bars represent ±1 standard deviation from the mean. Statistical significance was determined by unmatched two-tailed Student's 't' test analysis, where the null hypothesis was: Differences between chlamydial growth in cultures maintained in IMDM+2% FBS alone and cultures maintained in IMDM+2% FBS supplemented with 500 μg/ml of L-tryptophan occurred by chance. The null hypothesis was rejected at: P value<0.05 (*); P value<0.01 (**); and P value<0.001 (***).

Figure 5.4 The effects of L-NMMA on *C. psittaci* growth in ST.6 cells pretreated with ROvIFN-γ.

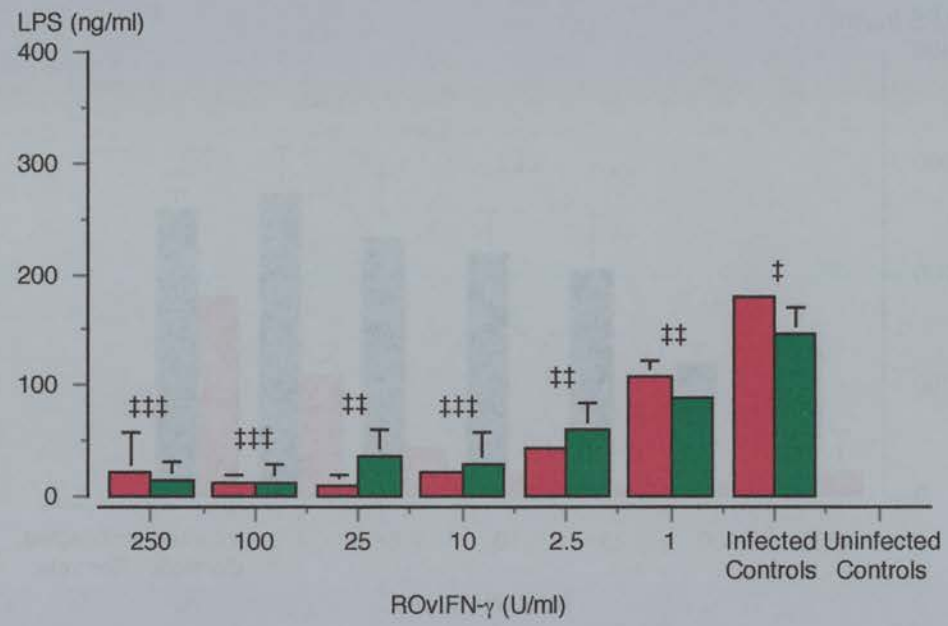

Triplicate cultures were maintained in IMDM+2% FBS alone (■) or IMDM+2% FBS containing 0.5 μM of L-NMMA (■). Error bars represent ±1 standard deviation from the mean. Statistical significance was determined by unmatched two-tailed Student's 't' test analysis, where the null hypothesis was: Differences between chlamydial growth in cultures maintained in IMDM+2% FBS alone and cultures maintained in IMDM+2% FBS containing 0.5 μM of L-NMMA occurred by chance. The null hypothesis accepted at: P value>0.05 (‡); P value>0.1 (‡‡); and P value>0.5 (‡‡‡).

Figure 5.5 The effects of L-NMMA and L-tryptophan on *C. psittaci* growth in ST.6 cells pretreated with ROvIFN-γ.

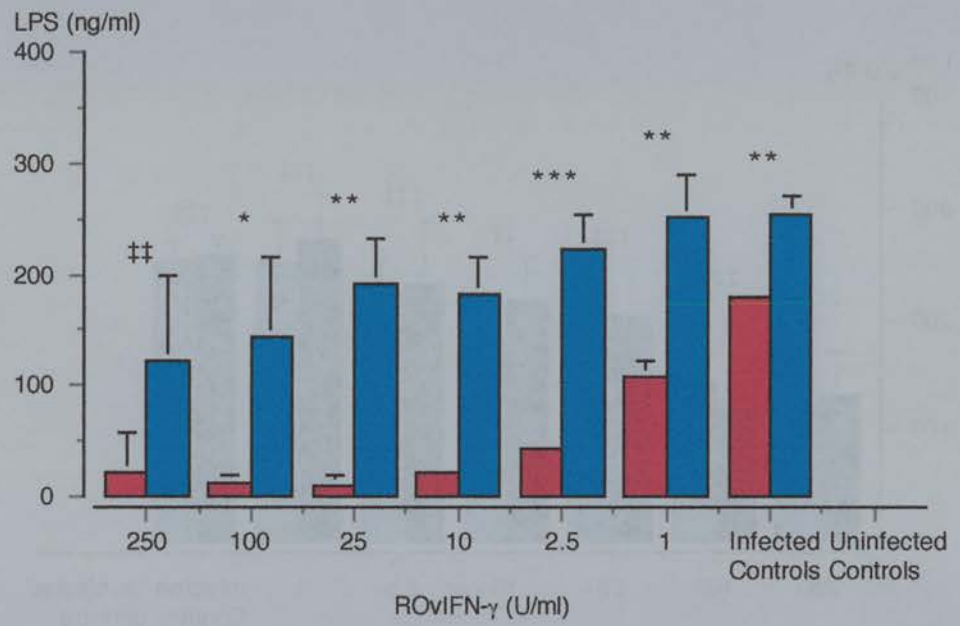

Triplicate cultures were maintained in IMDM+2% FBS alone (■) or IMDM+2% FBS containing 0.5 μM of L-NMMA and 500 μg/ml of L-tryptophan (■). Error bars represent ±1 standard deviation from the mean. Statistical significance was determined by unmatched two-tailed Student's 't' test analysis, where the null hypothesis was: Differences between chlamydial growth in cultures maintained in IMDM+2% FBS alone and cultures maintained in IMDM+2% FBS containing 0.5 μM of L-NMMA and 500 μg/ml of L-tryptophan occurred by chance. The null hypothesis was rejected at: P value<0.05 (*); P value<0.01 (**); and P value<0.001 (***). The null hypothesis accepted at: P value>0.1 (‡‡).

Figure 5.6 Comparative analysis of *C. psittaci* growth in ST.6 cells pretreated with ROvIFN-γ and maintained in the presence of L-tryptophan or L-NMMA and L-tryptophan.

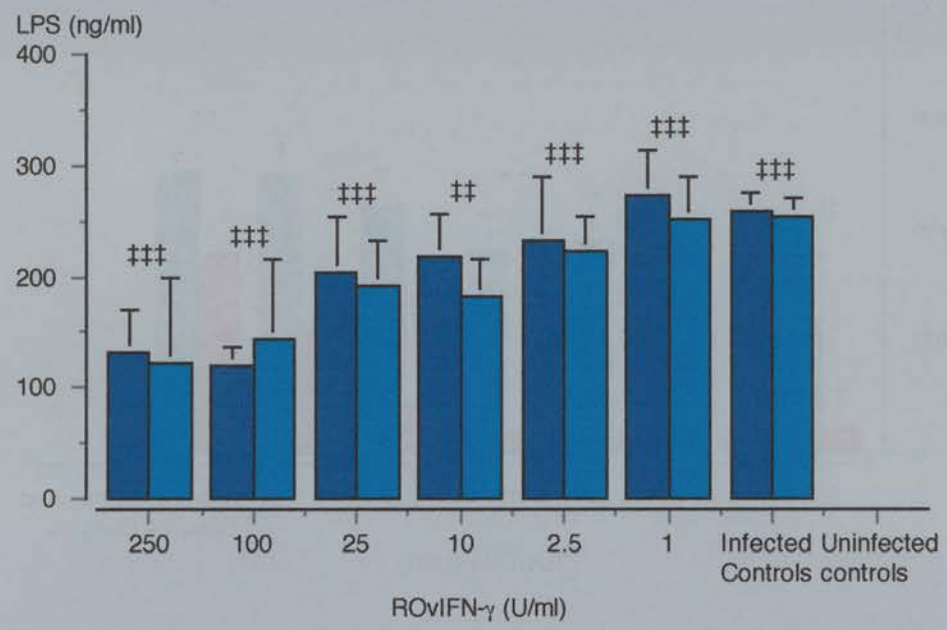

Triplicate cultures were maintained in IMDM+2% FBS supplemented with 500 μg/ml of L-tryptophan (■) or IMDM+2% FBS containing 0.5 μM of L-NMMA and 500 μg/ml of L-tryptophan (■). Error bars represent ±1 standard deviation from the mean. Statistical significance was determined by unmatched two-tailed Student's 't' test analysis, where the null hypothesis was: Differences between chlamydial growth in cultures maintained in IMDM+2% FBS containing 500 μg/ml of L-tryptophan and cultures maintained in IMDM+2% FBS containing 0.5 μM of L-NMMA plus 500 μg/ml of L-tryptophan occurred by chance. The null hypothesis was accepted at: P value>0.05 (‡); P value>0.1 (‡‡); and P value>0.5 (‡‡‡).

The ability of exogenous L-NMMA to reverse the anti-chlamydial effects ROvIFN-γ was further scrutinised in the context of ST.6 cultures maintained in IMDM+2% FBS supplemented with both L-tryptophan and L-NMMA. Whilst *C. psittaci* growth in these cultures was significantly enhanced compared to cultures maintained in IMDM+2% FBS alone (Figure 5.5), it did not differ significantly from cultures maintained in IMDM+2% FBS containing L-tryptophan (Figure 5.6). Analysis of culture supernatants using the Griess reaction indicated that NO• was not produced by any of the ST.6 cultures. Chlamydial LPS production was significantly reduced in cultures that were pretreated with ROvIFN-γ and maintained in IMDM+2% FBS alone or IMDM+2% FBS containing 0.5 μM of L-NMMA, but not in cultures that were maintained in IMDM+2% FBS containing 500 μg/ml of L-tryptophan or IMDM+2% FBS containing 500 μg/ml of L-tryptophan and 0.5 μM of L-NMMA (Table 5.4).

Table 5.4: Statistical analysis of the effects of L-tryptophan and L-NMMA on ROvIFN-γ mediated restriction of *C. psittaci* in ST.6 cells.

Biological Activity (U/ml)	*ROvIFN-γ P value =*	*+L-tryptophan P value =*	*+ L-NMMA P value =*	*+L-NMMA & L-tryptophan P value =*
250	0.0017 (-)	0.0910 (-)	0.0001 (-)	0.2634 (-)
100	0.0001 (-)	0.0051 (-)	0.0001 (-)	0.4265 (-)
25	0.0001 (-)	0.4866 (+)	0.0005 (-)	0.6643 (+)
10	0.0001 (-)	0.1629 (+)	0.0009 (-)	0.9756 (-)
2.5	0.0001 (-)	0.2045 (+)	0.0011 (-)	0.0841 (+)
1	0.0013 (-)	0.0191 (+)	0.0000 (-)	0.0285 (+)

Unmatched two-tailed Student's 't' test analysis where the null hypothesis is: Differences between chlamydial growth, measured indirectly by LPS-ELISA, in infected controls and cultures pretreated with ROvIFN-γ and maintained in IMDM+2% FBS alone or in conjunction with L-tryptophan and/or L-NMMA occurred by chance.(+/-) indicates increase/decrease.

Logarithmic transformation and linear regression were used to exclude the possibility that L-tryptophan increased *C. psittaci* growth in a manner that was independent of the anti-chlamydial effects of ROvIFN-γ. LPS concentrations were Log_2 transformed, based on the assumption that chlamydial LPS production was proportional to *C. psittaci* replication by binary fission. ROvIFN-γ concentrations were Log_{10} transformed to allow for the range of Log_{10} dilutions used in this experiment. A highly significant inverse linear relationship was observed between the concentration of chlamydial LPS (Log_2) produced by infected cultures and the concentration of ROvIFN-γ (Log_{10}) with which they were pretreated (Table 5.5). The intercepts and gradients of the regression lines obtained for cultures maintained in IMDM+2% FBS alone or IMDM+2% FBS containing 0.5 μM of L–NMMA were almost identical to each other. Similarly, linear regression of the ROvIFN-γ dose response of cultures maintained in IMDM+2% FBS supplemented with 500 μg/ml L-tryptophan or IMDM+2% FBS containing both L-tryptophan and L–NMMA produced virtually indistinguishable results. However, the gradient of the ROvIFN-γ dose response curve of cultures supplemented with exogenous L-tryptophan was significantly shifted towards 0 compared to that of cultures maintained in the absence of exogenous L-tryptophan (Figure 5.7 and Table 5.5).

Figure 5.7: Exogenous L-tryptophan abrogates the anti-chlamydial dose response of ST.6 cells to ROvIFN-γ.

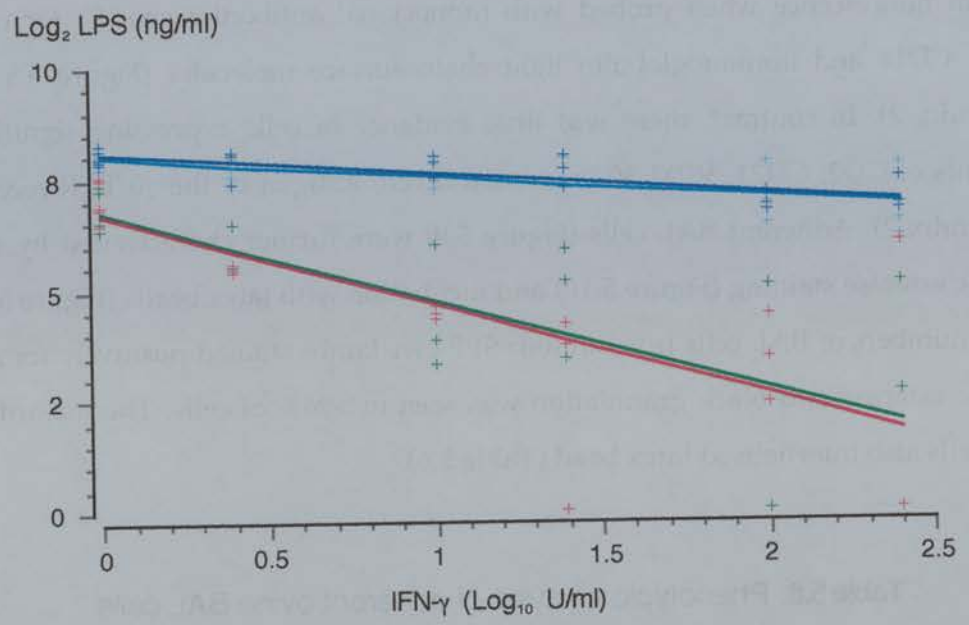

Anti-chlamydial dose response of ST.6 cells to ROvIFN-γ in the presence of IMDM+2% FBS alone (+: Regression values ———), IMDM+2% FBS supplemented with 500 μg/ml of L-tryptophan (+: Regression values ———), IMDM+2% FBS supplemented with 0.5 μM of L-NMMA (+: Regression values ———) and IMDM+2% FBS supplemented with 0.5 μM of L-NMMA and 500 μg/ml of L-tryptophan (+: Regression values ———).

Table 5.5: Linear regression of LPS (Log_2 ng/ml) and ROvIFN-γ (Log_{10} U/ml)

Culture Conditions	*Correlation Coefficient*	*Gradient*	*Intercept*	*P Value*
IMDM+2% FBS	-0.7745	-2.0403	6.6908	0.0000
L-tryptophan	-0.8246	-0.4671	8.0804	0.0000
L-NMMA	-0.7650	-1.9892	6.7470	0.0000
L-tryptophan & L-NMMA	-0.7359	-0.4752	8.0032	0.0001

5.3.4. Phenotypic analysis of ovine BAL cells

FACS analysis of ovine BAL cells revealed a single peak of cells with increased median fluorescence when probed with monoclonal antibodies specific for ovine CD45, CD14 and immunoglobulin light chain surface molecules (Figure 5.8 and Appendix 2). In contrast, there was little evidence of cells expressing significant amounts of CD2, CD21, VPM 30 (ruminant B-cell) antigen or the γδ TCR receptor (Appendix 2). Adherent BAL cells (Figure 5.9) were further characterised by non-specific esterase staining (Figure 5.10) and incubation with latex beads (Figure 5.11). Large numbers of BAL cells from all four SPF ewe lambs stained positively for non-specific esterase and black granulation was seen in >96% of cells. The majority of BAL cells also internalised latex bead (Table 5.6).

Table 5.6: Phenotypic analysis of adherent ovine BAL cells

SPF ewe lamb	*% of cells containing latex beads*	*% of non-specific esterase positive cells*
#1	95.04	99.38
#2	93.57	96.68
#3	91.08	98.6
#4	89.98	98.37

Figure 5.8A: CD14 expression on SPF ewe lamb #1 BAL cells

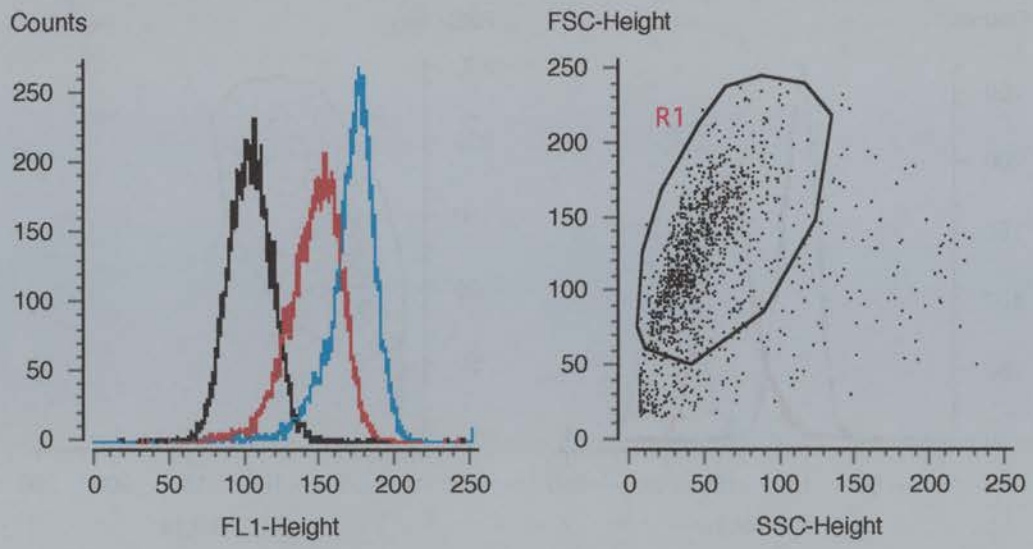

FACS analysis of ovine BAL cells from SPF ewe lamb #1. Control Mab VPM49: anti-Border Disease Virus (—), VPM65: anti-CD14 (—) and +ve control Mab SBU LCA (1.28): anti-CD45 (—) with gate (R1) set to exclude erythrocytes and dead cells.

Figure 5.8B: CD14 expression on SPF ewe lamb #2 BAL cells

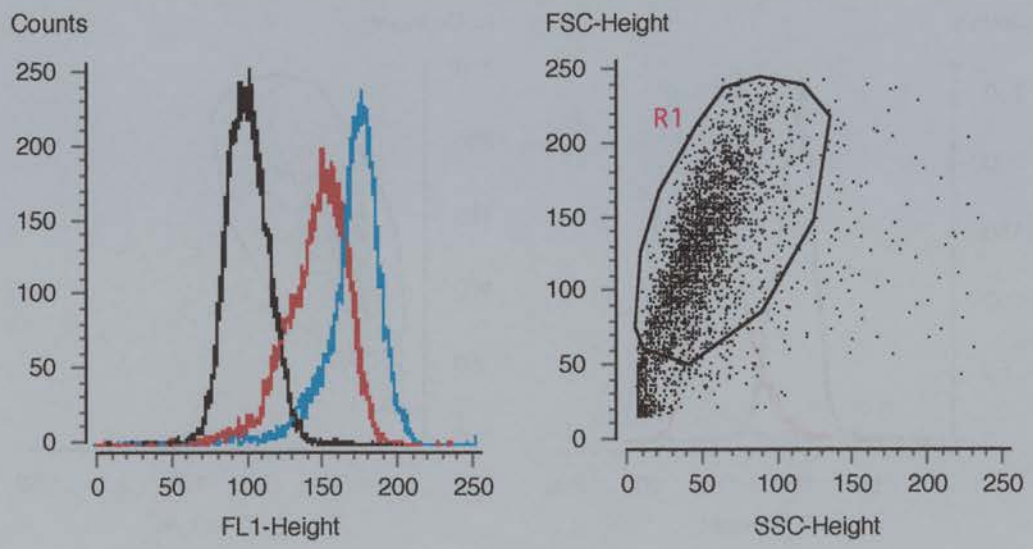

FACS analysis of ovine BAL cells from SPF ewe lamb #2. Control Mab VPM49: anti-Border Disease Virus (—), VPM65: anti-CD14 (—) and +ve control Mab SBU LCA (1.28): anti-CD45 (—) with gate (R1) set to exclude erythrocytes and dead cells.

Figure 5.8C: CD14 expression on SPF ewe lamb #3 BAL cells

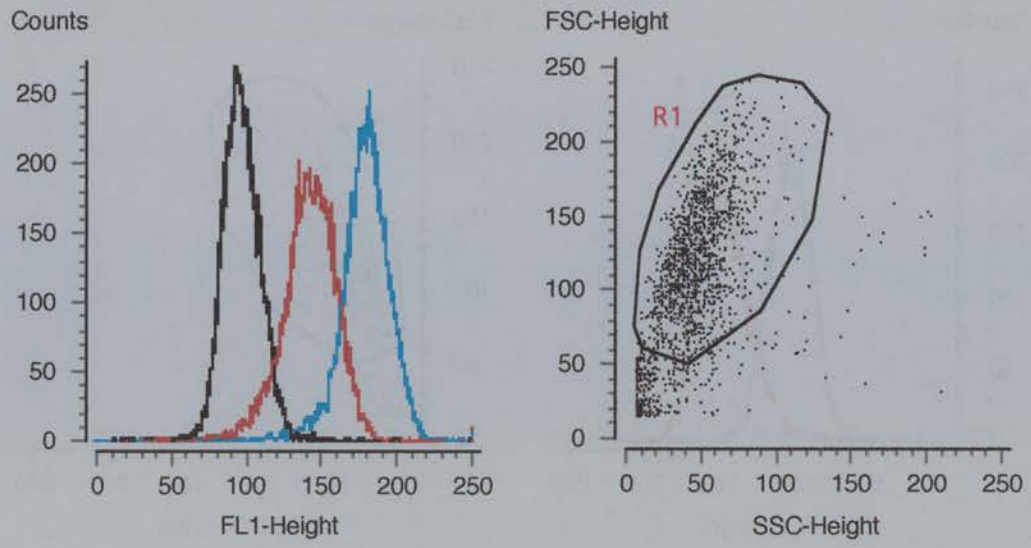

FACS analysis of ovine BAL cells from SPF ewe lamb #3. Control Mab VPM49: anti-Border Disease Virus (—), VPM65: anti-CD14 (—) and +ve control Mab SBU LCA (1.28): anti-CD45 (—) with gate (R1) set to exclude erythrocytes and dead cells.

Figure 5.8D: CD14 expression on SPF ewe lamb #4 BAL cells

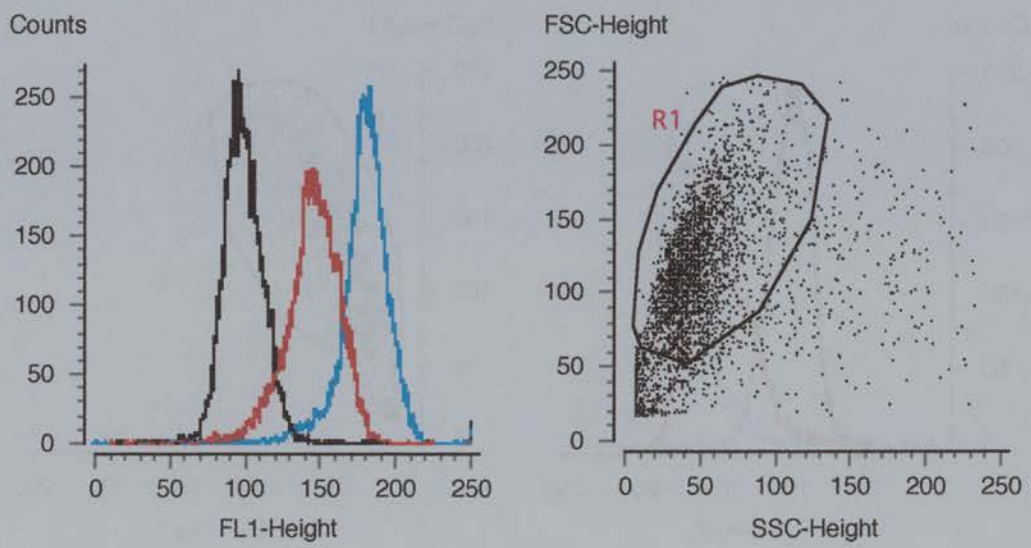

FACS analysis of ovine BAL cells from SPF ewe lamb #4. Control Mab VPM49: anti-Border Disease Virus (—), VPM65: anti-CD14 (—) and +ve control Mab SBU LCA (1.28): anti-CD45 (—) with gate (R1) set to exclude erythrocytes and dead cells.

Figure 5.9 Adherent ovine BAL cells (hematoxylin).

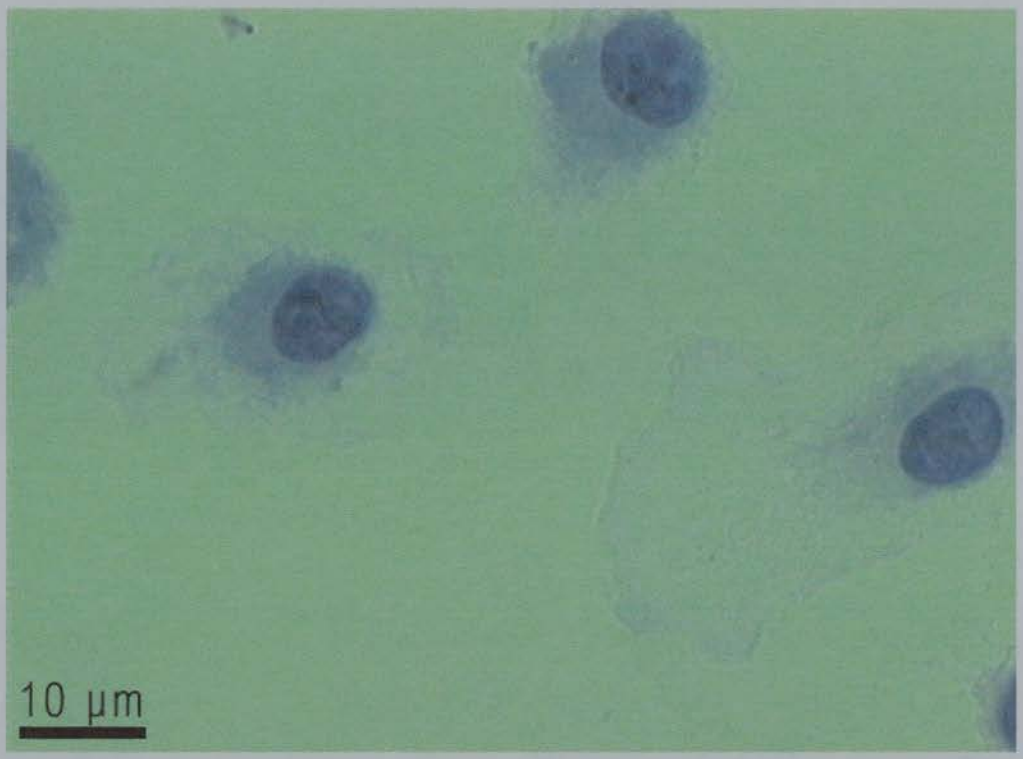

Figure 5.10 Non-specific esterase staining in adherent ovine BAL cells (hematoxylin counterstain).

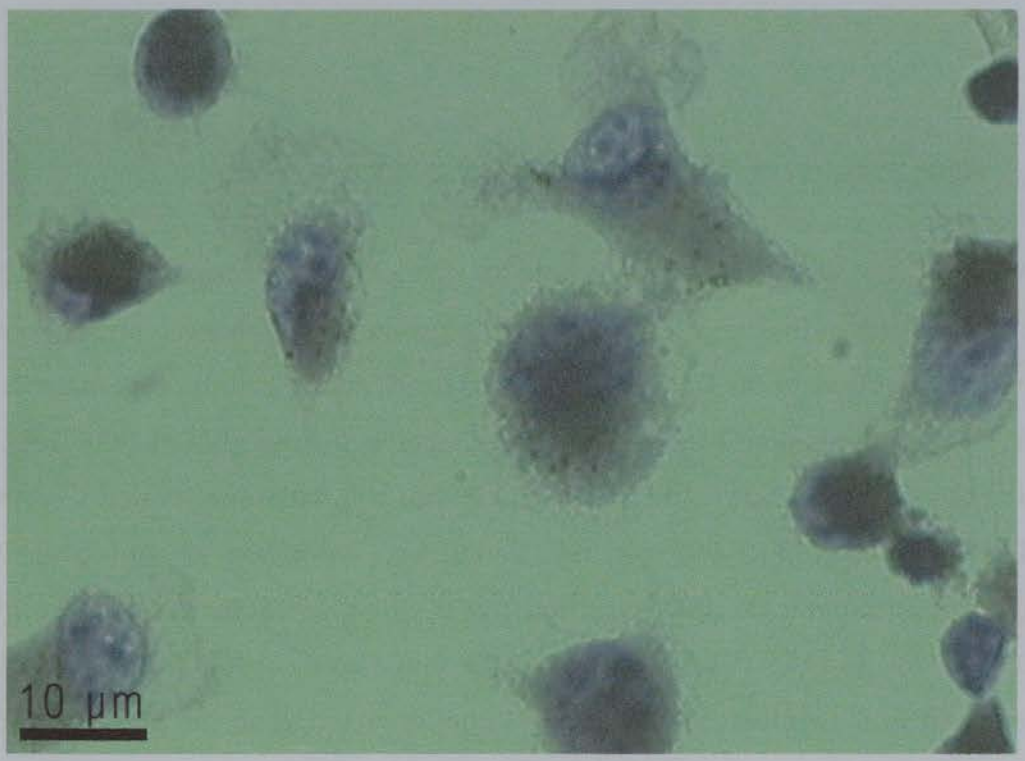

Figure 5.11 Uptake of latex beads by ovine BAL cells

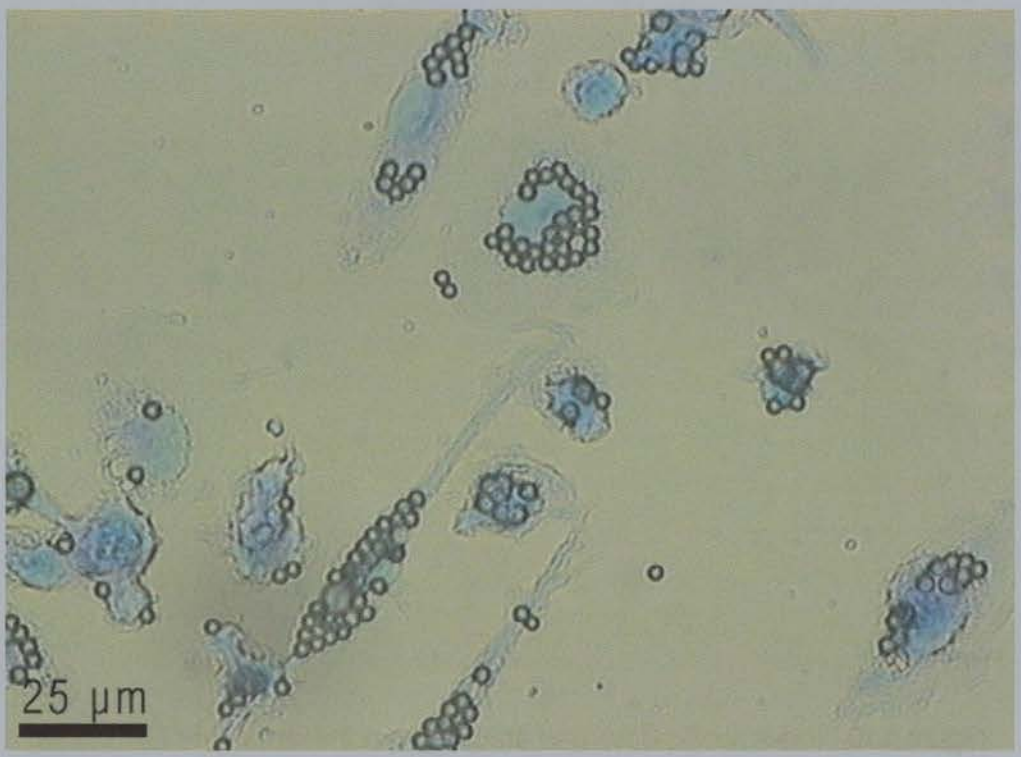

5.3.5. Nitric oxide production in murine RAW 264.7 cell controls

RAW 264.7 cells were used to determine the optimal concentrations of LPS, IFN-γ and *C. psittaci* required to induce nitric oxide production in this cell line (data not shown). Maximum levels of nitrite were detected in the culture supernatants of RAW 264.7 cells maintained for 48 hours or longer in the presence of $1x10^5$ IFU/ml of live *C. psittaci* and 500 U/ml or more of RMuIFN-γ. Heat inactivated *C. psittaci* and LPS (*S. minnesota* RE-595 or *E. coli* 026:b6) were less effective at inducing nitric oxide production in RAW 264.7 cells than live *C. psittaci*. Heat inactivated *C. psittaci* ($1x10^5$ EB/ml) and LPS (10 mg/ml) induced optimal levels of $NO^{\bullet}$ production when maintained in the culture conditions for 48 hours or longer in the presence of 500 U/ml of RMuIFN-γ.

5.3.6. Direct comparison of nitric oxide production in ovine BAL cells and murine RAW 264.7 cells

$NO^{\bullet}$ production was measured in ovine BAL and RAW 264.7 cultures maintained in various combinations of recombinant IFN-γ, LPS and heat inactivated or live *C. psittaci* for 48 hours (Figure 5.12). Ovine BAL and RAW 264.7 cultures maintained in DMEM+10% FBS supplemented with 3.9, 7.8, 15.6, 31.3, 62.5, 125, 250 or 500 U/ml of recombinant IFN-γ did not produce significant amounts of nitric oxide compared to cultures maintained in DMEM+10% FBS alone (unmatched two-tailed Student's 't' test analysis: P value = 1 in all cases). Significant (unmatched two-tailed Student's 't' test analysis: P value <0.01) amounts of nitric oxide were produced by RAW 264.7 cultures maintained in DMEM+10% FBS containing 1 μg/ml of LPS and 250 U/ml or more of RMuIFN-γ. Nitric oxide production reached a similar level of significance (unmatched two-tailed Student's 't' test analysis: P value <0.01) in RAW 264.7 cultures maintained in the presence of 250 U/ml or more of RMuIFN-γ and $1x10^5$ EB/ml of heat inactivated *C. psittaci*. RAW 264.7 cultures infected with $1x10^5$ IFU/ml of live *C. psittaci* produced significant (unmatched two-tailed Student's 't' test analysis: P value <0.01) amounts of nitric oxide in the presence of 62.5 U/ml or more of RMuIFN-γ (Figure 5.12A).

Figure 5.12: Nitric oxide production by murine RAW 264.7 cells and ovine BAL cells over 48 hours.

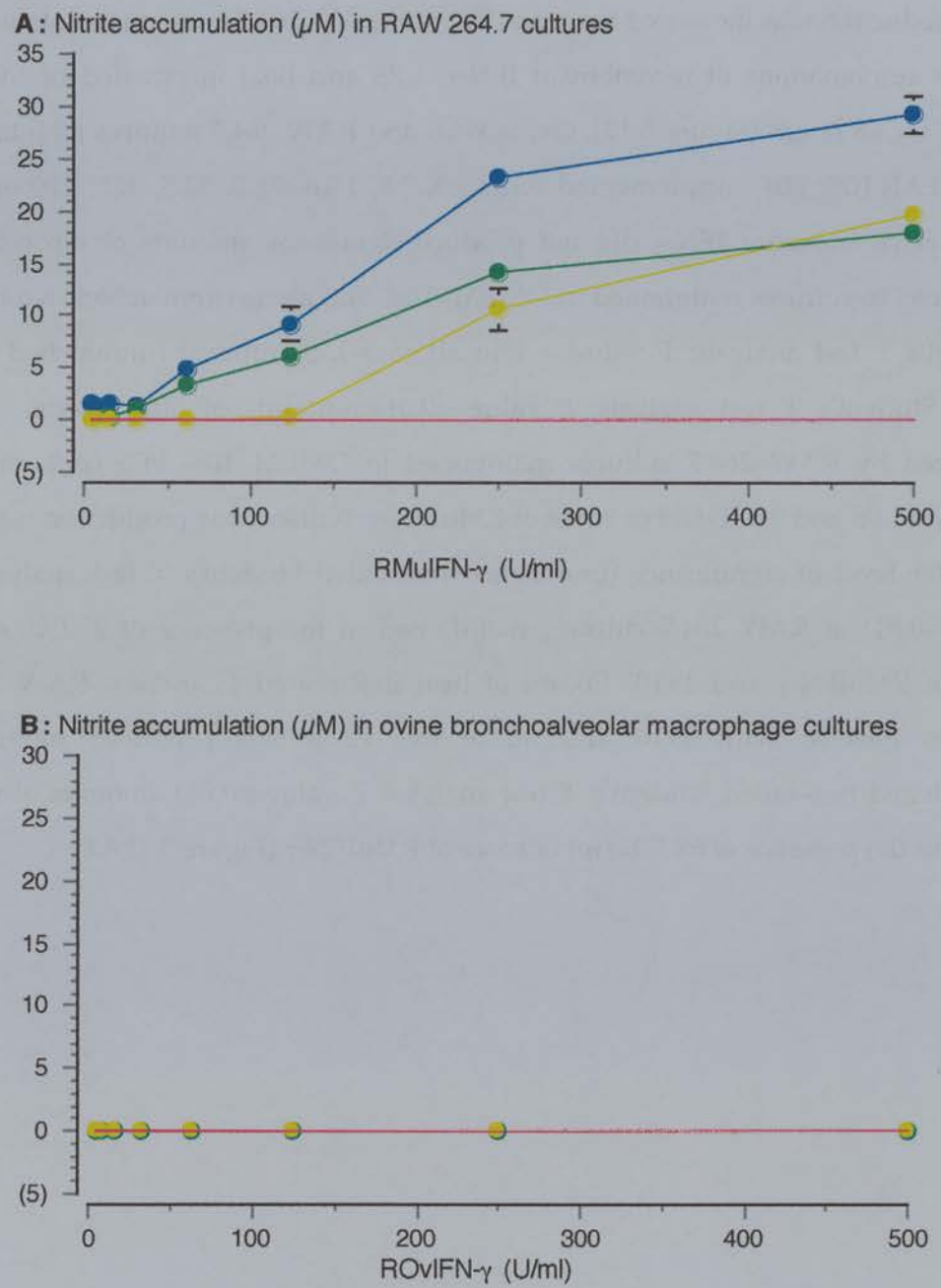

Nitrite accumulation in triplicate cultures of murine RAW 264.7 (**A**) and ovine BAL (**B**) cells over 48 hours incubation with various concentrations of IFN-γ and: DMEM+10% FBS alone (——); DMEM+10% FBS +1 μg/ml LPS (——●——); DMEM+10% FBS + $1x10^5$ IFU/m of *C. psittaci* (——●——, not visible in **B**); DMEM+10% FBS + $1x10^5$ EB/ml of heat inactivated *C. psittaci* (——●——, not visible in **B**). Error bars represent ±1 standard deviation from the mean.

Figure 5.13: Time course of nitric oxide production by murine RAW 264.7 cells and ovine BAL cells in the presence of carboxy–PTIO.

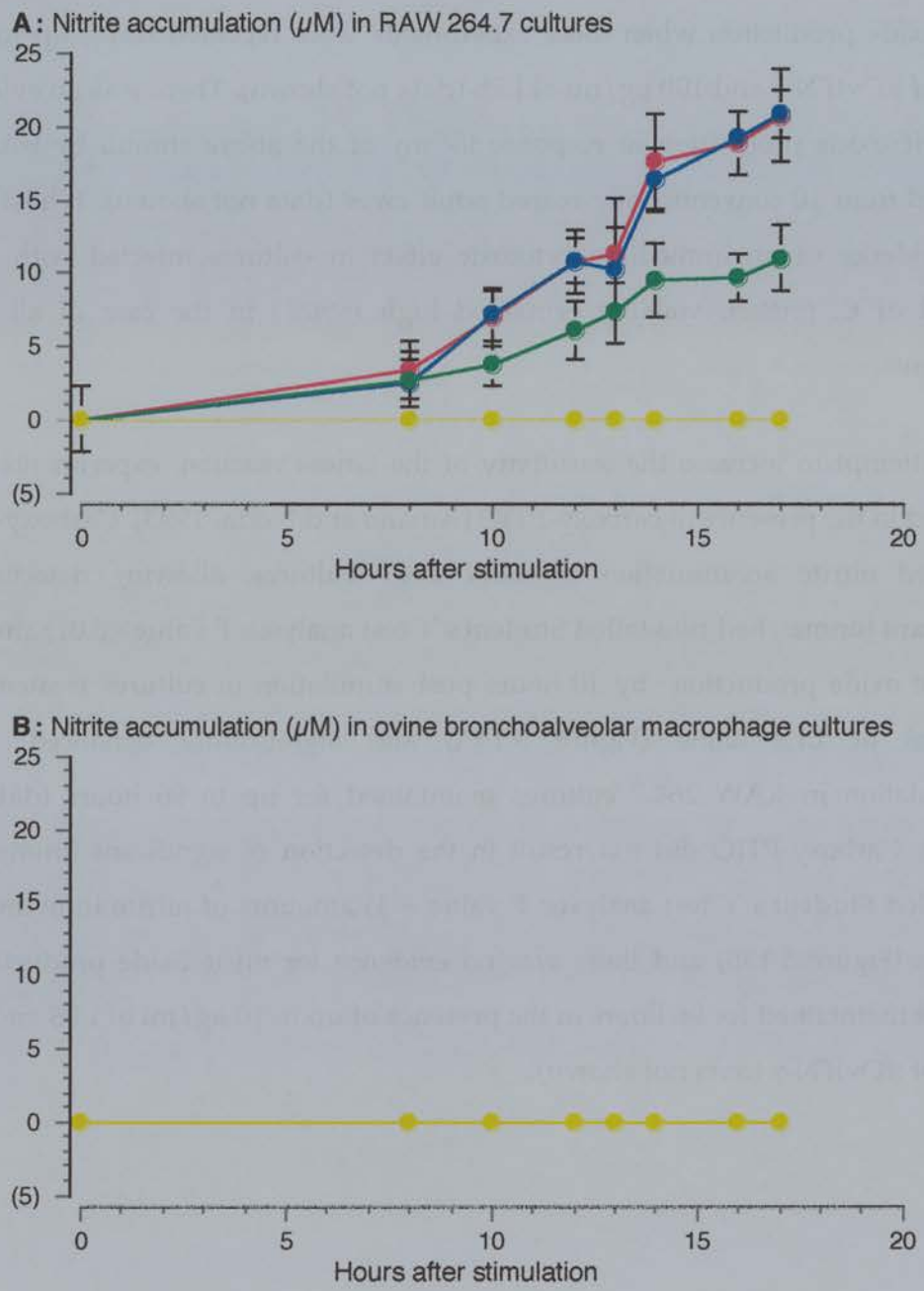

Nitrite accumulation in triplicate cultures of murine RAW 264.7 (**A**) and ovine BAL (**B**) cells over 17 hours post stimulation. Cultures were maintained in DMEM+10% FBS supplemented with 10 μg/ml of LPS (—●—, not visible in **B**), 1 μg/ml of LPS + 1000 U/ml of IFN-γ (—●—, not visible in **B**), or 10 μg/ml of LPS + 1000 U/ml of IFN-γ (—●—, not visible in **B**). Control cultures were maintained in DMEM+10% FBS alone (—●—). 100 μM carboxy PTIO was maintained in the culture conditions throughout the experiment. Error bars represent ±1 standard deviation from the mean.

Ovine BAL cells from all four SPF ewe lambs failed to produce significant levels of nitric oxide (unmatched two-tailed Student's 't' test analysis: P value =1 in all cases) in response to any of the stimuli (Figure 5.12A). There was no evidence of increased nitric oxide production when these experiments were repeated using up to 1000 U/ml of ROvIFN-γ and 100 μg/ml of LPS (data not shown). There was no evidence for nitric oxide production in response to any of the above stimuli by BAL cell obtained from 10 conventionally reared adult ewes (data not shown). Whilst there was evidence of an immediate cytotoxic effect in cultures infected with $1x10^5$ IFU/ml of *C. psittaci*, viability remained high (>90%) in the case of all other treatments.

In an attempt to increase the sensitivity of the Griess reaction, experiments were repeated in the presence of carboxy-PTIO [Amano and Noda, 1995]. Carboxy-PTIO increased nitrite accumulation in RAW 264.7 cultures, allowing detection of significant (unmatched two-tailed Student's 't' test analysis: P value <0.01) amounts of nitric oxide production by 10 hours post stimulation in cultures treated with 10μg/ml of LPS alone (Figure 5.13A) and significantly enhanced nitrite accumulation in RAW 264.7 cultures maintained for up to 96 hours (data not shown). Carboxy-PTIO did not result in the detection of significant (unmatched two-tailed Student's 't' test analysis: P value = 1) amounts of nitrite in ovine BAL cultures (Figure 5.13B) and there was no evidence for nitric oxide production in cultures maintained for 96 hours in the presence of up to 10 μg/ml of LPS and 1000 U/ml of ROvIFN-γ (data not shown).

5.3.7. ROvIFN-γ mediated restriction of chlamydial growth in ovine alveolar macrophages

Figure 5.14 Typical *C. psittaci* inclusion morphology (arrow) in untreated ovine alveolar macrophages (IPX/hematoxylin).

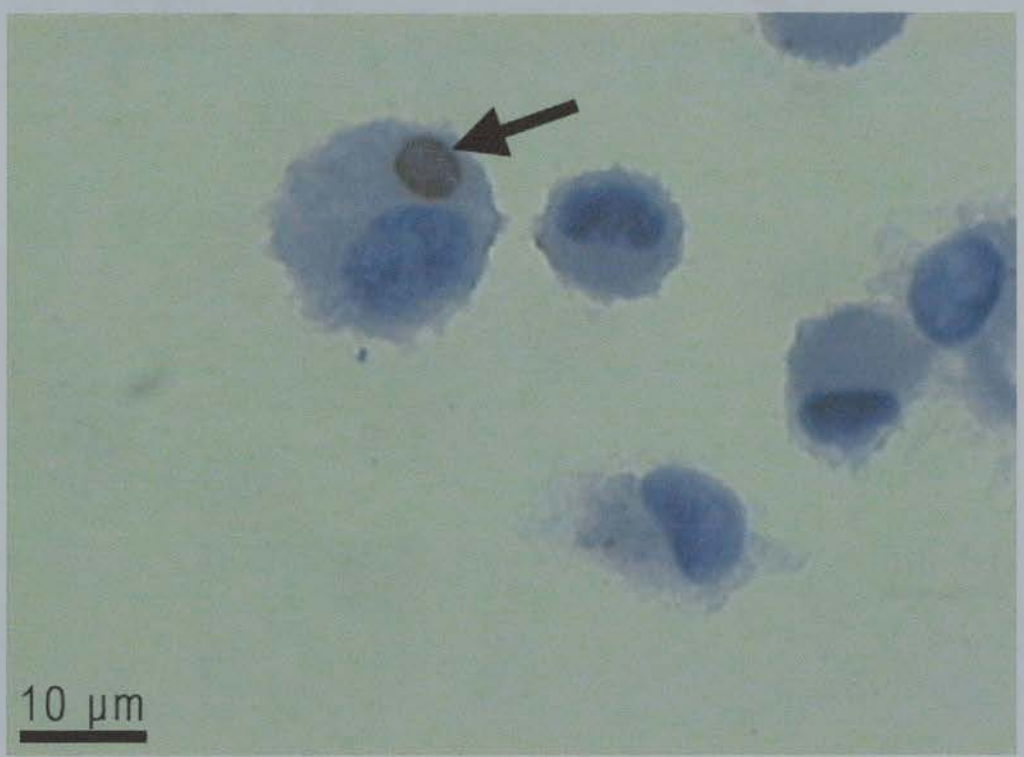

Approximately 20% of BAL cells in cultures which had not been pretreated with ROvIFN-γ developed a single large (5.8±2.4 µm diameter: n=100) inclusion body which stained intensely with MOMP-specific IPX (Figure 5.14). Multiple inclusion bodies (2-3/cell) were very rare in these cultures (>1% of cells) and were typically only marginally smaller than those in cells containing one body (3.2–1.7 µm diameter: n=30). This pattern was consistent in BAL cells from all four SPF lambs.

Figure 5.15 Typical (black arrow) and aberrant (red arrow) *C. psittaci* inclusion morphology in ovine BAL cells pretreated with 2.5 U/ml of ROvIFN-γ (IPX/hematoxylin).

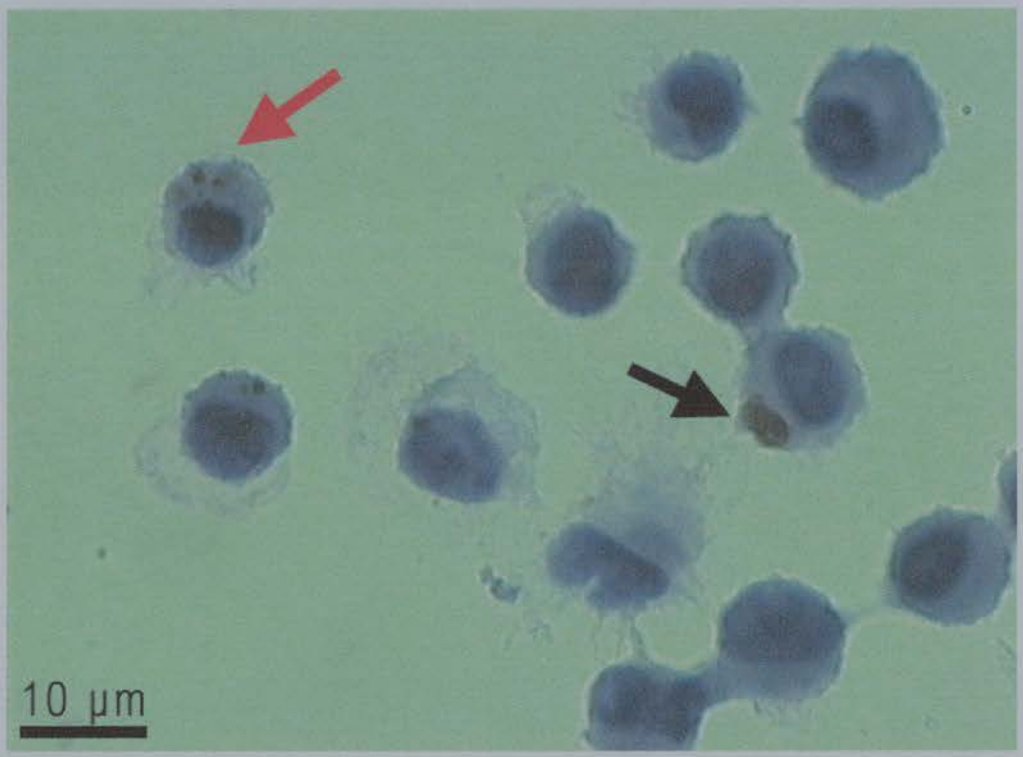

Cultures that had been pretreated with ROvIFN-γ prior to infection showed an increase in the amount of cells staining positively with IPX. Approximately 30% of BAL cells pretreated with 2.5 U/ml of ROvIFN-γ stained positively for *C. psittaci* MOMP. However, the majority of BAL cells pretreatment with 2.5 U/ml ROvIFN-γ contained aberrantly small (0.9±0.2 µm diameter: n=193) multiple inclusion bodies (Figure 5.15: Red arrow), although more typical inclusion bodies were also evident in these cultures (Figure 5.15: Black arrow). Cells containing multiple inclusion bodies also tended to exhibit increased plasma membrane projections. This pattern was consistent in BAL cells from all four sheep.

Figure 5.16 Aberrant *C. psittaci* inclusion morphology (arrow) in ovine BAL cells pretreated with 25 U/ml of ROvIFN-γ (IPX/hematoxylin).

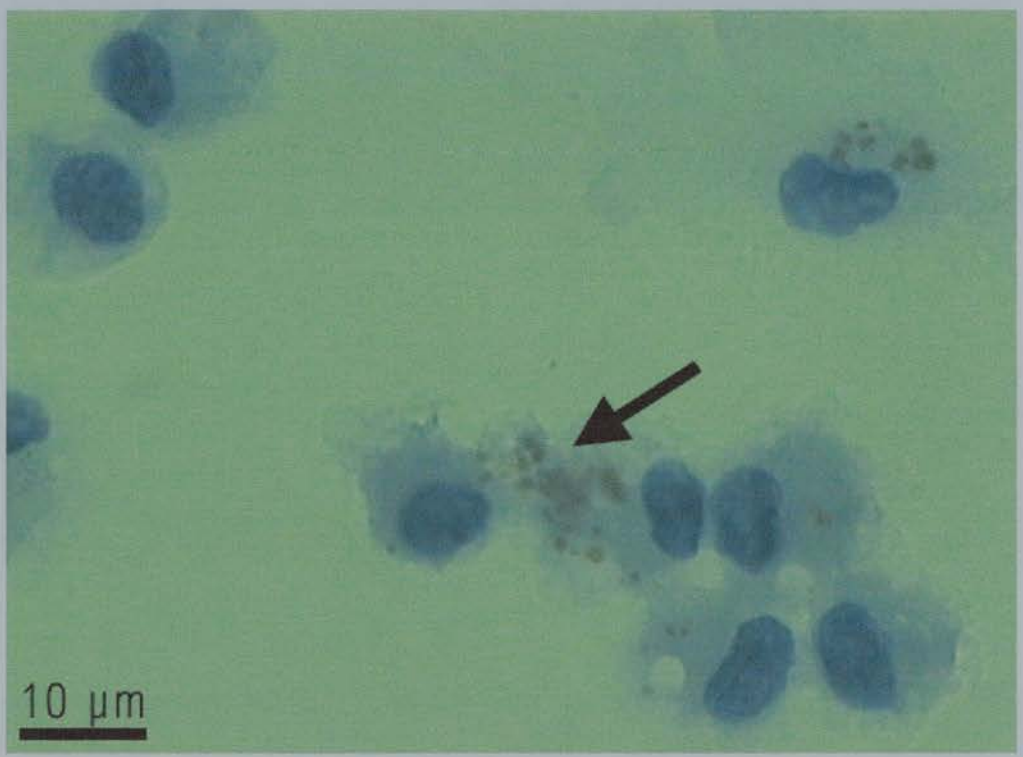

As the concentration of ROvIFN-γ was increased the frequency of cells staining positively for MOMP increased. However, very few cells treated with 25 U/ml of ROvIFN-γ contained morphologically "normal" inclusion bodies (<1% of cells containing inclusion bodies: n=112). Furthermore, the number of aberrant inclusion bodies within each cell increased, although the size remained constant (0.8±0.3 µm diameter: n=213). There was also evidence of increased plasma membrane projections in cells containing antigen and a change in the spatial arrangement of BAL cells toward a more clumped distribution (Figure 5.16). This pattern was consistent in BAL cells derived from all four sheep.

Figure 5.17 Aberrant *C. psittaci* inclusion morphology (arrow) in ovine BAL cells pretreated with 250 U/ml of ROvIFN-γ (IPX/hematoxylin).

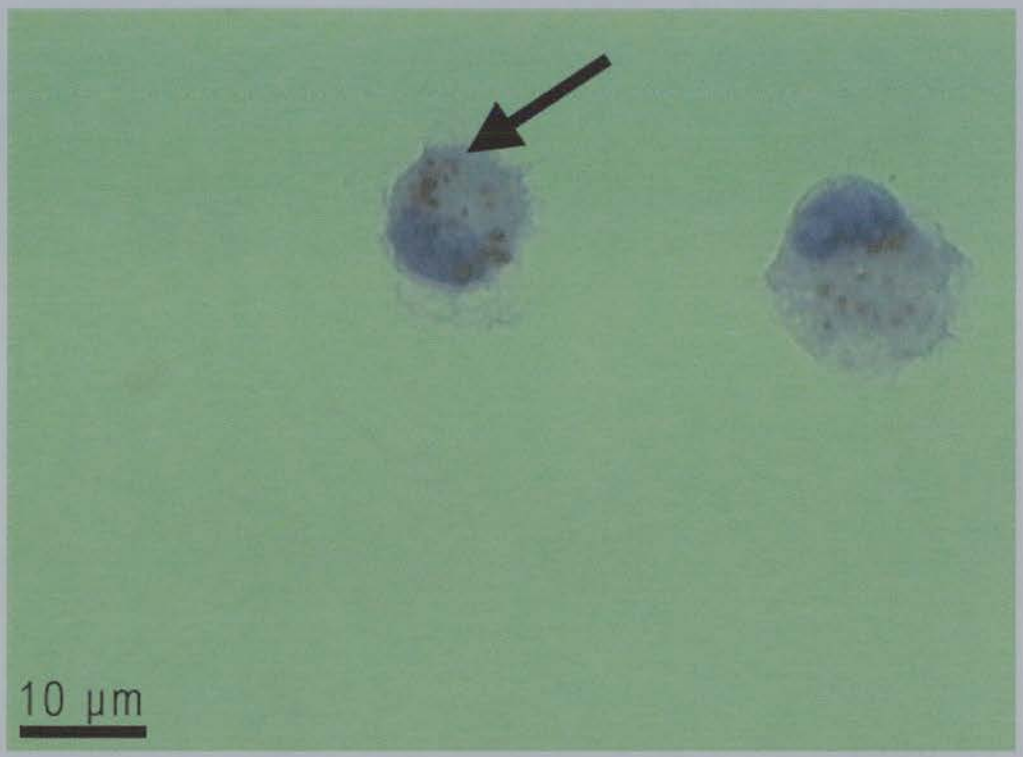

Approximately 40% of BAL cells from cultures which were pretreated with 250 U/ml of ROvIFN-γ contained vesicles which stained positively for MOMP by IPX. Morphologically "normal" inclusion bodies were not observed in any of the BAL cultures pretreated with 250 U/ml of ROvIFN-γ. Some cells contained as many as 20 small (1.0±0.2 µm diameter: n=198) vesicles of chlamydial antigen and exhibited increased plasma membrane projections (Figure 5.18). This pattern was consistent in BAL cells derived from all four sheep.

5.4. Discussion

Initial attempts to delineate the mechanisms through which ROvIFN-γ inhibits the growth of *C. psittaci* in ovine ST.6 cells suggested that they are independent from its anti-viral activities. Pretreatment of ST.6 cultures with ROvIFN-γ, Poly I: Poly C or RBovIFN-α prevented cytopathic growth of SFV in the ovine interferon bioassay. However, when used at concentrations matched for anti-viral activity, only ROvIFN-γ was shown to restrict the growth of *C. psittaci* in ST.6 cells (Figures 5.1 and 5.2). Although 150 U/ml of Poly I: Poly C appeared to restrict *C. psittaci* LPS production, this effect was due to a reduction in number of ST.6 host cells resulting from the cytotoxic effect of Poly I: Poly C at this concentration (500 μg/ml), rather than a direct anti-chlamydial effect. These findings parallel the results of previous studies in human macrophages and T24 cells which showed that RHuIFN-γ, but not recombinant human IFN-α (RHuIFN-α) or recombinant human IFN-β (RHuIFN-β), inhibited the growth of *C. psittaci*, *Toxoplasma gondii* and *Leishmania donovani* [Murray *et al*, 1989].

The mechanisms through which IFN-γ restricts the growth of chlamydiae in human and murine cells appear to be distinct [De La Maza *et al*, 1985; Murray and Teitelbaum, 1992]. Whilst initial studies in ovine ST.6 cells suggest a role for tryptophan depletion [Graham *et al*, 1995], the possibility that $NO^{\bullet}$ production contributes to the anti-chlamydial effects of ROvIFN-γ required clarification. Addition of exogenous L-tryptophan to ST.6 cultures that were pretreated with ROvIFN-γ resulted in significantly increased chlamydial growth (Figures 5.3 and Table 5.4). However, there was also evidence that exogenous L-tryptophan increased chlamydial growth in control cultures that were not pretreated with ROvIFN-γ (Figures 5.3). In contrast, $NO^{\bullet}$ production was not detected in the supernatants of ST.6 cells that had been pretreated with ROvIFN-γ (data not shown). In addition, there was no evidence that L-NMMA reversed the anti-chlamydial effects of ROvIFN-γ (Figures 5.4 - 5.6 and Table 5.4) and it would appear that $NO^{\bullet}$ production is unlikely to be involved in ROvIFN-γ mediated restriction of *C. psittaci* growth in ovine ST.6 cells. Whilst these findings show that exogenous L-tryptophan can enhance *C. psittaci* growth in ROvIFN-γ pretreated ST.6

cells, they do not rule out the possibility that this effect is unrelated to the anti-chlamydial effects of ROvIFN-γ.

To confirm that ROvIFN-γ and L-tryptophan depletion are directly related, the data were logarithmically transformed to allow linear regression of the ROvIFN-γ dose response. If exogenous L-tryptophan completely abrogates the anti-chlamydial effects of ROvIFN-γ in the absence of an independent increase in *C. psittaci* growth, the intercept of the dose response curve would remain constant regardless of whether cultures were maintained in L-tryptophan or not. However, the gradient of the dose response curve would be shifted to zero in cultures that were supplemented with exogenous L-tryptophan.

Alternatively, if exogenous L-tryptophan enhances *C. psittaci* growth through a mechanism that is independent of the anti-chlamydial effects of ROvIFN-γ, the gradient of the dose response curve for cultures supplemented with exogenous L-tryptophan would be identical to that of cultures maintained in IMDM+2% FBS alone. In this case only the intercept value would change in cultures supplemented with exogenous L-tryptophan, with the effect that the dose response curve would be shifted vertically but remain parallel to that obtained for cultures that were not supplemented with exogenous L-tryptophan.

Whilst the linear regressions obtained for the ROvIFN-γ dose responses in the experiment detailed here did not conform exactly to either of these two extremes, the gradients of the dose response curves obtained for cultures supplemented with exogenous L-tryptophan were markedly shifted towards zero suggesting that tryptophan availability and the ability of ROvIFN-γ to restrict *C. psittaci* growth are directly related (Figure 5.7 and Table 5.5). Despite the fact that *C. psittaci* growth was enhanced by exogenous L-tryptophan in cultures that were not pretreated with ROvIFN-γ, these results strongly support a role for tryptophan catabolism in ROvIFN-γ mediated restriction of *C. psittaci* growth in ovine ST.6 cells.

Although these finding suggest that the anti-chlamydial effects of ovine IFN-γ may share similarities with that of human IFN-γ [Byrne *et al*, 1986; Mehta *et al*, 1998;

Murray *et al*, 1989; Summersgill *et al*, 1995; Thomas *et al*, 1993], the mechanisms through which IFN-γ restricts the growth of chlamydiae are also likely to be affected by the phenotype of the target cell. Murray *et al* (1989) reported that whilst both RHuIFN-γ the type 1 interferons, RHuIFN-α and RHuIFN-β, upregulate tryptophan catabolism in human macrophages, only RHuIFN-γ was capable of restricting the growth of *C. psittaci*, *T. gondii* and *L. donovani*. However, they also reported that the anti-microbial effects of RHuIFN-γ were partially reversed by exogenous tryptophan and concluded that although tryptophan depletion contributes to the anti-microbial effects of IFN-γ it does not appear to be sufficient or required to restrict the growth of intracellular pathogens in human macrophages. Investigation of the mechanisms responsible for ROvIFN-γ mediated restriction of *C. psittaci* growth was subsequently extended to include *ex vivo* derived ovine BAL cells.

Phenotypic and functional analysis confirmed that BAL cells were analogous to macrophages. FACS analysis showed that ovine BAL cells comprised a single homogeneous population expressing CD45 and CD14 but not CD2, CD21, γδ TCR or VPM 30. Although there was little evidence for BAL cells expressing ovine CD21 or the ruminant B-cell marker, VPM 30 antigen [Hopkins *et al*, 1993], the entire population of BAL cells stained positively for immunoglobulin light chain (Appendix 2). The most likely explanation for these apparently conflicting results is that the anti-immunoglobulin antibody, VPM 8 [Bird *et al*, 1995], recognised *in vivo* acquired immunoglobulin bound to BAL cell Fc receptors. Furthermore, BAL cells were highly adherent, phagocytic and stained positively for non-specific esterase activity in a manner that suggests they were functionally analogous to macrophages [Yam *et al*, 1971].

The murine macrophage RAW 264.7 cell line produced abundant amounts of $NO^{\bullet}$ in response to stimulation with RMuIFN-γ in combination with LPS, heat inactivated S26/3 *C. psittaci* or live S26/3 *C. psittaci* (Figure 5.12). $NO^{\bullet}$ detection was enhanced when RAW 264.7 cultures were maintained in the presence of 100 μM of carboxy-PTIO (Figure 5.13), which increases nitrite accumulation and improves the sensitivity of the Griess reaction [Amano *et al*, 1995]. In contrast, $NO^{\bullet}$ production was not induced in ovine BAL macrophages from all four SPF ewe lambs, even

when they were stimulated with much higher concentrations of LPS and recombinant IFN-γ than were required for optimal NO• production in RAW 264.7 cultures. In addition, NO• production could not be induced in BAL macrophages derived from a further 10 conventionally reared adult ewes. Inclusion of carboxy-PTIO in the culture conditions did not result in the detection of significant amounts of nitrite in any of the BAL macrophages cultures examined here. These findings suggest that, like human macrophages [Murray and Teitelbaum, 1992] but in contrast to murine macrophages [Chen *et al*, 1996], NO• production is unlikely to be involved in ROvIFN-γ mediated restriction of *C. psittaci* in ovine macrophages.

Both human and murine macrophages have been shown to be susceptible to infection with *C. psittaci* or *C. trachomatis* [Manor and Sarov, 1986; Wyrick and Brownridge, 1978; Wyrick *et al*, 1978; Zhong and De La Maza, 1988]. In contrast, *C. pneumoniae* growth has been shown to be restricted in human macrophages infected *ex vivo* [Gaydos *et al*, 1996]. An immediate cytotoxic effect was observed in ovine BAL macrophages that were incubated with live S26/3 *C. psittaci* at ratio of 1.0 EB per macrophage, but in agreement with previous studies using murine macrophages [Wyrick and Brownridge; 1978, Wyrick *et al*, 1978; Su and Caldwell, 1995] and ovine BAL macrophages [Entrican *et al*, 1999], this effect was abolished when EB were heat inactivated or the ratio of EB to macrophages was reduced. Microscopic examination of ovine BAL macrophages, 60 hours after they were infected with *C. psittaci* at a ratio of 0.1 EB per macrophage, revealed large, typically singular, chlamydial inclusion bodies which stained intensely by IPX in approximately 20% of macrophages (Figure 5.14). These finding suggest that, not only do ovine BAL macrophages support *C. psittaci* growth, but they appear to be more susceptible to infection than the ST.6 cell line which was used to determine the number of *C. psittaci* EB (IFU/ml) of used in this experiment. The reason for this is not clear, but it may be related to differences in the phagocytic ability of the two cell types.

Whilst ROvIFN-γ did not induce NO• production in ovine BAL macrophages infected with *C. psittaci*, it did have a number of interesting effects on the growth of the pathogen. The finding that ROvIFN-γ increased the percentage of BAL macrophages that contained what appeared to be inclusion bodies is surprising

given that IFN-γ has been extensively shown to inhibit *C. psittaci* inclusion body formation in human and murine macrophages [Rothermel *et al*, 1983, 1986; Murray and Teitelbaum, 1992; Murray *et al*, 1989; Carlin and Weller, 1995]. Furthermore, ROvIFN-γ mediated restriction of *C. psittaci* LPS production in ST.6 cells is associated with a reduction in the number of cell containing inclusion bodies (data not shown). Interestingly, ROvIFN-γ also appeared to increase plasma membrane activity in BAL macrophages, an effect which was most notable in cultures which were pretreated with 250 U/ml of ROvIFN-γ (Figure 5.17). The increase in the percentage of cells containing MOMP suggests that this may reflect increased phagocytic activity.

Although ROvIFN-γ increased the percentage of BAL macrophages containing inclusion bodies it also had a highly marked effect on inclusion body morphology. Typical inclusion body morphology (Figure 5.14) was rare in BAL macrophages that were pretreated with 25 U/ml ROvIFN-γ and entirely absent from cultures pretreated with 250 U/ml. Instead, BAL macrophages from these culture contained multiple small (0.9±0.3 μm diameter), spherical vesicles which stained positively for *C. psittaci* MOMP by IPX (Figure 5.17).

There are a number of possible explanations for this finding. The vesicles of MOMP observed in BAL macrophages pretreated with ROvIFN-γ may be phagolysosomes containing MOMP derived from degraded *C. psittaci* rather that classical inclusion bodies containing viable replicating chlamydiae. Under these circumstances the increase in both the percentage of macrophages with vesicles containing MOMP and the number of vesicles per cell may be explained by the presence of large numbers of non-viable chlamydiae in inoculum used to infect the cultures. This is supported by the observation that during the preparation of tissue culture-derived stocks of the S26/3 *C. psittaci* (Chapter 2.1.8.) the titre of infectious EB (IFU/ml) commonly falls by over 1 Log_{10} after freezing in chlamydial transport medium (data not shown). Alternatively, ROvIFN-γ may block the aggregation of endosomes containing chlamydiae in BAL macrophages infected with multiple EB and normal inclusion body formation in a manner that is similar to effects of intracellular free Ca^{2+} depletion described in murine McCoy and human HeLa 229 cells infected with *C.*

trachomatis [Majeed *et al*, 1993; 1994]. Whilst this could represent a novel mechanism through which ROvIFN-γ restricts the growth of *C. psittaci* in ovine macrophages it does not explain the increase in the number of cells with vesicles containing MOMP. Another possibility is that *C. psittaci* initially forms normal inclusion bodies that are subsequently degraded in ROvIFN-γ pretreated BAL macrophages. Further studies incorporating confocal microscopy may help to clarify this novel effect of ROvIFN-γ in ovine macrophages.

Whilst it is clear that ROvIFN-γ induced aberrant *C. psittaci* inclusion body morphology in ovine BAL macrophages, these studies did not confirm whether infection of BAL macrophages was associated with the production of infectious chlamydiae or if ROvIFN-γ was capable of inhibiting *C. psittaci* growth in these cells. Future time course studies and titration of BAL macrophage supernatants for infectious chlamydiae would resolve this issue.

Chapter 6.0

Persistent *C. psittaci* Infection of Ovine Cells

6.1 Introduction

Persistent subclinical infection of the non-pregnant ewe with the agent responsible for OEA was first confirmed in 1951 [McEwen *et al*, 1951b]. The ability of *C. psittaci* to persist in the non-pregnant ewe without inducing protective immunity to OEA is not only critical for its survival and dissemination but also severely complicates the diagnosis and control of this pathogen [Buxton, 1994; Rodolakis, 1998]. However, the question as to how *C. psittaci* persists in immunocompetent sheep without inducing protective immunity remains largely unresolved. Given that *C. psittaci* does not appear to cause significant pathology prior to pregnancy [Amin and Wilsmore, 1995; Buxton *et al*, 1996; Huang *et al*, 1990], it can be assumed that the immune response in the naive non-pregnant ewe is able to restrict, but not eradicate, the pathogen. Current diagnostic technology is limited to the identification of ewes which have already aborted as a result of OEA and is consequently of limited prophylactic value. Identification of the immune mechanisms through which persistence is established and maintained in the ewe would not only provide a basis for the identification of persistently infected animals but might also have extensive ramification for vaccine design.

IFN-γ has been reported to induce and maintain persistent *C. trachomatis* infection in human HeLa 229 cells [Beatty *et al*, 1993; 1994a; 1994b; 1995] and more recently in polarised human epithelial cells [Kane and Byrne, 1998]. IFN-γ mediated persistence has also been reported in human HEp-2 cells infected with *C. pneumoniae* [Mehta *et al*, 1998]. Similarly, short term *in vitro* studies have shown that ROvIFN-γ can restrict the growth of the S26/3 strain of *C. psittaci* in ovine ST.6 cells [Graham *et al*, 1995] (Chapter 5) and ovine alveolar macrophages (Chapter 5) in a dose dependent manner. However, whether ROvIFN-γ eradicates chlamydiae from ovine cultures or simply restricts chlamydial growth in a reversible manner similar to that described in human cells [Beatty *et al*, 1995; Kane and Byrne, 1998; Mehta *et al*, 1998] has not been established. Consequently, it was of interest to determine the role, if any, ROvIFN-γ plays in establishing and maintaining persistence in ovine cells.

6.2 Materials and Methods

6.2.1 Infection of ST-6 cells and treatment with ROvIFN-γ

ST.6 cells were seeded into 25 cm^2 vented tissue culture flasks (Costar, High Wycombe, U.K.) at a density of $5x10^4$ cells/ml in 6 ml of IMDM+5% FBS (culture medium). After 3 days, when ST.6 cell monolayers were still sub-confluent, cells were incubated with 1 ml of culture medium containing $3x10^4$ *C. psittaci* strain S26/3 EB. Mock-infected controls were incubated with 1 ml of culture medium alone. After 6 hours, the supernatants were removed and replaced with 6 ml of culture medium containing concentrations of between 0 and 100 U/ml of ROvIFN-γ. The exact concentrations of ROvIFN-γ used in these experiments are displayed in Table 6.1.

Table 6.1: ST.6 culture treatments

Experiment Number	ROvIFN-γ (U/ml) Infected cultures	ROvIFN-γ (U/ml) uninfected cultures
6.3.1	0, 0.1, 0.5, 1.0, 5.0, 10.0	0
6.3.2	10, 100	0

6.2.2 Maintenance of persistently infected ST.6 cells

Cultures were passaged into fresh 25 cm^2 vented tissue culture flasks every 7 days following the procedure outlined in section 2, with the following adaptations. The cells were detached with trypsin/versene, washed in 10 ml of culture medium, centrifuged at 400 g for 5 minutes and resuspended in fresh culture medium. The cells from each flask were passaged at a 1 : 3 ratio and seeded into two fresh flasks in 6 ml volumes. ROvIFN-γ was then added to only one of each pair of new cultures to give the same final concentration of ROvIFN-γ that the cells had been maintained in during the previous 7 days. The other flask was maintained in ROvIFN-γ-free culture medium for the duration of the experiment or until chlamydiae lysed all the

ST.6 cells. This method of passaging cultures was used throughout the experiments. The procedure is represented diagrammatically in Figure 6.1.

6.2.3 Measurement of *C. psittaci* multiplication

Cultures were examined for evidence of *C. psittaci* growth at intervals of 7 days. Culture supernatants were collected prior to passage and assayed for chlamydial LPS by ELISA (Chapter 2.5.1.). In experiment 6.3.2, culture supernatants were also titrated on ST.6 cells to determine the numbers, if any, of infectious chlamydiae present (Chapter 2.5.2.). Giemsa stain was used to identify *C. psittaci* inclusion bodies (Chapter 2.4.3.).

6.2.4 Statistics

Spearman's Rank correlations were performed where evidence of dose dependent effects were observed. Triplicate data was generated by the LPS-ELISA and titration of supernatants. However, because each replicate represented the same culture supernatant it would be inappropriate to use these data for comparative statistics.

Figure 6.1: An *in vitro* model of persistent *C. psittaci* infection in ST.6 cells

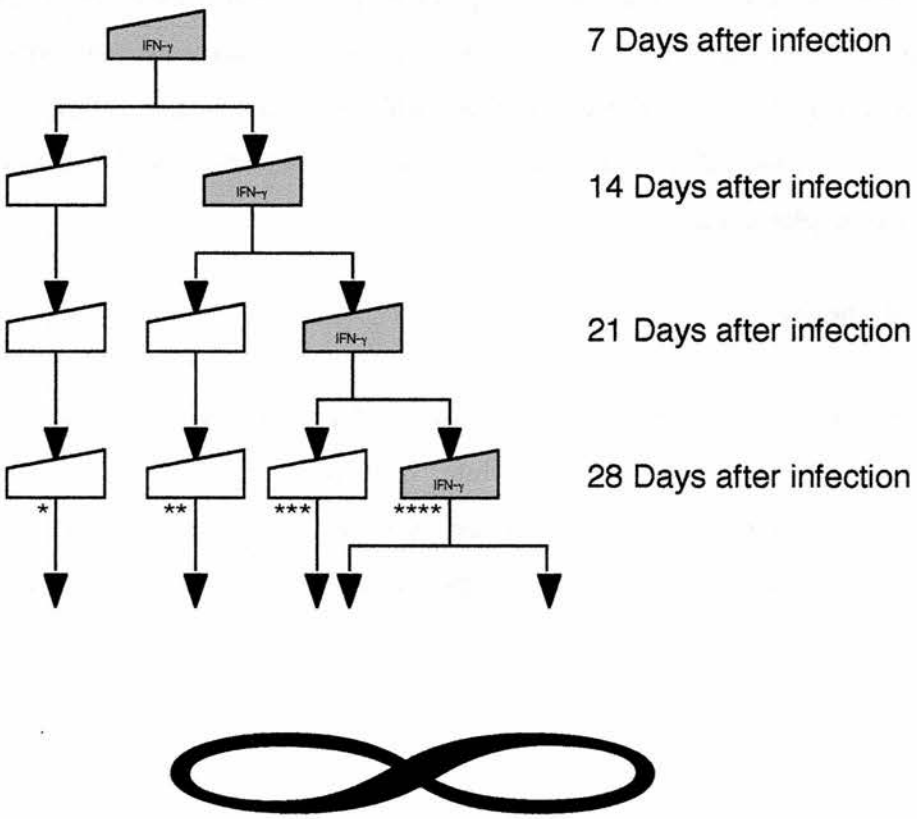

Figure 6.1: ROvIFN-γ was maintained in the culture medium for the duration of the experiment (▱). At each passage, secondary cultures were established and maintained in ROvIFN-γ-free culture medium (▱). This generated cultures in which ROvIFN-γ was maintained for: (*) the first 7 days after infection; (**) the first 14 days after infection; (***) the first 21 days after infection; (****) until the conclusion of the experiment.

6.3 Results

6.3.1 Restriction of *C. psittaci* growth in ovine ST.6 cells maintained in ROvIFN-γ for 21 days

25 cm^2 vented tissue culture flasks containing confluent monolayers of ST.6 cells were infected with $3x10^4$ *C. psittaci* strain S26/3 EB on day 0. An uninfected control culture was incubated in parallel with culture medium alone. One of the infected cultures was maintained in ROvIFN-γ-free culture medium and used as the infected control. The remaining infected cultures were maintained in culture medium containing 0.1, 0.5, 1, 5 or 10 U/ml of ROvIFN-γ for periods of 7, 14 and 21 days. The uninfected control was maintained for the duration of the experiment and used to provide background values for the LPS-ELISA.

The results of LPS-ELISA analysis of culture supernatants on day 14 are displayed in figure 6.2A. ROvIFN-γ reduced *C. psittaci* LPS production in a dose dependent manner, regardless of whether it was maintained in the culture medium for 7 or 14 days after infection (Spearman Rank Correlation Coefficient {ROvIFN-γ/ml : IFU/ml}: r_s = -1.00, $p<0.01$ in both cases). There was evidence of an increase in chlamydial growth when ROvIFN-γ was removed from the culture medium on day 7. LPS was not detected in the culture maintained for 14 days in 10 U/ml of ROvIFN-γ.

The results of LPS-ELISA analysis of culture supernatants on day 21 are displayed in figure 6.2B. Cultures treated with 5 or less U/ml of ROvIFN-γ failed to control chlamydial growth, resulting in complete lysis of these cultures and the absence of detectable dose dependent restriction of chlamydial LPS production (Spearman Rank Correlation Coefficient {ROvIFN-γ/ml : IFU/ml}: ROvIFN-γ maintained for 21 days r_s = 0.00, $p>1$ and for 14 days r_s = -0.3, $p>0.6$). LPS production was not detected in the culture maintained in 10 U/ml for 21 days. However, detectable concentrations of LPS were found when ROvIFN-γ was removed from the culture medium in the last 7 days of culture.

Figure 6.2: Recombinant OvIFN-γ mediated restriction of *C. psittaci* growth in ST.6 cells

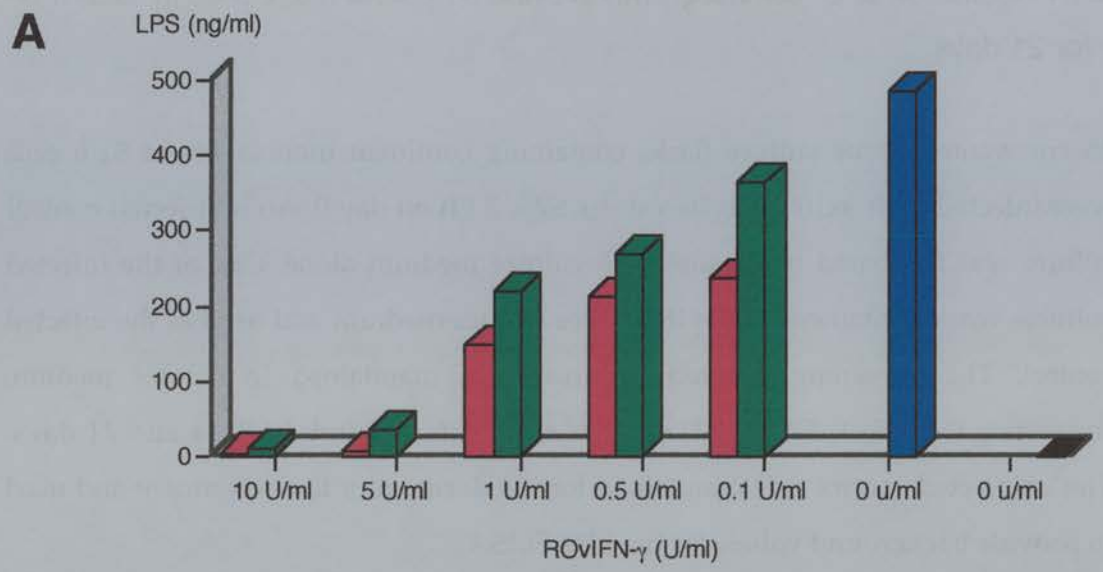

Chlamydial growth in ovine ST.6 cells 14 days after infection, measured indirectly using an LPS-ELISA to assay the concentration of chlamydial LPS in triplicate supernatant samples from each culture. ROvIFN-γ was maintained in cultures for 14 days (■) or for the first 7 days of culture (■). Infected control (■). Uninfected control (■).

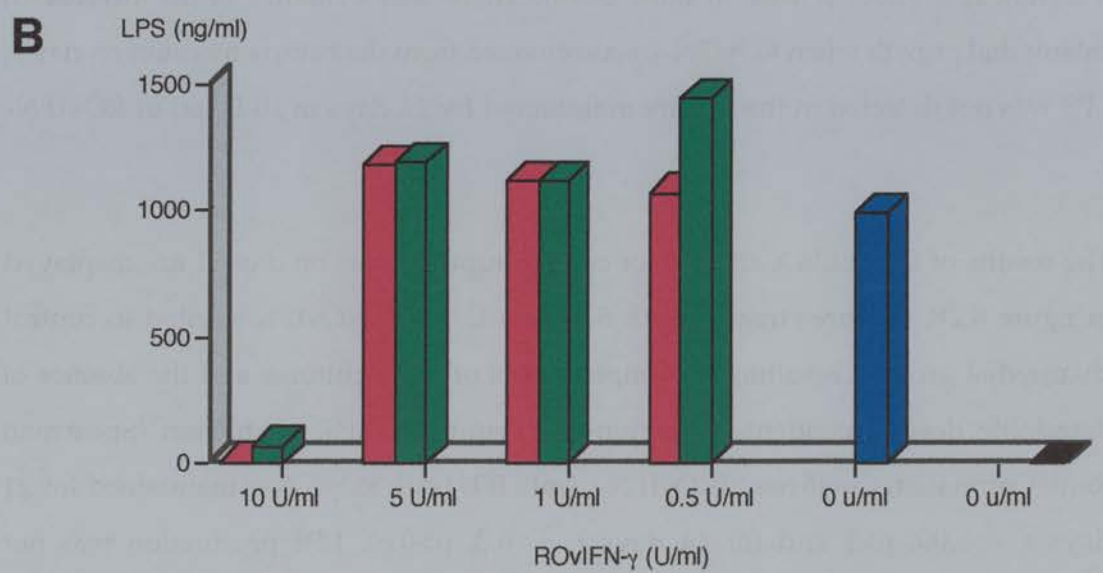

Chlamydial growth in ovine ST.6 cells 21 days after infection, measured indirectly using an LPS-ELISA to assay the concentration of chlamydial LPS in triplicate supernatant samples from each culture. ROvIFN-γ was maintained in cultures for 21 days (■) or for the first 14 days of culture (■). Infected control (■). Uninfected control (■).

Despite the absence of detectable chlamydial LPS in the culture supernatants, chlamydial inclusion bodies were clearly visible in all the infected cultures throughout this experiment.

6.3.2 Persistence *C. psittaci* infection of ovine ST.6 cells maintained in ROvIFN-γ for up to 28 days after infection.

The initial findings detailed in 6.3.1 suggested that it may be possible to induce persistent *C. psittaci* infection of ovine ST.6 cells through the action of ROvIFN-γ alone. The presence of replicating chlamydiae in cultures from which the supernatants were found to be negative for chlamydial LPS by ELISA indicated that the use of the LPS-ELISA alone was not suitable for determining whether chlamydial growth had been completely arrested. In the next experiment, the maximum concentration of ROvIFN-γ used was increased by a factor of 10, chlamydial LPS production was measured using the LPS-ELISA and the numbers of infectious EB present in the culture supernatants were determined by titration. 25 cm^2 vented tissue culture flasks containing confluent monolayers of ST.6 cells were infected with $3x10^4$ *C. psittaci* strain S26/3 EB on day 0. An uninfected control culture was incubated in parallel with culture medium alone. Infected cultures were maintained in culture medium containing 10 or 100 U/ml of ROvIFN-γ for periods of 7, 14, 21 and 28 days. The uninfected control was maintained for the duration of the experiment and used to provide negative controls for the LPS-ELISA and titration analysis.

Figure 6.3 Analysis of *C. psittaci* growth in ST.6 cells treated with ROvIFN-γ for 14 Days.

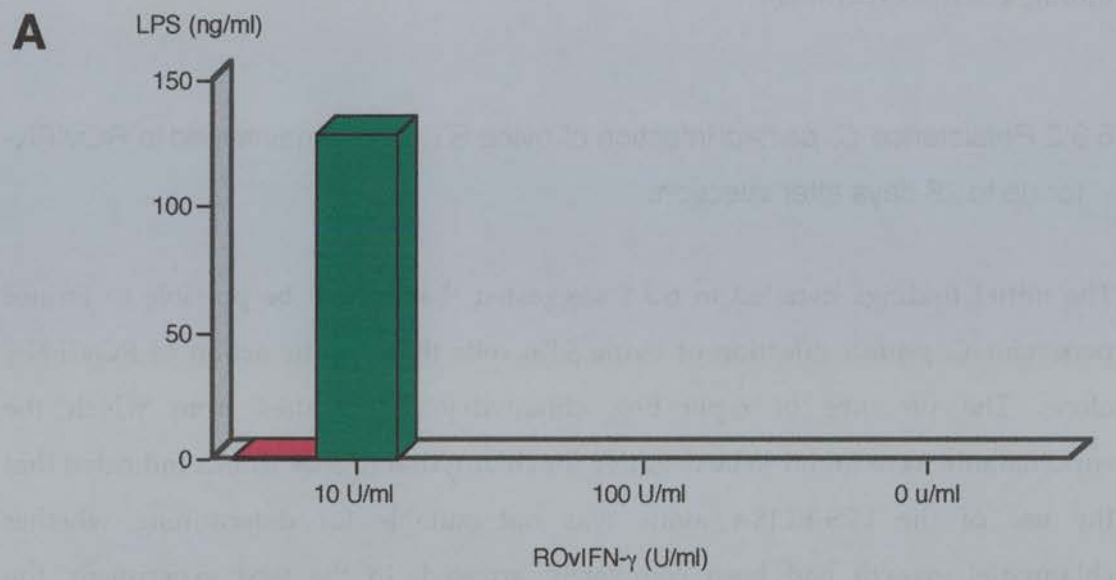

Chlamydial growth in ovine ST.6 cells 14 days after infection, measured indirectly using an LPS-ELISA to assay the concentration of chlamydial LPS in triplicate supernatant samples from each culture. ROvIFN-γ was maintained in cultures for 14 days (■) or for the first 7 days of culture (■). Uninfected control (■ not visible).

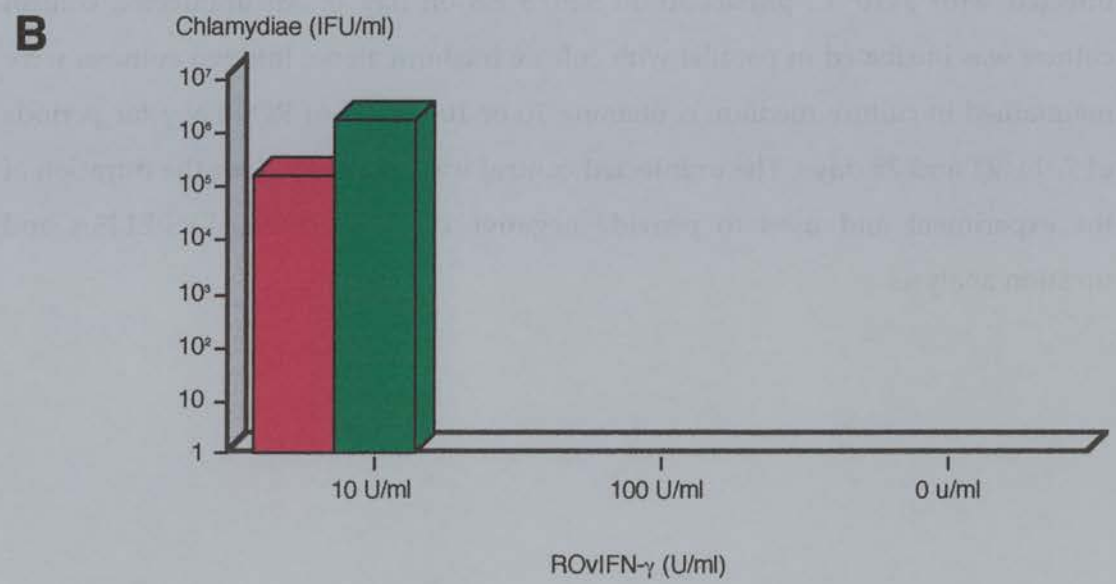

Chlamydial growth in ovine ST.6 cells 14 days after infection, measured by titration of inclusion forming units (IFU) in triplicate supernatant samples from each culture. ROvIFN-γ was maintained in cultures for 14 days (■) or for the first 7 days of culture (■). Uninfected control (■ not visible).

6.3.2.1 Analysis of *C. psittaci* growth on day 14

The results of LPS-ELISA analysis of culture supernatants on day 14 are displayed in figure 6.3A. LPS was not detected in cultures maintained for 14 days in medium containing ROvIFN-γ. When ROvIFN-γ was removed from the culture conditions on day 7, the amount of LPS increased in the culture treated with 10 U/ml, but remained at background levels in the culture treated with 100 U/ml. The results of titration analysis of culture supernatants for infectious chlamydiae on day 14 are displayed in figure 6.3B. Infectious EB were not detected in the supernatants of the cultures maintained for 7 or 14 days in medium containing 100 U/ml of ROvIFN-γ. Infectious EB were found in the supernatants of the cultures maintained in 10 U/ml for 7 and 14 days after infection. Removal of ROvIFN-γ from the culture conditions on day 7 resulted in a 10 fold increase in the numbers of infectious EB present in the supernatant of the culture that had been treated with 10 U/ml of ROvIFN-γ, but had no effect on the culture treated with 100 U/ml.

6.3.2.2 Analysis of *C. psittaci* growth on day 21

The results of LPS-ELISA analysis of culture supernatants on day 21 are displayed in figure 6.4A. Chlamydial LPS production was not detected when cultures were maintained in 10 or 100 U/ml of ROvIFN-γ for 21 days. Detectable amounts of LPS were recorded in cultures maintained in 10 U/ml for 7 and 14 days, and in the culture maintained in 100 U/ml for 7 days. The results of titration analysis of culture supernatants for infectious chlamydiae on day 21 are displayed in figure 6.4B. Infectious EB were found in all of the cultures that were treated with 10 U/ml of ROvIFN-γ, regardless of how long it was maintained in the culture medium. Infectious EB were not detected in cultures maintained for 14 or more days in 100 U/ml of ROvIFN-γ. However, infectious EB were recovered when ROvIFN-γ was removed from the culture conditions on day 7. In all cases, the shorter the duration of exposure to ROvIFN-γ, the higher the concentration of LPS and greater the number of infectious EB found in culture supernatants.

Figure 6.4: Analysis of *C. psittaci* growth in ST.6 cells treated with ROvIFN-γ for 21 Days.

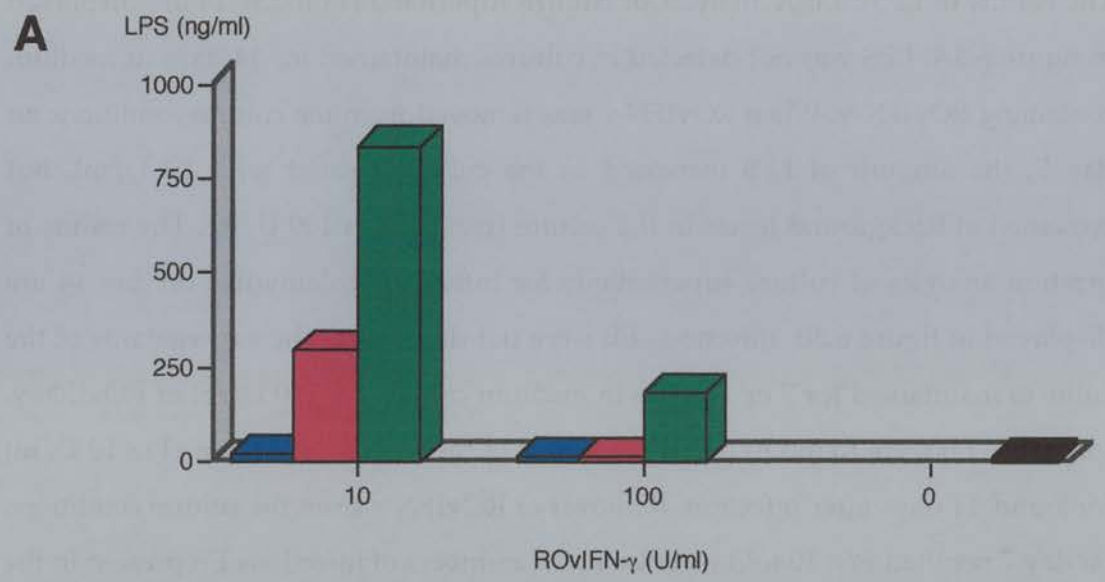

Chlamydial growth in ovine ST.6 cells 21 days after infection, measured indirectly using an LPS-ELISA to assay the concentration of chlamydial LPS in triplicate supernatant samples from each culture. ROvIFN-γ was maintained in cultures for 21 days (■), for the first 14 days (■) or for the first 7 days of culture (■). Uninfected control (■).

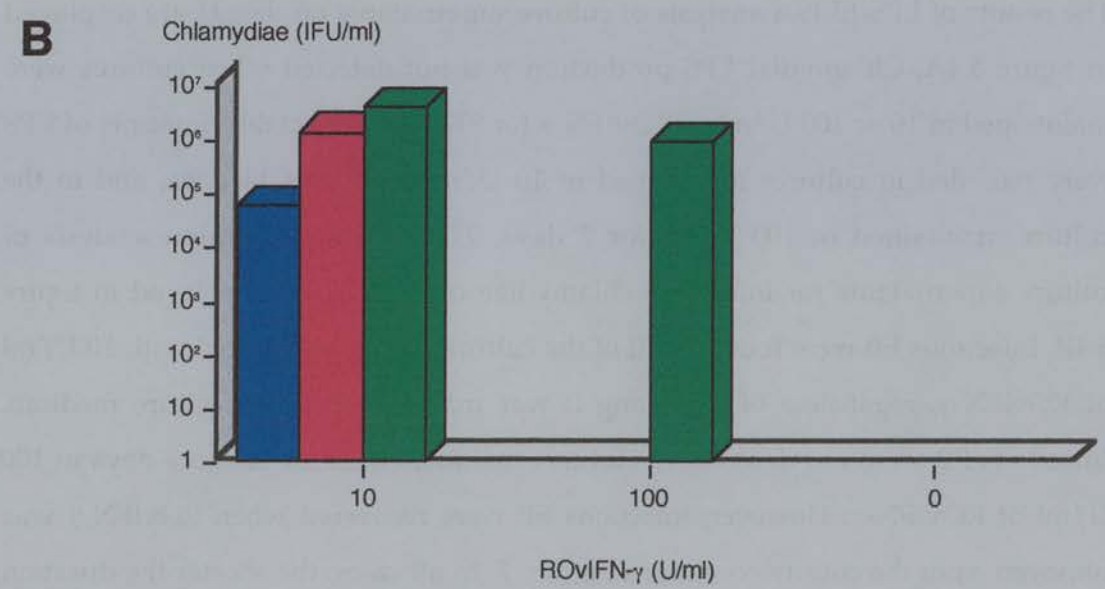

Chlamydial growth in ovine ST.6 cells 21 days after infection, measured by titration of inclusion forming units (IFU) in triplicate supernatant samples from each culture. ROvIFN-γ was maintained in cultures for 21 days (■), for the first 14 days (■) or for the first 7 days of culture (■). Uninfected controls (■ not visible).

Figure 6.5: Analysis of *C. psittaci* growth in ST.6 cells treated with ROvIFN-γ for 28 Days.

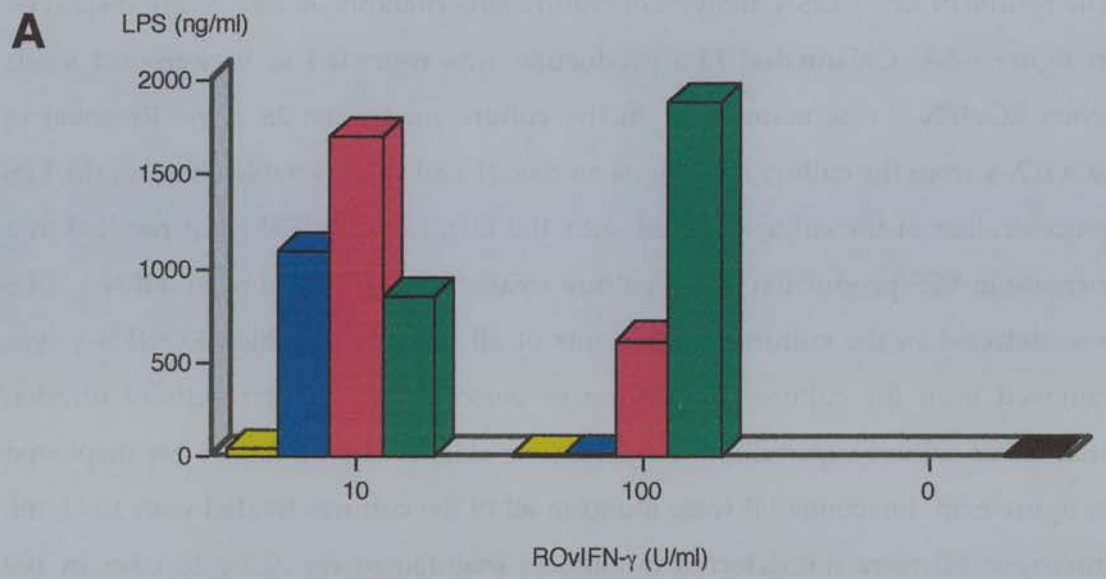

Chlamydial growth in ovine ST.6 cells 28 days after infection, measured indirectly using an LPS-ELISA to assay the concentration of chlamydial LPS in triplicate supernatant samples from each culture. ROvIFN-γ was maintained in cultures for 28 days (■), for the first 21 days (■), for the first 14 days (■) or for the first 7 days of culture (■). Uninfected control (■).

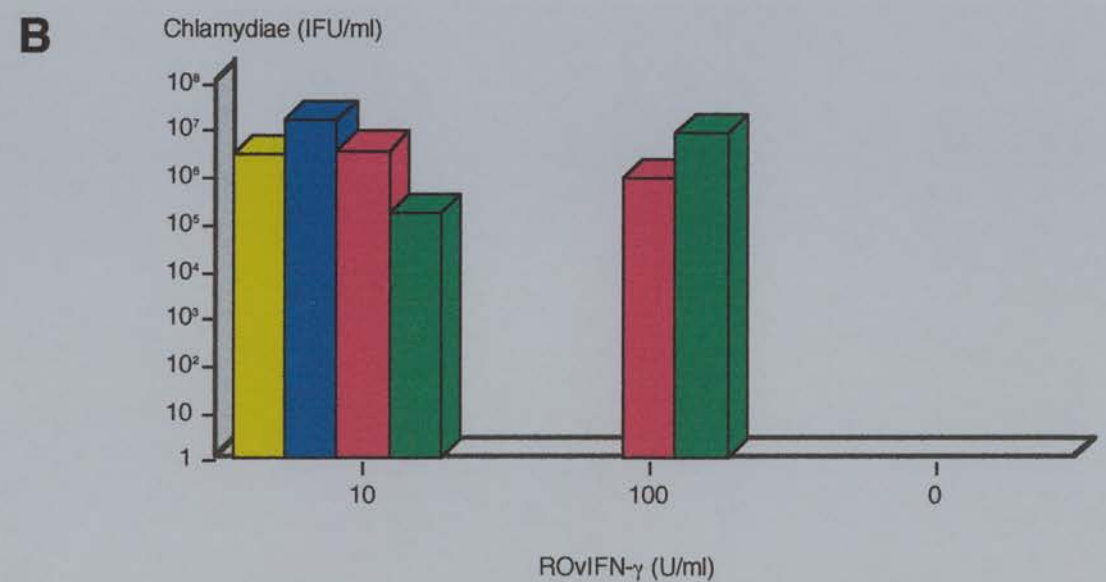

Chlamydial growth in ovine ST.6 cells 28 days after infection, measured by titration of inclusion forming units (IFU) in triplicate supernatant samples from each culture. rOvIFN-γ was maintained in cultures for 28 days (■), for the first 21 days (■), for the first 14 days (■) or for the first 7 days of culture (■). Uninfected controls were not inoculated with C.psittaci EB (■ not visible).

6.3.2.3 Analysis of *C. psittaci* growth on day 28

The results of LPS-ELISA analysis of culture supernatants on day 28 are displayed in figure 6.5A. Chlamydial LPS production was restricted to background levels when ROvIFN-γ was maintained in the culture media for 28 days. Removal of ROvIFN-γ from the culture conditions on day 21 had no detectable effect on the LPS concentration of the culture treated with 100 U/ml of ROvIFN-γ but resulted in a increase in LPS production in the culture treated with 10 U/ml of ROvIFN-γ. LPS was detected in the culture supernatants of all cultures in which ROvIFN-γ was removed from the culture medium on or before day 14. The results of titration analysis of culture supernatants for infectious chlamydiae on day 28 are displayed in figure 6.5B. Infectious EB were found in all of the cultures treated with 10 U/ml. Infectious EB were not detected in cultures maintained for 21 or 28 days in 100 U/ml of ROvIFN-γ. However, Infectious EB were detected when cultures treated with 100 U/ml of ROvIFN-γ were transferred into ROvIFN-γ-free culture medium on or before day 14.

6.4 Discussion

For IFN-γ to mediate persistent chlamydial infection, its effects must be nonlethal to the pathogen and must also be reversible. Beatty *et al* (1993; 1994a; 1994b) showed that treatment of HeLa 229 cells with 0.2 ng/ml of RHuIFN-γ shortly after infection with *C. trachomatis* (serovar A) could induce and maintain persistent infection. Removal of RHuIFN-γ from the culture conditions, up to 30 days after infection, resulted in the recovery of viable infectious chlamydiae and restored the normal cytolytic growth cycle of *C. trachomatis* [Beatty *et al*, 1995].

In the results of the initial experiment in ovine ST.6 cells, presented in section 6.3.1, relatively low concentrations of ROvIFN-γ (0.1 U/ml to 10 U/ml) were able to restrict chlamydial LPS production in ST.6 cells in a dose dependent manner but did not eradicate it completely from the cultures. Chlamydial LPS production was reduced to a level below the detection limit of the LPS-ELISA when ST.6 cells were maintained in 10 U/ml of ROvIFN-γ (figure 6.2). When ROvIFN-γ was removed from the culture medium on days 7 and 14 there was an increase in chlamydial LPS production, showing that the effects of ROvIFN-γ are reversible. However, whilst the concentrations of ROvIFN-γ used in this experiment were able to restrict the chlamydial LPS production, they did not prevent *C. psittaci*-mediated lysis of all the ST.6 cultures by day 35. The presence of replicating chlamydiae in these cultures in the absence of detectable levels of LPS indicated that the LPS-ELISA was not a suitable method for determining if *C. psittaci* growth had been completely inhibited. This finding also suggests *C. psittaci* LPS expression may be depressed in persistently infected ST.6 cultures in a similar manner to that described for persistent *C. trachomatis* infection in human cells [Beatty *et al*, 1993; 1994a; 1994b]. It was decided that traditional methods of assessing chlamydial growth by titration of infectious chlamydiae and visual enumeration of chlamydial inclusions would have to be used in conjunction with the LPS-ELISA in future experiments.

A second experiment was carried out using concentrations of 10 and 100 U/ml to establish whether ROvIFN-γ could inhibit chlamydial growth completely. The results of this experiment are presented in section 6.3.2. 10 U/ml of ROvIFN-γ was able to

reduce chlamydial LPS production to background levels (<1 ng/ml) when it was maintained in the culture medium for up to 21 days. However, LPS was not detected until more than $1x10^5$ IFU/ml were present in the culture supernatants and infectious chlamydiae were detected in the supernatant of the cultures treated with 10 U/ml, even when ROvIFN-γ was maintained in the culture medium throughout the experiment (Figures 6.3 - 6.5). In contrast, both chlamydial LPS and EB production were completely inhibited when ST.6 cells were maintained in culture medium containing 100 U/ml of ROvIFN-γ. Normal chlamydial growth resumed in cultures treated with 100 U/ml when they were transferred into ROvIFN-γ-free medium for more than 14 days (Figures 6.4 and 6.5). It therefore seem possible that IFN-γ could mediate persistent *C. psittaci* infection by restricting the growth and production of infectious chlamydiae in a reversible manner.

These experiments provided the first direct evidence that relatively low levels of ROvIFN-γ, less than half the concentration of OvIFN-γ produced *in vivo* by immune sheep after secondary challenge with live *C. psittaci* [Graham *et al*, 1995], can induce and maintain persistent infection of ovine cells with an OEA strain of *C. psittaci*. However, they did not provide any information on the morphology of persistent *C. psittaci* in ovine cells treated with ROvIFN-γ. RHuIFN-γ induced persistent *C. trachomatis* (serovar A) infection of HeLa 229 cells is characterised by small inclusion bodies containing large aberrant chlamydiae which fail to differentiate into infectious EB. When RHuIFN-γ was removed from this culture system, for more than 48 hrs, viable EB were recovered from culture supernatants and typical inclusion morphology was restored [Beatty *et al*, 1993; 1994a; 1995]. In contrast, the morphology of inclusion bodies in murine McCoy cells [Rodolakis *et al*, 1989] and murine L-cells [Perez-Martinez and Storz, 1985] persistently infected with OEA strains of *C. psittaci*, in the absence of IFN-γ or any other microbistatic agents, fluctuated temporally between periods where inclusions could not be found in cells and periods where cells contained abnormally large inclusion bodies.

None of the concentrations of ROvIFN-γ used in either of the experiments detailed here eradicated *C. psittaci* from infected cultures and it was clear that further work was required to determine if higher concentrations of ROvIFN-γ or prolonged

exposure to ROvIFN-γ could kill *C. psittaci*. In addition, persistent infection *in vivo* can be maintained from one breeding season to the next [Wilsmore *et al*, 1984] and the duration over which ROvIFN-γ could maintain persistence *in vitro* also required further examination.

Chapter 7.0

Long-Term Persistent *C. psittaci* Infection of Ovine Cells

7.1 Introduction

Beatty *et al* (1995) reported that treatment of HeLa 229 cells with 0.5 ng/ml of RHuIFN-γ shortly after infection with *C. trachomatis* could induce and maintain a persistent infection for up to 30 days *in vitro*. However, the same group have also shown that at higher concentrations (2 ng/ml), RHuIFN-γ was capable of eradicating *C. trachomatis* from infected HeLa 229 cultures [Beatty *et al*, 1993]. The results of the previous experiments (Chapter 6.0) showed that ROvIFN-γ could induce persistent infection of ovine ST.6 cells with the S26/3 OEA strain of *C. psittaci*, but was unable to eradicate *C. psittaci* from infected cells at concentrations of up to 100 U/ml of biological activity. These findings raised fundamental questions about the nature of ROvIFN-γ mediated persistence of *C. psittaci* in ovine cells.

- Can ROvIFN-γ maintain chlamydial persistence for prolonged periods of time, reflecting of the situation *in vivo* more accurately?

- Is there a critical concentration and/or exposure time above which ROvIFN-γ eradicates *C. psittaci* from infected ovine cells?

In order to address these questions the range of ROvIFN-γ concentrations used and duration over which cultures were maintained, both in the presence of ROvIFN-γ and after its removal, were extended in this experiment. Furthermore, because RHuIFN-γ mediated *C. trachomatis* persistence was shown to be associated with aberrant inclusion body morphology [Beatty *et al*, 1993; 1994a; 1994b; 1995], it was of interest to determine whether ROvIFN-γ mediated *C. psittaci* persistence was also associated with similar changes in inclusion morphology.

7.2 Materials and Methods

7.2.1 Infection of ST-6 cells and treatment with ROvIFN-γ

ST.6 cells were seeded into 25 cm^2 vented tissue culture flasks at a density of $5x10^4$ cells/ml in 6 ml IMDM+5% FBS (culture medium). After 3 days, when ST.6 cell monolayers were still sub-confluent, cells were incubated with 1 ml of culture medium containing $3x10^4$ *C. psittaci* strain S26/3 EB. Mock-infected controls were incubated with 1 ml of culture medium alone. After 6 hours, the supernatants were removed and replaced with 6 ml of culture medium containing 0 - 1000 U/ml of ROvIFN-γ.

7.2.2 Maintenance of persistently infected ST.6 cells

Cultures were passaged into fresh 25 cm^2 vented tissue culture flasks every 7 days (Chapter 2.1.4.), with the following adaptations. Cells were detached with trypsin/versene, washed in 10 ml of culture medium, centrifuged at 400 g for 5 minutes and resuspended in fresh culture medium. The cells from each flask were adjusted to a density of $5x10^4$ cells/ml before seeding into two fresh flasks in 6 ml volumes. ROvIFN-γ was then added to only one of each pair of new cultures to give the same final concentration of ROvIFN-γ that the cells had been maintained in during the previous 7 days. The other flask was maintained in ROvIFN-γ-free culture medium for the duration of the experiment or until chlamydiae lysed all the ST.6 cells.

7.2.3 Measurement of *C. psittaci* multiplication

Culture supernatants were assayed for chlamydial LPS by ELISA (see section 2) and titrated on fresh ST.6 cells to determine the numbers, if any, of infectious chlamydiae present (see section 2.5.2.) on the day of passage and at 2 and 4 days after passage. In addition, cytospins were performed on samples of cells taken at

the time of passage (see section 2.4.1.) and the percentage of cells containing chlamydial inclusions was initially quantified in 300 randomly sampled cells. If none were found in the first 300 cells the entire cytospin was examined. Giemsa stain was used to stain *C. psittaci* inclusion bodies (Chapter 2.4.3.).

7.2.4 Statistics

Spearman's Rank correlations were performed where evidence of dose dependent effects were observed. It was not possible to use replicates in these experiments because of the logistical problems associated with the exponential increase in the numbers of cultures generated at each passage. Triplicate data was generated by the LPS-ELISA and titration of supernatants. However, because each replica represented the same culture supernatant these data were not used for comparative statistics and are presented as mean values.

7.3 Results

25 cm^2 vented tissue culture flasks containing confluent monolayers of ST.6 cells were infected with $3x10^4$ *C. psittaci* strain S26/3 EB on day 0. Two uninfected control cultures were established in parallel. Two of the infected cultures were maintained in ROvIFN-γ-free culture medium and used as infected controls. The remaining infected cultures were maintained for up to 63 days in culture medium containing 5, 25, 100, 250 or 1000 U/ml of ROvIFN-γ. Cultures were maintained for 105 days after infection or until they were lysed by *C. psittaci*. Treatment of cultures with 1000 U/ml of ROvIFN-γ was stopped on day 35 due to the growth inhibitory effects of ROvIFN-γ on the ST.6 cells at this concentration. The uninfected controls were maintained for the duration of the experiment, one in culture medium containing 250 U/ml of ROvIFN-γ and one in culture medium alone. The mean LPS-ELISA, titration and cytospin data generated for these cultures were used to produce the baselines for the experiment. For the sake of clarity, data presented here has been limited to the results of analysis of culture supernatants and cytospins performed at the time of passage.

7.3.1 Infected control ST.6 Cell Cultures

C. psittaci completely lysed the infected control cultures by day 21 (figure 7.1). LPS was first detected in the supernatants of the infected controls on day 4 (data not shown). LPS production exceeded the maximum concentration detectable using the LPS-ELISA (without dilution of the samples = 110 ng/ml), by day 14 and remained above this level until the cultures were lysed by *C. psittaci* on day 21 (figure 7.1A). Infectious chlamydiae were detected in the supernatants of the infected controls from day 4 onward. Maximum numbers of infectious EB (mean=$1.92x10^6$ IFU/ml) were detected on day 14. Thereafter the number of infectious EB present in the supernatants fell by 15-fold to a mean value of $1.25x10^5$ on day 21 (Figures 7.1B). Inclusions were only found in the infected controls on day 14 (Figures 7.1C).

7.3.2 Cultures maintained in medium containing ROvIFN-γ for **7 Days**

The effects of maintaining ST.6 cultures in medium containing ROvIFN-γ for the first 7 days of the experiments are shown in figure 7.1. Chlamydial growth was restricted, when compared to the infected controls, during the time that cultures were maintained in the presence of ROvIFN-γ. Chlamydial growth increased following the removal of ROvIFN-γ on day 7. ROvIFN-γ retarded *C. psittaci* mediated lysis of cultures in a dose dependent manner (Spearman Rank Correlation Coefficient {ROvIFN-γ/ml : ST.6 culture survival/days} r_s = 0.8944, $p<0.05$). Cultures treated with 5, 25 and 100 U/ml were lysed by day 28. Cultures treated with 250 and 1000 U/ml were lysed by days 35 and 42 respectively.

The results of LPS-ELISA analysis of culture supernatants are shown in Figure 7.1A. LPS was not detected in any of the infected cultures during the time they were maintained in ROvIFN-γ. LPS production was retarded by approximately 7 days in cultures that had been treated with 5 or 25 U/ml of ROvIFN-γ, reaching detectable concentrations on day 14 and exceeding the detection limit of the LPS-ELISA on day 21. LPS was not detected in cultures that had been treated with 100, 250 or 1000 U/ml until day 21, 14 days after it was detected in the infected control cultures. Thereafter, chlamydial LPS production reached the maximum detection limit of the ELISA on day 21, in the culture that was treated with 100 U/ml, and day 28 in cultures that had been treated with 250 or 1000 U/ml.

The results of titration analysis of culture supernatants for infectious chlamydiae are displayed in figure 7.1B. In contrast to LPS, infectious EB were detected in the supernatants from all the infected cultures on day 7. ROvIFN-γ restricted the production of infectious EB on day 7 in a dose dependent manner (Spearman Rank Correlation Coefficient {ROvIFN-γ/ml : IFU/ml} r_s = -1.00, $p<0.01$). The supernatant of the culture treated with the lowest concentration of ROvIFN-γ contained approximately 7-fold fewer infectious EB ($9.4x10^2$ IFU/ml) compared to the infected controls ($7.04x10^3$ IFU/ml) on day 7. EB production increased in all the infected cultures after ROvIFN-γ was removed. Analogous to the results of the LPS-ELISA, maximal numbers of infectious EB were detected on day 21 in the

supernatants of cultures that had been treated with 5, 25 or 100 U/ml, and on day 28 in cultures that had been treated with 250 or 1000 U/ml. The maximum number of infectious EB detected in the supernatant of the culture treated with 5 U/ml of ROvIFN-γ was approximately 80-fold higher, at $1.58x10^8$ IFU/ml, than that seen in the infected control cultures. Peak EB production in cultures that had been treated with 25 and 100 U/ml of ROvIFN-γ was approximately 7-fold higher, at $1.2x10^7$ IFU/ml and $1.4x10^7$ IFU/ml respectively, than the maximum number of infectious EB recovered from the infected controls. The maximum numbers of infectious EB found in cultures treated with 250 and 1000 U/ml of ROvIFN-γ and were similar to those of the infected controls, at $2.6x10^6$ IFU/ml and $2.8x10^6$ IFU/ml respectively. In general, the number of infectious EB present in the culture supernatants fell by about 10-fold prior to culture lysis.

The percentage of ST.6 cells containing *C. psittaci* inclusions are shown in figure 7.1C. Inclusions were not detected in any of the cultures on day 7. Low numbers of inclusions were detected on day 14 in cultures which had been treated with 5, 25 and 100 U/ml of ROvIFN-γ and the maximum percentages of cells containing inclusions, two-three times that of the infected controls, were recorded in these cultures on day 21. Inclusions were not detected in cultures that had been treated with 250 or 1000 U/ml of ROvIFN-γ until day 21 and the percentage of cells containing inclusions peaked in these cultures on days 28 and 35 respectively.

7.3.3 Cultures maintained in medium containing ROvIFN-γ for **14 Days**

The effects of maintaining ST.6 cultures in medium containing ROvIFN-γ for the first 14 days of the experiments are shown in figure 7.2. Chlamydial growth was restricted, compared to the infected controls, when ROvIFN-γ was maintained in the culture medium. Chlamydial growth rate increased in cultures that had been treated with 5, 25 or 100 U/ml of ROvIFN-γ but remained undetectable in cultures treated with 250 or 1000 U/ml following removal of ROvIFN-γ on day 14. The culture treated with 5 U/ml of ROvIFN-γ was lysed by day 28 and cultures treated with 25 or 100 U/ml of ROvIFN-γ were lysed by day 35. Chlamydial mediated lysis did not

occur in cultures treated with 250 or 1000 U/ml of ROvIFN-γ and *C. psittaci* appeared to have been eradicated from these cultures.

The results of LPS-ELISA analysis of culture supernatants are shown in Figure 7.2A. Chlamydial LPS concentrations remained below the detection limit of the LPS-ELISA during the period that ROvIFN-γ was maintained in the culture media. Following removal of ROvIFN-γ, LPS production increased in cultures treated with 100 U/ml of ROvIFN-γ or less. LPS concentrations exceeded the maximum detection limit of the ELISA on day 21 in the culture that was treated with 5 U/ml of ROvIFN-γ and on days 28 and 35 in cultures that were treated with 25 and 100 U/ml of ROvIFN-γ. LPS was not detected at any time point in cultures that were treated with 250 or 1000 U/ml of ROvIFN-γ.

The results of titration analysis of culture supernatants for infectious chlamydiae are displayed in figure 7.2B. Production of infectious EB was restricted in a dose dependent manner when ROvIFN-γ was maintained in the culture media (Spearman Rank Correlation Coefficient {ROvIFN-γ/ml : IFU/ml} r_s = -0.812, $p<0.05$). ST.6 cells maintained in 5 U/ml produced fewer infectious EB than the infected controls. However, there was a 8-fold increase in the number of infectious EB present in the culture supernatant from day 7 to day 14 ($9.4x10^2$ IFU/ml to $7.5x10^3$ IFU/ml) despite the continual presence of ROvIFN-γ in the culture medium. The rate of EB production increased to a level similar to that of the infected controls when ROvIFN-γ was removed from the culture conditions. Maximum numbers of infectious EB were detected on day 21 ($3.9x10^6$ IFU/ml), after which numbers fell by over 5-fold to $7.5x10^5$ IFU/ml prior to lysis of the host culture. The numbers of infectious EB remained almost constant between days 7 and 14 when 25 U/ml of ROvIFN-γ was maintained in the culture medium. EB production increased to levels above the maximum rate seen in the infected controls when ROvIFN-γ was withdraw on day 14. Peak numbers of infectious EB, $4.5x10^7$ IFU/ml, were detected on day 28, 23-fold higher than the maximum numbers seen in the infected controls, after which it fell by over 100-fold prior to lysis of all the ST.6 cells in that culture on day 35. EB production was completely inhibited in cultures treated with 100 and 250 U/ml by day 14. When ROvIFN-γ was removed from the culture medium,

infectious EB were recovered from the supernatant of the culture treated with 100 U/ml but not the culture treated with 250 U/ml. Infectious EB peaked at $2.45x10^5$ IFU/ml in the culture treated with 100 U/ml on day 35 just before to host culture lysis. The supernatant from ST.6 cells treated with 1000 U/ml contained very low numbers of infectious EB on day 14 (20 IFU/ml). Infectious EB were not detected after day 14 in cultures treated with 250 or 1000 U/ml.

The percentage of ST.6 cells containing *C. psittaci* inclusions are shown in Figure 7.2C. Inclusion formation was prevented when ROvIFN-γ was maintained in the culture medium at concentrations of 25 U/ml or greater. The culture that was treated with 5 U/ml of ROvIFN-γ developed low numbers of inclusions during the period that ROvIFN-γ was present in the culture conditions and the percentage of cells containing inclusions rose to levels comparable to that of the infected controls after cells were transferred into ROvIFN-γ-free culture medium. Inclusion formation was retarded by 14 and 21 days respectively in cultures treated with 25 U/ml or 100 U/ml of ROvIFN-γ. Inclusions could not be demonstrated in cultures that were treated with 250 and 1000 U/ml at any point in the experiment.

7.3.4 Cultures maintained in medium containing ROvIFN-γ for **21 Days**

The effects of maintaining ST.6 cultures in medium containing ROvIFN-γ for the first 21 days of the experiment are shown in figure 7.3. Chlamydial growth was restricted during the time that ROvIFN-γ was maintained in the culture conditions. However, although 5 U/ml of ROvIFN-γ retarded chlamydial growth and ST.6 culture lysis by approximately 7 days, compared to the infected controls, there was an increase in chlamydial growth in this culture during the period that ROvIFN-γ was maintained in the culture conditions. The rate of chlamydial growth increased in cultures that were treated with 25 or 100 U/ml following removal of ROvIFN-γ from the culture conditions and eventually lysed these cultures on days 42 and 84 respectively. In contrast, no evidence of *C. psittaci* was found in cultures that were treated with 250 or 1000 U/ml of ROvIFN-γ after day 14.

The results of LPS-ELISA analysis of culture supernatants are shown in Figure 7.3A. LPS was detected on days 14 and 21 when ST.6 cells were maintained in 5 U/ml of ROvIFN-γ and the maximum concentration of LPS detectable using the LPS-ELISA was exceeded by day 28, 7 days after ROvIFN-γ was removed from the culture conditions. Chlamydial LPS was not detected during the first 21 days of the experiment when cultures were maintained in medium containing 25 or more U/ml of ROvIFN-γ. There was an immediate increase in LPS production in the culture that was treated with 25 U/ml when cells from this culture were transferred into ROvIFN-γ-free culture medium and the maximum detection limit of the ELISA was exceeded on day 35. LPS was not detected in the culture maintained in 100 U/ml of ROvIFN-γ until Day 91, 70 days after removal of ROvIFN-γ. Supernatants from cultures that had been treated with 250 or 1000 U/ml did not contain chlamydial LPS at concentrations detectable using the LPS-ELISA at any point in the experiment. Bacterial contamination of the culture that was treated with 250 U/ml of ROvIFN-γ occurred on day 50, preventing collection of data for this culture after day 49.

The results of titration analysis of culture supernatants for infectious chlamydiae are displayed in figure 7.3B. The culture that was treated with 5 U/ml of ROvIFN-γ produced large numbers of infectious EB during the period that ROvIFN-γ was maintained in the culture conditions. There was a slight increase in the rate of EB production following the removal of ROvIFN-γ from this culture on day 21 and peak numbers of $9x10^6$ IFU/ml of infectious EB were recorded on day 28, approximately 5-fold more than the maximum number of infectious EB detected in the infected controls. Infectious EB were also detected in the culture supernatant of cells treated with 25 U/ml of ROvIFN-γ. However, unlike the culture maintained in 5 U/ml, the number of infectious EB present in the supernatant of this culture declined with time, reaching 30 IFU/ml on day 21. When ROvIFN-γ was removed from the culture conditions the number of infectious EB increased, peaking at $1.9x10^7$ IFU/ml on day 35, 10-fold higher than the maximum number of infectious EB found in the infected controls, then falling to $6.36x10^5$ IFU/ml over the last 7 days of culture. Infectious EB were not detected in cultures when they were maintained in 100 or more U/ml of

ROvIFN-γ. Infectious EB were recovered from the culture treated with 100 U/ml, but only after ROvIFN-γ had been absent from the culture conditions for 63 days. Infectious EB were not detected after day 14 in cultures treated with 250 or 1000 U/ml of ROvIFN-γ.

The percentage of ST.6 cells containing *C. psittaci* inclusions are shown in Figure 7.3C. The culture that was treated with 5 U/ml of ROvIFN-γ developed similar numbers of inclusions as the infected controls during the period that ROvIFN-γ was present in the culture conditions, but inclusion formation was delayed by 7 days. Inclusions were not detected when ROvIFN-γ was maintained in the culture medium at concentrations of 25 U/ml or greater. Inclusion formation did not occur in cultures treated with 25 U/ml or 100 U/ml of ROvIFN-γ until 14 and 63 days after ROvIFN-γ was removed from the culture conditions. Inclusions could not be demonstrated in cultures that had been maintained in 250 and 1000 U/ml of ROvIFN-γ at any time point.

7.3.5 Cultures maintained in medium containing ROvIFN-γ for **28 Days**

The effects of maintaining ST.6 cultures in ROvIFN-γ for the first 28 days of the experiment are shown in figure 7.4. Chlamydial growth was restricted, compared to the infected controls, during the time that ROvIFN-γ was maintained in the culture medium. However, although the culture that was maintained in 5 U/ml restricted *C. psittaci* growth, it fail to control it completely and was lysed by day 28 despite the continual presence of ROvIFN-γ. Chlamydial growth rate increased in cultures treated with 25 or 100 U/ml when ROvIFN-γ was removed from the culture conditions on day 28 and completely lysed both cultures by days 42 and 91 respectively. There was no evidence of chlamydial growth after day 14 in cultures that were treated with 250 or 1000 U/ml of ROvIFN-γ.

The results of LPS-ELISA analysis of culture supernatants are shown in Figure 7.4A. LPS was detected in increasing concentrations on days 14, 21 and 28 in the culture maintained in 5 U/ml of ROvIFN-γ. Chlamydial LPS was not detected during the

first 28 days of the experiment when cultures were maintained in 25 U/ml or more of ROvIFN-γ. There was an immediate increase in LPS production in the culture that was treated with 25 U/ml when ROvIFN-γ was removed from the culture conditions, exceeding the maximum detection limit of the ELISA on day 42. LPS was not detected in the culture maintained in 100 U/ml until day 84, 56 days after the cells were transferred into ROvIFN-γ-free medium. Supernatants from cultures that had been treated with 250 or 1000 U/ml did not contain detectable concentrations of chlamydial LPS at any point during the experiment.

The results of titration analysis of culture supernatants for infectious chlamydiae are displayed in figure 7.4B. The culture that was treated with 5 U/ml of ROvIFN-γ produced less infectious EB than the infected controls, reaching a maximum of 1.07×10^5 IFU/ml on day 21. The number of infectious EB detected in the culture supernatant of cells treated with 25 U/ml of ROvIFN-γ declined with time, reaching its lowest level of 10 IFU/ml on day 28. As soon as ROvIFN-γ was removed from the culture there was an increase in EB production, reaching a maximum of 2.6×10^6 IFU/ml on day 35. Infectious EB were not detected in cultures treated with 100 U/ml or more after day 14 when ROvIFN-γ was maintained in the culture conditions. Infectious EB were found in the supernatant of the culture treated with 100 U/ml after ROvIFN-γ was removed from the culture conditions for more than 42 days. Infectious EB were not recovered from cultures treated with 250 or 1000 U/ml after day 7.

The percentage of ST.6 cells containing *C. psittaci* inclusions are shown in Figure 7.4C. Inclusion formation was prevented when 25 U/ml or more of ROvIFN-γ was present in the culture medium. The culture that was treated with 5 U/ml developed the same number of inclusions as the infected controls during the period that ROvIFN-γ was present in the culture medium, but inclusion formation was retarded by 7 days. Inclusions were not found in cultures treated with 25 U/ml or 100 U/ml until 7 and 56 days, respectively, after ROvIFN-γ was removed from the culture conditions. Inclusions were not found in cultures that were treated with 250 and 1000 U/ml of ROvIFN-γ at any time point in the experiment.

7.3.6 Cultures maintained in medium containing ROvIFN-γ for **35 Days**

The effects of maintaining ST.6 cultures in medium containing ROvIFN-γ for the first 35 days of the experiments are shown in figure 7.5. Chlamydial growth was inhibited completely by day 35 in the surviving cultures during the time that they were maintained in the presence of ROvIFN-γ. Chlamydial growth was restored after ROvIFN-γ was removed from cultures that had been treated with 25 or 100 U/ml but not in the cultures treated with 250 or 1000 U/ml of ROvIFN-γ. Cultures treated with 25 and 100 U/ml were lysed by days 42 and 91, seven and 56 days after cells were transferred into ROvIFN-γ-free culture medium. There was no evidence of *Chlamydial* growth in cultures that were treated with 250 or 1000 U/ml of ROvIFN-γ after day 14.

The results of LPS-ELISA analysis of culture supernatants are shown in Figure 7.5A. Chlamydial LPS was not detected during the first 35 days of the experiment when cultures were maintained in 25 or more U/ml of ROvIFN-γ. There was an immediate increase in LPS production in the culture that had been treated with 25 U/ml following the removal of ROvIFN-γ. The concentration of LPS exceeded the maximum detection limit of the ELISA on day 49 in this culture. LPS was not detected in the culture maintained in 100 U/ml of ROvIFN-γ until Day 77, 42 days after cells from this culture were transferred into ROvIFN-γ-free culture medium. Supernatants from cultures that had been treated with 250 or 1000 U/ml of ROvIFN-γ did not contain detectable levels of chlamydial LPS at any point in the experiment.

The results of titration analysis of culture supernatants for infectious chlamydiae are displayed in figure 7.5B. Infectious EB production was completely inhibited by day 35 in the culture treated with 25 U/ml of ROvIFN-γ. Infectious EB were recovered immediately after cells from this culture were transferred into ROvIFN-γ-free culture medium. Peak numbers of infectious EB (1.78×10^7 IFU/ml) were recorded on day 49, over 9-fold more than the maximum numbers detected in the infected controls. Infectious EB were not detected after day 7 in the culture treated with 100 units/ml during the time that ROvIFN-γ was maintained in the culture

conditions. Infectious EB were recovered from the supernatant of this culture when ROvIFN-γ had been absent from the culture conditions for more than 35 days and reached peak numbers ($1.16x10^6$ IFU/ml) on day 91. Infectious EB were not were not detected after day 14 in cultures treated with 250 or 1000 U/ml of ROvIFN-γ.

The percentage of ST.6 cells containing *C. psittaci* inclusions are shown in Figure 7.5C. Inclusion formation was prevented when ROvIFN-γ was maintained in the culture medium at concentrations of 25 U/ml or greater. Cultures treated with 25 or 100 U/ml of ROvIFN-γ only developed inclusions on days 42 and 77 after they had been transferred into ROvIFN-γ-free culture medium for 7 and 35 days respectively. Inclusions could not be demonstrated in cultures that had been maintained in 250 and 1000 U/ml of ROvIFN-γ at any point in the experiment.

7.3.7 Cultures maintained in medium containing ROvIFN-γ for **49 Days**

The effects of maintaining ST.6 cultures in medium containing ROvIFN-γ for the first 49 days of the experiments are shown in figure 7.6. Chlamydial growth was completely inhibited in all the surviving cultures after day 28 whilst ROvIFN-γ was maintained in the culture conditions. Chlamydial growth resumed shortly after cultures that were treated with 25 or 100 U/ml were transferred into ROvIFN-γ-free culture medium on day 49. Cultures treated with 25 and 100 U/ml were lysed by day 77 and day 63 respectively. Evidence of chlamydial growth was not detected after day 14 in cultures that were treated with 250 or 1000 U/ml of ROvIFN-γ.

The results of LPS-ELISA analysis of culture supernatants are shown in Figure 7.6A. Chlamydial LPS was not detected during the time that cultures were maintained in 25 or more U/ml of ROvIFN-γ. There was an increase in LPS production in the cultures that had been treated with 25 or 100 U/ml when ROvIFN-γ was removed from the culture conditions, reaching the maximum detection limit of the ELISA on days 70 and 63 respectively. Supernatants from the culture that had been treated with 250 U/ml did not contain detectable amounts of chlamydial LPS at any point in the experiment.

The results of titration analysis of culture supernatants for infectious chlamydiae are displayed in figure 7.6B. Infectious EB could not be demonstrated after day 35 in the culture that was treated with 25 U/ml of ROvIFN-γ. Removal of ROvIFN-γ from this culture on day 49 resulted in the recovery of infectious EB on day 63. The number of infectious EB peaked on day 77 ($1.94x10^5$ IFU/ml) in this culture, 10-fold less that the maximum number of infectious EB found in the infected controls. Infectious EB were not detected in the supernatant of the culture treated with 100 U/ml after day 7 when ROvIFN-γ was maintained in the culture conditions. Infectious EB were recovered from the supernatant of this culture 7 days after cells were transferred into ROvIFN-γ-free culture medium and reached peak numbers on day 63 ($3.57x10^6$ IFU/ml), approximately twice that of the infected controls. Infectious EB were not found in cultures treated with 250 U/ml of ROvIFN-γ after day 14.

The percentage of ST.6 cells containing *C. psittaci* inclusions are shown in Figure 7.6C. Inclusion formation was prevented during the time that ROvIFN-γ was maintained in the culture medium in the surviving cultures. Inclusion formation did not occur until 14 and 7 days after ROvIFN-γ was removed from the culture conditions in cultures treated with 25 U/ml or 100 U/ml respectively. Inclusions were not found at any point during the experiment in the culture that had been treated with 250 U/ml of ROvIFN-γ.

7.3.8 Cultures maintained in medium containing ROvIFN-γ for **63 Days**

The effects of maintaining ST.6 cultures in medium containing ROvIFN-γ for the first 63 days of the experiments are shown in figure 7.7. Chlamydial growth was completely inhibited in all the surviving cultures by day 35 and remained undetectable as long as ROvIFN-γ was maintained in the culture conditions. Chlamydial growth was restored when cells from the cultures that had been treated with 25 or 100 U/ml were transferred into ROvIFN-γ-free culture medium on day 63. Cultures treated with 25 and 100 U/ml were lysed by days 77 and day 91 respectively. Lysis did not occur in cultures that were treated with 250 U/ml of ROvIFN-γ.

The results of LPS-ELISA analysis of culture supernatants are shown in Figure 7.7A. Chlamydial LPS was not detected during the time that cultures were maintained in 25 or more U/ml of ROvIFN-γ. There was an increase in LPS production in the culture that had been treated with 25 U/ml when ROvIFN-γ was removed from the culture conditions, reaching the maximum detection limit of the ELISA on day 70. LPS was not detected in the culture maintained in 100 U/ml of ROvIFN-γ until day 84, 21 days after ROvIFN-γ was removed. Supernatants from the culture that had been treated with 250 U/ml of ROvIFN-γ did not contain detectable concentrations of chlamydial LPS at any point in the experiment.

The results of titration analysis of culture supernatants for infectious chlamydiae maintained in ROvIFN-γ for 63 days are displayed in figure 7.7B. After day 28, infectious EB were not found in the culture treated with 25 U/ml of ROvIFN-γ until day 70, seven days after ROvIFN-γ had been removed from the culture conditions. Maximum numbers of infectious EB ($1x10^6$ IFU/ml) were recovered from the supernatant of this culture on day 77. Infectious EB were not detected after day 7 in the culture treated with 100 units/ml while ROvIFN-γ was present in the culture conditions. *C. psittaci* EB production resumed when cells that had been treated for 63 days with 100 U/ml of ROvIFN-γ were transferred into ROvIFN-γ-free culture medium and peak numbers of infectious EB ($3.48x10^6$ IFU/ml) were recovered medium on day 84, 21 days after ROvIFN-γ was removed. Infectious EB were not detected after day 7 in the culture supernatant of cells treated with 250 U/ml of ROvIFN-γ.

The percentage of ST.6 cells containing *C. psittaci* inclusions are shown in Figure 7.7C. Inclusion formation was prevented in all the surviving cultures during the time that ROvIFN-γ was present in the culture conditions and inclusion formation did not occur until 7 and 21 days after cells from cultures treated with 25 U/ml or 100 U/ml of ROvIFN-γ were transferred into ROvIFN-γ-free medium. Inclusions could not be demonstrated in the culture that had been treated with 250 U/ml of ROvIFN-γ at any point in the experiment.

Figure 7.1: Cultures maintained in medium containing ROvIFN-γ for 7 Days

ST.6 cultures were incubated with ROvIFN-γ for the first 7 days after infection with *C. psittaci* at concentrations of:1000 U/ml (———), 250 U/ml (———), 100 U/ml (———), 25 U/ml (———), 5 U/ml (———). The Infected controls (———) were maintained in ROvIFN-γ-free culture medium until they were lysed by *C. psittaci*. Uninfected controls (—●—) were maintained for the duration of the experiment. The shaded area ( ) represents the period during which ROvIFN-γ was maintained in the cultures. *C. psittaci* mediated lysis of cultures occurred at the time point indicated by (*, *, *, *, * or *). *C. psittaci* mediated lysis occurred in the following 7 days, preventing further cytospin analysis (**, **, **, **, ** or **).

A: Mean concentration of chlamydial LPS in culture supernatants, measured by LPS-ELISA analysis of triplicate supernatant samples from each culture.

B: Mean number inclusion forming units (IFU/ml) present in culture supernatants, measured by titration of triplicate supernatant samples from each culture.

C: Percentage of cells containing chlamydial inclusion bodies.

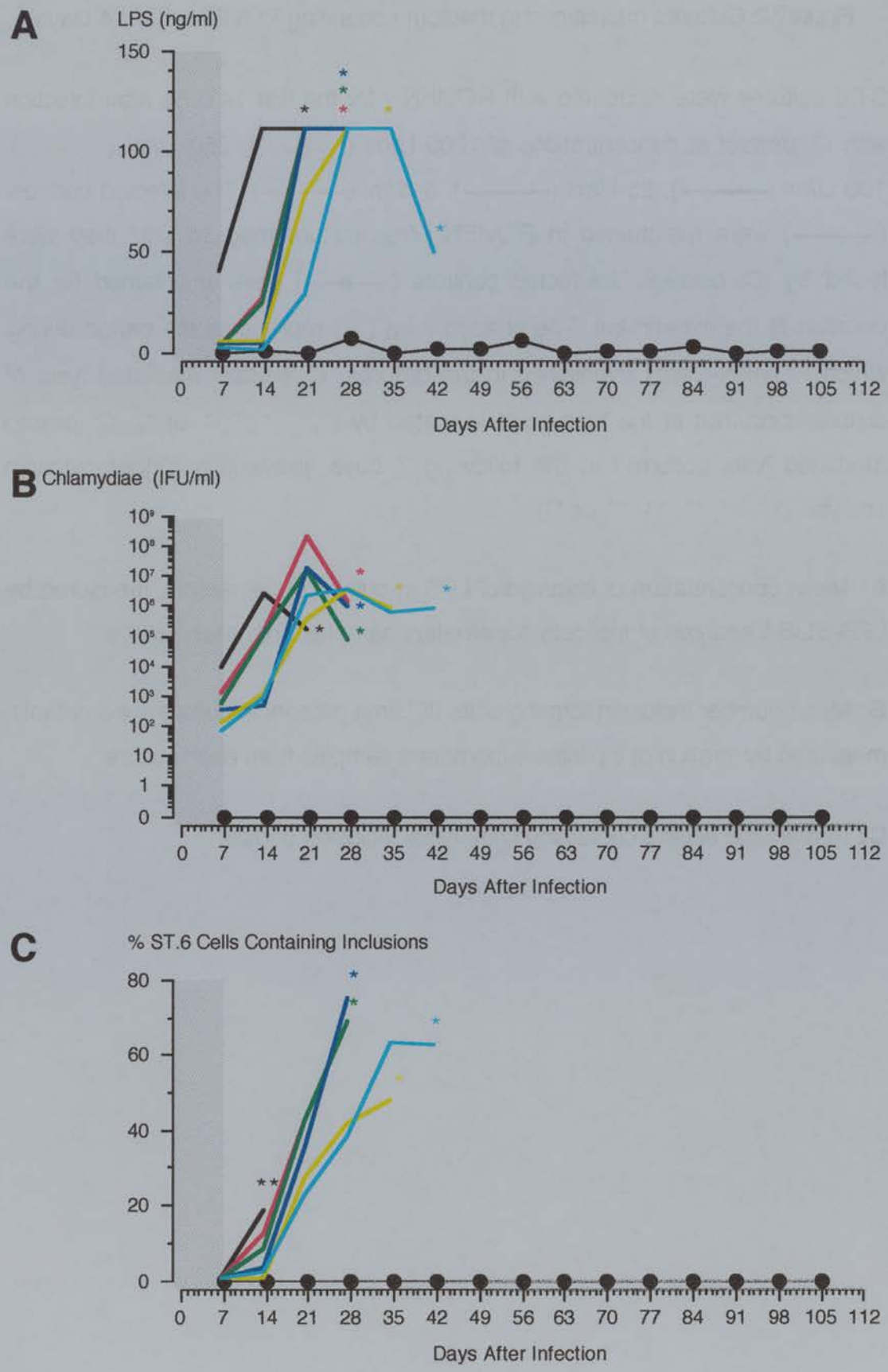
A
LPS (ng/ml)
150
100
50
0
0 7 14 21 28 35 42 49 56 63 70 77 84 91 98 105 112
Days After Infection
B
Chlamydiae (IFU/ml)
10^9
10^8
10^7
10^6
10^5
10^4
10^3
10^2
10
1
0
0 7 14 21 28 35 42 49 56 63 70 77 84 91 98 105 112
Days After Infection
C
% ST.6 Cells Containing Inclusions
80
60
40
20
0
0 7 14 21 28 35 42 49 56 63 70 77 84 91 98 105 112
Days After Infection

Figure 7.2: Cultures maintained in medium containing ROvIFN-γ for 14 Days

ST.6 cultures were incubated with ROvIFN-γ for the first 14 days after infection with *C. psittaci* at concentrations of:1000 U/ml (———), 250 U/ml (———), 100 U/ml (———), 25 U/ml (———), 5 U/ml (———). The Infected controls (———) were maintained in ROvIFN-γ-free culture medium until they were lysed by *C. psittaci*. Uninfected controls (—●—) were maintained for the duration of the experiment. The shaded area ( ) represents the period during which ROvIFN-γ was maintained in the cultures. *C. psittaci* mediated lysis of cultures occurred at the time point indicated by (*, *, *, *, * or *). *C. psittaci* mediated lysis occurred in the following 7 days, preventing further cytospin analysis (**, **, **, **, ** or **).

A: Mean concentration of chlamydial LPS in culture supernatants, measured by LPS-ELISA analysis of triplicate supernatant samples from each culture.

B: Mean number inclusion forming units (IFU/ml) present in culture supernatants, measured by titration of triplicate supernatant samples from each culture.

C: Percentage of cells containing chlamydial inclusion bodies.

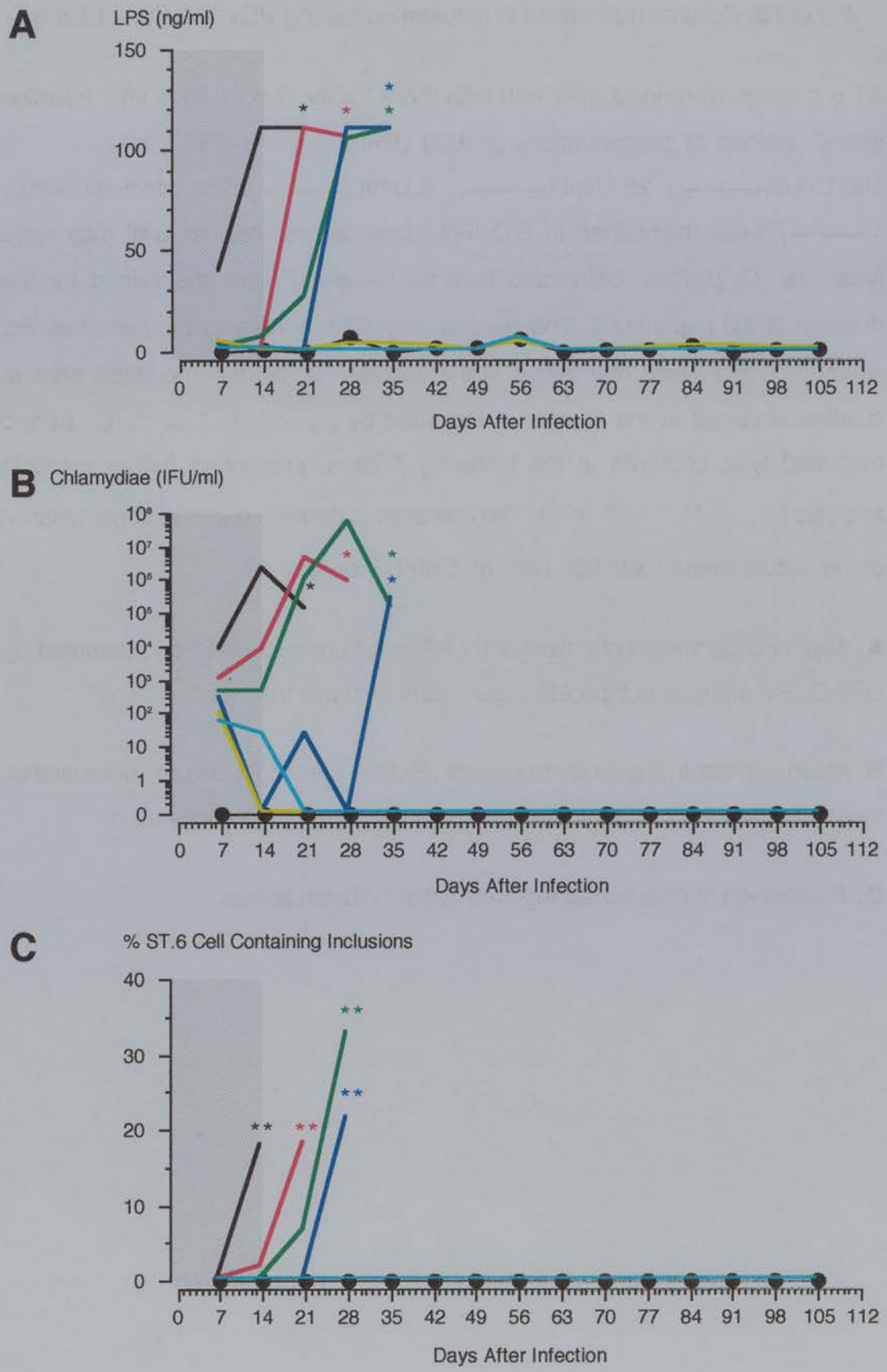
A
LPS (ng/ml)
150
100
50
0
0 7 14 21 28 35 42 49 56 63 70 77 84 91 98 105 112
Days After Infection
B
Chlamydiae (IFU/ml)
10^8
10^7
10^6
10^5
10^4
10^3
10^2
10
1
0
0 7 14 21 28 35 42 49 56 63 70 77 84 91 98 105 112
Days After Infection
C
% ST.6 Cell Containing Inclusions
40
30
20
10
0
0 7 14 21 28 35 42 49 56 63 70 77 84 91 98 105 112
Days After Infection

Figure 7.3: Cultures maintained in medium containing ROvIFN-γ for 21 Days

ST.6 cultures were incubated with ROvIFN-γ for the first 21 days after infection with *C. psittaci* at concentrations of:1000 U/ml (———), 250 U/ml (———), 100 U/ml (———), 25 U/ml (———), 5 U/ml (———). The Infected controls (———) were maintained in ROvIFN-γ-free culture medium until they were lysed by *C. psittaci*. Uninfected controls (—●—) were maintained for the duration of the experiment. The shaded area ( ) represents the period during which ROvIFN-γ was maintained in the cultures. *C. psittaci* mediated lysis of cultures occurred at the time point indicated by (*, *, *, *, * or *). *C. psittaci* mediated lysis occurred in the following 7 days, preventing further cytospin analysis (**, **, **, **, ** or **). The character x denotes bacterial contamination of the culture treated with 250 U/ml of rOvIFN-γ on day 49.

A: Mean concentration of chlamydial LPS in culture supernatants, measured by LPS-ELISA analysis of triplicate supernatant samples from each culture.

B: Mean number inclusion forming units (IFU/ml) present in culture supernatants, measured by titration of triplicate supernatant samples from each culture.

C: Percentage of cells containing chlamydial inclusion bodies.

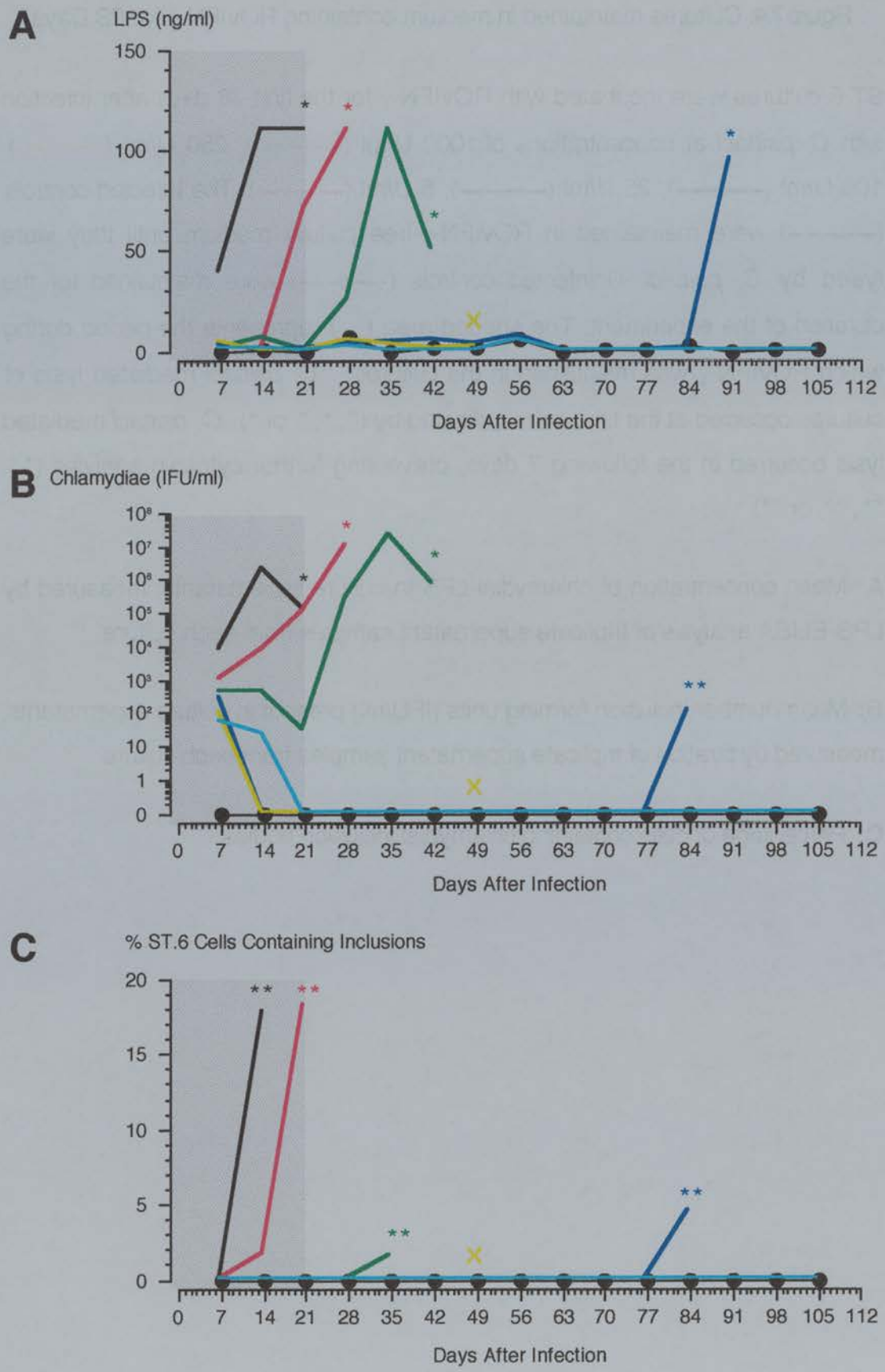
A
LPS (ng/ml)
150
100
50
0
0 7 14 21 28 35 42 49 56 63 70 77 84 91 98 105 112
Days After Infection
B
Chlamydiae (IFU/ml)
10⁸
10⁷
10⁶
10⁵
10⁴
10³
10²
10
1
0
0 7 14 21 28 35 42 49 56 63 70 77 84 91 98 105 112
Days After Infection
C
% ST.6 Cells Containing Inclusions
20
15
10
5
0
0 7 14 21 28 35 42 49 56 63 70 77 84 91 98 105 112
Days After Infection

Figure 7.4: Cultures maintained in medium containing ROvIFN-γ for 28 Days

ST.6 cultures were incubated with ROvIFN-γ for the first 28 days after infection with *C. psittaci* at concentrations of:1000 U/ml (———), 250 U/ml (———), 100 U/ml (———), 25 U/ml (———), 5 U/ml (———). The Infected controls (———) were maintained in ROvIFN-γ-free culture medium until they were lysed by *C. psittaci*. Uninfected controls (—●—) were maintained for the duration of the experiment. The shaded area ( ) represents the period during which ROvIFN-γ was maintained in the cultures. *C. psittaci* mediated lysis of cultures occurred at the time point indicated by (*, *, * or *). *C. psittaci* mediated lysis occurred in the following 7 days, preventing further cytospin analysis (**, **, ** or **).

A: Mean concentration of chlamydial LPS in culture supernatants, measured by LPS-ELISA analysis of triplicate supernatant samples from each culture.

B: Mean number inclusion forming units (IFU/ml) present in culture supernatants, measured by titration of triplicate supernatant samples from each culture.

C: Percentage of cells containing chlamydial inclusion bodies.

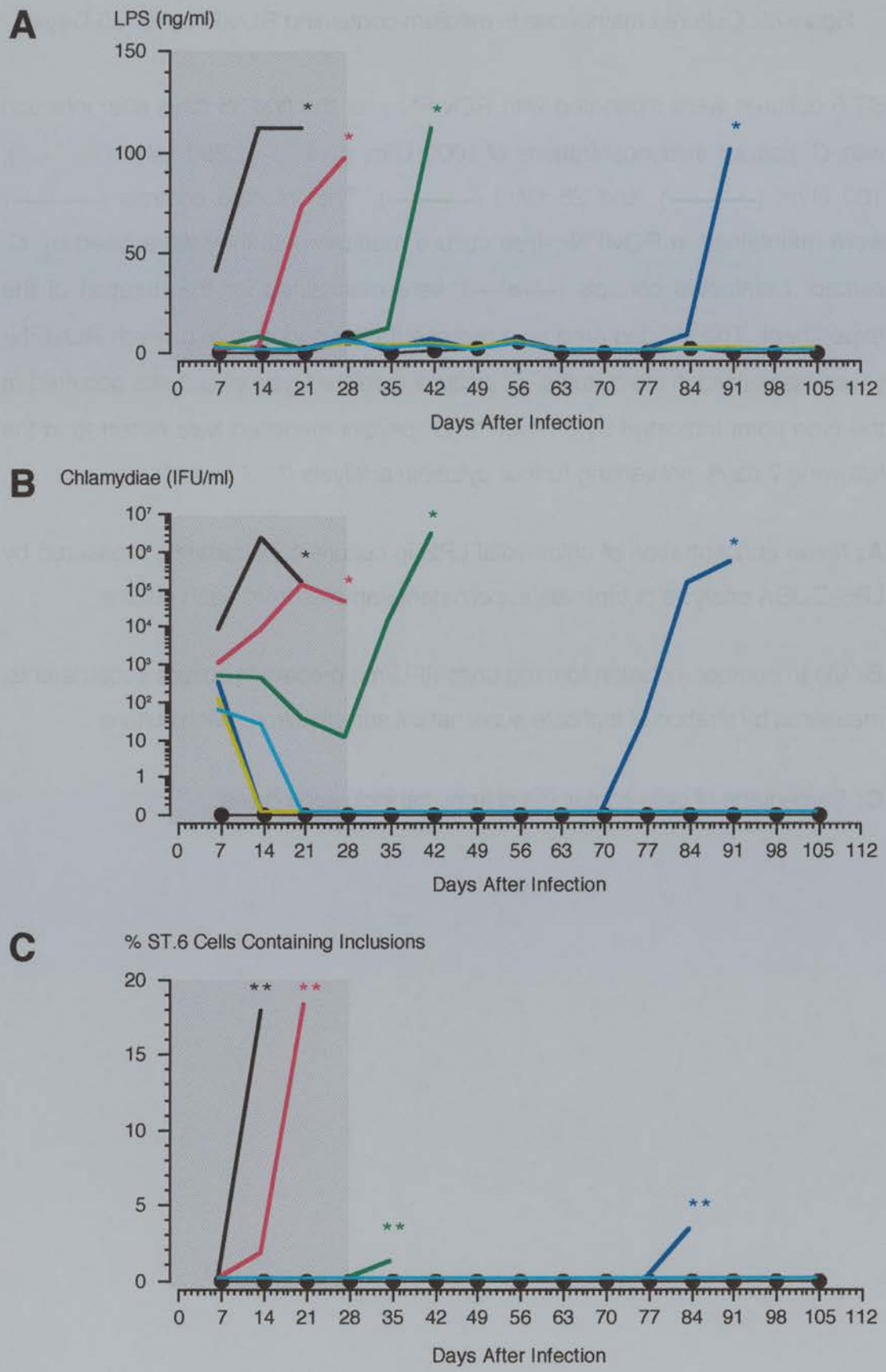
A
LPS (ng/ml)
150
100
50
0
0 7 14 21 28 35 42 49 56 63 70 77 84 91 98 105 112
Days After Infection
B
Chlamydiae (IFU/ml)
10⁷
10⁶
10⁵
10⁴
10³
10²
10
1
0
0 7 14 21 28 35 42 49 56 63 70 77 84 91 98 105 112
Days After Infection
C
% ST.6 Cells Containing Inclusions
20
15
10
5
0
0 7 14 21 28 35 42 49 56 63 70 77 84 91 98 105 112
Days After Infection

Figure 7.5: Cultures maintained in medium containing ROvIFN-γ for 35 Days

ST.6 cultures were incubated with ROvIFN-γ for the first 35 days after infection with *C. psittaci* at concentrations of:1000 U/ml (———); 250 U/ml (———); 100 U/ml (———); and 25 U/ml (———). The Infected controls (———) were maintained in ROvIFN-γ-free culture medium until they were lysed by *C. psittaci*. Uninfected controls (—●—) were maintained for the duration of the experiment. The shaded area ( ) represents the period during which ROvIFN-γ was maintained in the cultures. *C. psittaci* mediated lysis of cultures occurred at the time point indicated by (*, * or *). *C. psittaci* mediated lysis occurred in the following 7 days, preventing further cytospin analysis (**, ** or **).

A: Mean concentration of chlamydial LPS in culture supernatants, measured by LPS-ELISA analysis of triplicate supernatant samples from each culture.

B: Mean number inclusion forming units (IFU/ml) present in culture supernatants, measured by titration of triplicate supernatant samples from each culture.

C: Percentage of cells containing chlamydial inclusion bodies.

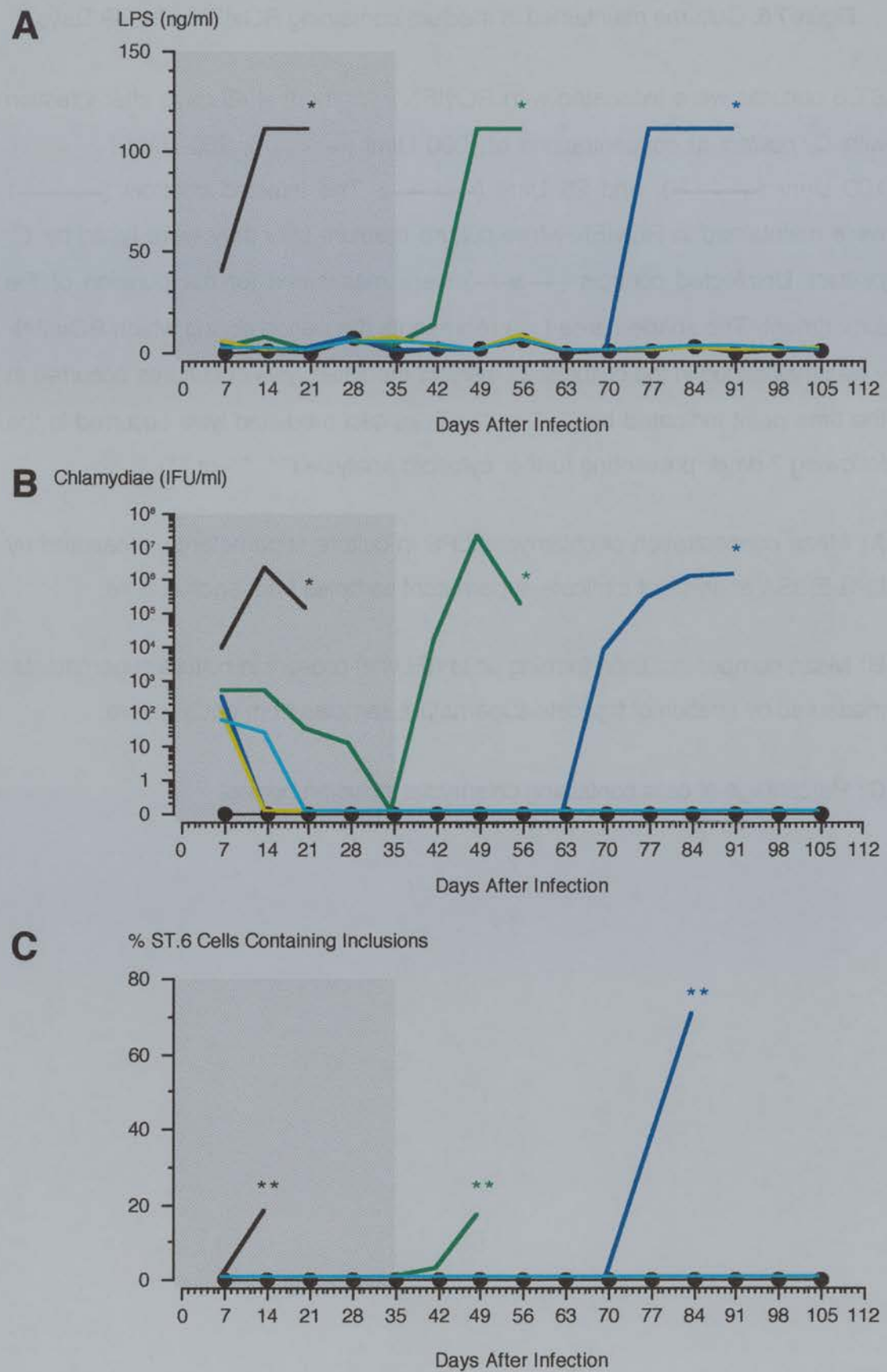
A
LPS (ng/ml)
150
100
50
0
*
*
*
0 7 14 21 28 35 42 49 56 63 70 77 84 91 98 105 112
Days After Infection
B
Chlamydiae (IFU/ml)
10⁸
10⁷
10⁶
10⁵
10⁴
10³
10²
10
1
0
*
*
*
0 7 14 21 28 35 42 49 56 63 70 77 84 91 98 105 112
Days After Infection
C
% ST.6 Cells Containing Inclusions
80
60
40
20
0
**
**
**
0 7 14 21 28 35 42 49 56 63 70 77 84 91 98 105 112
Days After Infection

Figure 7.6: Cultures maintained in medium containing ROvIFN-γ for 49 Days

ST.6 cultures were incubated with ROvIFN-γ for the first 49 days after infection with *C. psittaci* at concentrations of:1000 U/ml (———); 250 U/ml (———); 100 U/ml (———); and 25 U/ml (———). The Infected controls (———) were maintained in ROvIFN-γ-free culture medium until they were lysed by *C. psittaci*. Uninfected controls (—●—) were maintained for the duration of the experiment. The shaded area ( ) represents the period during which ROvIFN-γ was maintained in the cultures. *C. psittaci* mediated lysis of cultures occurred at the time point indicated by (*, * or *). *C. psittaci* mediated lysis occurred in the following 7 days, preventing further cytospin analysis (**, ** or **).

A: Mean concentration of chlamydial LPS in culture supernatants, measured by LPS-ELISA analysis of triplicate supernatant samples from each culture.

B: Mean number inclusion forming units (IFU/ml) present in culture supernatants, measured by titration of triplicate supernatant samples from each culture.

C: Percentage of cells containing chlamydial inclusion bodies.

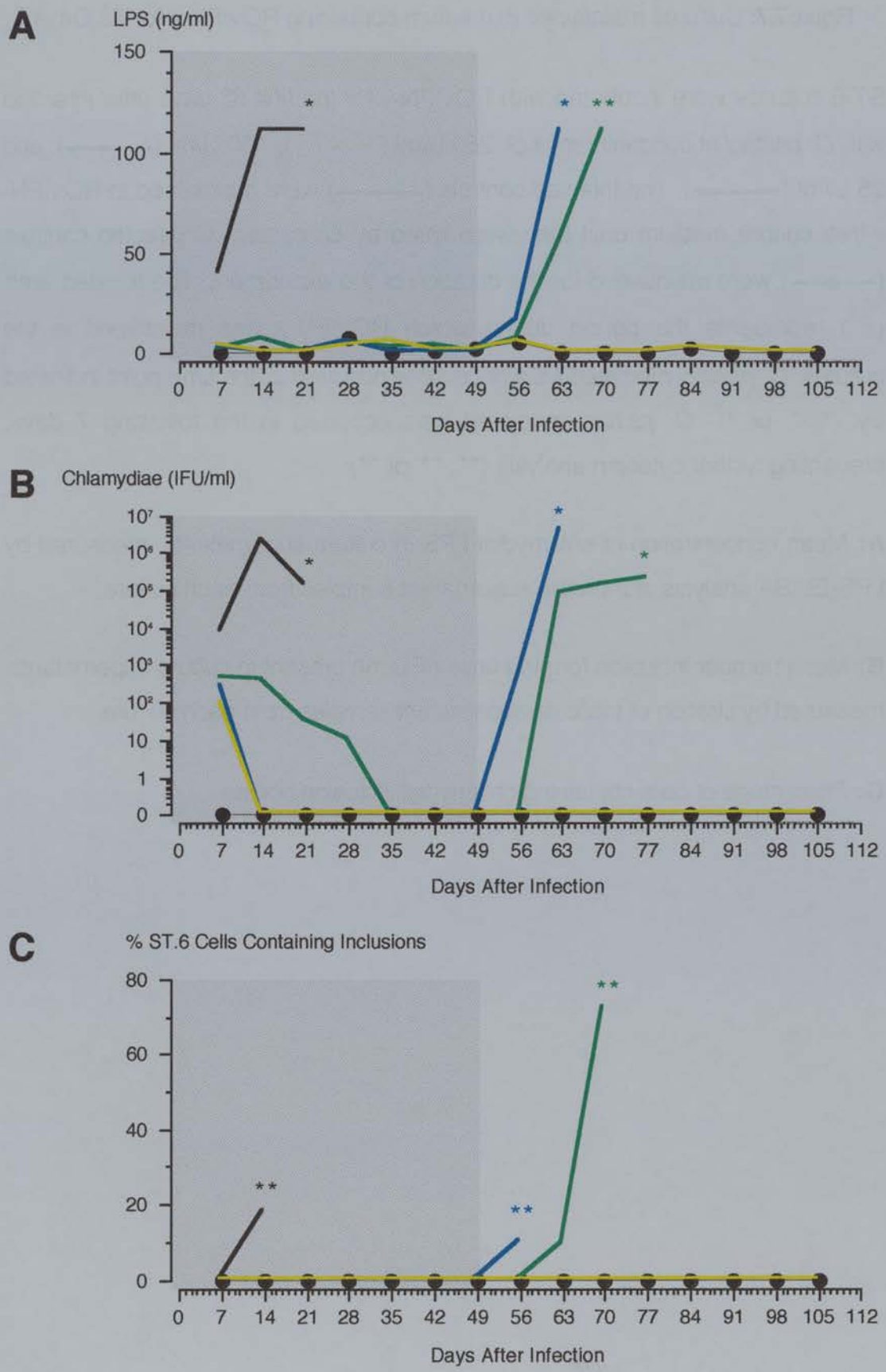
A
LPS (ng/ml)
150
100
50
0
0 7 14 21 28 35 42 49 56 63 70 77 84 91 98 105 112
Days After Infection
B
Chlamydiae (IFU/ml)
10⁷
10⁶
10⁵
10⁴
10³
10²
10
1
0
0 7 14 21 28 35 42 49 56 63 70 77 84 91 98 105 112
Days After Infection
C
% ST.6 Cells Containing Inclusions
80
60
40
20
0
0 7 14 21 28 35 42 49 56 63 70 77 84 91 98 105 112
Days After Infection

Figure 7.7: Cultures maintained in medium containing ROvIFN-γ for 63 Days

ST.6 cultures were incubated with ROvIFN-γ for the first 63 days after infection with *C. psittaci* at concentrations of: 250 U/ml (——); 100 U/ml (——); and 25 U/ml (——). The Infected controls (——) were maintained in ROvIFN-γ-free culture medium until they were lysed by *C. psittaci*. Uninfected controls (—●—) were maintained for the duration of the experiment. The shaded area ( ) represents the period during which ROvIFN-γ was maintained in the cultures. *C. psittaci* mediated lysis of cultures occurred at the time point indicated by (*, * or *). *C. psittaci* mediated lysis occurred in the following 7 days, preventing further cytospin analysis (**, ** or **).

A: Mean concentration of chlamydial LPS in culture supernatants, measured by LPS-ELISA analysis of triplicate supernatant samples from each culture.

B: Mean number inclusion forming units (IFU/ml) present in culture supernatants, measured by titration of triplicate supernatant samples from each culture.

C: Percentage of cells containing chlamydial inclusion bodies.

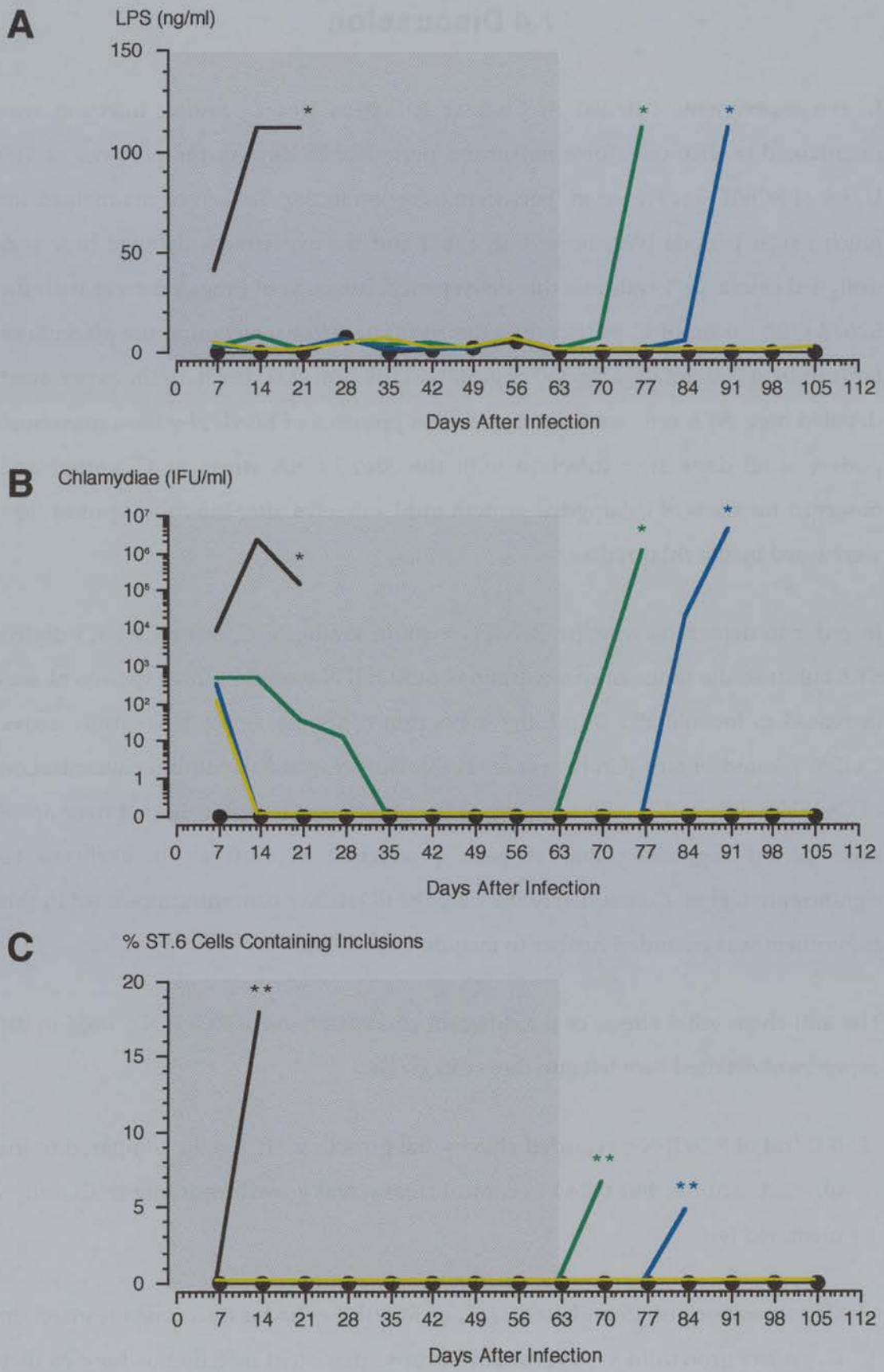
A
LPS (ng/ml)
150
100
50
0
0 7 14 21 28 35 42 49 56 63 70 77 84 91 98 105 112
Days After Infection
B
Chlamydiae (IFU/ml)
10⁷
10⁶
10⁵
10⁴
10³
10²
10
1
0
0 7 14 21 28 35 42 49 56 63 70 77 84 91 98 105 112
Days After Infection
C
% ST.6 Cells Containing Inclusions
20
15
10
5
0
0 7 14 21 28 35 42 49 56 63 70 77 84 91 98 105 112
Days After Infection

7.4 Discussion

In the experiments detailed in Chapter 6.0, persistent *C. psittaci* infection was maintained in ST.6 cells for a maximum period of 28 days in the presence of 100 U/ml of ROvIFN-γ. However, persistent infection in the ewe can be maintained for much longer periods [Wilsmore *et al*, 1984] and the experiment detailed here was designed primarily to address this discrepancy. Infection of pregnant ewes with the S26/3 OEA strain of *C. psittaci* does not result in active infection in the placenta or fetus until approximately day 60 of gestation [Buxton *et al*, 1990]. In the experiment detailed here, ST.6 cells were cultured in the presence of ROvIFN-γ for a maximum period of 63 days after infection with the S26/3 OEA strain of *C. psittaci* and observed for signs of chlamydial growth until 105 days after infection or until they were lysed by the chlamydiae.

In order to determine whether ROvIFN-γ could eradicate *C. psittaci* from infected ST.6 cultures, the range of concentrations of ROvIFN-γ used in this experiment was increased to include 250 U/ml, the maximum concentration of biologically active OvIFN-γ found *in vivo* [Graham *et al*, 1995]. However, the maximum concentration of OvIFN-γ detected *in vivo* was derived from efferent lymph collected over an 18 hour period suggesting that at peak production of OvIFN-γ is likely to be significantly higher. Consequently the range of ROvIFN-γ concentrations used in this experiment was extended further to include 1000 U/ml.

The anti-chlamydial effects of the different concentrations of ROvIFN-γ used in the experiment detailed here fell into three categories.

1. 5 U/ml of ROvIFN-γ retarded chlamydial growth in ST.6 cells, compared to the infected controls, but failed to control chlamydial growth resulting in *C. psittaci* mediated lysis.

2. Concentrations of 25 and 100 U/ml of ROvIFN-γ had a microbistatic effect on *C. psittaci* growth in ST-6 cells and induced persistent infection as long as they were maintained in the culture conditions.

3. Concentrations of 250 U/ml or 1000 U/ml of ROvIFN-γ, although initially microbistatic, appeared to become microbicidal when they were maintained in the culture conditions for 14 or more days.

Whilst ST.6 cells that were maintained in culture medium containing 5 U/ml of ROvIFN-γ failed to control *C. psittaci* growth completely and were lysed on day 28 (Figure 7.4), LPS production and inclusion formation were inhibited entirely when cultures were maintained in the presence 25 or 100 U/ml of ROvIFN-γ. In addition, ST.6 cultures maintained in 25 or 100 U/ml of ROvIFN-γ did not produce infectious chlamydiae after days 35 and 14 respectively. *C. psittaci* resumed its typical cytolytic developmental cycle when ST.6 cells were transferred into ROvIFN-γ-free culture medium, even after 63 days of culture in the presence of 25 or 100 U/ml of ROvIFN-γ. This suggested that these concentrations of ROvIFN-γ can induce and maintain *C. psittaci* persistence in ST.6 cells (Figure 7.7). Persistent *C. psittaci* infection was established more rapidly in cultures maintained in 100 U/ml of ROvIFN-γ than cultures maintained in 25 U/ml of ROvIFN-γ. With the exception of cultures treated with ROvIFN-γ for the first 49 days after infection, chlamydial growth recovered more rapidly following removal of ROvIFN-γ from cultures previously maintained in 25 U/ml of ROvIFN-γ compared to cultures that had been treated with 100 U/ml (Figure 7.6).

In the case of RHuIFN-γ mediated *C. trachomatis* persistence in human HeLa 229 cells, the recovery rate of infectious chlamydiae was shown to decrease over time [Beatty *et al*, 1995], suggesting that chlamydial growth was inhibited completely in this model. Here, the rate at which infectious *C. psittaci* were recovered from infected ovine cultures, following removal of ROvIFN-γ, did not decrease over time. By maintaining cultures that were initially infected with $3x10^4$ infectious EBs for 63 days, passaging cells at ratio of approximately 1:3 every 7 days, a static population of chlamydiae would effectively be diluted out of the cultures by day 63, reaching levels of about 2 infected cells/culture. This was clearly not the case in this experiment. In cultures that were treated with 100 U/ml of ROvIFN-γ, the rate at which chlamydial growth recovered following the removal of ROvIFN-γ actually appeared to increase with time (Spearman Rank Correlation Coefficient {Duration

of ROvIFN-γ treatment/days : ST.6 culture survival/days following removal of ROvIFN-γ} r_s = -0.9000, $p<0.05$, {Duration of ROvIFN-γ treatment/days : recovery of infectious EB} r_s = –0.9000, $p<0.05$). These findings suggest that despite the apparent absence of inclusion bodies in persistently infected cells or infectious chlamydiae and LPS in the culture supernatants, low level multiplication and transmission can occur in persistently infected ST.6 cultures. It is possible that very low numbers of EB (<10 IFU/ml) might be present in the supernatants of persistently infected ST.6. Alternatively, *C. psittaci* may enter adjacent cells through some as yet undefined method [Wyrick, 1998].

As in the case of RHuIFN-γ mediated restriction of *C. trachomatis* [Beatty *et al*, 1993], ovine ST.6 cells appear to be able to kill *C. psittaci* following treatment with higher concentrations, 250 and 1000 U/ml, of ROvIFN-γ. However, it would appear that ROvIFN-γ must be maintained in the culture conditions for at least 14 days to ensure elimination of *C. psittaci* from infected cultures (Figures 7.2).

These findings strongly support a role for OvIFN-γ both as a potential effector mechanism in immunity to *C. psittaci* and as a factor involved in the induction and maintenance of persistent infection in the non-pregnant ewe. Furthermore, the concentrations of ROvIFN-γ that induced persistent *C. psittaci* infection or effected eradication of *C. psittaci* from infected cultures were, with the exception of 1000 U/ml, within the range of OvIFN-γ produced by immune ewes following secondary challenge with live *C. psittaci* [Graham *et al*, 1995].

The nature of chlamydial persistence is likely to influence antigen presentation *in vivo* and have profound consequences on the outcome of the immune response. Persistent *C. trachomatis* (serovar A) described in human HeLa 229 treated with 0.2 or 0.5 ng/ml of RHuIFN-γ [Beatty, 1993; 1994a; 1994b; 1995] was characterised by small but conspicuous inclusion bodies containing large aberrant RBs which failed to differentiate into infectious EB. When IFN-γ was removed from the culture system for more than 48 hrs, viable EB were recovered from the culture supernatants and typical *C. trachomatis* inclusion morphology was restored [Beatty *et al*, 1995]. Similar reversible changes in chlamydiae morphology and developmental cycle have also

been reported following penicillin treatment of murine cells infected with *C. psittaci* [Matsumoto and Manire, 1970] and nutrient depletion [Coles *et al*, 1993]. In contrast, the inclusion morphology described for spontaneously occurring *C. psittaci* persistence in murine McCoy cells [Rodolakis *et al*, 1989] and murine L-cells [Perez-Martinez and Storz, 1985; Moulder *et al*, 1980] was reported to fluctuate between periods when inclusion bodies could not be demonstrated in infected cultures and periods of cytolytic chlamydial growth associated with unusually large and conspicuous inclusion bodies. More importantly, RHuIFN-γ mediated persistence was associated with changes in the relative expression of potentially protective and immunopathogenic chlamydial antigens. Expression of MOMP, the 60 KDa cysteine-rich OMP and LPS were down regulated compared to HSP 60 [Beatty *et al*, 1995]. Similar changes in the relative expression of MOMP and HSP 60 have been demonstrated in aberrant *C. trachomatis* isolated from the synovial tissues of patients with reactive arthritis [Gerard *et al*, 1998].

In the experiment detailed here, ROvIFN-γ mediated *C. psittaci* persistence was not associated with inclusions formation of any kind. Inclusion bodies were not found by light microscopy in cytospins prepared from persistently infected ST.6 cultures maintained in culture medium containing 25 or 100 U/ml of ROvIFN-γ. However, inclusion body formation was restored when these cultures were transferred into ROvIFN-γ-free culture medium (figure 7.7C). This may help to explain why *C. psittaci* is very difficult to detect by classical histology in ewes infected out-with pregnancy [Huang *et al*, 1990; Buxton *et al*, 1996].

The reasons for the apparent differences between persistent forms of *C. psittaci* and *C. trachomatis* in cells treated with IFN-γ are not clear. It is possible that the mechanism by which IFN-γ activates cells to inhibit chlamydial growth acts at different stages in the developmental cycle of each species or that differences in host cell species or phenotype are responsible. Further work is required to establish whether ROvIFN-γ mediated persistence of OEA strains of *C. psittaci* is associated with attenuated antigen expression, similar to that seen in *C. trachomatis*.

If the amount of IFN-γ produced *in vivo* is directly related to the amount of antigen

present, then persistent infection could develop as a result of low level antigenic stimulation at the time of initial infection. By entering a persistent state in response to low levels of IFN-γ produced early on in the ontogeny of the immune response, *C. psittaci* may be able to avoid inducing an acquired immune response to antigens that would protect the ewe against abortion. This would allow *C. psittaci* to persist until the next pregnancy, when IFN-γ production is thought to be down regulated [Raghupathy, 1997], invade the placenta, cause disease and spread to other ewes. The development of immunity to OEA which follows clinical disease may result from the massive antigenic stimulus associated with multiplication of *C. psittaci* in the placenta [Buxton *et al*, 1990].

It is unreasonable to assume that IFN-γ is the only factor involved in persistence. A number of other cytokines have been shown to exert anti-chlamydial effects *in vitro* through similar mechanisms to IFN-γ and may also play a role in persistence. TNF-α and IFN-β act in synergy to inhibit *C. trachomatis* in human HEp-2 cells [Shemer-Avni *et al*, 1988; 1989]. In addition, spontaneously occurring persistent infection has been reported in human peripheral blood monocytes infected *C. trachomatis* (serovar K) [Koehler *et al*, 1996; 1997]. Although there is no evidence in the literature support this in ovine monocytes it may have important ramifications for *C. psittaci* persistence in sheep.

The findings detailed here indicate that the S26/3 OEA strain of *C. psittaci* can persist in ovine cells *in vitro* for least 63 days in the presence of physiological levels of ROvIFN-γ. This has important implications for the persistence of *C. psittaci* in ewes infected outwith pregnancy and supports a role for the host immune response both in the maintenance of persistence and protection. These findings also demonstrated that OvIFN-γ is able to eradicate *C. psittaci* from infected ovine cells in the absence of other immunological factors. In addition, this work has provided an in vitro homologous model of OvIFN-γ mediated persistent infection of ovine cells with an ovine abortion isolate of *C. psittaci* which can now be used to further characterise chlamydial persistence in the context of OEA.

Chapter 8.0

A Role for the Tryptophan Pathway in Interferon-γ Mediated Persistence of *Chlamydia psittaci*

8.1 Introduction

The anti-chlamydial action of ROvIFN-γ on ovine ST.6 cells can be partially reversed by the addition of exogenous L-tryptophan [(Chapter 5.0); Graham *et al*, 1995]. In the previous experiments (Chapters 6.0 and 7.0) it was shown that concentrations of between 25-100 U/ml of ROvIFN-γ induced and maintained *C. psittaci* persistence, whereas 250 U/ml or more resulted in eradication of chlamydiae from infected ST.6 cultures. It was therefore of interest to determine whether L-tryptophan was able to abrogate the anti-chlamydial effects of ROvIFN-γ over a longer time course and to see what effects, if any, the addition of exogenous L-tryptophan had on the induction and maintenance of *C. psittaci* persistence in ST.6 cells.

The experiments detailed in this chapter were designed to address the following questions:

- Can the addition of exogenous L-tryptophan to ST.6 cultures at the time of initial infection prevent the induction of ROvIFN-γ-mediated *C. psittaci* persistence?

- Can exogenous L-tryptophan prevent eradication of *C. psittaci* from ST.6 cultures maintained in the presence of high concentrations of ROvIFN-γ?

- Can exogenous L-tryptophan abrogate the chlamydiastatic effects of 25-100 U/ml of ROvIFN-γ and induce cytolytic *C. psittaci* growth in persistently infected ST.6 cells.

8.2 Materials and Methods

8.2.1 Infection of ST-6 cells and treatment with ROvIFN-γ

ST.6 cells were seeded into sixteen 25 cm^2 vented tissue culture flasks at a density of $5x10^4$ cells/ml in 6 ml IMDM+5% FBS (culture medium). After 3 days, when the ST.6 cell monolayers were still sub-confluent, 10 of the flasks were incubated with 1 ml of culture medium containing $3x10^4$ *C. psittaci* strain S26/3 EB. The remaining 4 flasks were incubated with 1 ml of culture medium alone and used as uninfected controls. After 6 hours, the supernatants were removed and replaced with 6 ml of culture medium containing various concentrations of ROvIFN-γ and L-tryptophan (Table 8.1).

Table 8.1: Treatment protocols for ST.6 cultures

ROvIFN-γ (U/ml)	L-tryptophan (μg/ml)	*C. psittaci* (IFU/ml)
200	0	$3x10^4$
200	500	$3x10^4$
100	0	$3x10^4$
100	500	$3x10^4$
50 (x3)	0	$3x10^4$
50	500	$3x10^4$
25	0	$3x10^4$
25	500	$3x10^4$
0	0	$3x10^4$
0	500	$3x10^4$
50	0	0
50	500	0
0	0	0
0	500	0

8.2.2 Maintenance of persistently infected ST.6 cells

Cultures were passaged into fresh 25 cm^2 vented tissue culture flasks every 7 days (Chapter 2.1.4.) as follows. The cells were detached with trypsin/versene, washed in 10 ml of culture medium, centrifuged at 400 g for 5 minutes and resuspended in fresh culture medium. The cells from each flask were adjusted to a density of $5x10^4$

cells/ml before seeding into two fresh flasks in 6 ml volumes. ROvIFN-γ and/or 500 μg/ml of L-tryptophan was then added to only one of each pair of new cultures to give the same final concentrations that the cells had been maintained in during the previous 7 days. The other flask was maintained in culture medium alone for the duration of the experiment or until chlamydiae lysed all the ST.6 cells.

8.2.3 Measurement of *C. psittaci* multiplication

Culture supernatants were titrated in triplicate on fresh ST.6 cells to determine the numbers, if any, of infectious chlamydiae present (Chapter 2.5.2.). In addition, cytospins were prepared from samples of cells removed from cultures at the time of passage (Chapter 2.4.1.) and examined for the presence of ST.6 cells containing chlamydial inclusion bodies. Giemsa stain was used to stain *C. psittaci* inclusion bodies (Chapter 2.4.3.).

8.2.4 Addition of exogenous L-tryptophan to persistently infected cultures

Two flasks of ST.6 cells which had been infected with $3x10^4$ IFU/ml of *C. psittaci* were maintained in culture medium containing 50 U/ml of ROvIFN-γ and passaged as described in 8.2.2. Chlamydial growth was monitored by titration and cytospin analysis as described in 8.2.3. 500 μg/ml of L-tryptophan was added to one of the cultures seven days after *C. psittaci* persistence was first established. The other culture was maintained in ROvIFN-γ alone. Both cultures were maintained under these conditions for a further 14 days or until *C. psittaci* lysed all of the ST.6 cells in the cultures. Following the addition of exogenous L-tryptophan, chlamydial growth was measure by LPS ELISA (Chapter 2.5.1) and periodic titration of infectious EB onto fresh ST.6 cells (Chapter 2.5.2).

8.3 Results

8.3.1 Infected controls

Infectious chlamydiae were detected in the supernatants of the infected controls on days 7 and 14 and both cultures were completely lysed on day 14 (Figure 8.1). However, the supernatant from the infected control maintained in culture medium supplemented with 500 μg/ml of L-tryptophan contained approximately 7-fold fewer infectious EB ($2.65x10^5$ IFU/ml) than the control maintained in culture medium alone ($1.97x10^6$ IFU/ml) on day 14. Inclusion bodies were visible in cytospins prepared from both of the controls on day 7.

8.3.2 Induction of *C. psittaci* persistence by ROvIFN-γ

ROvIFN-γ restricted chlamydial growth in a dose dependent manner and removal of ROvIFN-γ from the cultures was associated with an increase in chlamydial growth. Concentrations of 12.5 U/ml (Figure 8.1) and 25 U/ml (Figure 8.2) of ROvIFN-γ reduced the number of infectious chlamydiae produced by infected ST.6 cells and delayed cell lysis. However, at these concentrations ROvIFN-γ failed to control chlamydial growth completely, resulting in total lysis of the ST.6 cell cultures by day 35, even when ROvIFN-γ was maintained in the culture conditions. Persistent *C. psittaci* infections were established when cultures were maintained in the presence of 50 U/ml (Figure 8.3) or 100 U/ml (Figure 8.4) of ROvIFN-γ for 21 and 14 or more days respectively. Persistent chlamydiae reverted to their normal lytic growth cycle when ROvIFN-γ was removed from the culture conditions (Table 8.2). In contrast, maintaining infected ST.6 cultures in the presence of 200 U/ml (Figure 8.5) of ROvIFN-γ for more than 14 days appeared to kill *C. psittaci*. Infectious EB and inclusion bodies were not found in this culture after day 14 (Table 8.2).

Figure 8.1: The effects of exogenous L-tryptophan on *C. psittaci* growth in ST.6 cells maintained in **12.5 U/ml** of ROvIFN-γ

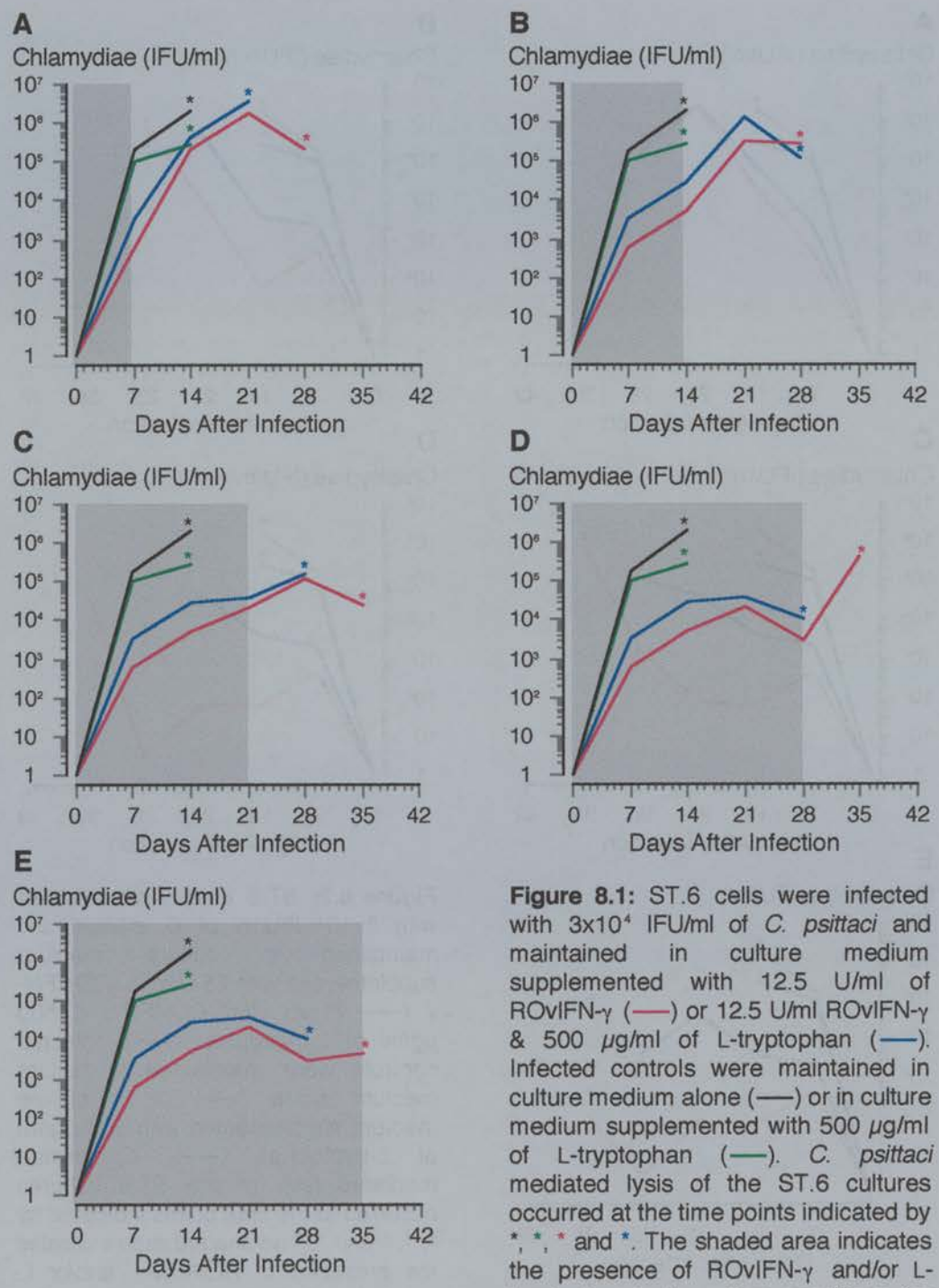

Figure 8.1: ST.6 cells were infected with $3x10^4$ IFU/ml of *C. psittaci* and maintained in culture medium supplemented with 12.5 U/ml of ROvIFN-γ (——) or 12.5 U/ml ROvIFN-γ & 500 μg/ml of L-tryptophan (——). Infected controls were maintained in culture medium alone (——) or in culture medium supplemented with 500 μg/ml of L-tryptophan (——). *C. psittaci* mediated lysis of the ST.6 cultures occurred at the time points indicated by *, *, * and *. The shaded area indicates the presence of ROvIFN-γ and/or L-tryptophan in the culture conditions for the first 7 (**A**), 14 (**B**), 21 (**C**), 28 (**D**) or 35 (**E**) days after infection ( ).

Figure 8.2: The effects of exogenous L-tryptophan on *C. psittaci* growth in ST.6 cells maintained in **25 U/ml** of ROvIFN-γ

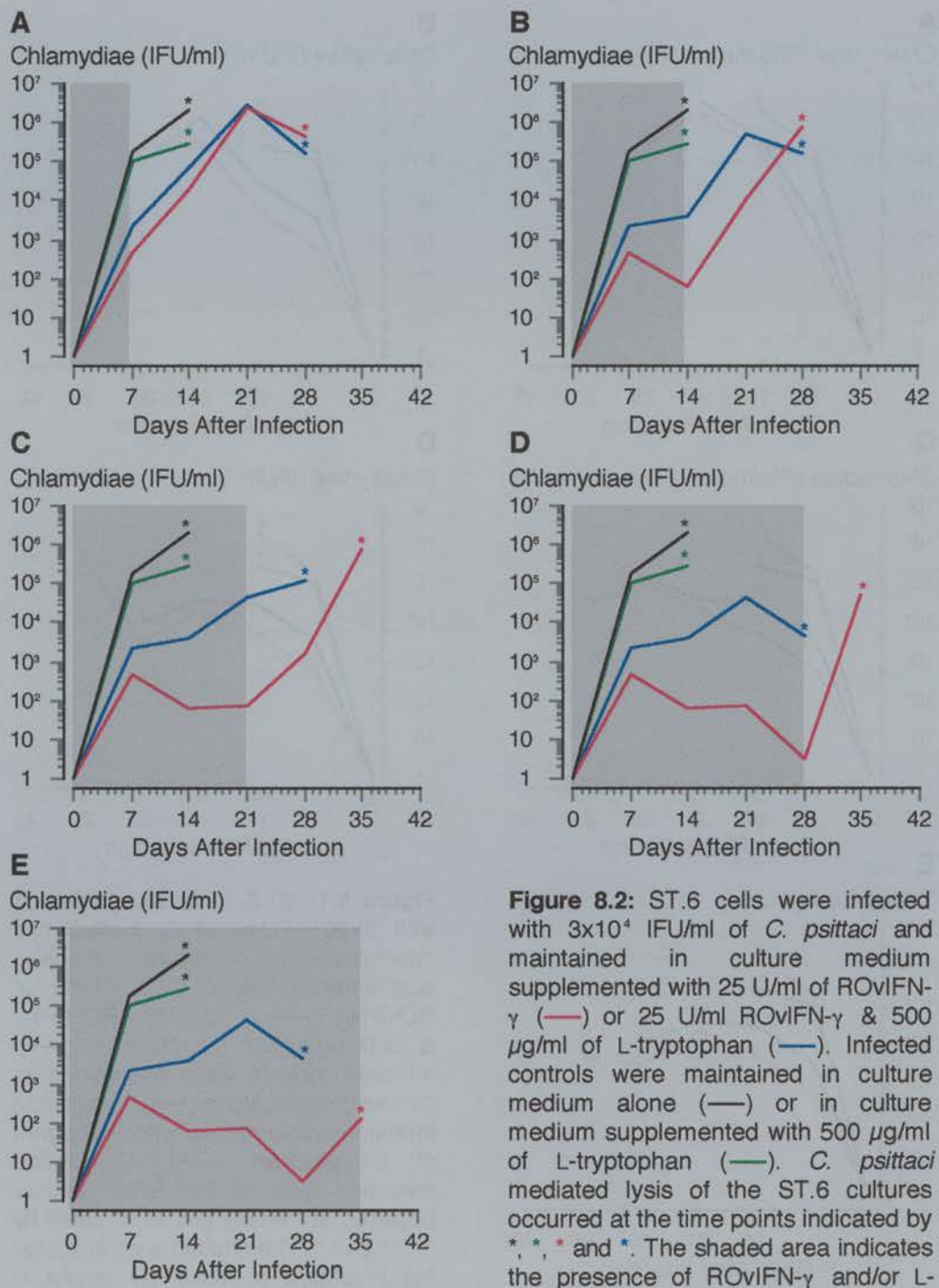

Figure 8.2: ST.6 cells were infected with $3x10^4$ IFU/ml of *C. psittaci* and maintained in culture medium supplemented with 25 U/ml of ROvIFN-γ (—) or 25 U/ml ROvIFN-γ & 500 μg/ml of L-tryptophan (—). Infected controls were maintained in culture medium alone (—) or in culture medium supplemented with 500 μg/ml of L-tryptophan (—). *C. psittaci* mediated lysis of the ST.6 cultures occurred at the time points indicated by *, *, * and *. The shaded area indicates the presence of ROvIFN-γ and/or L-tryptophan in the culture conditions for the first 7 (**A**), 14 (**B**), 21 (**C**), 28 (**D**) or 35 (**E**) days after infection ( ).

8.3.3 Addition of exogenous L-tryptophan to ST.6 cultures at the time of infection

ROvIFN-γ-mediated inhibition of *C. psittaci* growth in ST.6 cells was partially abrogated when 500 μg/ml of L-tryptophan was maintained in the culture conditions during the time that the cells were exposed to ROvIFN-γ. This effect was strictly dependent on both the concentration of ROvIFN-γ used and the time that the cultures were maintained in the presence of ROvIFN-γ and L-tryptophan.

The effects of exogenous L-tryptophan on chlamydial growth in cultures maintained in 12.5 U/ml of ROvIFN-γ are shown in Figure 8.1. There was a small increase in the number of infectious chlamydiae present in the culture supernatants (2 to 5.6-fold) when the culture medium was supplemented with 500 μg/ml of L-tryptophan during the time that the ST.6 cells were exposed to ROvIFN-γ (Figure 8.5E). In addition, cultures maintained in the presence of ROvIFN-γ and 500 μg/ml of L-tryptophan were typically lysed by *C. psittaci* 7 days earlier than cultures maintained in ROvIFN-γ alone. However, chlamydial growth and host cell lysis was retarded in cultures treated with ROvIFN-γ and L-tryptophan compared to the infected controls. Chlamydial growth increased when cells from these cultures were transferred into culture medium alone.

The effects of exogenous L-tryptophan were more marked in cultures treated with 25 U/ml of ROvIFN-γ (Figure 8.2). There was a small (3.4-fold) increase in the number of infectious chlamydiae present in the supernatants of cultures maintained in the presence of ROvIFN-γ and 500 μg/ml of L-tryptophan for 7 days compared to the culture maintained in ROvIFN-γ alone (Figure 8.2A). However, when ROvIFN-γ and L-tryptophan were maintained in the culture conditions for 14 days or more the number of infectious EB present in the culture supernatants rose to between 67 and 1406-fold more than that in the culture maintained in ROvIFN-γ alone (Figure 8.2D). In addition, the presence of exogenous L-tryptophan resulted in earlier lysis of the ST.6 cultures compared to the culture maintained in ROvIFN-γ alone (Figure 8.2E). Transfer of cells from the culture maintained in ROvIFN-γ and 500 μg/ml of L-tryptophan into culture medium alone on days 14 resulted in an increase in

chlamydial growth (Figure 8.2B).

Persistent *C. psittaci* infection was not established in cultures maintained in 50 U/ml of ROvIFN-γ and 500 μg/ml of L-tryptophan (Figure 8.3). On day 7 there was a 12.7-fold increase in the number of infectious chlamydiae present in the culture supernatant of ST.6 cells maintained in both ROvIFN-γ and L-tryptophan compared to the culture maintained in ROvIFN-γ alone. This discrepancy increased to 46.8-fold on day 14 (Figure 8.5B), after which chlamydial persistence was established in the culture maintained in ROvIFN-γ alone (Figure 8.5D). The number of infectious EB present in the supernatant of the culture maintained in the presence of both ROvIFN-γ and L-tryptophan remained constant at approximately $5x10^3$ IFU/ml until day 35 when it peaked at $1.1x10^5$ IFU/ml accompanied by lysis of the ST.6 cell culture (Figure 8.5E).

Persistent *C. psittaci* infection was not established in cultures maintained in culture medium containing both 100 U/ml of ROvIFN-γ and 500 μg/ml of L-tryptophan (Figure 8.4). On day 7 there was a 22-fold increase in the number of infectious chlamydiae present in the culture supernatant of ST.6 cells maintained in ROvIFN-γ and L-tryptophan compared to that in the culture maintained in ROvIFN-γ alone (Figure 8.4A). Infectious chlamydiae could not be demonstrated in the supernatant of cells maintained in culture medium containing 100 U/ml of ROvIFN-γ by day 14 (Figure 8.4C). In contrast, when infected ST.6 cells were maintained in the presence of both 100 U/ml of ROvIFN-γ and 500 μg/ml of L-tryptophan, the number of infectious chlamydiae in the culture supernatant remained static at approximately 100 IFU/ml until day 28, at which point no infectious EB could be demonstrated in the culture supernatant. However, this trend was reversed on day 35 when the number of infectious EB in the culture supernatant rose to $8.6x10^3$ IFU/ml and *C. psittaci* lysed all of the ST.6 cells in the culture.

Figure 8.3: The effects of exogenous L-tryptophan on *C. psittaci* growth in ST.6 cells maintained in **50 U/ml** of ROvIFN-γ

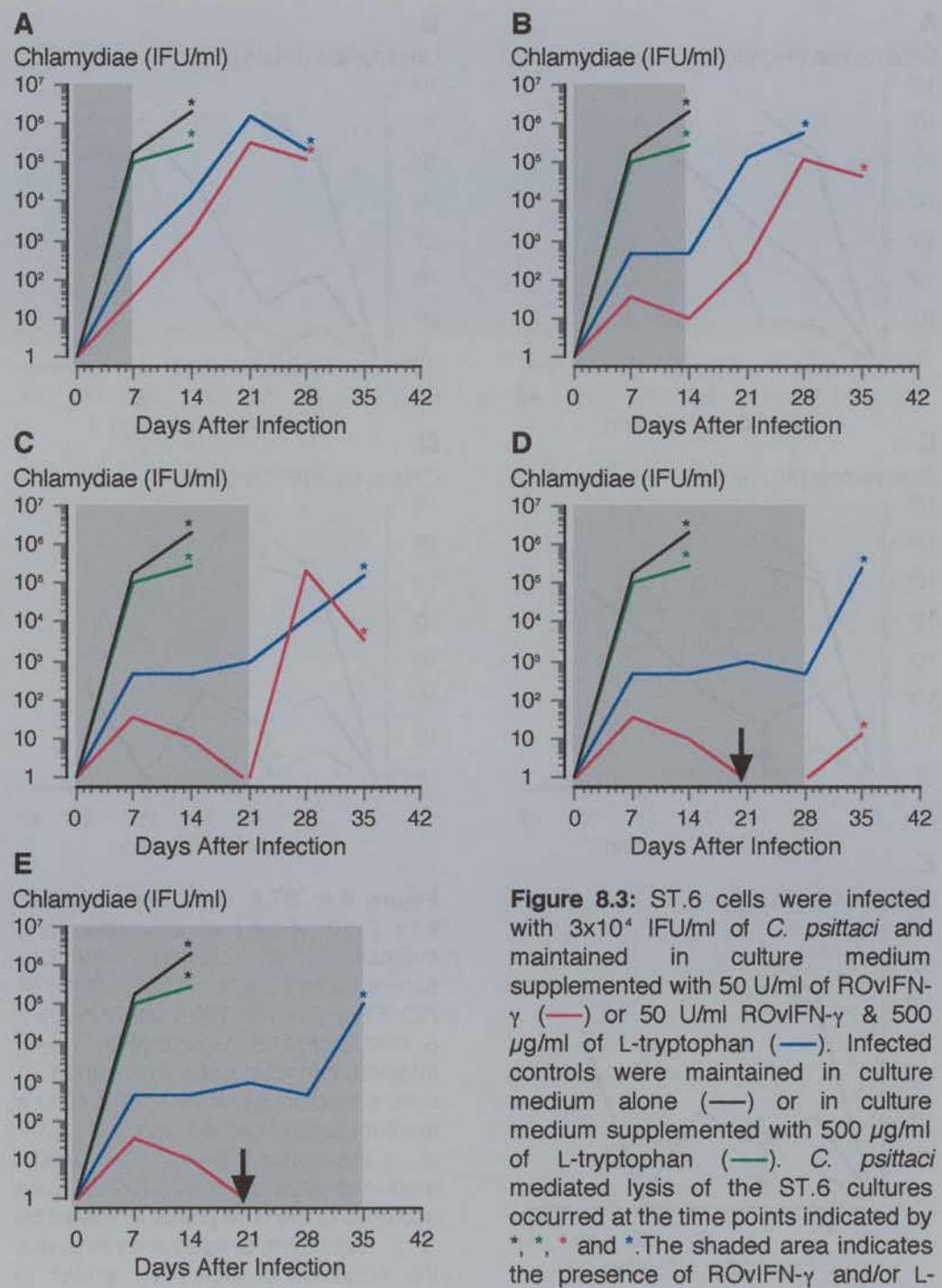

Figure 8.3: ST.6 cells were infected with $3x10^4$ IFU/ml of *C. psittaci* and maintained in culture medium supplemented with 50 U/ml of ROvIFN-γ (—) or 50 U/ml ROvIFN-γ & 500 μg/ml of L-tryptophan (—). Infected controls were maintained in culture medium alone (—) or in culture medium supplemented with 500 μg/ml of L-tryptophan (—). *C. psittaci* mediated lysis of the ST.6 cultures occurred at the time points indicated by *, *, * and *.The shaded area indicates the presence of ROvIFN-γ and/or L-tryptophan in the culture conditions for the first 7 (**A**), 14 (**B**), 21 (**C**), 28 (**D**) or 35 (**E**) days after infection ( ). Arrows indicate the point at which persistence was established.

Figure 8.4: The effects of exogenous L-tryptophan on *C. psittaci* growth in ST.6 cells maintained in **100 U/ml** of ROvIFN-γ

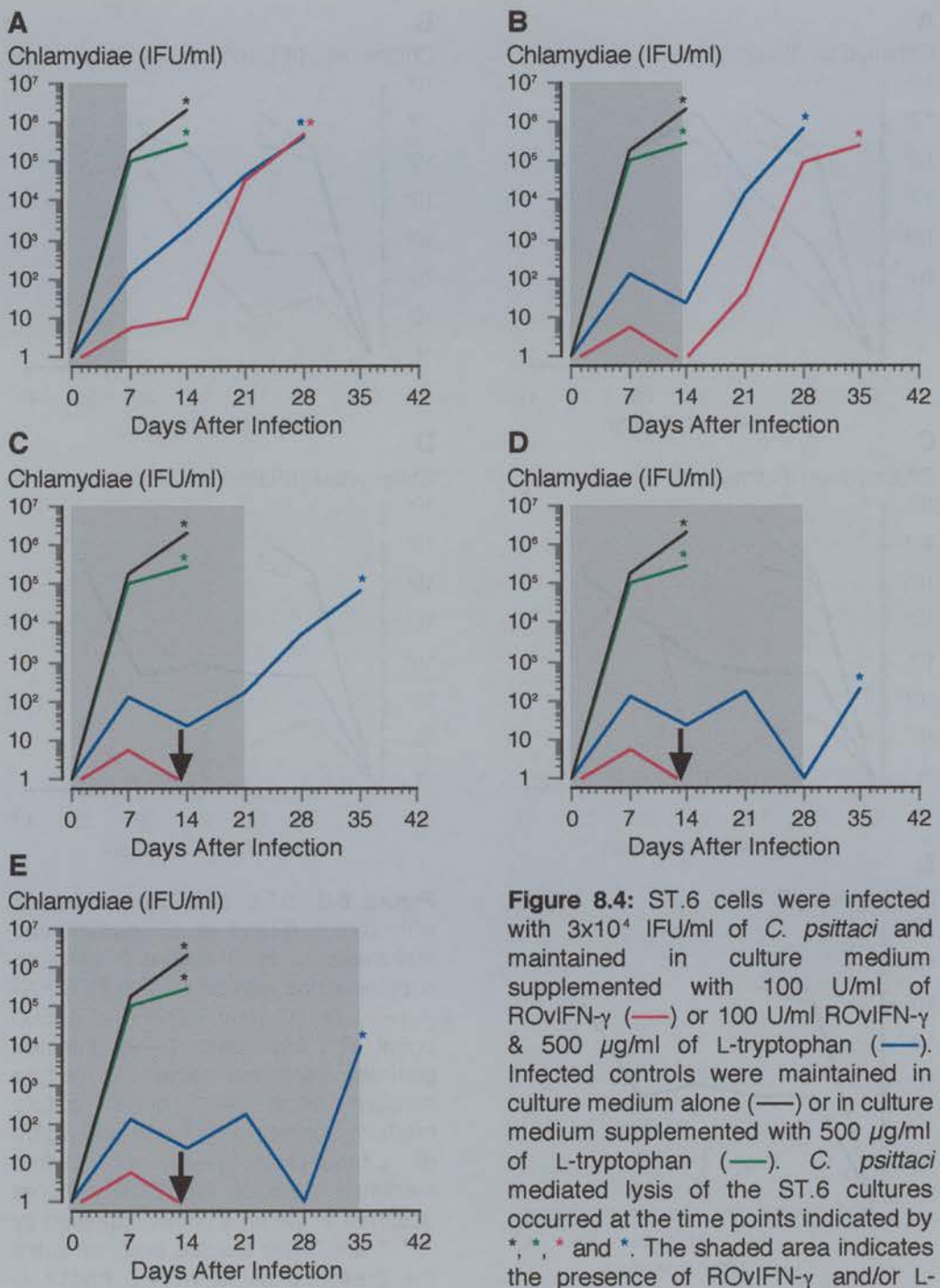

Figure 8.4: ST.6 cells were infected with $3x10^4$ IFU/ml of *C. psittaci* and maintained in culture medium supplemented with 100 U/ml of ROvIFN-γ (—) or 100 U/ml ROvIFN-γ & 500 μg/ml of L-tryptophan (—). Infected controls were maintained in culture medium alone (—) or in culture medium supplemented with 500 μg/ml of L-tryptophan (—). *C. psittaci* mediated lysis of the ST.6 cultures occurred at the time points indicated by *, *, * and *. The shaded area indicates the presence of ROvIFN-γ and/or L-tryptophan in the culture conditions for the first 7 (**A**), 14 (**B**), 21 (**C**), 28 (**D**) or 35 (**E**) days after infection ( ). Arrows indicate the point at which persistence was established.

Figure 8.5: The effects of exogenous L-tryptophan on *C. psittaci* growth in ST.6 cell maintained in 200 U/ml of ROvIFN-γ

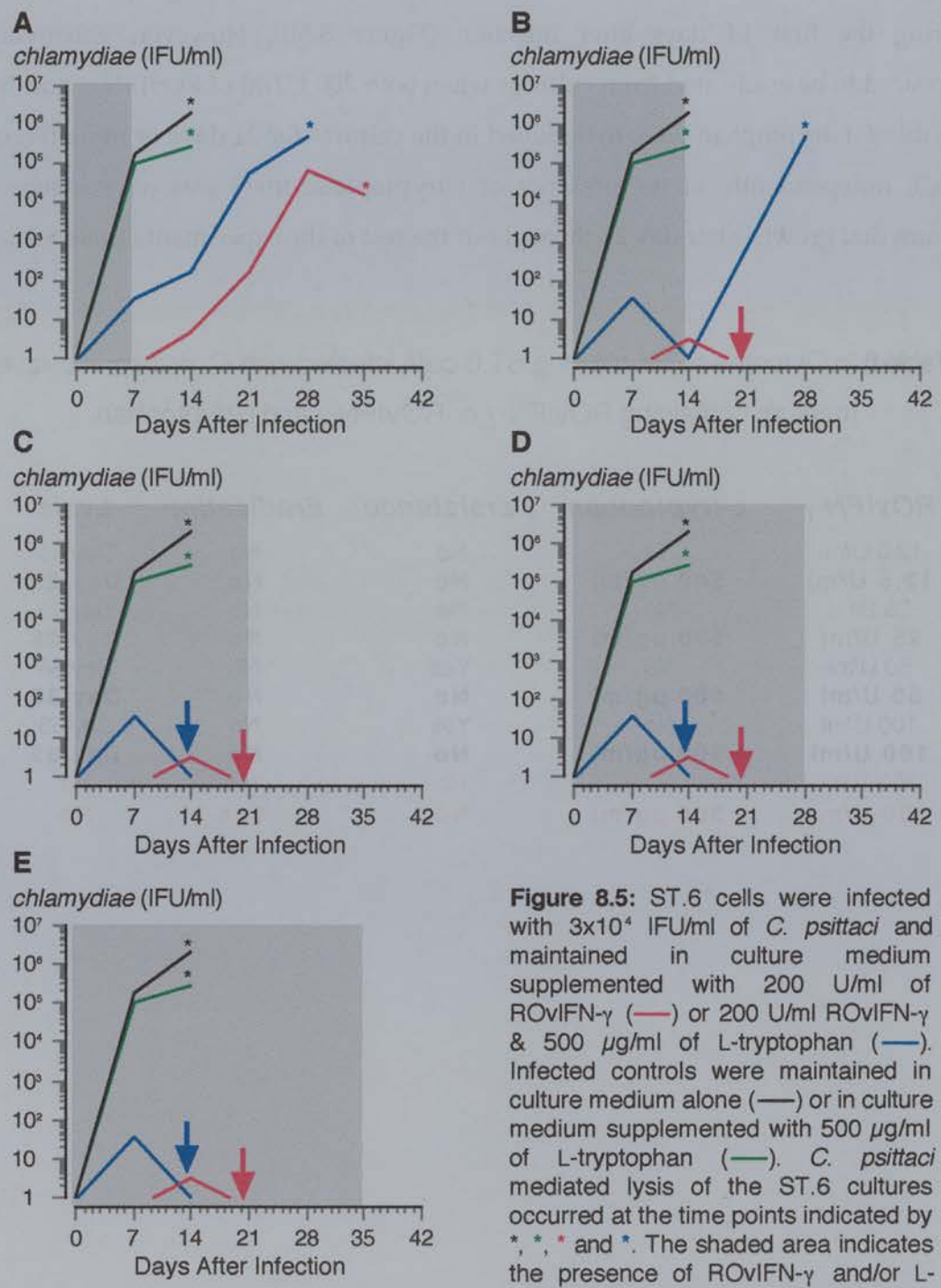

Figure 8.5: ST.6 cells were infected with $3x10^4$ IFU/ml of *C. psittaci* and maintained in culture medium supplemented with 200 U/ml of ROvIFN-γ (——) or 200 U/ml ROvIFN-γ & 500 μg/ml of L-tryptophan (——). Infected controls were maintained in culture medium alone (——) or in culture medium supplemented with 500 μg/ml of L-tryptophan (——). *C. psittaci* mediated lysis of the ST.6 cultures occurred at the time points indicated by *, *, * and *. The shaded area indicates the presence of ROvIFN-γ and/or L-tryptophan in the culture conditions for the first 7 (**A**), 14 (**B**), 21 (**C**), 28 (**D**) or 35 (**E**) days after infection ( ). Arrows indicate the point after which live *chlamydiae* were not recovered.

C. psittaci was eradicated from culture maintained in 200 U/ml of ROvIFN-γ and 500 μg/ml of L-tryptophan for 21 days or more (Figure 8.5). Cultures maintained in the presence of ROvIFN-γ and L-tryptophan failed to control chlamydial growth during the first 14 days after infection (Figure 8.5B). However, chlamydiae appeared to be eradicated from cultures when both 200 U/ml of ROvIFN-γ and 500 μg/ml of L-tryptophan were maintained in the cultures for 21 days or more (Figure 8.5C). Independently of the presence of L-tryptophan, there was no evidence of chlamydial growth after day 21 throughout the rest of the experiment (Table 8.2).

Table 8.2: Outcome of Maintaining ST.6 cells infected with *C. psittaci* in culture medium containing ROvIFN-γ or ROvIFN-γ and L-tryptophan.

ROvIFN-γ	L-tryptophan	Persistence	Eradication	Lysis
12.5 U/ml	No	No	No	Day 35
12.5 U/ml	**500 μg/ml**	**No**	**No**	**Day 28**
25 U/ml	No	No	No	Day 35
25 U/ml	**500 μg/ml**	**No**	**No**	**Day 28**
50 U/ml	No	Yes	No	Day 56
50 U/ml	**500 μg/ml**	**No**	**No**	**Day 35**
100 U/ml	No	Yes	No	Day 63
100 U/ml	**500 μg/ml**	**No**	**No**	**Day 35**
200 U/ml	No	No	Yes	No
200 U/ml	**500 μg/ml**	**No**	**Yes**	**No**

8.3.4 Addition of exogenous L-tryptophan to persistently infected ST.6 cells

In an experiment performed in parallel to that described in 8.3.3, persistent *C. psittaci* infections were established in two ST.6 cultures by maintaining them in culture medium supplemented with 50 U/ml of ROvIFN-γ for the first 35 days after infection.

Chlamydial growth was monitored periodically by titration and cytospin analysis to ensure that a persistent infection had been established. Infectious chlamydiae were not found in the supernatants of either of the cultures on day 35 and the ST.6 cells themselves were free from inclusion bodies. 500 μg/ml L-tryptophan was added to one of the cultures on day 35 and maintained in the culture conditions until day 70, at which point *C. psittaci* had lysed all of the ST.6 cells in the culture (Figure 8.6B) The other culture was maintained in the presence of 50 U/ml of ROvIFN-γ alone until day 84 (figure 8.6A). On days 35 and 49, cells from both cultures were transferred into ROvIFN-γ/L-tryptophan-free culture medium and maintained until *C. psittaci* lysed all of the ST.6 cells in the cultures (Figure 8.6).

Similar quantities of chlamydial LPS (Figure 8.6) and infectious chlamydiae (Table 8.3) were detected in the supernatants of both cultures following the removal of ROvIFN-γ on Day 35. Addition of exogenous L-tryptophan on day 35 resulted in more rapid recovery of chlamydial LPS (Figure 8.6B) and infectious EB (Table 8.3) when ST.6 cells were subsequently transferred into ROvIFN-γ-free culture medium on day 49. Chlamydial LPS (Figure 8.3A) and infectious EB (Table 8.3) were not found in the supernatants of the ST.6 culture maintained in the presence of ROvIFN-γ alone after day 21. However, addition of exogenous L–tryptophan on day 35 reversed this effect. Infectious EB (table 8.3) and chlamydial LPS (Figure 8.6B) were recovered from the culture supernatant on days 14 and 21 respectively and all of the ST.6 cells in this culture were lysed by day 70.

Figure 8.6A: ST.6 cells maintained in ROvIFN-γ alone

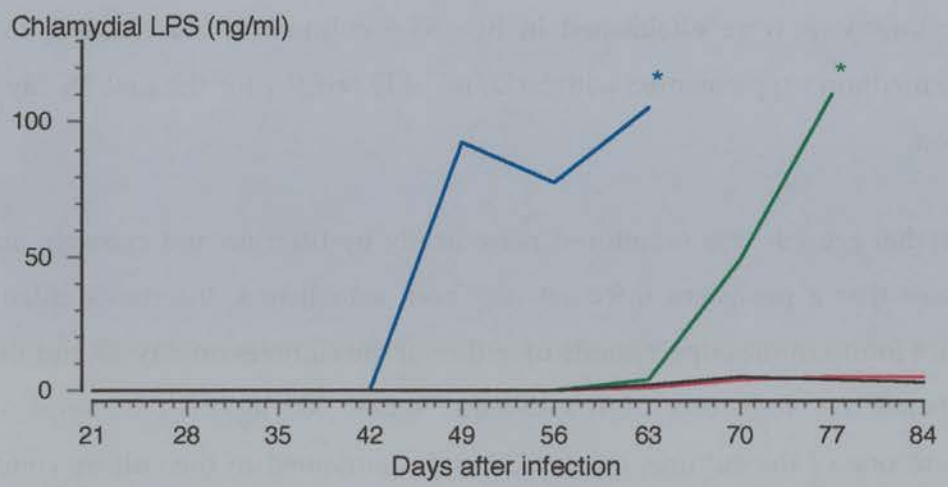

Figure 8.6A: ST.6 cells were infected with *C. psittaci* and maintained in culture medium supplemented with 50 U/ml ROvIFN-γ for 35 days (—), 49 Days (—) or 84 days (—). Uninfected controls (—) were maintained for the duration of the experiment. The asterisks (* and *) indicate *C. psittaci* mediated lysis of the ST.6 cultures.

Figure 8.6B: Addition of exogenous L-tryptophan to persistently infected ST.6 cells

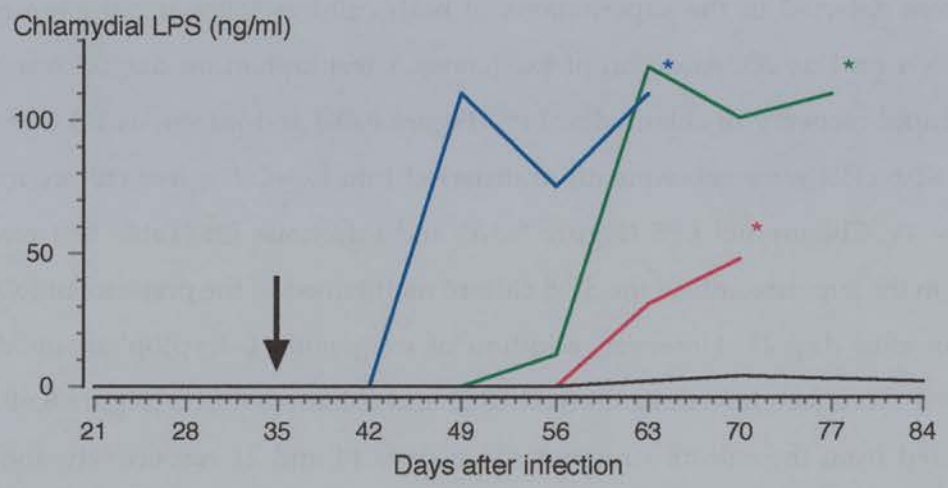

Figure 8.6B: ST.6 cells were infected with *C. psittaci* and maintained in culture medium supplemented with 50 U/ml of ROvIFN-γ for 35 days (—), on day 35 (arrow) 500 μg/ml of L-tryptophan was added to the culture maintained in ROvIFN-γ. ST.6 cells were maintained in the presence of ROvIFN-γ and L-tryptophan for a further 14 days (—) or until *C. psittaci* lysed all of the ST.6 cells in the culture (—). Uninfected controls (—) were maintained for the duration of the experiment.The asterisks (*, *, and *) indicate *C. psittaci* mediated lysis of the ST.6 cultures.

Table 8.3: Titration of infectious chlamydiae on days 49 and 77

ROvIFN-γ exposure (Days)	***L-tryptophan exposure (Days)***	***Day 49 (IFU/ml)***	***Day 77 (IFU/ml)***
0-35	-	4.35×10^5	Lysed on day 63
0-35	-	1×10^6	Lysed on day 63
0-49	-	0	1×10^3
0-49	35-49	0	1×10^8
0-84	-	0	0
0-70 (*lysis*)	35-70 (*lysis*)	5	Lysed on day 70
-ve Controls	*-ve Controls*	*0*	*0*

8.4 Discussion

These findings support a role for tryptophan depletion as a mechanism through which persistent *C. psittaci* infection of ovine ST.6 cells is induced and maintained by low levels (50-100 U/ml) of ROvIFN-γ. In addition, they lend further support to the role of OvIFN-γ in both microbistatic and microbicidal control of *C. psittaci* in ovine cells (Chapters 6.0 and 7.0). Similar studies in human HeLa 229 cells have demonstrated a role for tryptophan depletion in RHuIFN-γ mediated *C. trachomatis* persistence [Beatty *et al*, 1994a; 1995]. In those studies, the addition of exogenous tryptophan to persistently infected cultures maintained in 0.5 ng/ml of RHuIFN-γ was sufficient to restore normal *C. trachomatis* development and cytolytic growth. Furthermore, whilst RHuIFN-γ has been shown to upregulate tryptophan catabolism and induce *C. trachomatis* persistence in human ME180 cells, it does not increase tryptophan catabolism or chlamydial growth in the IDO deficient mutant cell line ME180-1R3B6A [Beatty *et al*, 1994a]. *C. trachomatis* persistence has also been shown to occur HeLa 229 cells maintained in tryptophan depleted culture medium in the absence of RHuIFN-γ [Beatty *et al* ; 1994a; 1995]. Similarly, amino acid deficient culture medium has been reported to induce *C. trachomatis* and *C. psittaci* persistence in McCoy cells [Coles *et al*, 1993].

Although the results detailed in this chapter support a role for tryptophan depletion in ROvIFN-γ mediated *C. psittaci* persistence in ovine ST.6 cells, cultures that were treated with both ROvIFN-γ and exogenous L–tryptophan restricted chlamydial growth more effectively than the infected controls. This agrees with previous studies in which ROvIFN-γ mediated restriction of *C. psittaci* growth in short-term culture experiments was only partially reversed by exogenous L-tryptophan [(Chapter 5.0); Graham *et al*, 1995].

There are several possible explanations for the failure of exogenous L–tryptophan to completely ablate the anti-chlamydial effects of ROvIFN-γ. Exogenous L-tryptophan may simply enhance *C. psittaci* growth in a manner that is independent from the effects of ROvIFN-γ. However, this seems unlikely because exogenous L-tryptophan did not result in increased *C. psittaci* growth in infected ST.6 cells maintained in

ROvIFN-γ-free culture medium (Figures 8.1 - 8.5). It is conceivable that the ST.6 cultures were able to catabolise all of the exogenous L-tryptophan present in the culture supernatants prior to it being replenished every 7 days. However, tryptophan catabolism was not measured in these studies and without further work, the ability of $1x10^6$ ST.6 cells (the approximate number of confluent ST.6 cells supported by a 25 cm^2 flask) to catabolise 3 mg of L-tryptophan in 7 days can only be speculated on. The failure of exogenous L-tryptophan to prevent eradication of chlamydiae from ST.6 cultures treated with 200 U/ml of ROvIFN-γ may therefore be due to the use of sub-optimal concentrations of L-tryptophan in this study. Alternatively, ROvIFN-γ may induce additional as yet undefined anti-chlamydial mechanisms in ovine cells, particularly at higher concentrations where exogenous L-tryptophan had little effect on the microbicidal effects of ROvIFN-γ. Further studies using the L-tryptophan agonist/IDO inhibitor 1-methyl-tryptophan [Munn *et al*, 1998] and/or semi quantitative RT-PCR analysis of IDO transcription should clarify this situation.

Chapter 9.0

Stimulation of *C. psittaci* specific PBM proliferation by recombinant MOMP

9.1. Introduction

Studies employing MHC II -/- and CD4 -/- mice have identified a requirement for CD4 +ve T–cells in the development of protective immunity to *C. trachomatis* in the mouse [Magee *et al*, 1995; Morrison *et al*, 1995; Williams *et al*, 1997]. The ability of different inbred strains of mice to resist primary infection with *C. trachomatis* has been shown to correlate with their ability to mount a Th1-like cytokine response [Darville *et al*, 1997] and more specifically to produce IFN-γ [Yang *et al*, 1996]. Whilst CD4 +ve and CD8 +ve T-cells are both capable of IFN-γ production [Simon *et al*, 1993; Magee *et al*, 1995], antibody-mediated depletion studies have shown that CD4 +ve T-cells contribute significantly more to both IFN-γ production and protective immunity in mice infected intranasally with *C. trachomatis* [Magee *et al*, 1995].

In vitro studies using ST.6 cells and BAL macrophages have shown that IFN-γ can restrict the growth of *C. psittaci* in ovine cells [Graham *et al*, 1995]. Little is known about the *in vivo* cellular source of IFN-γ production in sheep in response to *C. psittaci* infection or if its production is altered during pregnancy. However, generalised suppression of mitogen induced PBM proliferation has been reported in ewes during the later stages of pregnancy [Burrells *et al*, 1978; McCafferty, 1994].

Identification of the *C. psittaci*-specific T-cells responsible for IFN-γ production in immune sheep and to what extent its production is altered by hormonal changes during pregnancy would help to clarify which of the antigen-presentation pathways should be targeted in OEA vaccine design.

The experiments detailed in this chapter were designed to address these questions by employing dual label FACS analysis of surface marker expression and intracellular OvIFN-γ expression in PBM following stimulation with UV inactivated *C. psittaci* or recombinant MOMP and by quantitative ELISA analysis of the effects of various pregnancy associated hormones on the cytokine profiles of *C. psittaci*- and MOMP-specific T-cell lines derived from immune ewes.

9.2. Materials and Methods

9.2.1. Sheep

13 adult ewes which had aborted after subcutaneous injection with of $1x10^5$ egg lethal dose 50 of S26/3 *C. psittaci* on day 90 of gestation [Jones *et al,* 1995], were screened for *C. psittaci* specific PBM proliferation using a lymphocyte stimulation assay (LST assay; Chapter 2.7.). The interval between abortion and screening was 18 months. Two naive ewes which had previously been shown to be seronegative for chlamydiae-specific antibody by CFT were acquired from a *C. psittaci* free flock at MRI and used as negative controls.

9.2.2. Recombinant MOMP

Initial experiments were performed using FMOMP [Herring *et al,* 1994] which had been previously prepared for use in tissue culture by western blot and nitrocellulose resolubilisation as described by McCafferty (1992). Following a change in MOMP cloning strategy at MRI, FMOMP was replaced by TMOMP [Herring *et al,* 1998] in later experiments (Chapter 2.6).

9.2.3. *C. psittaci* specific lymphocyte stimulation assay

In initial experiments, PBM from immune ewes and controls were screened for proliferative responses to UV inactivated *C. psittaci* EB and FMOMP by LST assay (Chapter 2.7.). ConA (ICN Biomedicals) and *S. minnesota* RE-595 LPS (Sigma-Aldrich) were included in the assay as positive controls. Culture medium alone was used to provide negative control values. FMOMP was substituted with TMOMP in later LST screening experiments. Results were expressed as a stimulation index (SI).

$$SI = \frac{\text{CPM experimental}}{\text{Mean CPM of negative controls}}$$

9.3 Results

9.3.1. Screening of Post-OEA ewes and controls for FMOMP specific PBM proliferation

PBM from 13 adult post-OEA ewes and 2 controls were screened for proliferative responses to *C. psittaci* and FMOMP (Table 9.1).

Table 9.1: ^{3}H–thymidine incorporation by PBM from post-OEA and control ewes following stimulation with *C. psittaci* antigens

Sheep #	Antigen / mitogen	10 µg/ml	5 µg/ml	2.5 µg/ml	1.25 µg/ml	0.625 µg/ml	Mean CPM of -ve controls
2652	EB antigen	24.9	39.4	39.3	57.0	-	
Control	FMOMP	-	5.7	3.8	3.6	3.2	
ewe #1	ConA	-	292.2	-	243.4	-	
	LPS	6.9	-	-	-	-	47
2693	EB antigen	0.5	0.6	0.8	0.9	-	
Control	FMOMP	-	0.9	0.8	0.8	0.9	
ewe #2	ConA	-	32.8	-	28.1	-	
	LPS	3.8	-	-	-	-	54
2620	EB antigen	193.6	201.7	128.0	131.4	-	
OEA	FMOMP	-	193.0	128.7	77.3	56.7	
ewe #1	ConA	-	550.0	-	445.0	-	
	LPS	35.2	-	-	-	-	23.3
2628	EB	89.3	105.9	96.5	103.1	-	
OEA	FMOMP	-	23.2	19.0	18.9	16.7	
ewe #2	ConA	-	609.5	-	478.2	-	
	LPS	80.2	-	-	-	-	21.2
2629	EB antigen	28.4	30.1	21.0	13.6	-	
OEA	FMOMP	-	13.5	9.4	4.4	3.6	
ewe #3	ConA	-	191.1	-	169.2	-	
	LPS	22.9	-	-	-	-	59
2659	EB antigen	7.8	13.8	11.0	5.3	-	
OEA	FMOMP	-	23.9	13.6	9.8	5.3	
ewe #4	ConA	-	457.6	-	199.5	-	
	LPS	22.9	-	-	-	-	59.85
2662	EB antigen	1.9	2.3	1.6	2.7	-	
OEA	FMOMP	-	6.4	5.4	2.8	3.3	
ewe #5	ConA	-	22.4	-	17.3	-	
	LPS	17.9	-	-	-	-	546

Table 9.1: Results are expressed as mean SI values of duplicate cultures. Mean CPM values (1 SI) for the negative controls from each sheep are provided in the far right column.

Table 9.1 (continued): ^{3}H–thymidine incorporation by PBM from post-OEA and control ewes following stimulation with *C. psittaci* antigens

Sheep #	Antigen / mitogen	10 µg/ml	5 µg/ml	2.5 µg/ml	1.25 µg/ml	0.625 µg/ml	Mean CPM of -ve controls
2635	EB antigen	1.1	1.4	1.2	1.2	-	
	FMOMP	-	1.5	1.5	1.9	1.6	
	ConA	-	2.6	-	2.0	-	
	LPS	2.2	-	-	-	-	4792.5
2645	EB antigen	2.7	4.2	3.4	5.6	-	
	FMOMP	-	3.6	3.4	4.4	2.5	
	ConA	-	481.5	-	325.0	-	
	LPS	68.6	-	-	-	-	46
2664	EB antigen	0.2	0.3	0.5	0.7	-	
	FMOMP	-	2.0	2.0	1.8	1.7	
	ConA	-	2.0	-	1.5	-	
	LPS	2.1	-	-	-	-	6209
2669	EB antigen	1.9	4.1	6.4	7.6	-	
	FMOMP	-	13.6	13.1	14.8	16.1	
	ConA	-	29.3	-	26.9	-	
	LPS	25.0	-	-	-	-	445
2674	EB antigen	16.4	22.0	21.7	28.0	-	
	FMOMP	-	8.4	6.6	9.0	5.4	
	ConA	-	348.4	-	261.7	-	
	LPS	18.1	-	-	-	-	61
2691	EB antigen	11.8	15.6	17.9	17.2	-	
	FMOMP	-	8.9	12.5	7.3	5.1	
	ConA	-	565.5	-	512.4	-	
	LPS	11.0	-	-	-	-	25.3
2739	EB antigen	1.5	2.3	2.2	2.0	-	
	FMOMP	-	1.9	1.4	1.1	0.7	
	ConA	-	44.9	-	31.3	-	
	LPS	16.5	-	-	-	-	343
2741	EB antigen	0.8	1.4	1.4	1.3	-	
	FMOMP	-	0.5	0.8	0.7	0.7	
	ConA	-	13.5	-	11.6	-	
	LPS	1.7	-	-	-	-	1110

Table 9.1: Results are expressed as mean SI values of duplicate cultures. Mean CPM values (1 SI) for the negative controls from each sheep are provided in the far right column.

FMOMP induced proliferation in PBM derived from 8 of the post-OEA ewes. There was evidence of a dose dependent response to FMOMP in 5 of the post-OEA ewes (Table 9.2: highlighted in red) and these animals were selected for use in further experiments on this basis. There was also evidence of *C. psittaci* and FMOMP

specific proliferation in one of the controls (2652; control ewe #1) which had previously been shown to be seronegative for *C. psittaci*-specific antibody.

9.3.2. Screening of selected post-OEA ewes and controls for TMOMP specific PBM proliferation

Five post-OEA ewes, previously selected on the basis of dose dependent proliferation in response to FMOMP (Table 9.2: highlighted in red), were screened for TMOMP-specific PBM proliferation. TMOMP which had been prepared previously for use in tissue culture by western blot and nitrocellulose resolubilisation as described by McCafferty (1992) was cytotoxic and this approach was abandoned. TMOMP was subsequently prepared for use in tissue culture using polyacrylamide column chromatography (Chapter 2.6.4.). This technique allowed purification of large quantities (>2 mg/48 hours) of TMOMP which was non-toxic in cell culture at concentrations of up to 40 μg/ml.

Figure 9.1A: UV inactivated *C. psittaci* and TMOMP specific proliferation of PBM from control ewes

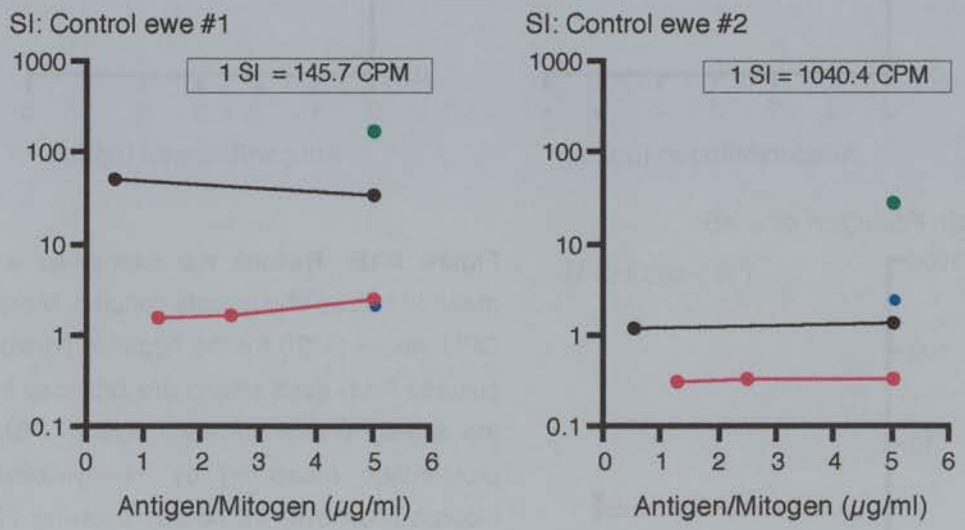

Figure 9.1A: Results are expressed as mean SI values of duplicate cultures. Mean CPM values (1 SI) for the negative control cultures from each sheep are provided in the top-right inset of each figure. PBM proliferation measured by ^{3}H–thymidine incorporation in duplicate cultures over 16 hours, following 72 hours incubation in the presence of UV inactivated *C. psittaci* EB (—●—), TMOMP (—●—), 5 μg/ml of ConA (●) or 5 μg/ml of LPS (●).

Figure 9.1B: Proliferation of PBM from post-OEA ewes in response the whole UV inactivated *C. psittaci* and TMOMP

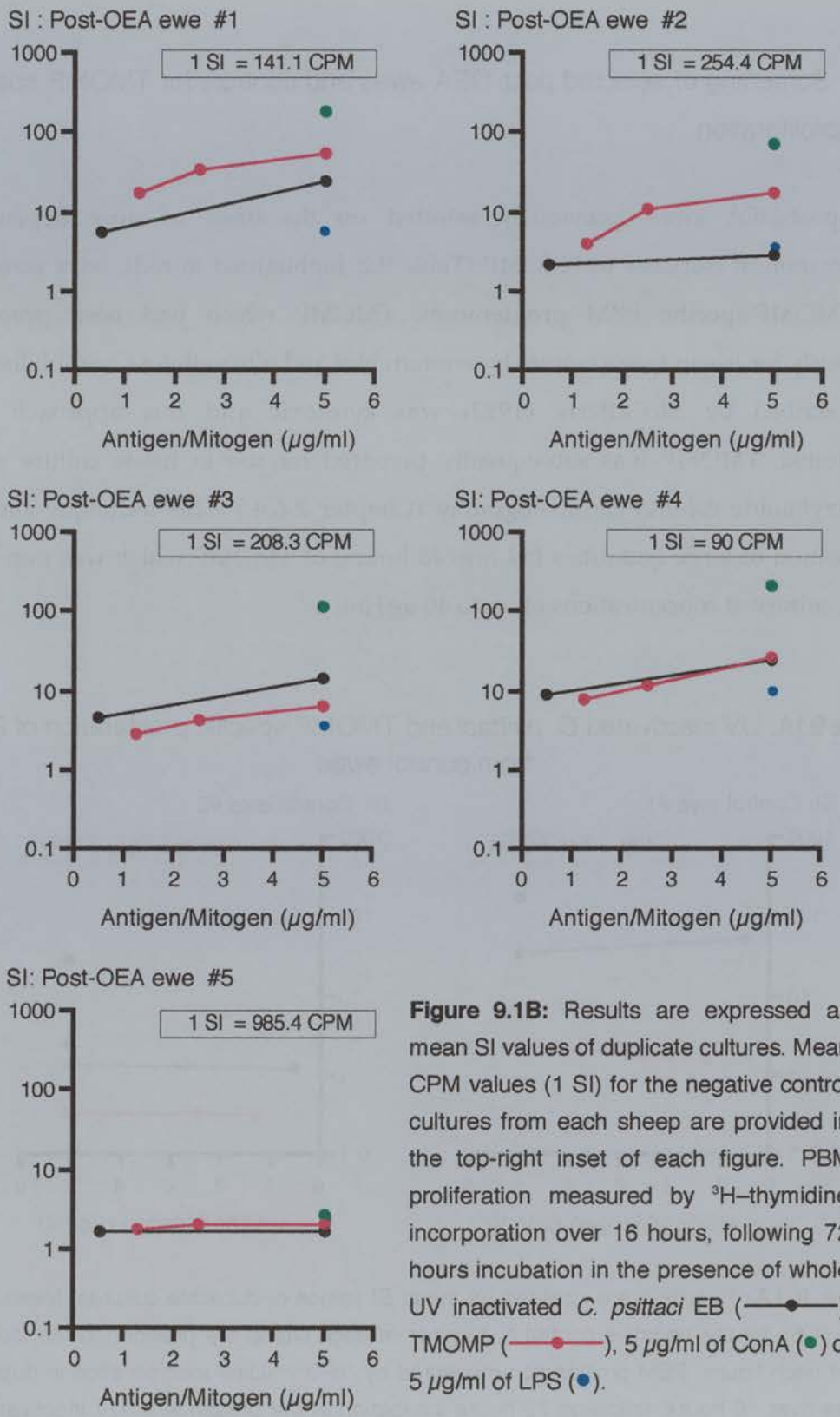

Figure 9.1B: Results are expressed as mean SI values of duplicate cultures. Mean CPM values (1 SI) for the negative control cultures from each sheep are provided in the top-right inset of each figure. PBM proliferation measured by ^{3}H–thymidine incorporation over 16 hours, following 72 hours incubation in the presence of whole UV inactivated *C. psittaci* EB (—●—), TMOMP (—●—), 5 μg/ml of ConA (●) or 5 μg/ml of LPS (●).

LST assays were performed on duplicate cultures, results are expressed as mean SI values. UV inactivated *C. psittaci* EB and TMOMP induced proliferation in PBM cultures derived from one of the controls (Figure 9.1A) and from 4 of the post-OEA ewes (Figure 9.1B). There was little evidence for antigen- or mitogen-driven proliferation in PBM cultures derived from post-OEA ewe #5 (Figure 9.1B). There was no evidence of *C. psittaci*- or TMOMP-specific proliferation in PBM cultures derived from the second control ewe (Figure 9.1A).

Large quantities (>200 mg) of TMOMP were produced for use in generating TMOMP-specific ovine T-cell lines using the *E. coli* expression system detailed in Chapter 2.6.1. The product was verified as TMOMP by direct dot-immunobinding assay (Chapter 2.6.2.) and quantified by SDS PAGE and 1D gel densitometery (Figure 9.2).

Figure 9.2: SDS-PAGE analysis of TMOMP (Coomassie Blue)

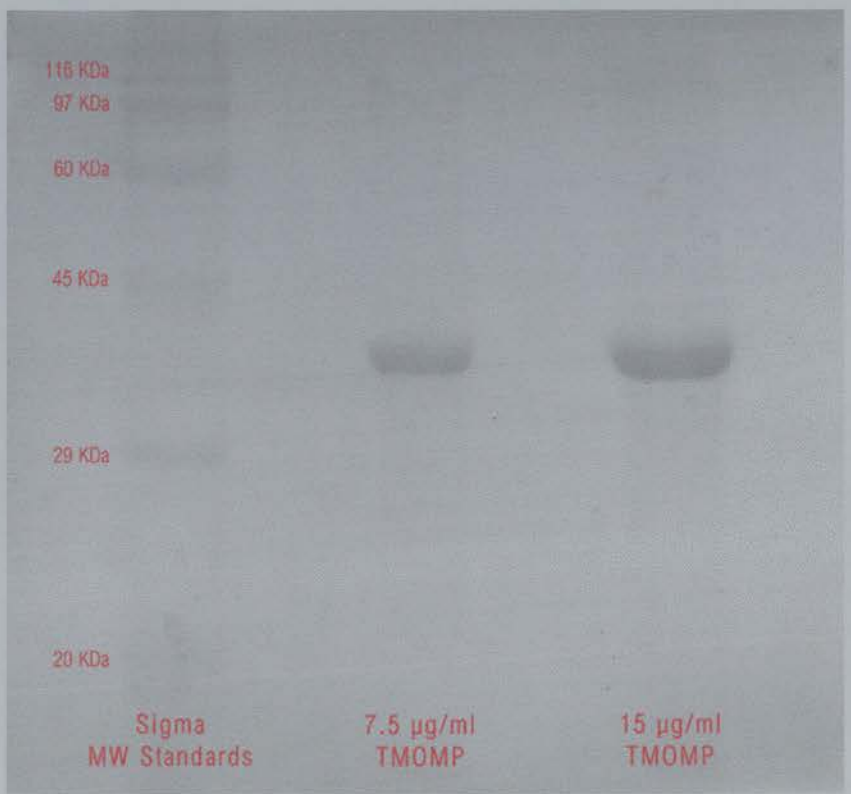

9.3.3. TMOMP-specific ovine T-cell lines

Attempts to extend these studies beyond the initial screening of PBM from immune ewes for *C. psittaci* and MOMP specific proliferation were hampered by animal fatalities and problems associated with generating sufficient amounts of TMOMP. Post-OEA ewe #5 died from natural causes in November 1996 (aged 6.5 years). Post-OEA ewe #1 inexplicably lambed in March 1997, despite having been housed under isolated conditions for over two years, and died as a result of trauma several days after giving birth (aged 7 years).

By the time that significant amounts of polyacrylamide column chromatography purified TMOMP were available for dual label FACS analysis and generating T-cell lines, little or no proliferation could be induced in the PBM of any of the remaining immune ewes in response to TMOMP or UV inactivated *C. psittaci* EB. Furthermore, there was no evidence of ConA or LPS mediated proliferation by PBM from any of the immune ewes despite repeated LST analysis (data not shown).

9.4. Discussion

Chlamydial MOMP has been the focus of a great deal of interest as a potential vaccine candidate against OEA strains of *C. psittaci* [Herring *et al*, 1998] and human strains of *C. trachomatis* [Stagg, 1998]. However, experimental OEA vaccines based on recombinant *C. psittaci* MOMP have so far proved largely ineffective at inducing protective immunity [Herring *et al*, 1998]. Differences in the efficacy of experimental OEA vaccines using the purified outer membrane of *C. psittaci* [Tan *et al*, 1990] and recombinant MOMP [Herring *et al*, 1994] have been attributed to the failure of the recombinant protein to adopt a trimeric conformation homologous to that of native MOMP [Herring *et al*, 1998]. However, conformational epitopes are not required for the induction MOMP specific T-cells. Vaccination of BALB/c H-2d mice with a fusion peptide derived from *C. trachomatis* MOMP (using the glutathione-S-transferase from *Schistosoma japonicum* which lacks T cell determinants recognised by BALB/c H-2d mice) has been shown to elicit both *C. trachomatis*-specific T-cell proliferation *ex vivo* and enhanced T-cell help for the production of protective antibodies following secondary challenge with heat-inactivated *C. trachomatis in vivo* [Allen *et al*, 1991]. Independent studies have identified a 12-mer peptide (TINKP) of MOMP which stimulates proliferation and IFN-γ production in T-cells from naive human donors [Stagg *et al*, 1993]. Anti-MHC II antibodies but not anti-MHC I antibodies block TINKP-specific proliferation suggesting that this epitope is recognised in the context of MHC II and CD4 +ve T-cells. In addition, intradermal vaccination of mice with TINKP induces chlamydiae-specific T-cell memory and provides partial protection against salpingitis during secondary challenge with live *C. trachomatis* [Knight *et al*, 1995].

Evaluation of the immune response elicited by OEA vaccines based on recombinant *C. psittaci* MOMP have thus far focused on antibody rather than T-cell responses [Herring *et al*, 1994; 1998]. It is notable that PBM derived from one of the control ewes (Control ewe #1) used in the experiments described here showed evidence of *C. psittaci*-specific proliferation despite having previously screened negative for *C. psittaci* specific antibody by CFT. Furthermore, efficacy studies have been restricted to ewes infected with *C. psittaci* for the first time during pregnancy and have not

taken into account the possibility that recombinant MOMP may increase the resistance of non-pregnant ewes to persistent infection by priming MOMP-specific T-cells. This is particularly important, not only because of the central role played by persistent infection in the epidemiology of OEA, but also because pregnancy is associated with a bias towards a Th2-like immune response and down regulation of Th1-like cytokines including IFN-γ [Raghupathy, 1997]. Evaluation of the the ability of recombinant MOMP to protect non-ewes against primary challenge with live *C. psittaci* would be more representative of the natural situation where ewes become persistently infected in one season and abort in the next [Wilsmore *et al*, 1984]. In addition, ewes were vaccinated subcutaneously in the experiments described by Herring *et al* (1994;1998), a route which has since been shown to induce few IFN-γ secreting T-cells or provide significant protection against secondary *C. trachomatis* infection in mice [Igietseme *et al*, 1998].

Both FMOMP and TMOMP induced proliferation in PBM derived from immune ewes in the experiments detailed here (Table 9.1 and Figure 9.1B) suggesting that linear epitopes within MOMP are recognised by PBM from immune ewes. Dual labelling of cell surface phenotypic antigens and intracellular OvIFN-γ in PBM challenged with TMOMP or UV inactivated *C. psittaci ex vivo* would have provided an extremely useful insight into which ovine cell types are responsible for OvIFN-γ production in response to secondary challenge with *C. psittaci in vivo* [Graham *et al*, 1995]. Similarly, it was hoped that quantitative analysis of the effects of oestrogen and progesterone on the production of ROvIFN-γ by TMOMP-specific T-cell lines would help to explain how persistent *C. psittaci* may become reactivated during pregnancy. However, technical difficulties prevented further characterisation of *C. psittaci*- and TMOMP-specific PBM or the generation of T-cell lines from responding PBM.

Chapter 10.0
General Discussion

The overall aim of this thesis was to further the understanding of the interaction between the ovine immune system and *C. psittaci*, with the ultimate objective of improving diagnosis and prophylactic control of OEA. To this end, two main avenues of research were pursued.

1. The development of an automated image analysis system for quantification of chlamydial growth *in vitro* that would provide a viable alternative to counting chlamydial inclusions by eye.
2. Investigation of the effects of ROvIFN-γ on *C. psittaci* growth in ovine cells, focusing on the mechanisms through which it restricts chlamydial growth and its role in the induction and maintenance of persistence *in vitro*.

Quantifying chlamydial growth is often one of the major rate limiting steps in experiments involving the study of anti-chlamydial pharmaceuticals or immune effector mechanisms. Prior to the development of Inclusion Counter, an LPS-ELISA [Graham *et al*, 1995] was routinely used to quantify *C. psittaci* growth in many of the experiments detailed in this thesis (Chapters 5.0, 6.0, 7.0 and 8.0). Whilst the LPS-ELISA provides a more rapid means of quantifying *C. psittaci* growth *in vitro* than counting inclusion bodies by eye, there are a number of technical considerations. The LPS-ELISA provides an indirect measure of chlamydial growth as a function of the amount of LPS released into the extracellular milieu by infected cells *in vitro* and it does not appear to be as sensitive as titration of culture supernatants for the presence of infectious EB (Chapter 7.0). This is particularly true of cultures maintained in the presence of ROvIFN-γ where the sensitivity of the LPS-ELISA appears to be reduced compared to cultures maintained in ROvIFN-γ-free culture medium (Figure 7.2). The reason for this is not clear, but it may be due to IFN-γ mediated changes in *C. psittaci* LPS levels similar to that describe for *C. trachomatis* [Beatty, 1993]. RHuIFN-γ-mediated *C. trachomatis* persistence in HeLa 229 cells is associated with the formation of aberrant chlamydiae which exhibit reduced levels of LPS, MOMP and the 60-kDa cysteine-rich OMP when compared to *C. trachomatis* grown in HeLa 229 cells under control conditions. In contrast, chlamydial HSP60 production does not appear to be downregulated by chlamydiastatic concentrations

of RHuIFN-γ [Beatty, 1993; 1994c]. Similar changes in chlamydiae morphology and antigen production have also be reported with chlamydiastatic concentrations of penicillin, ampicillin and hydroxyurea [Cevenini *et al*, 1988; Rosenkranz *et al*, 1973; Sardinia *et al*, 1988].

The possibility that chlamydial antigen expression may be modulated in response to immunological and pharmaceutical stress has serious implications for the detection and quantification of chlamydiae. Any technique based on the recognition of a single chlamydial antigen or RNA sequence is likely to be open to misinterpretation if the chosen antigen is preferentially upregulated or downregulated by chlamydiae as a consequence of the host's immune response *in vivo* or in response to immune factors or antibiotics *in vitro*. Consequently, monoclonal antibody and RT-PCR based techniques may not be the best solution for quantifying chlamydial growth *in vitro* or detecting chlamydiae in tissues *ex vivo*. This is particularly true of RT-PCR, where there is little scope for direct verification of the results since both the host cells and inclusion bodies are destroyed in the process of extracting RNA [Khan *et al*, 1996].

The use of monoclonal antibodies may adversely effect the interpretation of immunohistochemistry and immunofluorescence. Inclusion bodies containing aberrant *C. trachomatis*, which develop in HeLa 229 cells treated with chlamydiastatic concentrations of RHuIFN-γ, stain poorly with anti-MOMP monoclonal antibodies compared to normal inclusion bodies from control cultures [Beatty *et al*, 1993]. Similarly, chlamydiastatic concentrations of ampicillin, hydroxyurea and penicillin completely inhibit production of the cysteine-rich 60-kDa *C. trachomatis* OMP but do not eradicate the pathogen from infected cultures [Cevenini *et al*, 1988; Sardinia *et al*, 1988].

Differential downregulation of chlamydial antigens may explain why the anatomical and cellular location of *C. psittaci* has has yet to be identified in the persistently infected ewe. Monoclonal antibodies have been used to detect *C. psittaci* in tissue sections derived from experimentally infected non-pregnant ewes with varying degrees of success [Amin and Wilsmore, 1995; Buxton *et al*, 1996; Huang *et al*, 1990]. However, *C. psittaci* becomes increasingly difficult to detect *in vivo* with anti-

LPS monoclonal antibodies 6 days after infection despite the continual presence of *C. psittaci* DNA, as determined by PCR [Buxton *et al*, 1996]. Similarly, Amin and Wilsmore (1995) were only able to detect *C. psittaci* during the first 6 days after infection using monoclonal antibodies specific for a 57-kDa *C. psittaci* protein [Bollo *et al*, 1992] and chlamydial-LPS. Recent attempts to detect *C. psittaci* in chronically infected non-pregnant ewes which have previously aborted or experienced fetopathology following experimental infection with *C. psittaci* have been more successful [Papp *et al*, 1998]. Using a monoclonal antibody which is specific for OEA strains of *C. psittaci* [Andersen, 1991], Papp *et al* (1998) were able to demonstrate chlamydiae in cells collected from the cervix and vagina of 100% of non-pregnant ewes that had experienced *C. psittaci* induced abortion three years previously. Although the target antigen for the monoclonal antibody used by Papp *et al* (1998) remains unspecified, it is reasonable to speculate that its ability to detect chronic *C. psittaci* infection in non pregnant ewes where the Clearview test did not is a result of differential antigen expression by *C. psittaci* in the chronically infected ewe.

Diffuse staining of chlamydial inclusion bodies is particularly problematic for image analysis since efficient segmentation of inclusion bodies from cellular background not only depends on the specificity of the staining procedure employed, but also on the intensity of stain taken up by the chlamydiae. This is especially true for automated approaches to image analysis including Inclusion Counter. Consequently, selection of a staining procedure which provides specific and uniformly intense staining of inclusion bodies regardless of the developmental status of the chlamydiae is of paramount importance. Polyclonal antibodies raised against live chlamydiae offer the most straightforward solution to this problem. The chief argument against using polyclonal antibodies is their potential to cross-react with different species and strains of chlamydiae. Whilst this does not present a problem under controlled *in vitro* conditions or *in vivo* experiments using specific pathogen free animals, it has the potential to confound diagnosis of OEA because polyclonal antibodies may also detect non-pathogenic stains of *C. pecorum* or polyarthritis strains of *C. psittaci*. However, it is worth noting that anti-LPS monoclonal

antibodies commonly used for diagnostic purposes such as Clearview and IMAGEN™ (Celltech) are genus-specific rather than species-specific. Furthermore, the anti-LPS monoclonal antibody 13/4 used by Huang *et al* (1990) and Buxton *et al* (1996) not only recognises LPS from all four species of *Chlamydia* but also RE-strain LPS from other bacteria including *Salmonella Spp*, which can also cause abortion in ewes.

In situ DNA-hybridisation offers an attractive alternative to antibody based technologies. It allows the use of strain specific oligonucleotides which can be designed such that they only hybridise to DNA and are thus unlikely to be affected by relative changes in chlamydial antigen expression. It also offers tighter regulation of fluorochrome or substrate deposition than antibody-antigen based approaches. Signal amplification can be achieved by using combinations of oligonucleotides tagged with multiple moieties, direct biotin-streptavidin amplification, anti-moiety biotinylated antibodies or biotinylated anti-Ig F(ab)2 fragments to enhance inclusion body segmentation from cellular background. Alternatively, *in situ* PCR can be used to amplify target DNA sequences prior to *in situ* hybridisation.

Whilst Inclusion Counter was designed and assessed using images of *C. psittaci* inclusion bodies stained with MZN it has been developed to cope with the wide diversity of staining procedures available for differentiating chlamydial inclusion bodies from cellular background. This was initially achieved by generating 8-bit greyscale images from combinations of the red, green and blue components of the original 24-bit RGB colour images so as to maximise the contrast between inclusion bodies and cellular background and thereby facilitate their segmentation (Chapter 3.0). In Inclusion Counter v2.0 (Chapter 4.0), a true 24-bit colour segmentation system was developed using both the RGB and HSV colour models to allow automated enumeration and measurement of inclusion bodies to be independent of the colour of stain used. Inclusion Counter v2.0 can also be configured to ignore RGB or HSV channels in which cellular background and inclusion bodies share similar grey scale values. This feature is particularly effective at excluding particulate background artefacts when used in conjunction with the HSV colour model (Chapter 4.0: Figure 4.6).

The latest version of Inclusion Counter (v2.0) is not only highly accurate with regard to counting inclusion bodies, but also provides accurate values for inclusion body length, width, area, and total area/percentage of the field of view occupied by inclusion bodies. These parameters are simply not available using flow cytometry [Dessus-Babus *et al*, 1998] and are prohibitively time consuming to perform by eye or by non-automated image analysis based approaches. Inclusion Counter discriminates inclusion bodies from background using fixed threshold values and size parameters for any given series of images, therefore the level of error inherent in the system remains constant and is not open to operator bias. Furthermore, images of control cultures can be used to determine the level of error inherent in the system, a feature which is unavailable when counting inclusion bodies by eye. Further measurement parameters such as morphological measurements like roundness or width/length (aspect ration) can be added to Inclusion Counter v2.0 as required without incurring significant development costs.

The range of measurement possible with Inclusion Counter should allow more precise analysis of the effects of anti-chlamydial agents such as cytokines and antibiotics than currently available techniques. Agents which target both intracellular and extracellular chlamydiae are likely to affect inclusion body size and frequency. Reductions in *C. trachomatis* inclusion body number and size have been observed following pretreatment of murine McCoy or L-cells with IFN-γ [Byrne and Krueger, 1983; Mayer *et al*, 1993]. Treatment of HeLa 229 cells with RHuIFN-γ six hours after infection with *C. trachomatis* is associated with a significant reduction in inclusion body size [Beatty *et al*, 1994b]. Agents which act exclusively on chlamydial EB in the extracellular milieu or prevent internalised EB from escaping phagolysosomal fusion would be expected to result in a reduction in the number of inclusion bodies per field of view in the absence of significant changes in inclusion body size or morphology. Consequently, Inclusion Counter may be useful in determining whether novel pharmaceutical compounds penetrate infected cells and act on established intracellular chlamydiae or simply inactivate extracellular EB. The ability of Inclusion Counter to return accurate values for inclusion body size may also be used to ensure that putative neutralising antibodies do not cause a

significant reduction in inclusion body size that might otherwise indicate the presence of contaminating cytokines such as IFN-γ which influence inclusion body size [Beatty *et al*, 1993; Byrne and Krueger, 1983; Mayer *et al*, 1993]. Conversely, reduced inclusion body size in the absence of a reduction in inclusion body numbers would be expected following treatment of infected cells with anti-chlamydial agents which do not effect establishment of the inclusion body but restrict RB binary fission. Agents which block the aggregation of endosomes containing chlamydiae in cells infected with multiple EB, similar to that described for *C. trachomatis* in McCoy and HeLa 229 cells after intracellular free Ca^{2+} depletion [Majeed *et al*, 1993; 1994], should result in increased numbers of significantly smaller inclusion bodies compared to controls. Future versions of Inclusion Counter will incorporate roundness and aspect ratio measurements since significant changes in these morphology parameters may indicate damage to inclusion body integrity in the later stages of the chlamydial developmental cycle.

The same approach employed to segment inclusion bodies from cellular background can also be used to calculate the area of the cell monolayer which was lysed due to chlamydial growth. This allows the progression of the infectious process to be measured after the first cycle of chlamydial growth and host cell lysis, providing additional information about the effects of anti-chlamydial agents beyond the initial phase of infection.

The major limitation of Inclusion Counter is that it has been designed primarily for use with confluent monolayers of cells. It cannot, in its present format, be used for applications such as determining the percentage of infected cells in primary macrophage cultures or cytospins. However, an updated version of Inclusion Counter v2.0 is under development which does address this requirement. In addition to its designated application, Inclusion Counter has a number of other potential uses. Inclusion Counter can be used to allow rapid and accurate quantification of a wide variety of histological features both inside and outside chlamydial biology, including cytokine expression, pathological changes and infectious processes that would otherwise be difficult to quantify.

The completed version of Inclusion Counter v2.0 (Chapter 4.0) is freely available in the public domain and can be downloaded from the U.S. National Institute of Health via the internet (ftp://codon.nih.gov/pub/nih-image/user-macros/). However, Inclusion Counter is constantly evolving to accommodate new applications and more recent versions of the software along with online instruction manuals for Inclusion Counter v2.0 use can be downloaded from the Inclusion Counter Home Page at (http://www.image-analysis.co.uk).

Whilst clinical OEA appears to be restricted to fetopathology and abortion in the ewe, the interaction between *C. psittaci* and the ovine immune system is highly complex. Infection during pregnancy commonly results in abortion at or just before the time of normal parturition [Buxton *et al*, 1990]. Non-pregnant ewes appear to be able to control OEA strains of *C. psittaci* and do not develop demonstrable pathology. However, many ewes infected in this manner fail to resolve the infection or develop protective immunity, remain persistently infected for prolonged periods and often go on to experience clinical disease during their next pregnancy [Wilsmore *et al*, 1984]. Furthermore, although ewes which experience OEA appear to develop protective immunity to clinical disease in future pregnancies, the exact nature of this immunity remains unclear.

Protective immunity to OEA may not to be synonymous with sterile immunity to *C. psittaci*, since immune ewes may remain chronically infected for several years after experiencing clinical OEA [Papp *et al*, 1994; 1998; Papp and Shewen, 1996b]. Delineation of the immune mechanisms involved in persistent infection in non-immune ewes and chronic infection of the vaginal and cervical epithelium of immune ewes is likely to have major implications for OEA vaccine design.

ROvIFN-γ restricts the growth of the S26/3 OEA strain of *C. psittaci* in a dose dependent manner in ovine ST.6 cells and has a marked effect on chlamydial inclusion body morphology in ovine BAL macrophages (Chapter 5.0). ROvIFN-γ appears to inhibit *C. psittaci* growth through both microbistatic and microbicidal mechanisms in ST.6 cells. Concentrations of 1 to 25 U/ml of ROvIFN-γ restrict but do not completely inhibit *C. psittaci* growth in ST.6 cells. In contrast, *C. psittaci*

growth is completely inhibited when infected ST.6 cells are maintained in the presence of concentrations of 25 U/ml or more of ROvIFN-γ. This effect appears to become microbicidal when the concentration of ROvIFN-γ is increased to 200 U/ml or more (Chapters 6.0, 7.0 and 8.0).

Pretreatment of ST.6 cells with RBovIFN-α or synthetic double stranded RNA at concentrations matched with ROvIFN-γ in terms of anti-viral activity does not significantly affect *C. psittaci* growth, suggesting that the mechanisms through which ROvIFN-γ restricts *C. psittaci* in ovine cells are independent from its anti-viral activities (Chapter 5.0). ROvIFN-γ does not induce the production of detectable amounts of $NO^{\bullet}$ in ST.6 cells or ovine BAL macrophages infected with the S26/3 OEA strain of *C. psittaci*. Indeed, direct comparison with the murine RAW 264.7 macrophage cell line strongly suggests that ovine BAL macrophages are incapable of $NO^{\bullet}$ synthesis, even when stimulated with combinations of IFN-γ and LPS or *C. psittaci* which induce maximal production of $NO^{\bullet}$ in RAW 264.7 cultures. These finding concur with previous data published by Bogdan *et al* (1997) which showed that ovine BAL macrophages do not produce significant amounts of $NO^{\bullet}$ in response to live bacteria and supernatants from *Corynebacterium pseudotuberculosis* and *Pasteurella haemolytica* cultures; purified *E. coli* or *P. haemolytica* LPS either alone or in combination with IFN-γ or lymphocyte conditioned medium; or ovine lentivirus. Furthermore, whilst L-NMMA has been shown to reverse the anti-chlamydial effects of IFN-γ in murine RAW 264.7 and McCoy cells [Chen *et al*, 1996; Mayer *et al*, 1993], it has no effect of the anti-chlamydial effects of ROvIFN-γ in ST.6 cells infected with *C. psittaci* (Chapter 5.0). Similarly, neither L-NMMA nor depletion of L-arginine by the enzyme arginase reduce the capacity of human peripheral blood monocyte derived macrophages stimulated with IFN-γ *in vitro* or monocytes from patients undergoing IFN-γ therapy to restrict intracellular growth of *C. psittaci*, *T. gondii* and *L. donovani* [Murray and Teitelbaum, 1992]. These findings suggest that in contrast to the situation in mice and homologous to that in humans, iNOS and $NO^{\bullet}$ are unlikely to participate in the anti-chlamydial activities of IFN-γ in sheep.

Despite the body of evidence in support of the role of IFN-γ mediated $NO^{\bullet}$

production in restricting chlamydial growth in the mouse, several recent studies have cast doubt on the relevance of iNOS/NO• in murine immunity to chlamydiae. Result from experiments comparing the susceptibility of iNOS KO mice (iNOS -/- mice) and normal control mice to MoPn suggest that NO• production is not required for the resolution of chlamydial infections *in vivo* [Ramsey *et al*, 1998; Perry *et al*, 1998], although iNOS -/- mice were marginally more susceptible to systemic infection [Igietseme *et al*, 1998]. In addition, Ramsey *et al* (1998) demonstrated that macrophages and primary cell lines (lung and urinary bladder cells) explanted from iNOS -/- mice were not significantly different from cells derived from control mice in terms of their ability to restrict *C. trachomatis* growth following treatment with IFN-γ *in vitro*. In light of these findings, IFN-γ mediated NO• production may accompany rather than mediate the anti-chlamydial effects of this cytokine in the mouse. Moreover, the lack of evidence of a role for NO• production in IFN-γ mediated restriction of chlamydial growth in sheep or humans suggests that the mouse model may have little value in this context.

In contrast to the apparent lack of involvement of NO• production, there is considerable evidence to support a role for the induction of tryptophan catabolism by in ROvIFN-γ mediated inhibition of *C. psittaci* replication in ovine cells. In agreement with previously published data [Graham *et al*, 1995], addition of exogenous L-tryptophan to ROvIFN-γ pretreated ST.6 cultures partially ablates their ability to restrict the growth of the S26/3 OEA strain of *C. psittaci* (Chapter 5.0). Furthermore, regression analysis suggests that exogenous L-tryptophan reverses the anti-chlamydial effects of ROvIFN-γ rather than simply increasing *C. psittaci* growth in a generalised manner (Chapter 5.0). These findings echo the results of studies in human cells [Byrne *et al*, 1986; Mehta *et al*, 1998; Murray *et al*, 1989; Summersgill *et al*, 1995; Thomas *et al*, 1993].

Tryptophan catabolism may not be the only anti-chlamydial mechanism induced by ROvIFN-γ in ovine cells. Long-term culture of *C. psittaci* infected ST.6 cells in the presence of ROvIFN-γ has allowed delineation of the microbistatic and microbicidal activities of this cytokine (Chapter 7.0). Induction and maintenance of *C. psittaci* persistence in ST.6 cells by microbistatic concentrations of ROvIFN-γ is ablated

when cultures are maintained in the presence of exogenous L-tryptophan. In contrast, exogenous L-tryptophan does not rescue *C. psittaci* from the microbicidal effects of concentrations of 200 U/ml or more of ROvIFN-γ (Chapter 8.0). The reason for this disparity is not clear, but it seems plausible that additional microbicidal mechanisms may be induced when cells are maintained in the presence of high concentrations of ROvIFN-γ for prolonged periods of time. However, what is clear is that further analysis is required in order to rule out the possibility the microbicidal effects of ROvIFN-γ are mediated by tryptophan catabolism alone.

Current opinion favours the down regulation of Th1-like immunity in favour of Th2-like immunity during successful pregnancy [Raghupathy, 1997]. A number of factors are thought to contribute towards biasing the immune system away from Th1-like immunity during pregnancy. Wegmann *et al* (1993) reported spontaneous production of the Th2-like cytokines IL-4, IL-5 and IL-10 by murine decidual cells cultured *ex vivo* throughout pregnancy. Progesterone biases antigen-specific human CD4 +ve T-cell lines and clones towards Th2-like cytokine production [Piccinni *et al*, 1995]. Progesterone-induced blocking factor (PIBF) has a similar effect on murine spleen cells [Szekeres-Bartho and Wegmann, 1996] and has been shown to suppress NK cell cytotoxicity toward human embryonic fibroblast cells and TNF production [Szekeres-Bartho *et al*, 1989]. Suppressed PIBF production is also associated with recurrent spontaneous abortion in women [Szekeres-Bartho *et al*, 1995]. Supernatants from human placental and trophoblast cells appear to have more generalised immunoregulatory functions, including down regulation of murine and human mixed lymphocyte reactions, mitogen induced T-cell proliferation, murine graft-versus-host responses and CTL activity [Krishnan *et al*, 1991; 1995].

Constitutive expression of IDO by trophoblast cells has been proposed as a potential mechanisms for preventing allogeneic fetal rejection. IDO activity increases in human syncytiotrophoblast cells after 14 weeks gestation and is maintained at high levels until shortly before parturition [Kamimura *et al*, 1991]. Munn *et al* (1998) have recently described a similar pattern for IDO transcription in the murine placenta. Furthermore, inhibition of IDO activity by the tryptophan analogue 1-methyl-tryptophan induces abortion in pregnant mice carrying allogeneic concepti

but has no effect on syngeneic pregnancies. In light of these findings and what is know about the role of tryptophan catabolism in IFN-γ mediated restriction of chlamydial growth in human and ovine cells [Byrne *et al*, 1986; Graham *et al*, 1995; Mehta *et al*, 1998; Murray *et al*, 1989; Summersgill *et al*, 1995; Thomas *et al*, 1993; (Chapters 5.0 and 8.0)] it seems unlikely that trophoblast cells would support the growth of OEA strains of *C. psittaci*. However, *C. psittaci* inclusion bodies are readily detectable in ovine trophoblast cells from approximately 90 days gestation onward *in vivo* [Buxton *et al*, 1990]. *C. psittaci* inclusion bodies have also been found in murine trophoblast cells *in vivo* [Banks *et al*, 1982; Buendia *et al*, 1998] and in the syncytiotrophoblast of pregnant women who have aborted as a consequence of zoonotic infection with OEA strains of *C. psittaci* [Hyde and Benirschke, 1997].

The involvement of tryptophan deprivation in IFN-γ mediated restriction of *C. psittaci* growth in ovine cells does not exclude the possibility that it also plays a role in preventing allogeneic fetal rejection in the ewe. Whilst the ability of *C. psittaci* to infect cells in which the availability of tryptophan is likely to be heavily restricted until the later stages of pregnancy is surprising, constitutive expression of IDO by trophoblast cells may actually explain the delay between invasion of the placenta at around day 60 of gestation and the onset of pathology after 90 days gestation in OEA.

The finding that ROvIFN-γ can mediate persistent *C. psittaci* infection in an ovine cell line *in vitro* suggests that IFN-γ may be involved in maintaining persistence *in vivo* (Chapters 6.0, 7.0 and 8.0). It is therefore conceivable that down regulation of Th1-like cytokines, including IFN-γ, may be responsible the transition from persistent to active *C. psittaci* infection during pregnancy, similar to the reduction in resistance to *L. major* infection observed in C57BL mice during pregnancy [Krishnan *et al*, 1996a]. Fetopathology may occur as a direct result of chlamydial replication in the placenta. Alternatively, massive *C. psittaci* replication in the placenta may induce a localised Th1-like response at the maternal-fetal interface and subsequent allogeneic fetal rejection similar to that seen in pregnant mice injected with TNF-α, IFN-γ or IL-2 [Chaouat *et al*, 1990].

Whilst downregulation of Th1-like cytokines provides an attractive hypothesis for the reactivation of persistent *C. psittaci* during pregnancy, it does not explain why ewes develop protective immunity to OEA after experiencing clinical disease. However, the interaction between *Plasmodium falciparum* and the human immune system during pregnancy may offer an explanation. Primary immunity to *P. falciparum* infection in humans is thought to be mediated by CMI and is associated with the production of Th1-like cytokines [Harpaz *et al*, 1992]. In contrast, protective immunity to secondary infection is thought to be mediated by antibody [Smith, 1996]. In highly endemic areas where acquired immunity is common, clinical manifestations of malarial infection are not usually exacerbated during pregnancy. In areas of low endemicity where acquired immunity is rare, pregnant women infected with *P. falciparum* often suffer from exacerbated pathology during pregnancy, possible as a result of suppressed Th1-like immunity [Smith, 1996]. Although it is not not clear whether protective immunity to OEA is predominantly mediated by antibody or CMI, it is conceivable that immunity to OEA strains of *C. psittaci* is regulated in a similar manner to that described for *P. falciparum*. Primary infection in the non-pregnant ewe may be controlled by a Th1-like response, whereas protective immunity to clinical OEA may be mediated by antibody. However, both DTH and antibody responses to *C. psittaci* antigens are significantly enhanced in immune ewes [Dawson *et al*, 1986].

Changes in the physiology of the ewe during pregnancy may induce *C. psittaci* to express antigens which mediate its sequestration to the placenta. Protective immunity may therefore be directed against an antigen which is only expressed by *C. psittaci* during the pregnancy. Once again a parallel may be drawn between OEA and *P. falciparum* infection in pregnant women. Malaria can cause complications during pregnancy that arise as a result of *P. falciparum* infection of the placenta leading to low birthweight babies and increased neonatal mortality [Steketee *et al*, 1996]. Sequestration of the parasite to the placenta is mediated by the adhesion of parasitised erythrocytes to chondriotin sulphate A (CSA) expressed on the surface of the syncytiotrophoblast [Fried and Duffy, 1996; 1998] where the parasite appears induce a localised Th1-like response [Fried *et al*, 1998a]. However, such

complications are most common in women during their first pregnancy and it appears that women exposed to *P. falciparum* during pregnancy develop antibody which specifically blocks the interaction of parasitised erythrocytes with CSA expressed on the surface of the placenta [Fried *et al*, 1998b; Miller and Smith, 1998]. The existence of similar *C. psittaci* antigens may explain why immune ewes do not experience clinical OEA despite the fact that they can remain chronically infected with *C. psittaci* [Papp *et al*, 1994; 1998; Papp and Shewen, 1996b].

Broadly speaking, the interaction between the ovine immune system and OEA strains of *C. psittaci* can be divided into three stages.

1. Persistent infection in the non-pregnant ewe in the absence of protective immunity against abortion or pathology.

2. Active infection and invasion of the placenta with subsequent fetopathology during pregnancy.

3. Persistent infection in the immune ewe in the absence of pathology outwith or during subsequent pregnancies.

To be effective, the minimum requirement of an OEA vaccine would be the induction of protective immunity to clinical OEA. In other words, the vaccine would be required to induce an immune response that mimics naturally acquired immunity to OEA but would not necessarily be required to induce sterile immunity to *C. psittaci* itself. However, it is not clear which components of the acquire immune response to OEA strains of *C. psittaci* are responsible for preventing fetopathology. Given the complexity of the protective immune response to OEA, it seems unlikely that an effective sub-component vaccine will be achieved by selecting target antigens merely on the basis that they are expressed on the outer membrane of the EB and that they are recognised by sera from immune ewes.

Whilst protective antigens must by definition be immunogenic, immunogenic antigens are not necessarily protective. Recombinant MOMP is recognised by sera from immune ewes and it is the major constituent of the *C. psittaci* EB outer membrane but

it does not induce protective immunity to OEA [Herring *et al*, 1994, 1998]. Although Herring *et al* (1998) suggest that the the reason for the lack of protection achieved using experimental vaccines based on recombinant MOMP is due to its failure to adopt native conformation, it may equally well be that immunologic recognition MOMP is not required for protective immunity to OEA. Further work is required to determine which *C. psittaci* antigens are involved in sequestration of the pathogen to the placenta during pregnancy and whether their expression is modulated by pregnancy. The identification of such an antigen might allow the development of a vaccine which blocks *C. psittaci* invasion of the placenta similar to that envisaged by Miller and Smith (1998) for preventing sequestration of *P. falciparum* infected erythrocytes to the syncytiotrophoblast in pregnant women.

One of the major drawbacks of a vaccine which induces protective immunity to clinical OEA rather that *C. psittaci* itself is that immunised ewes may still be susceptible to persistent infection similar to that described in naturally immune ewes [Papp *et al*, 1994; 1998; Papp and Shewen, 1996b]. Although this type of vaccine may reduce transmission at lambing by preventing abortion and the subsequent shedding of large quantities of infectious *C. psittaci* into the local environment, it is not clear whether it would prevent persistently infected immune ewes from shedding *C. psittaci* during estrus. Consequently, OEA vaccines which simulate natural immunity in the ewe are unlikely to be useful for wholesale eradication of *C. psittaci* from infected flocks.

An alternative approach to OEA vaccine design would be to target persistent infection in the non-immune ewe by boosting Th1-like immune responses to *C. psittaci*. Under these circumstance, IFN-γ production may be increased from microbistatic to microbicidal levels and thus lead to eradication (Chapter 7.0) and the induction of sterile immunity rather that persistence in the non-pregnant ewe. Appropriate target antigens could be extrapolated from the *in vitro* model of *C. psittaci* persistence in ovine ST.6 cells (Chapters 6.0, 7.0 and 8.0) by Western blot or RT-PCR analysis. The possibility that persistently infected ovine cells present *C. psittaci* antigens in the context of MHC that would make this approach feasible is supported by the observation that IFN-γ mediated persistent *C. psittaci* and *C.*

trachomatis infected murine L-cells are efficiently recognised and killed by cytotoxic CD8 +ve T cells [Rasmussen *et al*, 1996].

Although a vaccine which induces a strong Th1-like immune response might run the risk of exacerbating fetopathology in ewes infected with *C. psittaci* during pregnancy, it would be preferable to vaccines which mimic naturally acquired protective immunity to OEA since it would in theory induce sterile immunity to *C. psittaci*. Such a vaccine could be employed either prophylactically or curatively to eradicate *C. psittaci* from infected flocks. The *in vitro* model of IFN-γ-mediated *C. psittaci* persistence in ovine cells may aid in the identification of putative target antigens for this type of vaccine.

References

Aitken, I. D. (1991): Human infection with *Chlamydia psittaci*, pp. 369-370. In Aitken, I. D. and Martin. W. B. (Ed.): *Diseases of Sheep*, Blackwell Scientific Publications, Oxford.

Aitken, I. D., Clarkson, M. J. and Linklater, K. (1990): Enzootic abortion of ewes. *Veterinary Record* **126**, 136-138.

Aitken, I. D., Robinson, G. W. and Anderson, I. E. (1981): Recent experimental studies on chlamydial abortion in ewes. *Sheep Veterinary Society Proceedings* **5**, 553-590.

Allen, J. E., Locksley, R. M. and Stephens, R. S. (1991): A single peptide from the major outer membrane protein of *Chlamydia trachomatis* elicits T cell help for the production of antibodies to protective determinants. *Journal of Immunology* **147**, 674-679.

Amano, F. and Noda, T. (1995): Improved detection of nitric oxide radical ($NO^{\bullet}$) production in an activated macrophage culture with a radical scavenger, carboxy-PTIO, and Griess reagent. *Federation of European Biochemical Societies Letters* **368**, 425-428.

Amin, J. D. and Wilsmore, A. J. (1994): Detection of *Chlamydia psittaci* (ovis) antigen in tissue sections and McCoy cells using streptavidin-biotin and the IMAGEN staining method. *British Veterinary Journal* **150**, 555-560.

Amin, J. D. and Wilsmore, A. J. (1995): Studies on the early phase of the pathogenesis of ovine enzootic abortion in the nonpregnant ewe. *British Veterinary Journal* **151**, 141-155.

Andersen, A. A. (1991): Serotyping of *Chlamydia psittaci* isolates using serovar-specific monoclonal antibodies with the microimmunofluorescence test. *Journal of Clinical Microbiology* **29**, 707-711.

Anderson, I. E., Herring, A. J., Jones, G. E., Low, J. C. and Greig, A. (1995): Development and evaluation of an indirect ELISA to detect antibodies to abortion strains of *Chlamydia psittaci* in sheep sera. *Veterinary Microbiology* **43**, 1-12.

Appleyard, W. T., Aitken, I. D. and Anderson, I. E. (1985): Attempted venereal transmission of *Chlamydia psittaci* in sheep. *Veterinary Record* **116**, 535-538.

Baker, C. C. and Cooper, B. (1983): A case of good management. *Journal of Infection* **6**, 71-3.

Bancroft, G. J. (1993): The role of natural killer cells in innate resistance to infection. *Current Opinion in Immunology* **5**, 503-10.

Banks, J., Glass, R., Spindle, A. I., and Schachter, J. (1982): *Chlamydia trachomatis* infection of mouse trophoblasts. *Infection and Immunity* **38**, 368-370.

Barteneva, N., Theodor, I., Peterson, E. M. and De La Maza, L. M. (1996): Role of neutrophils in controlling early stages of a *Chlamydia trachomatis* infection. *Infection and Immunity* **64**, 4830-4833.

Beatty, W. L., Belanger, T. A., Desai, A. A., Morrison, R. P. and Byrne, G. I. (1994a): Tryptophan depletion as a mechanism of gamma interferon-mediated chlamydial persistence. *Infection and Immunity* **62**, 3705-3711.

Beatty, W. L., Byrne, G. I. and Morrison, R. P. (1993): Morphologic and antigenic characterization of interferon-γ-mediated persistent *Chlamydia trachomatis* infection *in vitro*. *Proceedings of the National Academy of Sciences of the United States of America* **90**, 3998-4002.

Beatty, W. L., Morrison, R. P. and Byrne, G. I. (1995): Reactivation of Persistent *Chlamydia trachomatis* Infection in Cell Culture. *Infection and Immunity* **63**, 199-205.

Beatty, W. L., Morrison, R. P., and Byrne, G. I. (1994b): Immunoelectron-microscopic quantitation of differential levels of chlamydial proteins in a cell culture model of persistent *Chlamydia trachomatis* infection. *Infection and Immunity* **62**, 4059-4062.

Bianchi, A., Dosquet, C., Henry, S., Couderc, M., Ferchal, F. and Scieux, C. (1997): *Chlamydia trachomatis* growth stimulates interleukin 8 production by human monocytic U-937 cells. *Infection and Immunity* **65**, 2434-6.

Bird, P., Jones, P., Allen, D., Donachie, W., Huntley, J., McConnell, I. and Hopkins, J. (1995): Analysis of the expression and secretion of isotypes of sheep B cell immunoglobulins with a panel of isotype-specific monoclonal antibodies. *Research in Veterinary Science* **59**, 189-94.

Bobo, L., Novak, N., Mkocha, H., Vitale, S., West, S. and Quinn, T. C. (1996): Evidence for a predominant proinflammatory conjunctival cytokine response in individuals with trachoma. *Infection and Immunity* **64**, 3273-3279.

Bogdan, J. R., Newlands-Monteith, C. F., and Ellis, J. A. (1997): Nitric oxide production following in vitro stimulation of ovine pulmonary alveolar macrophages. *Veterinary Immunology And Immunopathology* **56**, 299-310.

Bollo, E., Biolatti, B., Donn, A., Turilli, C., and Wilsmore, A. J. (1992): Preparation and use of a monoclonal antibody to detect *Chlamydia psittaci* antigen in paraffin-embedded tissue sections. *Research in Veterinary Science* **53**, 393-396.

Boman, J., Soderberg, S., Forsberg, J., Birgander, L., Allard, A., Persson, K., Jidell, E., Kumlin, U., Juto, P., Waldenstrom, A. and Wadell, G. (1998): High prevalence of *Chlamydia pneumoniae* DNA in peripheral blood mononuclear cells in patients with cardiovascular disease and in middle-aged blood donors. *Journal of Infectious Diseases* **178**, 274-7.

Buendia, A., Sanchez, J., Martinez, M., Camara, P., Navarro, J., Rodolakis, A. and Salinas, J. (1998): Kinetics of infection and effects on placental cell populations in a murine model of *Chlamydia psittaci*-induced abortion. *Infection and Immunity* **66**, 2128-34.

Burrells, C. (1985): Cellular and humoral elements of the lower respiratory tract of sheep. Immunological examination of cell and fluid obtained by bronchoalveolar lavage of normal lungs. *Veterinary Immunology and Immunopathology* **10**, 225-243.

Burrells, C., Wells, P. W. and Sutherland, A. D. (1978): Reactivity of ovine lymphocytes to phytohaemagglutinin and pokeweed mitogen during pregnancy and in the immediate post-parturient period. *Clinical and Experimental Immunology* **33**, 410-5.

Buxton, D. (1994): Pregnancy: infectious ovine abortion. Recent developments in the control of chlamydial and *Toxoplasma* abortion, pp. 77-85. In Goodier, J and Spence, J. (Ed): *Science serving sheep: Volume 17. Proceedings of the Third International Sheep Veterinary Conference.*

Buxton, D., Barlow, R. M., Finlayson, J., Anderson, I.E. and Mackellar, A. (1990): Observations on the pathogenesis of *Chlamydia psittaci* infection in pregnant sheep. *Journal of Comparative Pathology* **102**, 221-237.

Buxton, D., Rae, A. G., Maley, S. W., Thomson, K. M., Livingstone, M., Jones, G. E. and Herring, A. J. (1996): Pathogenesis of *Chlamydia psittaci* infection in sheep: detection of the organism in a serial study of the lymph node. *Journal of Comparative Pathology* **114**, 221-230.

Buzoni-Gatel, D., Bernard, F., Andersen, A. and Rodolakis, A. (1990): Protective effect of polyclonal and monoclonal antibodies against abortion in mice infected by *Chlamydia psittaci*. *Vaccine* **8**, 342.

Byrne, G. I. and Faubion, C. L. (1982): Lymphokine-mediated microbistatic mechanisms restrict *Chlamydia psittaci* growth in macrophages. *Journal of Immunology* **128**, 469-74.

Byrne, G. I. and Krueger, D. A. (1983): Lymphokine-mediated Inhibition of *Chlamydia* Replication in mouse fibroblasts is neutralised by anti-Gamma Interferon immunoglobulin. *Infection and Immunity* **42**, 1152-1158.

Byrne, G. I., Lehmann, L. K. and Landry, G. J. (1986): Induction of tryptophan catabolism is the mechanism for gamma-interferon- mediated inhibition of intracellular *Chlamydia psittaci* replication in T24 cells. *Infection and Immunity* **53**, 347-351.

Byrne, G. I., Schobert, C. S., Williams, D. M. and Krueger, D. A. (1989): Characterization of gamma interferon-mediated cytotoxicity to *Chlamydia*-infected fibroblasts. *Infection and Immunity* **57**, 870-874.

Carlin, J. M. and Weller, J. B. (1995): Potentiation of interferon-mediated inhibition of *Chlamydia* infection by interleukin-1 in human macrophage cultures. *Infection and Immunity* **63**, 1870-5.

Cella, M., Scheidegger, D., Palmer-Lehmann, K., Lane, P., Lanzavecchia, A. and Alber, G. (1996): Ligation of CD40 on dendritic cells triggers production of high levels of interleukin-12 and enhances T cell stimulatory capacity: T-T help via APC activation. *Journal of Experimental Medicine* **184**, 747-52.

Cevenini, R., Donati, M., and Laplaca, M. (1988): Effects of penicillin on the synthesis of membrane-proteins of *Chlamydia trachomatis* LGV2 serotype. *FEMS Microbiology Letters* **56**, 41-46.

Cevenini, R., Donati, M., Brocchi, E., De, S., F, and La, P., M (1991): Partial characterization of an 89-kDa highly immunoreactive protein from *Chlamydia psittaci* A/22 causing ovine abortion. *FEMS Microbiology Letters* **65**, 111-115.

Chalmers, W., Simpson, J., Lee, S. and Baxendale, W. (1997): Use of a live chlamydial vaccine to prevent ovine enzootic abortion. *Veterinary Record* **141**, 63-7.

Chen, B., Stout, R. and Campbell, W. F. (1996): Nitric oxide production: a mechanism of *Chlamydia trachomatis* inhibition in interferon-gamma-treated RAW264.7 cells. *FEMS Immunology and Medical Microbiology* **14**, 109-120.

Cicco, N. A., Lindemann, A., Content, J., Vandenbussche, P., Lubbert, M., Gauss, J., Mertelsmann, R. and Herrmann, F. (1990): Inducible production of interleukin-6 by human polymorphonuclear neutrophils: role of granulocyte-macrophage colony-stimulating factor and tumor necrosis factor-alpha. *Blood* **75**, 2049-52.

Coalson, J. J., Winter, V. T., Bass, L. B., Schachter, J., Grubbs, B. G. and Williams, D. M. (1987): *Chlamydia trachomatis* pneumonia in the immune, athymic and normal BALB mouse. *British Journal of Experimental Pathology* **68**, 399-411.

Coles, A. M., Reynolds, D. J., Harper, A., Devitt, A. and Pearce, J. H. (1993): Low-nutrient induction of abnormal chlamydial development: a novel component of chlamydial pathogenesis? *FEMS Microbiology Letters* **106**, 193-200.

Corkish, J. D. and Bevan, B. J. (1991): Diagnosis of psittacosis. *Veterinary Record* **128**, 42-43.

Cotter, T. W., Meng, Q., Shen, Z. L., Zhang, Y. X., Su, H. and Caldwell, H. D. (1995): Protective efficacy of major outer membrane protein-specific immunoglobulin A (IgA) and IgG monoclonal antibodies in a murine model of *Chlamydia trachomatis* genital tract infection. *Infection and Immunity* **63**, 4704-4714.

Cotter, T., Ramsey, K., Miranpuri, G., Poulsen, C. and Byrne, G. (1997): Dissemination of *Chlamydia trachomatis* chronic genital tract infection in gamma interferon gene knockout mice.*Infection and Immunity* **65**, 2145-52.

Cox, R. L., Kuo, C-C, Grayston, J. T. and Campbell, L. A. (1988): Deoxyribonucleic acid relatedness of Chlamydia Sp. strain TWAR to *Chlamydia trachomatis* and *C. psittaci*. *International Journal of Systematic Bacteriology* **38**, 265-268.

Cvenkel, B. and Globocnik, M. (1997): Conjunctival scrapings and impression cytology in chronic conjunctivitis. Correlation with microbiology. *European Journal of Ophthalmology* **7**, 19-23.

Darville, T., Andrews C. W. J., Laffoon, K., Shymasani, W., Kishen, L. and Rank, R. (1997): Mouse strain-dependent variation in the course and outcome of chlamydial genital tract infection is associated with differences in host response. *Infection and Immunity* **65**, 3065-73.

Darville, T., Laffoon, K. K., Kishen, L. R. and Rank, R. G. (1995): Tumor necrosis factor alpha activity in genital tract secretions of guinea pigs infected with chlamydiae. *Infection and Immunity* **63**, 4675-4681.

Dawson, M., Zaghloul, A and Wilsmore A. J. (1986): Ovine enzootic abortion: experimental studies of immune responses. *Research in Veterinary Science* **40**, 59-64.

De La Maza, L. M., Peterson, E. M., Fennie, C. W. and Czarniecki, C. W. (1985): The anti-chlamydial and anti-proliferative activities of recombinant murine interferon-gamma are not dependent on tryptophan concentrations. *Journal of Immunology* **135**, 4198-4200.

De La Maza, L., Peterson, E. M., Burton, L. E., Gray, P. W., Rinderknecht, E. and Czarniecki, C. W. (1987a): The antichlamydial, antiviral, and antiproliferative activities of human gamma interferon are dependent on the integrity of the C terminus of the interferon molecule. *Infection and Immunity* **55**, 2727-2733.

De La Maza, L., Plunkett, M. J., Carlson, E. J., Peterson, E. M. and Czarniecki, C. W. (1987b): Ultrastructural analysis of the anti-chlamydial activity of recombinant murine interferon-gamma. *Experimental and Molecular Pathology* **47**, 13-25.

De Sa, C., Souriau, A., Bernard, F., Salinas, J. and Rodolakis, A. (1995): An oligomer of the major outer membrane protein of *Chlamydia psittaci* is recognized by monoclonal antibodies which protect mice from abortion. *Infection and Immunity* **63**, 4912-4916.

Del Prete, G. (1998): The concept of type-1 and type-2 helper T cells and their cytokines in humans. *International Reviews of Immunology* **16**, 427-55.

Delannoy, I., Lekeux, P. and Miossec, P. (1993): Cytokine and anti-cytokine strategies in inflammatory reaction modulation. *Veterinary Research* **24**, 449-67.

Dessus-Babus, S., Belloc, F., Bebear, C., Poutiers, F., Lacombe, F., Bebear, C. and de Barbeyrac, B. (1998): Antibiotic susceptibility testing for *Chlamydia trachomatis* using flow cytometry. *Cytometry* **31**, 37-44.

Dille, B. J., Butzen, C. C. and Birkenmeyer, L. G. (1993): Amplification of *Chlamydia trachomatis* DNA by ligase chain reaction. *Journal of Clinical Microbiology* **31**, 729-731.

Dinarello, C. A. (1998): Interleukin-1, interleukin-1 receptors and interleukin-1 receptor antagonist. *International Reviews of Immunology* **16**, 457-99.

Donn, A., Jones, G., Ruiu, A., Ladu, M., Machell, J. and Stancanelli, A. (1997): Serological diagnosis of chlamydial abortion in sheep and goats: comparison of the complement fixation test and an enzyme-linked immunosorbent assay employing solubilised proteins as antigen. *Veterinary Microbiology* **59**, 27-36.

Dubravec, D. B., Spriggs, D. R., Mannick, J. A. and Rodrick, M. L. (1990): Circulating human peripheral blood granulocytes synthesize and secrete tumor necrosis factor alpha. *Proceedings of the National Academy of Sciences of the United States of America* **87**, 6758-61.

Dutia, B. M., Entrican, G. and Nettleton, P. F. (1990): Cytopathic and non-cytopathic biotypes of border disease virus express polypeptides of different molecular weight with common antigenic determinants. *Journal of General Virology* **71**, 1227-1232.

Entrican, G. (Unpublished Results): Personal communication.

Entrican, G., Haig, D. M. and Norval, M. (1989): Identification of ovine interferons: Differential activities derived from fibroblast and lymphoid cells. *Veterinary Immunology and Immunopathology* **21**, 187-195.

Entrican, G., McInnes, C. J., Rothel, J. S. and Haig, D. M. (1992): Kinetics of ovine interferon-gamma production: detection of mRNA and characterisation of biological activity. *Veterinary Immunology and Immunopathology* **33**, 171-178.

Entrican, G., Wilkie, R., McWaters, P., Scheerlinck, J-P., Wood, P. R. and Brown, J. (1999): Cytokine release by ovine macrophages following infection with *Chlamydia psittaci*. *Clinical and Experimental Immunology* (In Press).

Evans, R. T. and Taylor-Robinson, D. (1982): Development and evaluation of an enzyme-linked immunosorbent assay (ELISA), using chlamydial group antigen, to detect antibodies to *Chlamydia trachomatis*. *Journal of Clinical Pathology* **35**, 1122-1128.

Fried, M., and Duffy, P. E. (1996): Adherence of *Plasmodium falciparum* to chondroitin sulfate A in the human placenta. *Science* **272**, 1502-4.

Fried, M., and Duffy, P. E. (1998): Maternal malaria and parasite adhesion. *Journal of Molecular Medicine* **76**, 162-71.

Fried, M., Muga, R. O., Misore, A. O., and Duffy, P. E. (1998a): Malaria elicits type 1 cytokines in the human placenta: IFN-gamma and TNF-alpha associated with pregnancy outcomes. *Journal of Immunology* **160**, 2523-30.

Fried, M., Nosten, F., Brockman, A., Brabin, B. J., and Duffy, P. E. (1998b): Maternal antibodies block malaria [letter]. *Nature* **395**, 851-2.

Fukushi, H. and Hirai, K. (1992): Proposal of *Chlamydia pecorum* sp. nov. for *Chlamydia* strains derived from ruminants. *International Journal of Systematic Bacteriology* **42**, 306-308.

Gaydos, C. A., Summersgill, J. T., Sahney, N. N., Ramirez, J. A. and Quinn, T. C. (1996): Replication of *Chlamydia pneumoniae in vitro* in human macrophages, endothelial cells, and aortic artery smooth muscle cells. *Infection and Immunity* **64**, 1614-1620.

Gerard, H., Branigan, P., Schumacher H. R, J. and Hudson, A. (1998): Synovial *Chlamydia trachomatis* in patients with reactive arthritis/Reiter's syndrome are viable but show aberrant gene expression. *Journal of Rheumatology* **25**, 734-42.

Gibbs, R. G., Carey, N. and Davies, A. H. (1998): *Chlamydia pneumoniae* and vascular disease. *British Journal of Surgery* **85**, 1191-7.

Graham, S. P., Jones, G. E., MacLean, M., Livingstone, M. and Entrican, G. (1995): Recombinant Ovine Interferon Gamma Inhibits the Multiplication of *Chlamydia psittaci* in Ovine Cells. *Journal of Comparative Pathology* **112**, 185-195.

Grayston, J. T., Kuo, C.-C., Cambell, L. A. and Wang, S. P. (1989): *Chlamydia pneumoniae* sp. nov. for *Chlamydia sp.* strain TWAR. *International Journal of Systematic Bacteriology* **39**, 88-90.

Greig, J. R. (1936): Enzootic abortion in ewes*Veterinary Record* **48**, 1225-1227.

Griffiths, P. C., Plater, J. M., Horigan, M. W., Rose, M. P. M., Venables, C. and Dawson, M. (1996): Serological diagnosis of ovine enzootic abortion by comparative inclusion immunofluorescence assay, recombinant lipopolysaccharide enzyme linked immunosorbent assay, and complement-fixation test. *Journal of Clinical Microbiology* **34**, 1512-1518.

Grusby, M. J., Johnson, R. S., Papaioannou, V. E. and Glimcher, L. H. (1991): Depletion of CD4+ T cells in major histocompatibility class II deficient mice. *Science* **253**, 1417-1420.

Gupta, S. L., Carlin, J. M., Pyati, P., Dai, W., Pfefferkorn, E. R., and Murphy, M. J. (1994): Antiparasitic and antiproliferative effects of indoleamine 2,3-dioxygenase enzyme expression in human fibroblasts. *Infection and Immunity* **62**, 2277-2284.

Gupta, V. K., McConnell, I., Dalziel, R. G. and Hopkins, J. (1996): Identification of the sheep homologue of the monocyte surface molecule-CD14. *Veterinary Immunology and Immunopathology* **51**, 89-99.

Hadley, K. M., Carrington, D., Frew, C. E., Gibson, A. A. and Hislop, W. S. (1992): Ovine chlamydiosis in an abattoir worker. *Journal of Infection* **25 Suppl 1**, 105-109.

Hansen, P. J. a. L., W. -J (1996): Immunological aspects of pregnancy: concepts and speculations using the sheep as a model. *Animal Reproduction Science* **42**.

Harpaz, R., Edelman, R., Wasserman, S. S., Levine, M. M., Davis, J. R., and Sztein, M. B. (1992): Serum cytokine profiles in experimental human malaria. Relationship to protection and disease course after challenge. *Journal of Clinical Investigation* **90**, 515-23.

Heinemann, M., Susa, M., Simnacher, U., Marre, R. and Essig, A. (1996): Growth of *Chlamydia pneumoniae* induces cytokine production and expression of CD14 in a human monocytic cell line. *Infection and Immunity* **64**, 4872-4875.

Herring, A. J., Jones, G. E., Dunbar, S. M., Nettleton, P. F., Fitzgerald, T. A., Anderson, I. E., Chapman, S. N. and Wilson, T. M. A. (1998): Recombinant vaccines against *Chlamydia psittaci*-an overview of results using bacterial expression and a new approach using a plant virus 'overcoat' system, pp 434-437. In R. S. Stephens., Byrne, G. I., Christiansen, G., Clarke, I. N., Grayston, J. T., Rank, R. G., Ridway, G. L., Saikku, P., Schachter, J. and Stamm, W. E. (Ed) Eighth International Symposium on Human Chlamydial Infections, Napa, Californian, USA

Herring, A. J., McCafferty, M. C., Jones, G. E., Dunbar, S. and Andersen, A. A. (1994): Vaccination against chlamydial abortion in sheep: Problems and progress with a recombinant vaccine, pp. 118-121. In R. S Stephens., Byrne, G. I., Christiansen, G., Clarke, I. N., Grayston, J. T., Rank, R. G., Ridway, G. L., Saikku, P., Schachter, J. and Stamm, W. E. (Ed) Eighth International Symposium on Human Chlamydial Infections, Napa, Californian, USA.

Herring, A. J., Tan, T. W., Baxter, S., Inglis, N. F. and Dunbar, S. (1989): Sequence analysis of the major outer membrane protein gene of an ovine abortion strain of *Chlamydia psittaci*. *FEMS Microbiology Letters* **53**, 153-8.

Heufler, C., Koch, F., Stanzl, U., Topar, G., Wysocka, M., Trinchieri, G., Enk, A., Steinman, R. M., Romani, N. and Schuler, G. (1996): Interleukin-12 is produced by dendritic cells and mediates T helper 1 development as well as interferon-gamma production by T helper 1 cells. *European Journal of Immunology* **26**, 659-68.

Hewinson, R. G., Griffiths, P. C., Rankin, S. E. S., Dawson, M. and Woodward, M. J. (1991): Towards a differential polymerase chain reaction test for *Chlamydia psittaci*. *Veterinary Record* **128**, 381-382.

Holland, M., Conway, D., Blanchard, T., Mahdi, O., Bailey, R., Whittle, H. and Mabey, D. (1997): Synthetic peptides based on *Chlamydia trachomatis* antigens identify cytotoxic T lymphocyte responses in subjects from a trachoma-endemic population. *Clinical and Experimental Immunology* **107**, 44-9.

Hopkins, J., Ross, A., and Dutia, B. M. (1993): Summary of workshop findings of leukocyte antigens in sheep. *Veterinary Immunology and Immunopathology* **39**, 49-59.

Hu, B., Bruce, D., Hissong, B. D. and Carlin, J. M. (1995): Interleukin-1 enhances indoleamine 2,3-dioxygenase activity by increasing specific mRNA expression in human mononuclear phagocytes. *Journal of Interferon and Cytokine Research* **15**, 617-24.

Huang, H. S., Buxton, D. and Anderson, I. E. (1990): The ovine immune response to *Chlamydia psittaci;* histopathology of the lymph node. *Journal of Comparative Pathology* **102**, 89-97.

Huebner, R. E. and Byrne, G. I. (1988): *In vivo*-activated mononuclear phagocytes and protective immunity to chlamydiae in mice. *Infection and Immunity* **56**, 1492-1499.

Hunig, T. (1985): The cell surface molecule recognized by the erythrocyte receptor of T lymphocytes. Identification and partial characterization using a monoclonal antibody. *Journal of Experimental Medicine* **162**, 890-901.

Hyde, S. and Benirschke, K. (1997): Gestational psittacosis: case report and literature review. *Modern Pathology* **10**, 602-7.

Igietseme, J. U. (1996): Molecular mechanism of T-cell control of *Chlamydia* in mice: role of nitric oxide *in vivo*. *Immunology* **88**, 1-5.

Igietseme, J. U., Magee, D. M., Williams, D. M. and Rank, R. G. (1994): Role for CD8+ T cells in antichlamydial immunity defined by *Chlamydia*- specific T-lymphocyte clones. *Infection and Immunity* **62**, 5195-5197.

Igietseme, J. U., Uriri, I. M., Kumar, S. N., Ananaba, G. A., Ojior, O. O., Momodu, I. A., Candal, D. H. and Black, C. M. (1998): Route of infection that induces a high intensity of gamma interferon-secreting T cells in the genital tract produces optimal protection against *Chlamydia trachomatis* infection in mice. *Infection and Immunity* **66**, 4030-5.

Igietseme, J., Perry, L., Ananaba, G., Uriri, I., Ojior, O., Kumar, S., and Caldwell, H. (1998): Chlamydial infection in inducible nitric oxide synthase knockout mice. *Infection and Immunity* **66**, 1282-6.

Ingalls, R. R., Rice, P. A., Qureshi, N., Takayama, K., Lin, J. S. and Golenbock, D. T. (1995): The inflammatory cytokine response to *Chlamydia trachomatis* infection is endotoxin mediated. *Infection and Immunity* **63**, 3125-3130.

Jack, R. M. and Fearon, D. T. (1988): Selective synthesis of mRNA and proteins by human peripheral blood neutrophils. *Journal of Immunology* **140**, 4286-93.

Johansson, M., Schon, K., Ward, M. and Lycke, N. (1997b): Genital tract infection with *Chlamydia trachomatis* fails to induce protective immunity in gamma interferon receptor-deficient mice despite a strong local immunoglobulin A response. *Infection and Immunity* **65**, 1032-44.

Johansson, M., Ward, M. and Lycke, N. (1997a): B-cell-deficient mice develop complete immune protection against genital tract infection with *Chlamydia trachomatis*. *Immunology* **92**, 422-8.

Johnson, F. W. A. (1975): A comparison of staining techniques for demonstrating group A *Chlamydia* in tissue culture. *Medical Laboratory Technology* **32**, 233-238.

Johnson, F. W. A., Chancerelle, L. Y. J. and Hobson, D. (1978): An improved method of demonstrating the growth of chlamydiae in tissue culture. *Medical Laboratory Sciences* **35**, 67-74.

Jones, G. E. and Anderson, I. E. (1988): *Chlamydia psittaci*: is tonsillar tissue the portal of entry in ovine enzootic abortion? *Research in Veterinary Science* **44**, 260-261.

Jones, G. E., Jones, K. A., Machell, J., Brebner, J., Anderson, I. E. and How, S. (1995): Efficacy trials with tissue-culture grown, inactivated vaccines against chlamydial abortion in sheep. *Vaccine* **13**, 715-723.

Jones, G., Low, J., Machell, J. and Armstrong, K. (1997): Comparison of five tests for the detection of antibodies against chlamydial (enzootic) abortion of ewes. *Veterinary Record* **141**, 164-8.

Jorgensen, D. (1997): Gestational psittacosis in a Montana sheep rancher. *Emerging Infectious Diseases* **3**, 191-4.

Kaltenboeck, B., Kousoulas, K. G. and Storz, J. (1993): Structures of and allelic diversity and relationships among the major outer membrane protein (ompA) genes of the four chlamydial species. *Journal of Bacteriology* **175**, 487-502.

Kamimura, S., Eguchi, K., Yonezawa, M., and Sekiba, K. (1991): Localization and developmental change of indoleamine 2,3-dioxygenase activity in the human placenta. *Acta Medica Okayama* **45**, 135-9.

Kane, C. D. and Byrne, G. I. (1998): Differential effects of gamma interferon on *Chlamydia trachomatis* growth in polarized and nonpolarized human epithelial cells in culture. *Infection and Immunity* **66**, 2349-51.

Kaufmann, S. (1993): Immunity to intracellular bacteria. *Annual Review of Immunology* **11**, 129-63.

Kaukoranta-Tolvanen, S-S. E., Teppo, A. M., Laitinen, K., Saikku, P., Linnavuori, K. and Leinonen, M. (1996): Growth of *Chlamydia pneumoniae* in cultured human peripheral-blood mononuclear-cells and induction of a cytokine response. *Microbial Pathogenesis* **21**, 215-221.

Khan, M. A., Potter, C. W. and Sharrard, R. M. (1996): A reverse transcriptase-PCR based assay for in-vitro antibiotic susceptibility testing of *Chlamydia pneumoniae*. *Journal of Antimicrobial Chemotherapy* **37**, 677-685.

Killeen, N., Sawada, S. and Littman, D. R. (1993): Regulated expression of human CD4 rescues T cell helper development in mice lacking expression of endogenous CD4. *EMBO Journal* **12**, 1547-1553.

Kimsey, P. B., Kennedy, P. C., Bushnell, R. B., Casaro, A. P., BonDurant, R. H., Oliver, M. N. and Kendrick, J. W. (1983): Studies on the pathogenesis of epizootic bovine abortion. *American Journal of Veterinary Research* **44**, 1266-1271.

Kitamura, D., Roes, J., Kuhn, R. and Rajewsky, K. (1991): A B cell-deficient mouse by targeted disruption of the membrane exon of the immunoglobulin mu chain gene. *Nature* **350**, 423-6.

Knight, S. C. and Stagg, A. J. (1993): Antigen-presenting cell types. *Current Opinion in immunology* **5**, 374.

Knight, S. C., Iqball, S., Woods, C., Stagg, A., Ward, M. E. and Tuffrey, M. (1995): A peptide of *Chlamydia trachomatis* shown to be a primary T-cell epitope *in vitro* induces cell-mediated immunity *in vivo*. *Immunology* **85**, 8-15.

Koehler, L., Bonk, C., Nettelnbreker, E., Wollenhaupt, J., Kuipers, J. G., Zeidler, H., Hudson, A. P. and Gerard, H. (1996): Persistence of *Chlamydia trachomatis* (*ct*) in human monocytes in a nonreplicative but viable state. *Arthritis and Rheumatism* **39**, 941.

Koehler, L., Nettelnbreker, E., Hudson, A. P., Ott, N., Gerard, H. C., Branigan, P. J., Schumacher, H. R., Drommer, W. and Zeidler, H. (1997): Ultrastructural and molecular analyses of the persistence of *Chlamydia trachomatis* (serovar K) in human monocytes. *Microbial Pathogenesis* **22**, 133-142.

Krishnan, L., Guilbert, L. J., Wegmann, T. G., Belosevic, M., and Mosmann, T. R. (1996): T helper 1 response against Leishmania major in pregnant C57BL/6 mice increases implantation failure and fetal resorptions. Correlation with increased IFN-gamma and TNF and reduced IL-10 production by placental cells. *Journal of Immunology* **156**, 653-62.

Krishnan, L., Menu, E., Chaouat, G., Talwar, G. P., and Raghupathy, R. (1991): In vitro and in vivo immunosuppressive effects of supernatants from human choriocarcinoma cell lines. *Cellular Immunology* **138**, 313-25.

Krishnan, L., Sad, S., and Raghupathy, R. (1995): Characterization of an immunosuppressive factor secreted by a human trophoblast-derived choriocarcinoma cell line. *Cellular Immunology* **162** , 295-308.

Linklater, K. A. and Dyson, D. A. (1979): Field studies on enzootic abortion of ewes in south east Scotland. *Veterinary Record* **105**, 387-389.

Longbottom, D., Findlay, J., Vretou, E. and Dunbar, S. (1998a): Immunoelectron microscopic localisation of the OMP90 family on the outer membrane surface of *Chlamydia psittaci*. *FEMS Microbiology Letters* **164**, 111-7.

Longbottom, D., Rusell, M., Jones, G. E., Lainson, F. A. and Herring, A. J. (1996): Identification of a multigene family coding for the 90 kda proteins of the ovine abortion subtype of *Chlamydia psittaci*. *FEMS Microbiology Letters* **142**, 277-281.

Longbottom, D., Russell, M., Dunbar, S., Jones, G. and Herring, A. (1998b): Molecular cloning and characterization of the genes coding for the highly immunogenic cluster of 90-kilodalton envelope proteins from the *Chlamydia psittaci* subtype that causes abortion in sheep. *Infection and Immunity* **66**, 1317-24.

Lord, P. C., Wilmoth, L. M., Mizel, S. B. and McCall, C. E. (1991): Expression of interleukin-1 alpha and beta genes by human blood polymorphonuclear leukocytes. *Journal of Clinical Investigation* **87**, 1312-21.

Lore, K., Sonnerborg, A., Spetz, A. L., Andersson, U. and Andersson, J. (1998): Immunocytochemical detection of cytokines and chemokines in Langerhans cells and *in vitro* derived dendritic cells. *Journal of Immunological Methods* **214**, 97-111.

Macatonia, S. E., Hosken, N. A., Litton, M., Vieira, P., Hsieh, C. S., Culpepper, J. A., Wysocka, M., Trinchieri, G., Murphy, K. M. and OqGarra, A. (1995): Dendritic cells produce IL-12 and direct the development of Th1 cells from naive CD4+ T cells. *Journal of Immunology* **154**, 5071-9.

Mackay, C. R., Hein, W. R. and Brown, M. H. (1988): Unusual expression of CD2 in sheep: Implication for T-cell interaction. *European Journal of Immunology* **18**, 1681-1688.

Maddox, J. F., Mackay, C. R. and Brandon, M. R. (1985): The sheep analogue of leukocyte common antigen (LCA). *Immunology* **55**, 347-353.

Magee, D. M., Igietseme, J. U., Smith, J. G., Bleicker, C. A., Grubbs, B. G., Schachter, J., Rank, R. G. and Williams, D. M. (1993): *Chlamydia trachomatis* pneumonia in the severe combined immunodeficiency (SCID) mouse. *Regional Immunology* **5**, 305-311.

Magee, D. M., Smith, J. G., Bleicker, C. A., Carter, C. J., Bonewald, L. F., Schachter, J. and Williams, D. M. (1992): *Chlamydia trachomatis* pneumonia induces *in vivo* production of interleukin-1 and -6. *Infection and Immunity* **60**, 1217-1220.

Magee, D. M., Williams, D. M., Smith, J. G., Bleicker, C. A., Grubbs, B. G., Schachter, J. and Rank, R. G. (1995): Role of CD8 T cells in primary *Chlamydia* infection. *Infection and Immunity* **63**, 516-521.

Magee, D. M., Williams, D. M., Wing, E. J., Bleicker, C. A. and Schachter, J. (1991): Production of colony-stimulating factors during pneumonia caused by *Chlamydia trachomatis*. *Infection and Immunity* **59**, 2370-2375.

Majeed, M., Ernst, J. D., Magnusson, K. E., Kihlstrom, E. a. and Stendahl, O. (1994): Selective translocation of annexins during intracellular redistribution of *Chlamydia trachomatis* in HeLa and McCoy cells. *Infection and Immunity* **62**, 126-134.

Majeed, M., Gustafsson, M., Kihlstrom, E. and Stendahl, O. (1993): Roles of Ca2+ and F-actin in intracellular aggregation of *Chlamydia trachomatis* in eukaryotic cells. *Infection and Immunity* **61**, 1406-1414.

Manor, E. and Sarov, I. (1986): Fate of *Chlamydia trachomatis* in human monocytes and monocyte-derived macrophages. *Infection and Immunity* **54**, 90-95.

Manor, E., Schmitz, E. and Sarov, I. (1993): TNF and PGE(2) in human monocyte-derived macrophages infected with *Chlamydia trachomatis*. *Mediators of Inflammation* **2**, 367-371.

Markey, B. K., McNulty, M. S. and Todd, D. (1993): Comparison of serological tests for the diagnosis of *Chlamydia psittaci* infection of sheep. *Veterinary Microbiology* **36**, 233-252.

Matsumoto, A. and Manire, G. P.(1970): Electron microscopic observations on the effects of penicillin on the morphology of *Chlamydia psittaci*. *Journal of Bacteriology* **101**, 278-285.

Mayer, J., Woods, M. L., Vavrin, Z. and Hibbs, J. B. (1993): Gamma-interferon-induced nitric-oxide production reduces *Chlamydia trachomatis* infectivity in McCoy cells. *Infection and Immunity* **61**, 491-497.

McCafferty, M. C. (1992): Ovine cell mediated immunity to *Chlamydia psittaci*, pp. 53-54: *The Department of Pathology, Faculty of Medicine*, The University of Edinburgh, Edinburgh.

McCafferty, M. C. (1994): The development of proliferative responses of ovine peripheral blood mononuclear cells to *Chlamydia psittaci* during pregnancy. *Veterinary Immunology and Immunopathology* **41**, 173-180.

McCafferty, M. C., Herring, A. J., Andersen, A. A. and Jones, G. E. (1995): Electrophoretic analysis of the major outer membrane protein of *Chlamydia psittaci* reveals multimers which are recognized by protective monoclonal antibodies. *Infection and Immunity* **63**, 2387-2389.

McCafferty, M. C., Maley, S. W., Entrican, G. and Buxton, D. (1994): The importance of interferon-gamma in an early infection of *Chlamydia psittaci* in mice. *Immunology* **81**, 631-636.

McClarty, G. (1994): Chlamydiae and the biochemistry of intracellular parasitism. *Trends In Microbiology* **2**, 157-163.

McClenaghan, M., Herring, A. J. and Aitken, I. D. (1984): Comparison of *Chlamydia psittaci* isolates by DNA restriction endonuclease analysis. *Infection and Immunity* **45**, 384-389.

McEwen, A. D, Littlejohn, A. I. and Foggie, A (1951a): Enzootic abortion in ewes: some aspects of infection and resistance. *Veterinary Record* **63**, 489-492.

McEwen, A. D., Dow, J. B. and Anderson, R. D. (1955): Enzootic abortion in ewes. An adjuvant vaccine prepared from eggs. *Veterinary Record* **67**, 393-394.

McEwen, A. D., Stamp, J. T. and Littlejohn, A. I. (1951b): Enzootic abortion in ewes II. Immunisation and infection experiments. *Veterinary Record* **63**, , 197.

McInnes, C. J., Logan, M., Redmond, J., Entrican, G. and Baird, G. D. (1990): The molecular cloning of the ovine gamma-interferon cDNA using the polymerase chain reaction. *Nucleic Acids Research* **18**, 4012.

McKercher, D. G., Wada, E. M., Ault, S. K. and Theis, J. H. (1980): Preliminary studies on transmission of *Chlamydia* to cattle by ticks (Ornithodoros coriaceus). *American Journal of Veterinary Research* **41**, 922-924.

Megran, D. W., Stiver, H. G. and Bowie, W. R. (1985): Complement activation and stimulation of chemotaxis by *Chlamydia trachomatis*. *Infection and Immunity* **49**, 670-673.

Mehta, S. J., Miller, R. D., Ramirez, J. A. and Summersgill, J. T. (1998): Inhibition of *Chlamydia pneumoniae* replication in HEp-2 cells by interferon-gamma: role of tryptophan catabolism. *Journal of Infectious Diseases* **177**, 1326-1331.

Moazed, T. C., Kuo, C. C., Grayston, J. T. and Campbell, L. A. (1998): Evidence of systemic dissemination of *Chlamydia pneumoniae* via macrophages in the mouse. *Journal of Infectious Diseases* **177**, 1322-1325.

Mohammed, N. R. and Hillary, I. B. (1984): Detection of *Chlamydia trachomatis* inclusions in McCoy and HeLa-229 cells: an alternative staining technique using toluidine blue. *Journal of Clinical Pathology* **37**, 682-5.

Mohanty, S., Satpathy, G., Mittal, S. and Panda, S. K. (1996): Development of an antigen capture enzyme immuno assay using genus specific monoclonal antibodies for detection of *Chlamydia* in clinical specimens. *Indian Journal of Medical Research* **103**, 77-83.

Molestina, R., Dean, D., Miller, R., Ramirez, J. and Summersgill, J. (1998): Characterization of a strain of *Chlamydia pneumoniae* isolated from a coronary atheroma by analysis of the omp1 gene and biological activity in human endothelial cells. *Infection and Immunity* **66**, 1370-6.

Monno, R., Vena, G., Cafforio, P. and Milone, E. (1991): Polymorphonuclear cell-function impairment in patients with *Chlamydia trachomatis* urogenital infections. *Acta Microbiologica Hungarica* **38**, 75-79.

Moore, F. D. J., Jack, R. M. and Antin, J. H. (1992): Peripheral blood neutrophils in chronically neutropenic patients respond to granulocyte-macrophage colony-stimulating factor with a specific increase in CR1 expression and CR1 transcription. *Blood* **79**, 1667-71.

Morrison, R. P., Feilzer, K. and Tumas, D. B. (1995): Gene knockout mice establish a primary protective role for major histocompatibility complex class II-restricted responses in *Chlamydia trachomatis* genital tract infection. *Infection and Immunity* **63**, 4661-4668.

Moulder, J. W. (1991): Interaction of chlamydiae and host cells *in vitro*. *Microbiological Reviews* **55**, 143-190.

Moulder, J. W., Levy, N. J. and Schulman, L. P. (1980): Persistent infection of mouse fibroblasts (L cells) with *Chlamydia psittaci*: evidence for a cryptic chlamydial form. *Infection and Immunity* **30**, 874-883.

Munn, D. H., Zhou, M., Attwood, J. T., Bondarev, I., Conway, S. J., Marshall, B., Brown, C., and Mellor, A. L. (1998): Prevention of allogeneic fetal rejection by tryptophan catabolism. *Science* **281**, 1191-3.

Murray, H. W. and Teitelbaum, R. F. (1992): L-arginine-dependent reactive nitrogen intermediates and the antimicrobial effect of activated human mononuclear phagocytes. *Journal of Infectious diseases* **165**, 513-517.

Murray, H. W., Szuro-Sudol, A., Wellner, D., Oca, M. J., Granger,. M., Libby, D. M., Rothermel, C. D. and Rubin, B. Y. (1989): Role of tryptophan degradation in respiratory burst-independent antimicrobial activity of gamma interferon-stimulated human macrophages. *Infection and Immunity* **57**, 845-849.

Naessens, J. and Howard, C. J. (1991): Monoclonal antibodies reacting with bovine B cells (BoWC3, BoWC4, BoWC5). *Veterinary Immunology and Immunopathology* **27**, 77-85.

Nettleton, P. F. and Entrican, G. (1995): Ruminant Pestiviruses. *British Veterinary Journal* **151**, 615-641.

Neuman, E., Huleatt, J. W. and Jack, R. M. (1990): Granulocyte-macrophage colony-stimulating factor increases synthesis and expression of CR1 and CR3 by human peripheral blood neutrophils. *Journal of Immunology* **145**, 3325-32.

Norval, M., Head, K. W., Else, R. W., Hart, H. and Neill, W. A (1981): Growth in culture of adenocarcinoma cells from the small intestine of sheep. *British Journal of Experimental Pathology* **62**, 270-282.

Ojcius, D. M., Souque, P., Perfettini, J. L. and Dautry-Varsat, A. (1998a): Apoptosis of epithelial cells and macrophages due to infection with the obligate intracellular pathogen *Chlamydia psittaci*. *Journal of Immunology* **161**, 4220-6.

Ojcius, D., Bravo de Alba, Y., Kanellopoulos, J., Hawkins, R., Kelly, K., Rank, R. and Dautry-Varsat, A. (1998b): Internalization of *Chlamydia* by dendritic cells and stimulation of *Chlamydia*-specific T cells. *Journal of Immunology* **160**, 1297-303.

Ojcius, D., Hellio, R. and Dautry-Varsat, A. (1997): Distribution of endosomal, lysosomal, and major histocompatibility complex markers in a monocytic cell line infected with *Chlamydia psittaci*. *Infection and Immunity* **65**, 2437-42.

Page, L. A. (1968): Proposal for the recognition of two species of in the genus *Chlamydia*. *International Journal of Systematic Bacteriology* **18**, 51-66.

Paguirigan, A. M., Byrne, G. I., Becht, S. and Carlin, J. M. (1994): Cytokine-mediated indoleamine 2,3-dioxygenase induction in response to *Chlamydia* infection in human macrophage cultures. *Infection and Immunity* **62**, 1131-1136.

Pal, S., Theodor, I., Peterson, E. and De La Maza, L. (1997): Monoclonal immunoglobulin A antibody to the major outer membrane protein of the *Chlamydia trachomatis* mouse pneumonitis biovar protects mice against a chlamydial genital challenge. *Vaccine* **15**, 575-82.

Palmer, H. M., Gilroy, C. B., Thomas, B. J., Hay, P. E., Gilchrist, C. and Taylor-Robinson, D. (1991): Detection of *Chlamydia trachomatis* by the polymerase chain reaction in swabs and urine from men with non-gonococcal urethritis. *Journal of Clinical Pathology* **44**, 321-325.

Papp, J. and Shewen, P. (1997): *Chlamydia psittaci* infection in sheep: a paradigm for human reproductive tract infection. *Journal of Reproductive Immunology* **34**, 185-202.

Papp, J. R. and Shewen, P. E. (1996a): Pregnancy failure following vaginal infection of sheep with *Chlamydia psittaci* prior to breeding. *Infection and Immunity* **64**, 1116-1125.

Papp, J. R. and Shewen, P. E. (1996b): Localization of chronic *Chlamydia psittaci* infection in the reproductive tract of sheep.*Journal of Infectious Diseases* **174**, 1296-1302.

Papp, J. R., Shewen, P. E. and Gartley, C. J. (1994): Abortion and subsequent excretion of chlamydiae from the reproductive tract of sheep during estrus. *Infection and Immunity* **62**, 3786-3792.

Papp, J., Shewen, P., Thorn, C. and Andersen, A. (1998): Immunocytologic detection of *Chlamydia psittaci* from cervical and vaginal samples of chronically infected ewes. *Canadian Journal of Veterinary Research* **62**, 72-4.

Perez-Martinez, J. A. and Storz, J. (1985): Persistent infection of L cells with an ovine abortion strain of *Chlamydia psittaci*. *Infection and Immunity* **50**, 453-458.

Perry, L. L., Feilzer, K. and Caldwell, H. D. (1997): Immunity to *Chlamydia trachomatis* is mediated by T helper 1 cells through IFN-gamma-dependent and -independent pathways. *Journal of Immunology* **158**, 3344-3352.

Perry, L., Feilzer, K., and Caldwell, H. (1998): Neither interleukin-6 nor inducible nitric oxide synthase is required for clearance of *Chlamydia trachomatis* from the murine genital tract epithelium. *Infection and Immunity* **66**, 1265-9.

Peterson, E., Cheng, X., Motin, V. and De La Maza, L. (1997): Effect of immunoglobulin G isotype on the infectivity of *Chlamydia trachomatis* in a mouse model of intravaginal infection. *Infection and Immunity* **65**, 2693-9.

Piccinni, M. P., Giudizi, M. G., Biagiotti, R., Beloni, L., Giannarini, L., Sampognaro, S., Parronchi, P., Manetti, R., Annunziato, F., Livi, C., and et, a. (1995): Progesterone favors the development of human T helper cells producing Th2-type cytokines and promotes both IL-4 production and membrane CD30 expression in established Th1 cell clones. *Journal of Immunology* **155**, 128-33.

Pitche, P., Plinga, A. and Tchangai-Walla, K. (1998): [Lymphogranuloma venereum]. *Sante* **8**, 239-44.

Pizzichini, M., Pizzichini, E., Efthimiadis, A., Clelland, L., Mahony, J., Dolovich, J. and Hargreave, F. (1997): Markers of inflammation in induced sputum in acute bronchitis caused by *Chlamydia pneumoniae*. *Thorax* **52**, 929-31; discussion 926-7.

Pudjiatmoko, Fukushi, H., Ochiai, Y., Yamaguchi, T. and Hirai, K. (1998): *In vitro* susceptibility of *Chlamydia pecorum* to macrolides, tetracyclines, quinolones and beta-lactam. *Microbiology and Immunology* **42**, 61-3.

Pudjiatmoko, H. F., Ochiai, Y., Yamaguchi, T. and Hirai, K. (1997): Phylogenetic analysis of the genus *Chlamydia* based on 16S rRNA gene sequences. *International Journal of Systematic Bacteriology* **47**, 425-431.

Pugh, S. F., Slack, R. C. B., Caul, E. O., Paul, I. D., Appleton, P. N. and Gatley, S. (1985): Enzyme amplified immunoassay - a novel technique applied to direct detection of *Chlamydia trachomatis* in clinical specimens. *Journal of Clinical Pathology* **38**, 1139-1141.

Raghupathy, R. (1997): Th1-type immunity in incompatible with successful pregnancy. *Immunology Today* **18**, 478-482.

Rahemtulla, A., Fung-Leung, W. P., Schilham, M. W., Kundig, T. M., Sambhara, S. R., Narendran, A., Arabian, A., Wakeham, A., Paige, C. J., Zinkernagel, R. M. and et, a. (1991): Normal development and function of CD8+ cells but markedly decreased helper cell activity in mice lacking CD4. *Nature* **353**, 180-4.

Ramsey, K. H., Miranpuri, G. S., Poulsen, C. E., Marthakis, N. B., Braune, L. M., and Byrne, G. I. (1998): Inducible nitric oxide synthase does not affect resolution of murine chlamydial genital tract infections or eradication of chlamydiae in primary murine cell culture. *Infection and Immunity* **66**, 835-8.

Ramsey, K. H., Soderberg, L. S. F. and Rank, R. G. (1988): Resolution of chlamydial genital infection in B-cell-deficient mice and immunity to reinfection. *Infection and Immunity* **56**, 1320.

Ramsey, K., Miranpuri, G., Poulsen, C., Marthakis, N., Braune, L. and Byrne, G. (1998): Inducible nitric oxide synthase does not affect resolution of murine chlamydial genital tract infections or eradication of chlamydiae in primary murine cell culture. *Infection and Immunity* **66**, 835-8.

Rank, R. G., Ramsey, K. H., Pack, E. A. and Williams, D. M. (1992): Effect of gamma interferon on resolution of murine chlamydial genital infection. *Infection and Immunity* **60**, 4427-4429.

Rapoza, P. A., Tahija, S. G., Carlin, J. P., Miller, S. L., Padilla, M. L. and Byrne, G. I. (1991): Effect of interferon on a primary conjunctival epithelial cell model of trachoma. *Investigative Ophthalmology and Visual Science* **32**, 2919-2923.

Rasband, W. S. and Bright, D. S. (1995): NIH Image: A public domain image processing program for the Macintosh. *Microbeam Analysis* **4**, 137 - 149.

Raschke, W. C., Baird, S., Ralph, P. and Nakoinz, I. (1978): Functional macrophage cell lines transformed by Abelson leukemia virus. *Cell* **15**, 261-7.

Rasmussen, S. J. (1998): Chlamydial immunology. *Current Opinion in Infectious Disease* **11**, 37-41.

Rasmussen, S. J., Douglas, F. P. and Timms, P. (1992): PCR detection and differentiation of *Chlamydia pneumoniae, Chlamydia psittaci* and *Chlamydia trachomatis*. *Molecular and Cellular Probes* **6**, 389-394.

Rasmussen, S. J., Eckmann, L., Quayle, A. J., Shen, L., Zhang, Y. X. Anderson, D. J., Fierer, J., Stephens, R. S. and Kagnoff, M. F. (1997): Secretion of proinflammatory cytokines by epithelial cells in response to *Chlamydia* infection suggests a central role for epithelial cells in Chlamydial pathogenesis. *Journal of Clinical Investigation* **99**, 77-87.

Rasmussen, S. J., Timms, P., Beatty, P. R., and Stephens, R. S. (1996): Cytotoxic-T-lymphocyte-mediated cytolysis of L cells persistently infected with *Chlamydia spp. Infection and Immunity* **64**, 1944-1949.

Reacher, M. H., Pe'er, J., Rapoza, P. A., Whittum-Hudson, J. A. and Taylor, H. R. (1991): T cells and trachoma. Their role in cicatricial disease. *Ophthalmology* **98**, 334-341.

Register, K. B., Davis, C. H., Wyrick, P. B., Shafer, W. M. and Spitznagel, J. K. (1987): Nonoxidative antimicrobial effects of human polymorphonuclear leukocyte granule proteins on *Chlamydia spp. in vitro. Infection and Immunity* **55**, 2420-2427.

Register, K. B., Morgan, P. A. and Wyrick, P. B. (1986): Interaction between *Chlamydia spp.* and human polymorphonuclear leukocytes *in vitro. Infection and Immunity* **52**, 664-670.

Roblin, P. and Hammerschlag, M. (1998): *In vitro* activity of a new ketolide antibiotic, HMR 3647, against *Chlamydia pneumoniae. Antimicrobial Agents Chemotherapy* **42**, 1515-6.

Rodolakis, A. and Bernard, F. (1984): Vaccination with temperature-sensitive mutant of *Chlamydia psittaci* against enzootic abortion of ewes. *Veterinary Record* **114**, 193-194.

Rodolakis, A. and Souriau, A. (1979): Clinical evaluation of a commercial vaccine against chlamydial abortion of ewes. *Annales de Recherches Veterinaires* **10**, 41-48.

Rodolakis, A. and Souriau, A. (1983): Response of ewes to temperature-sensitive mutants of *Chlamydia psittaci* (var ovis) obtained by NTG mutagenesis. *Annales de Recherches Veterinaires* **14**, 155-161.

Rodolakis, A. and Souriau, A. (1986): Response of goats to vaccination with temperature-sensitive mutants of *Chlamydia psittaci* obtained by nitrosoguanidine mutagenesis. *American Journal of Veterinary Research* **47**, 2627-2631.

Rodolakis, A. and Souriau, A. (1989): Variations in virulence of strains of *Chlamydia psittaci* for pregnant ewes. *Veterinary Record* **125**, 87-90.

Rodolakis, A., Bernard, F., Souriau, A., Layachi, K. and Buzoni-Gatel, D. (1989): Relationship between virulence of *Chlamydia psittaci* and establishment of persistent infection of McCoy cells. *Veterinary Microbiology* **19**, 65-73.

Rodolakis, A., Gestin, L. and Bertin, A. (1981): Methode de controle des vaccins contre la chlamydiose abortive ovine utilisant la souris gestante. *Annales de Recherches Veterinaires* **12**, 371-377.

Rodolakis, A., Salinas, J. and Papp, J. (1998): Recent advances on ovine chlamydial abortion. *Veterinary Research* **29**, 275-288.

Rodolakis, G. (1983): *In vitro* and *in vivo* properties of chemically induced temperature-sensitive mutants of *Chlamydia psittaci* var. ovis: screening in a murine model. *Infection and Immunity* **42**, 525-530.

Romani, L., Bistoni, F. and Puccetti, P. (1997): Initiation of T-helper cell immunity to *Candida albicans* by IL-12: the role of neutrophils. *Chemical Immunology* **68**, 110-35.

Rosenkranz, H. S., Gutter, B., and Becker, Y. (1973): Studies on the developmental cycle of *Chlamydia trachomatis*: selective inhibition by hydroxyurea. *Journal of Bacteriology* **115**, 682-90.

Rothermel, C. D., Rubin, B. Y. and Murray, H. W. (1983): Gamma-interferon is the factor in lymphokine that activates human macrophages to inhibit intracellular *Chlamydia psittaci* replication. *Journal of Immunology* **131**, 2542-2544.

Rothermel, C. D., Rubin, B. Y., Jaffe, E. A. and Murray, H. W. (1986): Oxygen-independent inhibition of intracellular *Chlamydia psittaci* growth by human monocytes and interferon-gamma-activated macrophages. *Journal of Immunology* **137**, 689-692.

Russ, J. C. (1998): *The Image Processing Hand Book*. CRC Press.

Salti-Montesanto, V., Tsoli, E., Papavassiliou, P., Psarrou, E., Markey, B., Jones, G. and Vretou, E. (1997): Diagnosis of ovine enzootic abortion, using a competitive ELISA based on monoclonal antibodies against variable segments 1 and 2 of the major outer membrane protein of *Chlamydia psittaci* serotype 1. *American Journal of Veterinary Research* **58**, 228-35.

Sanghi, A., Morgan-Capner, P., Hesketh, L. and Elstein, M. (1997): Zoonotic and viral infection in fetal loss after 12 weeks. *British Journal of Obstetrics and Gynaecology* **104**, 942-5.

Sardinia, L. M., Segal, E., and Ganem, D. (1988): Developmental regulation of the cysteine-rich outer-membrane proteins of murine *Chlamydia trachomatis*. *Journal of General Microbiology* **134**, 997-1004.

Shemer-Avni, Y., Wallach, D. and Sarov, I. (1988): Inhibition of *Chlamydia trachomatis* growth by recombinant tumor necrosis factor. *Infection and Immunity* **56**, 2503-2506.

Shemer-Avni, Y., Wallach, D. and Sarov, I. (1989): Reversion of the antichlamydial effect of tumor necrosis factor by tryptophan and antibodies to beta interferon. *Infection and Immunity* **57**, 3484-3490.

Simon, A. K., Seipelt, E., Wu, P., Wenzel, B., Braun, J. and Sieper, J. (1993): Analysis of cytokine profiles in synovial T cell clones from chlamydial reactive arthritis patients: predominance of the Th1 subset. *Clinical and Experimental Immunology* **94**, 122-126.

Smith, J. A. (1994): Neutrophils, host defence, and inflammation: a double-edged sword. *Journal of Leukocyte Biology* **56**, 672-86.

Smith, N. C. (1996): An immunological hypothesis to explain the enhanced susceptibility to Malaria during pregnancy. *Parasitology Today* **12**, 4-6.

Souriau, A. and Rodolakis, A. (1986): Rapid detection of *Chlamydia psittaci* in vaginal swabs of aborted ewes and goats by enzyme linked immunosorbent assay (ELISA). *Veterinary Microbiology* **11**, 251-259.

Souriau, A., Bosseray, N., Rodolakis, A., Lantier, F. and Plommet, M. (1988): Anti-chlamydial immunity in ewes conferred by vaccination with a combination of three live *Chlamydia*, *Brucella* and *Salmonella* vaccines. *Veterinary Record* **123**, 12, 29-32.

Stagg, A. (1998): Vaccines against *Chlamydia*: approaches and progress. *Molecular Medicine Today* **4**, 166-73.

Stagg, A. J., Elsley, W. A., Pickett, M. A., Ward, M. E. and Knight, S. C. (1993a): Primary human T-cell responses to the major outer membrane protein of *Chlamydia trachomatis*. *Immunology* **79**, 1-9.

Stagg, A. J., Stackpoole, A. Elsley, W. J. and Knight, S. C. (1993b): Acquisition of chlamydial antigens by dendritic cells and monocytes, pp. 581. In Kamperdijk *et al* (Ed.): *Fundamental and Clinical Immunology*, Plenum Press, New York.

Stagg, A., Tuffrey, M., Woods, C., Wunderink, E. and Knight, S. (1998): Protection against ascending infection of the genital tract by *Chlamydia trachomatis* is associated with recruitment of major histocompatibility complex class II antigen-presenting cells into uterine tissue.*Infection and Immunity* **66**, 3535-44.

Stamp, J. T., McEwen, A. D., Watt, J. A. A. and Nisbet, D. I. (1950): Enzootic abortion of ewes: transmission of the disease. *Veterinary Record* **62**, 251-254.

Starnbach, M. N., Bevan, M. J. and Lampe, M. F. (1994): Protective cytotoxic T lymphocytes are induced during murine infection with *Chlamydia trachomatis*. *Journal of Immunology* **153**, 5183-5189.

Steketee, R. W., Wirima, J. J., Slutsker, L., Heymann, D. L., and Breman, J. G. (1996): The problem of malaria and malaria control in pregnancy in sub-Saharan Africa. *American Journal of Tropical Medicine And Hygiene* **55**, 2-7.

Stephens, R. S., Kalman, S., Lammel, C., Fan, J., Marathe, R., Aravind, L., Mitchell, W., Olinger, L., Tatusov, R. L., Zhao, Q., Koonin, E. V., and Davis, R. W. (1998): Genome sequence of an obligate intracellular pathogen of humans: *Chlamydia trachomatis*. *Science* **282**, 754-9.

Sternberg, S. R. (1983): Biomedical Image Processing. *IEEE Computer* **January**, 22 - 34.

Sting, R. and Hafez, H. M. (1992): Purification of *Chlamydia psittaci* antigen by affinity chromatography on polymyxin B agarose for use in the enzyme-linked immunosorbent assay (ELISA). *Zentralblatt fur Bakteriologie* **277**, 436-445.

Su, H. and Caldwell, H. (1998): Sulfated polysaccharides and a synthetic sulfated polymer are potent inhibitors of *Chlamydia trachomatis* infectivity *in vitro* but lack protective efficacy in an *in vivo* murine model of chlamydial genital tract infection. *Infection and Immunity* **66**, 1258-60.

Su, H. and Caldwell, H. D. (1995): Kinetics of chlamydial antigen processing and presentation to T cells by paraformaldehyde-fixed murine bone marrow-derived macrophages. *Infection and Immunity* **63**, 946-953.

Su, H., Feilzer, K., Caldwell, H. and Morrison, R. (1997): *Chlamydia trachomatis* genital tract infection of antibody-deficient gene knockout mice. *Infection and Immunity* **65**, 1993-9.

Su, H., Spangrude, G. J. and Caldwell, H. D. (1991): Expression of Fc gamma RIII on HeLa 229 cells: possible effect on *in vitro* neutralization of *Chlamydia trachomatis*. *Infection and Immunity* **59**, 3811-3814.

Summersgill, J. T., Sahney, N. N., Gaydos, C. A., Quinn, T. C. and Ramirez, J. A. (1995): Inhibition of *Chlamydia pneumoniae* growth in HEp-2 cells pretreated with gamma interferon and tumor necrosis factor alpha. *Infection and Immunity* **63**, 2801-2803.

Szekeres-Bartho, J., and Wegmann, T. G. (1996): A progesterone-dependent immunomodulatory protein alters the Th1/Th2 balance. *Journal of Reproductive Immunology* **31**, 81-95.

Szekeres-Bartho, J., Autran, B., Debre, P., Andreu, G., Denver, L., and Chaouat, G. (1989): Immunoregulatory effects of a suppressor factor from healthy pregnant women's lymphocytes after progesterone induction. *Cellular Immunology* **122**, 281-94.

Szekeres-Bartho, J., Faust, Z., and Varga, P. (1995): The expression of a progesterone-induced immunomodulatory protein in pregnancy lymphocytes. *American Journal of Reproductive Immunology* **34**, 342-348.

Takahashi, T., Masuda, M., Tsuruno, T., Mori, Y., Takashima, I., Hiramune, T. and Kikuchi, N. (1997): Phylogenetic analyses of *Chlamydia psittaci* strains from birds based on 16S rRNA gene sequence. *Journal of Clinical Microbiology* **35**, 2908-14.

Tan, T. W., Herring, A. J., Anderson, I. E. and Jones, G. E. (1990): Protection of sheep against *Chlamydia psittaci* infection with a subcellular vaccine containing the major outer membrane protein. *Infection and Immunity* **58**, 3101-8.

Taylor-Robinson, D. (1997): Evaluation and comparison of tests to diagnose *Chlamydia trachomatis* genital infections. *Human Reproduction* **12**, 113-20.

Thomas, S. M., Garrity, L. F., Brandt, C. R., Schobert, C. S., Feng, G. S., Taylor, M. W., Carlin, J. M. and Byrne, G. I. (1993): IFN-gamma-mediated antimicrobial response. Indoleamine 2,3-dioxygenase- deficient mutant host cells no longer inhibit intracellular *Chlamydia spp.* or *Toxoplasma growth. Journal of Immunology* **150**, 5529-5534.

Tseng, C-T. K. and Rank, R. G. (1998): The Contribution of NK cells to the regulation of Chlamydial genital infection, pp. 470-473. In R. S. Stephens, Byrne, G.I., Christiansen, G., Clarke, I. n., Grayston, J.T., Rank, R. G., Ridway, G. L., Saikku, P., Schachter, J. and Stamm, W. E. (Ed.): *Chlamydial Infections*, Proceedings of the Ninth International Symposium on Human Chlamydial Infection, Napa, Californian, USA.

Van Ooij, C., Apodaca, G. and Engel, J. (1997): Characterization of the *Chlamydia trachomatis* vacuole and its interaction with the host endocytic pathway in HeLa cells. *Infection and Immunity* **65**, 758-66.

Van Westreenen, M., Pronk, A., Diepersloot, R., de Groot, P. and Leguit, P. (1998): *Chlamydia trachomatis* infection of human mesothelial cells alters proinflammatory, procoagulant, and fibrinolytic responses. *Infection and Immunity* **66**, 2352-5.

Vanrompay, D., Ducatelle, R. and Haesebrouck, F. (1995): *Chlamydia psittaci* infections: a review with emphasis on avian chlamydiosis. *Veterinary Microbiology* **45**, 93-119.

Verhasselt, V., Buelens, C., Willems, F., De Groote, D., Haeffner-Cavaillon, N. and Goldman, M. (1997): Bacterial lipopolysaccharide stimulates the production of cytokines and the expression of costimulatory molecules by human peripheral blood dendritic cells: evidence for a soluble CD14-dependent pathway. *Journal of Immunology* **158**, 2919-25.

Veterinary Laboratories Agency., Welsh Office Agriculture Department., Ministry of Agriculture, Fisheries and Food and Scottish Office Agriculture and Fisheries Department. (1997): Veterinary Investigation Surveillance Report 1989-1996, UK Government.

Vischer, N. O. E., Huls, P. G. and Woldringh, C. L. (1994): Object-Image: An interactive image analysis program using structured point collection. *Binary* **6**, 1994 BioLine, pp 160.

Vivino, M. (1992): Cell colony macros, NIH Image FTP Site, ftp://codon.nih.gov/pub/nih-image/user-macros/

Ward, M. E. (1995): The immunobiology and immunopathology of chlamydial infections. *Acta Pathology, Microbiology and Immunology Scandinavia* **103**, 769-796.

Wegmann, T. G., Lin, H., and Mosmann, T. R. (1993): Bidirectional cytokine interactions in the maternal-fetal relationship: is successful pregnancy a TH2 phenomenon? *Immunology Today* **14**, 353-356.

Williams, D. M, Grubbs, B., Pack, E., Kelly, K. and Rank, R. (1997): Humoral and cellular immunity in secondary infection due to murine *Chlamydia trachomatis*. *Infection and Immunity* **65**, 2876-82.

Williams, D. M., Byrne, G. I., Grubbs, B., Marshal, T. J. and Schachter, J. (1988): Role *in vivo* for gamma interferon in control of pneumonia caused by *Chlamydia trachomatis* in mice. *Infection and Immunity* **56**, 3004-3006.

Williams, D. M., Grubbs, B. and Schachter, J. (1987b): Primary murine *Chlamydia trachomatis* pneumonia in B-cell-deficient mice. *Infection and Immunity* **55**, 2387-2390.

Williams, D. M., Grubbs, B. G., Kelly, K. W., Pack, E., Rank, R. G. and Kelly, K. (1996): Role of gamma-delta T cells in murine *Chlamydia trachomatis* infection. *Infection and Immunity* **64**, 3916-3919.

Williams, D. M., Grubbs, B. G., Schachter, J. and Magee, D. M. (1993): Gamma interferon levels during *Chlamydia trachomatis* pneumonia in mice. *Infection and Immunity* **61**, 3556-3558.

Williams, D. M., Schachter, J. and Grubbs, B. (1987a): Role of natural killer cells in infection with the mouse pneumonitis agent (murine *Chlamydia trachomatis*). *Infection and Immunity* **55**, 223-226.

Williams, D. M., Schachter, J., Drutz, D. J. and Sumaya, C. V. (1981): Pneumonia due to *Chlamydia trachomatis* in the immunocompromised (nude) mouse. *Journal of Infectious Diseases* **143**, 238-41.

Williams, D. M., Schachter, J., Grubbs, B. and Sumaya, C. V. (1982): The role of antibody in host defence against the agent of mouse pneumonitis. *Journal of Infectious Diseases* **145**, 200.

Wilsmore, A. J., Parsons, V. and Dawson, M. (1984): Experiments to demonstrate routes of transmission of ovine enzootic abortion. *British Veterinary Journal* **140**, 380-391.

Wu, X., Dolecki, G. J. and Lefkowith, J. B. (1995): GRO chemokines: a transduction, integration, and amplification mechanism in acute renal inflammation. *American Journal of Physiology* **269**, F248-56.

Wu, X., Wittwer, A. J., Carr, L. S., Crippes, B. A., DeLarco, J. E. and Lefkowith, J. B. (1994): Cytokine-induced neutrophil chemoattractant mediates neutrophil influx in immune complex glomerulonephritis in rat. *Journal of Clinical Investigation* **94**, 337-44.

Wyrick, P. B. (1998): Cell biology of chlamydial infection: A journey in the host epithelial cell by the ultimate cellular microbiologist, 69-78. In R. S Stephens., Byrne, G. I., Christiansen, G., Clarke, I. N., Grayston, J. T., Rank, R. G., Ridway, G. L., Saikku, P., Schachter, J. and Stamm, W. E. (Ed) Eighth International Symposium on Human Chlamydial Infections, Napa, Californian, USA.

Wyrick, P. B. and Brownridge, E. A. (1978): Growth of *Chlamydia psittaci* in macrophages. *Infection and Immunity* **19**, 1054-1060.

Wyrick, P. B. and Davis, C. H. (1984): Elementary body envelopes from *Chlamydia psittaci* can induce immediate cytotoxicity in resident mouse macrophages and l-cells. *Infection and Immunity* **45**, 297-298.

Wyrick, P. B., Brownridge, E. A. and Ivins, B. E. (1978): Interaction of *Chlamydia psittaci* with mouse peritoneal macrophages. *Infection and Immunity* **19**, 1061-1067.

Yam, L. T., Li, C. Y. and Crosby, W. H. (1971): Cytochemical identification of monocytes and granulocytes. *American Journal of Clinical Pathology* **55**, 283-90.

Yancopoulos, G. D. and Alt, F. W. (1988): Reconstruction of an immune system. *Science* **241**, 1581-3.

Yang, X., HayGlass, K. T. and Brunham, R. C. (1996): Genetically determined differences in IL-10 and IFN-gamma responses correlate with clearance of *Chlamydia trachomatis* mouse pneumonitis infection. *Journal of Immunology* **156**, 4338-4344.

Yang, Z. P., Cummings, P. K., Patton, D. L. and Kuo, C. C. (1994): Ultrastructural lung pathology of experimental *Chlamydia pneumoniae* pneumonitis in mice. *Journal of Infectious Diseases* **170**, 464-467.

Yoneda, C., Dawson, C. R., Daghfous, T., Hishiwara, I., Jones, P., Messadi, M. and Schachter. (1975): Cytology as a guide to the presence of chlamydial inclusions in Giemsa-stained conjunctival smears in severe endemic trachoma. *British Journal of Ophthalmology* **59**, 116.

Yong, E. C., Chi, E. Y. and Kuo, C. C. (1987): Differential antimicrobial activity of human mononuclear phagocytes against the human biovars of *Chlamydia trachomatis*. *Journal of Immunology* **139**, 1297-1302.

Yong, E. C., Chi, E. Y., Chen, W. J. and Kuo, C. C. (1986): Degradation of *Chlamydia trachomatis* in human polymorphonuclear leukocytes: an ultrastructural study of peroxidase-positive phagolysosomes. *Infection and Immunity* **53**, 427-431.

Yong, E. C., Klebanoff, S. J. and Kuo, C. C. (1982): Toxic effect of human polymorphonuclear leukocytes on *Chlamydia trachomatis*. *Infection and Immunity* **37**, 422-426.

Yu, C. L., Sun, K. H., Shei, S. C., Tsai, C. Y., Tsai, S. T., Wang, J. C., Liao, T. S., Lin, W. M., Chen, H. L., Yu, H. S. *et al* (1994): Interleukin 8 modulates interleukin-1 beta, interleukin-6 and tumor necrosis factor-alpha release from normal human mononuclear cells. *Immunopharmacology* **27**, 207-14.

Zhang, Y., Ramos, B. F., Jakschik, B., Baganoff, M. P., Deppeler, C. L., Meyer, D. M., Widomski, D. L., Fretland, D. J. and Bolanowski, M. A. (1995): Interleukin 8 and mast cell-generated tumor necrosis factor-alpha in neutrophil recruitment. *Inflammation* **19**, 119-32.

Zhong, G. M. and De La Maza, L, M. (1988): Activation of mouse peritoneal macrophages *in vitro* or *in vivo* by recombinant murine gamma interferon inhibits the growth of *Chlamydia trachomatis* serovar L1. *Infection and Immunity* **56**, 3322-3325.

Zvillich, M. and Sarov, I. (1985): Interaction between human polymorphonuclear leukocytes and *Chlamydia trachomatis* elementary bodies - electron-microscopy and chemi- luminescent response. *Israel Journal of Medical Sciences* **21**, 177.

Appendix

Appendix 1

1.1 PBS (MRI scientific services)

- 900 ml deionised water
- 8 g NaCl (Sigma-Aldrich)
- 1.15 g Na_2HPO_4 (Sigma-Aldrich)
- 0.2 g KH_2PO_4 (Sigma-Aldrich)
- 0.2 g KCL (Sigma-Aldrich)
- Adjusted to 1 L in volume at pH 7.4, autoclaved and stored at RT.

1.2 trypsin/versene

- 20% Trypsin solution (MRI scientific services)
    - 40 g of NaCl (Sigma-Aldrich)
    - 3.8 g of KCl (Sigma-Aldrich)
    - 0.5 g of Na_2HPO_4 (Sigma-Aldrich)
    - 15 g of Tris (hydroxymethyl)methylamine (Sigma-Aldrich)
    - 7.5 ml of 1% Phenol red solution (Sigma-Aldrich)
    - 12.5 g Trypsin (Difco Laboratories, Surrey, UK)
    - Made up to 5 L in deionised water pH 7.6.

- 80% Versene solution (MRI scientific services)
    - 48.0 g of NaCl (Sigma-Aldrich)
    - 1.2 g of KCl (Sigma-Aldrich)
    - 6.9 g of Na_2HPO_4 (Sigma-Aldrich)
    - 1.2 g of KH_2PO_4 (Sigma-Aldrich)
    - 1.2 g Versene (Ethylene Diamine Tetra acetic acid (Disodium salt: Dihydrate)) (Sigma-Aldrich)
    - 9.0 ml of 1% Phenol red solution (Sigma-Aldrich)
    - Made up to 6 L in deionised water pH 7.2.

1.3 chlamydial transport medium (MRI scientific services)

- 373 g of Sucrose (Sigma-Aldrich)
- 2.560 g of KH_2PO_4 (Sigma-Aldrich)
- 6.185 g of K_2HPO_4 (Sigma-Aldrich)
- 3.605 g of L-glutamic acid (Sigma-Aldrich)
- Made up to 5 L in deionised water
- 20 ml 0.4% phenol red solution (Sigma-Aldrich) added
- 500 ml of FBS (GIBCO BRL) added
- 25 ml (1/4 vial) of gentacin (GIBCO BRL) added
- 0.5 g of streptomycin (GIBCO BRL) added
- Filtered and 25 ml 10 000 U/ml Nystatin suspension added

1.4 Carbonate coating buffer (pH 9.6)

- 4.9 L of deionised water
- 10.6 g Na_2CO_3 (Sigma-Aldrich)
- 16.8 g $NaHCO_3$ (Sigma-Aldrich)
- Adjusted to 5 L in volume at (pH 9.6) aliquoted and stored at -20°C.

1.5 L-broth

- 900 ml of deionised water
- 10 g Tryptone (Difco Laboratories)
- 5 g Yeast Extract (Difco Laboratories)
- 5 g NaCl (Sigma-Aldrich)
- Adjusted to 1 L in volume at (pH 7.2), autoclaved and stored at 4°C.

1.6 L-agar

- 900 ml of deionised water
- 10 g Tryptone (Difco Laboratories)
- 5 g Yeast Extract (Difco Laboratories)
- 10 g NaCl (Sigma-Aldrich)
- 15 g Agar (Difco Laboratories)
- Adjusted to 1 L in volume (pH 7.2), autoclaved and cooled to 50°C before pouring under class I flow bench. Set and stored upside down at 4°C.

1.7 40 mM Phosphate buffer (pH 7.4)

- 162 ml of 0.2 M Na_2HPO_4 (Sigma-Aldrich)
- 38 ml of 0.2 M NaH_2PO_4 (Sigma-Aldrich)
- Autoclave and store at RT
- Diluted 1/5 in deionised water to yield 1 L of pH 7.4 40 mM Phosphate buffer prior to use.

1.8 12% acrylamide resolving gel (10 ml)

- 4.0 ml acrylamide/Bis solution (30% acrylamide/0.8% N' N'-bis-methylene-acrylamide; Severn Biotech LTD, Kidderminster, UK).
- 3.35 ml deionised water
- 2.5 ml 1.5 M (pH 8.8) Tris-HCL (Sigma-Aldrich)
- 0.1 ml 10% SDS in deionised water (Sigma-Aldrich)
- 100 µl 10% ammonium persulfate (APS; BIO-RAD) and 10 µl TEMED (BIO-RAD) were added to catalyse polymerisation before to adding gel to the cast.

1.9 4% acrylamide stacking gel (5 ml)

- 1.15 ml acrylamide/Bis solution (30% acrylamide/0.8% N' N'-bis-methylene-acrylamide; Severn Biotech LTD, Kidderminster, UK).
- 3.09 ml deionised water
- 1.25 ml 0.5 M (pH 6.8) Tris-HCL (Sigma-Aldrich)
- 140 µl 10% SDS in deionised water (Sigma-Aldrich)
- 100 µl 10% ammonium persulfate (APS; BIO-RAD) and 10 µl TEMED (BIO-RAD) were added to catalyse polymerisation before adding gel to the cast.

1.10 5x Electrode buffer (3 L)

- 45 g Tris base (Sigma-Aldrich)
- 216 g Glycine (Sigma-Aldrich)
- 15 g SDS (Sigma-Aldrich)
- Made up to 3 L in deionised water, diluted 1/5 in deionised water prior to use.

1.11 Sample buffer (5 ml)

- 3.8 ml deionised water
- 1 ml 0.5 M (pH 6.8) Tris-HCL (Sigma-Aldrich)
- 0.8 ml Glycerol (Sigma-Aldrich)
- 1.6 ml 10% SDS in deionised water (Sigma-Aldrich)
- 0.4 ml 2-mercaptoethanol (ICN Biomedicals)
- 0.4 ml 0.05% bromophenol blue in deionised water (Sigma-Aldrich)

1.12 Acid-alcohol (Destain for Coomassie blue)

- 900 ml deionised water
- 500 ml absolute alcohol (Fisher Scientific)
- 200 ml acetic acid (Fisher Scientific)

1.13 Griess reagent

- Reagent A: 1% sulfanilamide (Sigma-Aldrich) in 5% phosphoric acid (Sigma-Aldrich), stored in the dark at 4°C.
- Reagent B: 0.1% *N* -1-napthylethylenediamine dihydrochloride (Sigma-Aldrich) in deionised water, stored in the dark at 4°C.
- Mix Reagent A and reagent B in equal parts immediately before use.

Appendix 2: Surface marker expression of ovine BAL cells

Antibody	Specificity	#1 M1 % (Gated) /Median FITC green fluorescence	#2 M1 % (Gated) /Median FITC green fluorescence	#3 M1 % (Gated) /Median FITC green fluorescence	#4 M1 % (Gated) /Median FITC green fluorescence
No primary/No secondary	*-ve control*	*0.23/87.00*	*0.00/76.00*	*0.00/74.00*	*0.05/76.00*
No primary	*-ve control*	*0.73/103.00*	*0.70/99.00*	*0.41/96.00*	*0.69/98.00*
VPM49	*BDV (-ve control MAb)*	*1.08/105.00*	*0.80/102.00*	*0.77/99.00*	*0.95/101.00*
VPM 22 & 49	*BDV (-ve control Ab)*	*1.14/107.00*	*1.84/105.00*	*1.99/102.00*	*1.30/106.00*
SBU LCA (1.28)	CD45 (+ve control Mab)	93.43/176.00	88.92/175.00	96.48/183.00	95.65/184.00
36F	CD2 (T cells/NK cells)	9.81/118.00	12.21/116.00	6.36/114.00	13.67/120.00
86D	γδ TCR (γδ T cells)	0.90/106.00	0.79/103.00	0.79/101.00	1.04/104.00
CC21	CD21 (CR2: B cells)	0.89/106.00	0.91/102.00	3.50/101.00	0.81/103.00
VPM30	B cell marker	0.88/105.00	0.59/101.00	0.79/98.00	0.57/102.00
VPM 65	CD14	67.65/150.00	67.92/151.00	61.09/146.00	68.82/149.00
VPM 67	CD14	65.81/149.00	65.14/150.00	52.95/143.00	60.48/146.00
VPM 8	Immunoglobulin light chain	55.39/145.00	58.60/147.00	59.02/145.00	58.89/145.00

Appendix 3: Peer reviewed publications arising from the work detailed in this thesis

Brown, J and Entrican, G. (1996) Interferon-γ mediates long-term persistent *Chlamydia psittaci* infection *in vitro*. *Journal of Comparative pathology* **115**, 373-383.

Brown, J., Coulon, C., Howie S, E, M and Entrican G. (1998) Automated measurement of chlamydial inclusion bodies using NIH Image, 115 - 118. In R. S Stephens., Byrne, G. I., Christiansen, G., Clarke, I. N., Grayston, J. T., Rank, R. G., Ridway, G. L., Saikku, P., Schachter, J. and Stamm, W. E. (Ed) Eighth International Symposium on Human Chlamydial Infections, Napa, Californian, USA.

Entrican, G., Brown, J & Graham S. (1998) Cytokines and the protective host response to *Chlamydia psittaci*. *Comparative Immunology, Microbiology and Infectious Diseases* **21**, 15 - 26.

McInnes C, J., Innes E, A., Brown, J, Entrican, G. (1997) A current perspective on ovine cytokines, 87-99. In: M. C. Horzinek and V. E. C. J. Schijns (Ed) Cytokines in Veterinary medicine, CAB International Publications, Wallingford, UK.